THE BIOLOGY OF TUBERCULOUS GRANULOMAS

by Mi Jeong Kim

THE BIOLOGY OF TUBERCULOUS GRANULOMAS

A Dissertation

Presented to the Faculty of the Graduate School

of Cornell University

In Partial Fulfillment of the Requirements for the Degree of

Doctor of Philosophy

by

Mi Jeong Kim

August 2010

THE BIOLOGY OF TUBERCULOUS GRANULOMAS

Mi Jeong Kim, Ph. D.

Cornell University 2010

Mycobacterium tuberculosis (Mtb) infection results in the formation of a granuloma by the host immune response. The well-structured tuberculous (TB) granuloma confines the bacilli at the local foci, preventing the systemic infection. Most of Mtb-infected individuals are able to control the infection and stay healthy. However, by still unknown mechanisms, the TB granuloma can liquefy and erode into the airway space, thereby releasing bacilli and transmitting TB to other hosts. Despite the importance of granulomas in TB pathogenesis, our understanding is still unclear. This work was performed to advance our knowledge on the biology of TB granuloma by using human TB tissues and *in vitro* and *in vivo* models.

Our microarray analysis on human TB granulomas shows upregulation of biological processes including inflammation, lipid metabolism, tissue remodeling, and apoptosis. Immunohistological analysis on human TB lung tissues reveals that proteins responsible for lipid synthesis and accumulation are disproportionately expressed in granulomas; adipose differentiation-related protein (ADFP), acyl-CoA synthetase long chain family member 1 (ACSL1), and saposin C (SapC) are most strongly expressed in caseous granulomas but not in resolved granulomas. The biochemical analysis shows that the caseum of TB granulomas is enriched with neutral lipids and glycosphingolipids, which are tightly associated with the upregulated expression of ADFP, ACSL1, and SapC. In addition, Mtb infection in macrophages *in vitro* induces similar changes of transcript and protein expression when compared to that of human pulmonary TB granulomas, suggesting that the host lipid metabolism is perturbed by

Mtb infection. Furthermore, murine granulomas induced by the Mtb-cell wall component, trehalose dimycolate (TDM), accumulate extensive amounts of lipids in cells, and this phenomenon is not dependent on the presence of B- or T-cells, indicating that innate immunity is mainly responsible for the accumulation of lipids in cells in response to TDM. In addition to lipid accumulation, the microarray analysis shows that the murine TDM-granuloma is strikingly reminiscent of human TB granuloma; e.g. tissue remodeling and degeneration, cell death, and angiogenesis. In summary, these data demonstrate (1) human TB granulomas undergo dysregulated lipid metabolism, which culminates in the formation of lipid-filled caseum, (2) Mtb bacilli infection affects the lipid metabolism in macrophages *in vitro*, (3) the Mtb cell wall lipid, TDM, induces the formation of lipid-filled foam cells in mice *in vivo*, and (4) TDM-induced granulomas resemble the pathology of human TB granulomas.

BIOGRAPHICAL SKETCH

Born in South Korea, Mi Jeong Kim obtained her bachelor's degree in Pharmacy in 2000 and master's degree in Pharmacy in 2002. Mi Jeong worked as a pharmacist in pharmacies and for a pharmaceutical company and also as a tutor and volunteer in South Korea until she joined Dr. David Russell's lab for her Ph.D. in 2005.

To my loving parents, Kim Tae-Hong and Park Choon-Rye,

and my siblings, Kim Ki-Kyung, Kim Yun-Hwan, and Kim Nak-Hyun

ACKNOWLEDGMENTS

I'd like to thank my advisor, Dr. David G. Russell, who has supported my study for so many years. I am very fortunate and happy to know and work for him.

I give endless thanks to my committee members, Dr. Lisa Fortier, Dr. David Lin, and Dr. Cynthia Leifer for their sincere support and advices. They have kept me on the right track.

I thank Dr. Helen Wainwright and Dr. Genevieve Learmonth at University of Cape Town Medical School for their support, friendship, enthusiasm, and love. I am deeply obliged to Dr. Eung-Chil Choi and Dr. Chang-Yuil Kang at Seoul National University School of Pharmacy for their warmth and support.

I send my sincere thanks to all the past and present Russell lab members including Brian VanderVen, Robert Abramovitch, Elizabeth Rhoades, Róisín Owens, and Robin Yates. Especially, I thank Ute Schwab, Luis Camacho, and Kaori Sakamoto for being the most magnificent friends and mentors in my life. Without them, I couldn't have gone through these years.

Friends in Ithaca have been very kind and caring; Meilman family, Alice, Phil, Anna, and Laura, Leesun Kim, Andy Moorhead, Inês Veiga, Jill Thurman, Walter Iddings, Xiangjie Sun, Kui Yang, Rod Getchell, Najet Chbab, Becky Mitchell, Sachiko Funaba, AnnMarie Butler, Dr. Klaus Osterrieder, Karsten Tischer, and Jens Von Einem. I send my heartfelt thanks to all of my loving friends in South Korea and other countries, especially Kim Yang-Joong, Sister Liberata, Song Yeo-Ok, Lee Yoo-Soon, Lee Seung-Hee, Bae Sung-Yoon, Park Eun-Kyung, Jeong Jae-Hee, and Anina Hicks.

I give zillions of thanks to Nature for nourishing my soul.

Mostly and lastly, I thank my parents and family from my deepest heart.

Everyone I have met is essential to my life; I have become myself, thanks to love and support from all of them. Thank you very much!

TABLE OF CONTENTS

LIST OF FIGURES

LIST OF TABLES

LIST OF ABBREVIATIONS

ABHD5	Abhydrolase domain containing 5
ACLY	ATP citrate lyase
ACSL1	Acyl-CoA synthetase long chain family member 1
ADAMTS1	ADAM metallopeptidase with thrombospondin
ADFP	Adipose differentiation-related protein
AFB	Acid fast bacilli
AIDS	Acquired immune deficiency syndrome
APAF1	Apoptotic peptidase activating factor 1
aRNA	antisense RNA
ATF2	Activating transcription factor 2
BALF	Bronchial alveolar lavage fluid
BCG	*Mycobacterium bovis* Bacille Calmette-Guérin
β_2m	beta 2-microglobulin
BMMΦ	Bone marrow-derived macrophages
C3AR1	Complement component 3a receptor 1
C5AR1	Complement component 5a receptor 1
CAD	Collisionally activated dissociation
CALR	Calreticulin
CANX	Calnexin
CASP1	Caspase 1
CCL	Chemokine (C-C motif) ligand
CD	Cluster of differentiation
CE	Cholesteryl esters
CHI3L1	Chitinase-3-like 1

CHO	Cholesterol
CHOP	CCAAT/enhancer-binding protein homologous protein
CKLF	Chemokine-like factor
CMKLR1	Chemokine-like receptor 1
COL1A1	Collagen, type I, alpha 1
CR	Complement receptor
CRAT	Carnitine O-acetyltransferase
CSF1	Colony stimulating factor 1
CTGF	Connective tissue growth factor
CXCL	Chemokine (C-X-C motif) ligand
CYCS	Cytochrome c, somatic
CYP1B1	Cytochrome P450, family 1, subfamily B, polypeptide 1
Dapk1	Death associated protein kinase 1
DC	Dendritic cell
DC-SIGN	DC-specific intercellular adhesion molecule-3-grabbing non-integrin
DEGS1	Degenerative spermatocyte homolog 1, lipid desaturase
DHCR7	7-dehydrocholesterol reductase
DMEM	Dulbecco's Modified Eagle Medium
DOTS	Directly Observed Therapy Short Course
EBP	Emopamil binding protein
EDEM1	ER degradation enhancer, mannosidase alpha-like 1
EEA1	Early endosome antigen 1 protein
EHS	Engelbreth-Holm-Swarm
EI	Electron impact
ELISA	Enzyme-Linked Immunosorbent Assay

ELOVL5	Elovl family member 5, elongation of long chain fatty acids
ER	Endoplasmic reticulum
ERO1L	Endoplasmic oxidoreductin-1-like protein
FADS1	Fatty acid desaturase 1
FASLG	Fas ligand
FBLN2	Fibulin 2
FCER1G	Fc fragment of IgE, high affinity I, receptor for; gamma polypeptide
FCGR2A	Fc fragment of IgG, low affinity, IIa, receptor
FCGR2B	Fc fragment of IgG, low affinity, IIIa, receptor
FCGR3A	Fc fragment of IgG, low affinity, IIIb, receptor
FDPS	Farnesyl diphosphate synthase
Gadd34	Growth arrest and DNA-damage-inducible 34
Gadd45b	Growth arrest and DNA-damage-inducible 45 beta
GBA	Glucosidase, beta, acid
GLA	Galactosidase, alpha
GLB1	Galactosidase, beta 1
GC/MS	Gas chromatography/mass spectrometry
GlcCer	Glucosylceramide
GPD2	Glycerol-3-phosphate dehydrogenase 2
HADHA	Hydroxyacyl-Coenzyme A dehydrogenase/3-ketoacyl-Coenzyme A thiolase/enoyl-Coenzyme A hydratase, alpha subunit
H&E	Hematoxylin and eosin
HERPUD1	Homocysteine-inducible, ER stress-inducible, ubiquitin-like domain member 1

HIF1A	Hypoxia inducible factor 1, alpha subunit
HI-FCS	Heat-inactivated fetal calf serum
HIV	Human immunodeficiency virus
HLA	Human leukocyte antigen
HMGCR	3-hydroxy-3-methyl-glutaryl-CoA reductase
HSP90B1	Heat shock protein 90 kDa beta (Grp94), member 1
hVPS34	Phosphatidylinositol-3-OH-kinase
ICAM3	Intercellular adhesion molecule 3
IDI1	Isopentenyl-diphosphate delta isomerase 1
IFIT1	Interferon-induced protein with tetratricopeptide repeats 1
IFN-γ	Interferon-gamma
IFNGR1	Interferon gamma receptor 1
IL	Interleukin
IL6ST	Interleukin 6 signal transducer (gp130)
ILIs	Intracellular lipophilic inclusions
INHBA	Inhibin, beta A
INSIG1	Insulin induced gene 1
IRAK2	Interleukin-1 receptor-associated kinase 2
ITGA5	Integrin, alpha 5
ITGB1	Integrin, beta 1
IVT	*In vitro* transcription
Juk1	Mitogen-activated protein kinase 8
KO	Knockout
LacCer	Lactosylceramide
LAM	Lipoarabinomannan
LCFA	Long-chain fatty acid

LCM	Laser Capture Microdissection
LDL	Low density lipoprotein
LDLR	Low density lipoprotein receptor
LIPA	Lipase A, lysosomal acid, cholesterol esterase
LSS	Lanosterol synthase
LTA	Lymphotoxin alpha
LTB	Lymphotoxin beta
LUM	Lumican
ManLAM	Mannose-capped lipoarabinomannan
MAP	Mitogen-activated protein
MAP3K5	Mitogen-activated protein kinase kinase kinase 5
MAPK1	Mitogen-activated protein kinase
MARCO	Macrophage receptor with collagenous structure
MCP-1	Monocytes chemoattractant protein-1
MDR-TB	Multidrug resistant tuberculosis
MGC	Multinucleated giant cell
MHC	Major histocompatibility complex
MIF	Macrophage migration inhibitory factor
MIP-1	Macrophage inflammatory protein-1
MMP	Matrix metalloproteinase
MR	Mannose receptor
MRC1	Mannose receptor, C type 1
MRC2	Mannose receptor, C type 2
MS	Mass spectrometry
MSN	Moesin
MSR1	Macrophage scavenger receptor 1

MST1	Macrophage stimulating 1
Mtb	*Mycobacterium tuberculosis*
MyD88	Myeloid differentiation factor 88
NADPH	Nicotinamide adenine dinucleotide phosphate
NKT	Natural killer T cells
NO	Nitric oxide
Nramp-1	Natural resistance-associated macrophage protein 1
NRP1	Neuropilin 1
OADC	Oleic acid/albumin/dextrose/catalase
PAG1	Phosphoprotein associated with glycosphingolipid microdomains 1
PBMC	Peripheral blood mononuclear cell
PBMM	Peripheral blood monocytes-derived macrophages
PDGFC	Platelet derived growth factor C
PDGFRA	Platelet derived growth factor, alpha polypeptide
PDIA4	Protein disulfide isomerase family A, member 4
PG	Phosphatidylglycerol
PIM	Phosphatidyl-*myo*-inositol mannoside
PLAU	Plasminogen activator, urokinase
PLAT	Plasminogen activator, tissue
PLSCR1	Phospholipid scramblase 1
PPAR	Peroxisome proliferator-activated receptor
PSAP	Prosaposin
Rag1	Recombination activating gene 1
RT-PCR	Reverse transcription polymerase chain reaction
SapC	Saposin C

SCARA5	Scavenger receptor class A, member 5
SCARB2	Scavenger receptor class B, member 2
SCARF1	Scavenger receptor class F, member 1
SC5DL	Sterol-C5-desaturase
SCD	Stearoyl-CoA desaturase
SCYE1	Small inducible cytokine subfamily E, member 1
SERPINA1	Serpin peptidase inhibitor, clade A, member 1
SMAD3	SMAD (mothers against decapentaplegic) family member 3
SMC	Smooth muscle cell
SOAT1	Sterol O-acyltransferase 1
SP	Surfactant protein
SPHK2	Sphingosine kinase 2
STAT6	Signal transducer and activator of transcription 6, interleukin 4-induced
SYK	Spleen tyrosine kinase
TACO	Tryptophan-alanine-rich coat protein
TAG	Triacylglycerols
TAP	Transporter associated with antigen processing
TB	Tuberculosis or tuberculous
TDM	Trehalose dimycolate
TGF-β	Transforming growth factor beta
TGFBR1	Transforming growth factor, beta receptor 1
THBS2	Thrombospondin 2
TIC	Total ion current
TIMP1	TIMP metallopeptidase inhibitor 1
TLC	Thin layer chromatography

TLR	Toll-like receptor
TNF-α	Tumor necrosis factor alpha
TNFAIP1	TNF, alpha-induced protein 1
TNFRSF1A	TNF receptor superfamily, member 1A
TNFSF4	TNF (ligand) superfamily, member 4
TNIP3	TNFAIP3 interacting protein 3
TPI1	Triosephosphate isomerase 1
TRAF1	TNF receptor-associated factor 3
TUNEL	Terminal deoxylnucleotidyl transferase dUTP nick end labeling
VCAN	Versican
VEGFA	Vascular endothelial growth factor A
XBP1	X-box binding protein 1
XDR-TB	Extreme drug resistant tuberculosis

CHAPTER ONE

INTRODUCTION

Mycobacterium tuberculosis and Tuberculosis

The causative agent of tuberculosis (TB), *Mycobacterium tuberculo*sis (Mtb) bacillus, was first identified by Robert Koch in 1882 [1]. Mtb belongs to genus of *Mycobacterium*, family of Mycobacteriaceae, suborder of Corynebacterineae, order of Actinomycetales, and phylum of Actinobacteria. A group of *Mycobacterium* species that can cause TB is called the Mtb complex, which includes Mtb, *M. canettii*, *M. africanum* subtype 1 *M. pinnipedii*, *M. microti*, *M. bovis* subsp. *caprae*, and *M. bovis*. Mtb complex members are known to have different host preferences; Mtb for humans, *M. bovis* for bovids, and *M. pinnipedii* for marine mammals [2-3].

Mtb is reported to have around 4,000 putative genes, with 52% having known functions [4-5]. A large number of genes are involved in lipid metabolism and environmental regulation, which reflects the versatility of Mtb under extreme conditions [6-7]. Lipids in Mtb permit the characteristic acid-fastness and resistance to drying and antibiotics, and affect the host immune response [8-9]. Mtb is a slow grower, with replication time of 12~24 hours *in vitro*, and it is known to replicate much slower during acute or chronic infection *in vivo* [10-11]. TB transmission occurs when active TB patients cough up Mtb-containing aerosol droplets, which in turn are engulfed by phagocytes. Mtb-containing phagocytes secrete various cytokines and chemokines, recruiting other leukocytes from the circulation to the site of infection. This leads to the formation of TB granuloma, where Mtb bacilli reside. During the chronic infection, the granuloma protects not only the host from the bacterial transmission but also provides a shelter to Mtb. When the disease becomes

active, Mtb bacilli replicate actively and escape from the localized TB granuloma, infecting other new hosts.

TB is the second leading infectious cause of death worldwide, following acquired immune deficiency syndrome (AIDS), and it claims 2 million lives and 9 million new individuals are infected with Mtb per year [12]. TB is more problematic in AIDS patients, whose immunity is severely compromised [13-15], and especially, sub-Saharan Africa is heavily afflicted by TB and human immunodeficiency virus (HIV) co-infection [15]. WHO has initiated the Directly Observed Therapy Short-Course (DOTS) program in 1990 in Peru, and now worldwide, covering 62% of the world's population [16-17]. DOTS has been very effective in improving treatment outcomes and preventing deaths and it is especially important in HIV care provision, because of the strong epidemiological link between TB and HIV and the high prevalence of HIV infection among TB patients. The emergence of multidrug resistant TB (MDR-TB), extreme drug resistant TB (XDR-TB), and the poor socioeconomic conditions are another hurdle for reducing TB burden. Expansion of DOTS program, early detection of TB, and novel strategies of reducing mortality from TB and TB-HIV co-infection are urgently needed to improve the global TB control.

Treatment of Tuberculosis

The available vaccine for TB prevention is an attenuated strain of *M. bovis* Bacille Calmette-Guérin (BCG). BCG is administered to infants in more than 167 countries and is effective in preventing TB in about 80% of children. But its effectiveness is variable against TB in adults [18]. Modified BCG, attenuated Mtb, and protein or DNA subunit vaccines are actively being developed for TB prevention [19-21].

Treatment of TB with drug-susceptible Mtb requires at least 6-months of therapy with the first-line drugs: ethambutol, isoniazid, pyrazinamide, and rifampicin for 2 months, and then isoniazid and rifampicin for further 4 months. MDR-TB treatment takes longer, at least 18 months. Due to severe side-effects during the long regimen of antibiotic treatment, poor compliance of TB patients, and emergence of drug-resistant Mtb, it is necessary to develop novel therapeutics for TB treatment. One of the promising drugs is R207910 (TMC207, developed by Johnson & Johnson), diarylquinoline, an inhibitor of bacterial ATP synthase, that was very effective in TB treatment in mice, in combination with rifampicin and pyrazinamide [22-23]. Linezolid and PNU-100480, oxazolidinone antibiotics that inhibit bacterial protein synthesis, is another promising agent against Mtb including drug-resistant strains [24-26]. When administered with rifampicin and pyrazinamide, moxifloxacine was very effective in reducing Mtb burden by inhibiting DNA gyrase and topoisomerases [27]. Inhibition of Mtb cell wall synthesis has been shown effective in treating TB. SQ-109, a novel diamine antibiotic, in combination with rifampicin, pyrazinamide, and isoniazid, improved the outcome of TB treatment [28]. Bicyclic nitroimidazoles such as PA-824 and OPC 67683 have proven to be effective against replicating and non-replicating Mtb possibly by acting as nitric oxide (NO) donors and therefore augmenting the innate immunity-mediated killing mechanism [29-30].

First described in the literature back in 18th century, lung resection has been performed on patients with MDR-TB, complications of TB such as hemoptysis, bronchiectasis, or empyema, or difficult diagnosis between TB and cancer [31-36]. Surgical cure rates of over 90% have been reported and the resection together with antibiotic treatment is important in treating TB patients lung resection is highly recommended to reduce the burden of infection.

Immunity to Tuberculosis

A. Cytokines and Chemokines

Mtb bacilli entering macrophage can block the phagosome maturation and the lysosomal fusion, therefore surviving within the phagocyte; but the host cell is not quiescent. The host cells that phagocytose Mtb bacilli via various receptors such as complement receptor, mannose receptors, scavenger receptors, TLRs, and other unidentified receptors secrete various cytokines and chemokines. In response to tumor necrosis factor (TNF)-α, chemokine (C-C motif) ligand 2 (CCL2), chemokine (C-X-C motif) ligand (CXCL9), CXCL10, interleukin (IL)-1α, IL-1β, and IL-18, neutrophils are recruited and secrete more effector molecules such as TNF-α, CCL2, CCL3, CCL4, CCL5, CXCL9, and CXCL10 [37-38]. Successively, γδ T cells, natural killer T (NKT) cells, monocytes, and granulocytes arrive at the site of infection, followed by effector B and T cells. Cluster of differentiation (CD) molecules, major histocompatibility complex (MHC) molecules, toll-like receptors, cytokines, and chemokines, implicated in TB pathogenesis are shown in Table 1.1 and 1.2.

Tumor Necrosis Factor-α

TNF-α is a primary mediator of immune regulation and the inflammatory response and has been implicated as a beneficial and harmful factor. It is produced by numerous cells including monocytes, eosinophils, neutrophils, basophils, NKT cells, B cells, T cells, macrophages, granulosa cells, mast cells, Kupffer cells, astrocytes, osteoblasts, spermatogenic cells, retinal pigment epithelial cells fibroblasts, smooth muscle cells, glia, neurons, keratinocytes, and tumor cells. TNF-α synthesis is tightly regulated so that it is rapidly synthesized and secreted in activated cells induced by infections. TNF-α is critical in Mtb infection by stimulating neutrophils and macrophages in an autocrine and paracrine fashion to promote cell apoptosis and

Table 1.1 Cluster of Differentiation (CD) antigen, Major Histocompatibility Complex (MHC) molecule, and Toll-Like Receptor (TLR)

CD antigen	Leukocyte	Function
CD1a-e; MHC class I-like	Dendritic cells, B cells, Langerhans cells, monocytes, activated T cells, some thymocytes, epithelial cells	Display of non-peptide and glycolipid antigens for T-cell activation
CD3	Thymocytes, T cells, natural killer (NK) cells	Adhesion molecule involved in T-cell activation
CD4	MHC class II-restricted T cells, some thymocytes, monocytes, macrophages, granulocytes	Co-receptor for MHC class II-restricted T-cell activation; thymic differentiation marker for T cells; a receptor for HIV
CD8	MHC class I-restricted T cells, thymocytes, subset of dendritic cells	Co-receptor for MHC class I-restricted T cells
DC-SIGN (dendritic-cell-specific intercellular adhesion molecule-3-grabbing non-integrin); C-type lectin; CD209	Dendritic cells	Dendritic cell-mediated adhesion to endothelial cells and antigen endocytosis and degradation; binding to HIV
MHC	**Cell type**	**Function**
MHC class I	All nucleated cells; composed of α-chain and β_2-microglobulin	Presents antigens to cytotoxic $CD8^+$ T cells
MHC class II	antigen-presenting cells; dendritic cells, macrophages, B cells, epithelial cells, fibroblasts, thymic epithelial cells, thyroid epithelial cells, glial cells, pancreatic beta cells, vascular endothelial cells	Presents antigens to helper $CD4^+$ T cells
Receptor	**Ligand**	**Cell type**
TLR2	Lipopeptides, lipoproteins, glycolipids, lipoteichoic acid, heat-shock protein 70, zymosan	Monocytes, macrophages, myeloid dendritic cells, mast cells
TLR4	Lipopolysaccharide, heat-shock proteins, fibrinogen, heparan sulfate fragments, hyaluronic acid fragments	Monocytes, macrophages, myeloid dendritic cells, mast cells, intestinal epithelium

Table 1.2 Cytokines and Chemokines

Cytokine	Sources	Activity
Interleukin-1 (IL-1), α & β	Monocytes, macrophages, dendritic cells, B cells, T cells, NK cells, vascular epithelium, fibroblasts, some smooth muscle cells	Induces fever and acute phase response; stimulates neutrophil production; regulates hematopoiesis; increases vascular permeability; promotes fibroblast proliferation; activates B cells and T cells; produces platelets
IL-2; T cell growth factor	T cells	Stimulates growth and differentiation of B cells, T cells, and NK cells
IL-4; B cell stimulating factor 1	Mast cells, bone marrow stromal cells, T cells	Promotes of growth and development of B cells, T cells, and monocytes; induces B-cell class switch to IgE; upregulates of MHC class II molecule
IL-6; B cell stimulating factor 2; hybridoma/plasmacytoma growth factor; hepatocyte-stimulating factor	B cells, T cells, macrophages, bone marrow stromal cells, fibroblasts, endothelial cells, astrocytes	Induces fever and acute phase response; regulates B cells and T cells; regulates hematopoiesis; increases vascular permeability; produces platelets; increases immunoglobulin synthesis
IL-10; cytokine synthesis inhibitor	Activated subset of $CD4^+$ and $CD8^+$ T cells	Stimulates proliferation of B cells, mast cells, and thymocytes together with transforming growth factor-β; stimulates IgA synthesis and secretion by B cells; antagonizes generation of TH1 cells
IL-12; NK cells stimulatory factor; Cytotoxic lymphocyte maturation factor	Dendritic cells, macrophages	Induces differentiation of TH1 cells; induces interferon gamma production by T cells and NK cells; enhances NK-cell activity
IL-18; interferon gamma-inducing factor	Monocytic cells, dendritic cells	Promotes TH1 differentiation; induces interferon gamma production of T cells; enhances NK-cell cytotoxicity
Interferon gamma; macrophage-activating factor; T-cell interferon	$CD4^+$ and $CD8^+$ T cells, NK cells	Promotes leukocyte adhesion; induces activation, growth, and differentiation of macrophages, B cells, T cells, and NK cells; upregulates MHC expression on antigen-presenting cells; promotes TH1 cell differentiation
Transforming growth factor beta; differentiation-inhibiting factor	Many nucleated cell types and also found in platelets	Affects tissue remodeling, wound repair, development, and hematopoiesis; induces B-cell class switch to IgA; induces cell apoptosis; promotes $CD25^+$ regulatory T cells

Table 1.2 (Continued)

Cytokine/Chemokine	Sources	Activity
Tumor necrosis factor alpha; cachectin; TNF ligand superfamily member 2	Monocytes, macrophages, neutrophils, fibroblasts, activated T cells, NK cells	Induces fever and acute phase response; cytotoxic to transformed cells; promotes angiogenesis, bone resorption, and thrombotic processes; suppresses lipogenetic metabolism; a potent chemoattractant for neutrophils; stimulates macrophages; increases insulin resistance
Chemokine (C-C motif) ligand 2; monocytes chemotactic protein-1	Produced by tumor cells and a variety of cell types; inducible by oxidative stress, cytokines, or growth factors	Recruits monocytes, dendritic cells, and memory T cells to the site of tissue injury and infection; promotes osteoclast differentiation; causes degranulation of mast cells and eosinophils
CCL3 & 4; macrophage inflammatory protein-1 α & β	Inducible in most hematopoietic cells; monocytes, macrophages, neutrophils, B cells, T cells, dendritic cells, mast cells, NK cells, platelets, osteoblasts, astrocytes, microglia, epithelial cells, fibroblasts	Activates granulocytes leading to acute neutrophilic inflammation; induces synthesis and secretion of IL-1, IL-6, and TNF-α; recruits T cells, NK cells, monocytes, and many other immune cells; HIV suppressive factor; implicated in many diseases including arthritis, multiple sclerosis, granuloma formation, asthma, sepsis, and myeloid leukemia
CCL5; regulated upon activation, normal T-cell expressed, and secreted (RANTES)	Many cell types including monocytes, macrophages, T cells, fibroblasts, renal and pulmonary epithelium, endothelium, and airway smooth muscle	Recruits T cells, eosinophils, basophils to the inflammatory site; induces proliferation and activation of NK cells; causes the release of histamine from basophils and activated eosinophils
Chemokine (C-X-C motif) ligand 9	Dendritic cells, B cells, macrophages, endothelial cells	Recruits T cells NK cells to the inflammatory site; suppresses tumor growth
CXCL10; 10 kDa interferon gamma induced protein	Monocytes, endothelial cells, fibroblasts	Recruits monocytes, macrophages, T cells, NK cells, and dendritic cells; promotes T-cell adhesion to the endothelium; inhibits tumor growth, bone marrow colony formation, and angiogenesis

reactive oxygen and nitrogen intermediate production [39-42]. It also organizes the formation of TB granuloma, as manifested by TB reactivation in individuals who receive anti-TNFα therapy [37, 43-44]. On the other hand, uncontrolled synthesis of TNF-α is responsible for fever, wasting, and lung pathology in TB patients [43, 45]. In the presence of mycobacterial infection, TNF-α upregulates the production of matrix metalloproteinases and urokinase, and thereby leads to the destruction of the structural components of the lung [45-47].

Interferon-γ

Interferon-γ (IFN-γ), produced by $CD4^+$ T cells, $CD8^+$ T cells, and NKT cells, activates infected macrophages to overcome the mycobacterial inhibition of phagosomal maturation and to destroy the pathogen. The importance of IFN-γ in granuloma formation, downregulation of proinflammatory response and macrophage activation has been described using the murine model [48-49]. Although both $CD4^+$ and $CD8^+$ T cells are crucial for the effective control of Mtb, TH1-polarized $CD4^+$ T cells seem to be more important in controlling TB, by secreting IFN-γ [38, 48-50].

Interleukins

A member of IL-1 family, IL-1β, is produced by macrophages, dendritic cells (DCs), monocytes, and fibroblasts, and nearly all microbes and microbial products induce production of IL-β. It plays an important role in anti-mycobacterial response and is implicated in disease severity and fever in TB patients [51-53]. IL-6 is produced by both lymphoid and non-lymphoid cells and regulates immune response, acute-phase reactions, and haematopoiesis [54]. A high level of IL-6 was detected in pleural effusion in TB patients, and bronchoalveolar lavage cells from TB patients released significantly increased amounts of IL-6 together with IL-1β and TNF-α [55-

57]. Unlike IL-1, IL-6, or TNF-α, the secretion of IL-4 is restricted to certain cell types: activated T cells, mast cells, and basophils. IL-4, a TH2 cytokine, appears to exacerbate the tissue damage by synergizing with TNF-α, and IL-4 was observed in lavage fluid and peripheral blood samples from patients with cavitary TB [58].

B. Innate Immune Cells

Innate immune cells are capable of recognizing and responding to microbes and mediate the appropriate initiation of the acquired immunity, which in turn activates phagocytes to eliminate the infection. Phagocytes are critical in wound healing, inflammation, and host defense; professional phagocytes include macrophages, monocytes, and neutrophils, and DCs are considered paraprofessional phagocytes.

Dendritic cells

Immature DCs of myeloid lineage are able to phagocytose microbes and process antigens, and then they become mature, presenting antigens to naïve T cells. The roles of DCs in Mtb infection are still under investigations. DCs are known to phagocytose Mtb via a specialized C-type lectin known as DC-specific intercellular adhesion molecule-3-grabbing non-integrin (DC-SIGN) [59-61]. Specifically, the mycobacterial cell wall component, mannose-capped lipoarabinomannan (ManLAM), was demonstrated to bind to DC-SIGN, which resulted in the production of anti-inflammatory cytokine, IL-10, and it was proposed that Mtb infection downregulates DC-mediated immunity [59, 62]. However, these data are in contrast to the observation made by Schaefer *et al.* that DC-SIGN may promote protection by limiting Mtb-induced pathology [63].

Macrophages

Originated from blood monocytes, macrophages are distributed throughout all tissues and important as a first line defense against infection [64]. Macrophages are involved in both innate and acquired immunity; detect microbial invasion, restrict microbial spread by phagocytosis and killing, recruit immune cells by releasing cytokines and inflammatory mediators, activate lymphocytes by presenting antigens and producing cytokines, kill microbes by cell-mediated immunity, and participate in humoral immunity by binding antibodies and complements. Macrophages are also important in resolving the inflammation by producing anti-inflammatory factors including IL-10 and transforming growth factor β (TGF-β). Macrophages also serve as a niche for many pathogens including Mtb. Mtb bacilli are recognized by pattern recognition receptors (PRRs) such as complement receptors (CRs), mannose receptor (MR), CD14, and surfactant protein A receptor [65]. The microbes within phagosomes are killed by low pH and lysosomal fusion, limitation of nutrients, and the generation of reactive oxygen and nitrogen intermediates; however, Mtb has the ability to arrest phagosomal maturation [66]. Many studies have been done to understand how Mtb interferes with endocytic pathway, thereby evading the host immune response. The Mtb cell wall lipid, ManLAM, has been shown to be able to block the recruitment of Rab5A effectors, early endosome antigen 1 protein (EEA1) and phosphatidylinositol-3-OH-kinase (hVPS34) [67-69]. Mtb also produces a phosphatase, SapM, which hydrolyzes phosphatidylinositol-3-phosphate, inhibiting the fusion of phagosome and late-endosome [70], and it is resistant to the acidification of phagosome, by excluding the vesicular proton ATPase [71]. The confined environment of Mtb-phagosome have limited nutrients, however, Mtb can obtain iron by binding iron with a higher affinity than the host molecule [72]. Moreover, polymorphisms in natural resistance-associated macrophage protein 1 (Nramp-1)

which is thought to play a role in the removal of iron from the phagosome are significantly associated with TB [73]. The macrophage respiratory burst producing reactive oxygen intermediates is one of Mtb-killing mechanism, and mice lacking nicotinamide adenine dinucleotide phosphate-oxidase (NADPH oxidase) were shown to have increased numbers of Mtb bacilli during the early infection [74]. Reactive nitrogen intermediates generated in phagocytes are also effective in killing microbes; transposon mutants screening revealed that Mtb proteasome confers the resistance to oxidative or nitrosative stress [75]. Mtb is also shown to downregulate the surface expression of CD1, inhibiting T cell activation [76].

C. Acquired immune cells

The innate immune response against microbial infection is followed by acquired immune response, which is initiated by the recognition of foreign antigens. The antigen-specific response is divided into cell-mediated immunity of T cell activation and effector mechanism and humoral response of B cell maturation and antibody production.

B cells

The role of humoral response in TB pathogenesis is still unclear. It was shown that the absence of humoral response does not change the course of Mtb infection in mice [77-78]. However, a recent study in B cell deficient mice infected with Mtb showed increased recruitment of pulmonary neutrophils, exacerbated lung pathology, elevated production of IL-10, and uncontrolled bacterial growth [79]. Furthermore, lymphoid-like B cell aggregates were found in proximity to granulomas in mice and human, emphasizing the involvement of B cells in modulating the inflammatory response during TB infection [79-83].

$CD4^+$ T cells

MHC class II-restricted $CD4^+$ T cells are required to form TB granulomas and to produce IL-2, IL-12, IFN-γ, and TNF-α [84]. Patients with severe pulmonary TB showed higher percentage of $CD4^+$ T cells and increased ratios of $CD4^+/CD8^+$ in bronchoalveolar lavage fluid but not in peripheral blood [85]. $CD4^+$ T cells have been shown to be required for the resistance to Mtb infection in mice; especially IFN-γ and nitric oxide synthase 2 induced by $CD4^+$ T cells were critical in the early immunological response and granuloma formation [86]. Another example of the importance of $CD4^+$ T cells is that HIV/AIDS patients who have low $CD4^+$ counts are more susceptible to TB progression and TB is responsible for the major cause of death in TB/AIDS patients.

$CD8^+$ T cells

The development of most of $CD8^+$ T cells requires the recognition of antigenic peptides in the context of MHC class Ia molecule complexed with β_2-microglobulin (β_2m). Experiments using mice deficient in transporter associated with antigen processing (TAP), $CD8^+$ T cells, or MHC class Ia heavy chain showed that $CD8^+$ T cells are protective against TB [87-89]. $CD8^+$ T cells specific for Mtb antigens are able to produce IFN-γ and TNF-α [90]. IFN-γ plays a key role in protection to Mtb infection and in activation of macrophages to produce reactive nitrogen intermediates and to kill intracellular Mtb. In addition to cytokines, $CD8^+$ T cells are also equipped with a pore forming protein, perforin, in the cytotoxic granules, which lyses infected macrophages [91-93]. Perforin was shown to be critical in regulating TB in mice [94]. $CD8^+$ T cells also produce TNF-α, which is a key molecule for macrophage activation and granuloma formation and maintenance. In TB patients, the number of IFN-γ producing $CD8^+$ T cells is decreased whereas the number of IL-4 producing $CD8^+$ T

cells is increased [95]. Even though memory $CD8^+$ T cells were observed in the murine lungs infected with Mtb, the overall levels of $CD8^+$ T cells responding to the secondary Mtb infection were not high [96].

CD1-restricted T cells

The unconventional MHC Ib and CD1-restrcted T cells also play a role in Mtb infection. CD1 molecule is associated with β_2 on the cell surface and its heavy chain is composed of three domains that accommodate lipid tails of glycolipids [97-98]. There are five forms of CD1 in humans, CD1a, CD1b, CD1c, CD1d, and CD1e, and mice have CD1e. Mtb has a thick cell wall mainly composed of glycolipids, which are known to be presented to T cells by CD1 [99]. Free and monoglycosylated mycolic acids, lipoarabinomannan (LAM), phosphatidyl-*myo*-inositol mannosides (PIMs), and diacylated sulfoglycolipids are presented by CD1b or CD1d [100-102]. Moreover, the presentation of LAM by CD1b is shown to require saposin C (SapC), which transfers lipid antigens from the intralysosomal membranes to CD1b [103].

Tuberculous Granuloma

Mtb-containing aerosols expectorated from open cavitary TB granuloma are inhaled by a new host, and Mtb bacilli travel through the respiratory tract and are implanted mostly near the pleura. Mtb is mainly phagocytosed by the front line immune cells such as alveolar macrophages, neutrophils, and sometimes DC, but type II lung epithelial cells are also known to harbor Mtb [104-105]. One single Mtb bacillus is known to be sufficient for successful infection [106]. Infected macrophages are activated through toll-like receptor 2 (TLR2) and TLR4 and rapidly secrete pro- and anti-inflammatory cytokines such as TNF-α, IL-1β, IL-6, IL-10, and IL-12, and recruit macrophages, monocytes, neutrophils, B cells, NKT cells, $CD4^+$ T cells, and

$CD8^+$ T cells [107-110]. These cells secrete additional cytokines and chemokines to recruit more leukocytes to the site of infection [39-40, 82, 111]. This response leads to the establishment of an early granuloma. Mtb bacilli are also drained into the regional lymph nodes presumably by DC. Typically, in response to Mtb infection, a well-organized granuloma develops; infected macrophages are surrounded by epithelioid cells (activated macrophages, commonly seen in granulomatous response), foam cells, foreign-body giant cells, and Langhans giant cells (formed by the fusion of epithelioid cells), which become encircled by lymphocytes and fibroblasts that form a tight fibrous capsule (Figure 1.1). If the granuloma progresses, it undergoes caseation (Figure 1.1). This primary site of Mtb infection is called Ghon focus, and together with the inflamed regional lymph nodes is known as Ghon complex. Immunocompetent adults can control Mtb infection by forming a tightly structured granuloma or resolve the lesion completely, whereas infants, children, elders, immunocompromised individuals are more prone to the development of disseminated and extrapulmonary TB [112-113]. Typically, about 10% of Mtb-infected individuals develop active TB disease; primary TB starts in the lung and spreads hematogenously to the body, whereas secondary (or post-primary) TB develops in individuals who already have developed immunity against the primary infection. Primary TB shows subtle clinical symptoms, whereas secondary TB is accompanied by symptoms such as fever, anorexia, dyspnea, hemoptysis, empyema, bronchiectasis, night sweats, and weight loss. Secondary TB is also characterized by liquefaction of caseum and cavitation of granuloma.

Foamy Macrophages in Tuberculous Granuloma

The chronic inflammatory response to Mtb infection leads to the formation of a granuloma in which mononuclear phagocytes are predominant; macrophages,

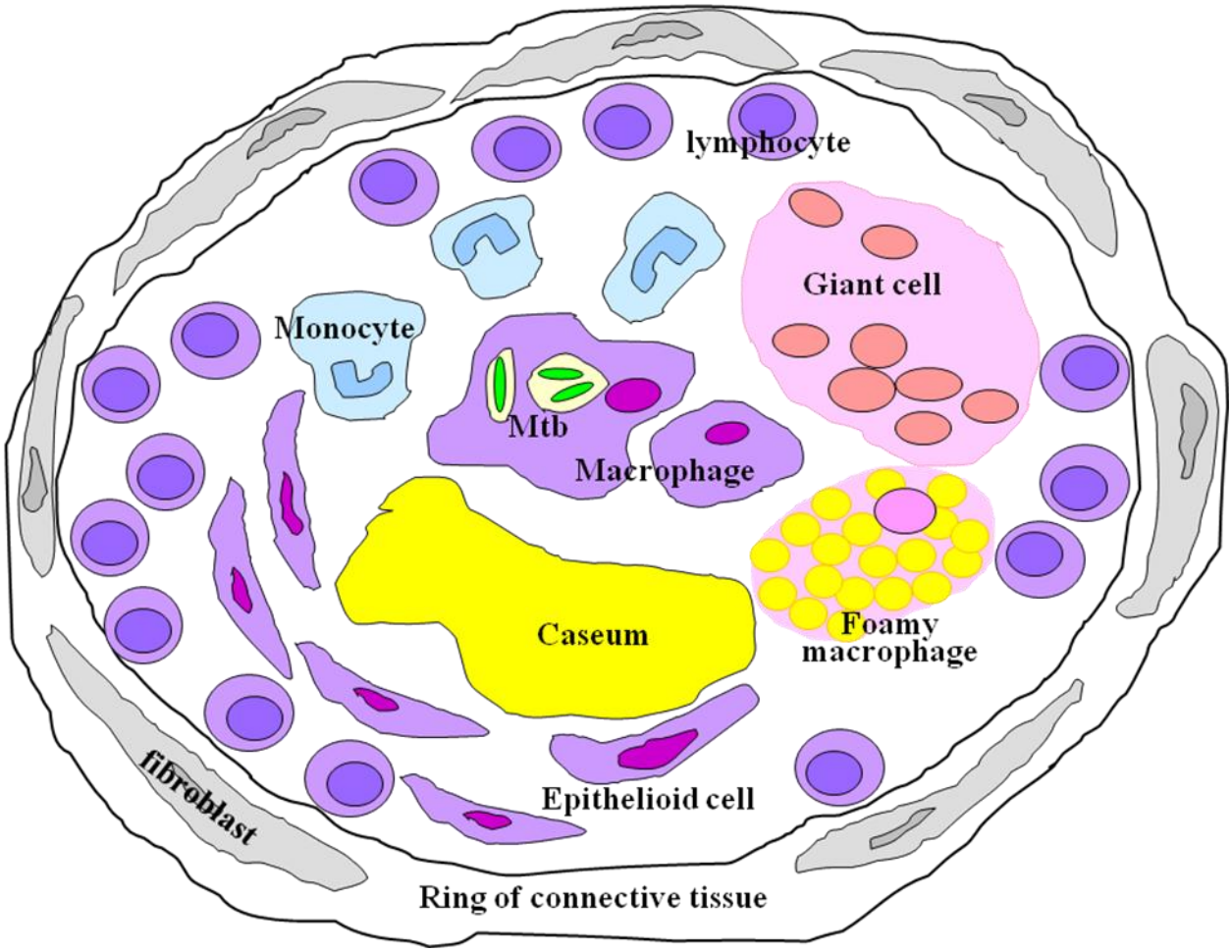

Figure 1.1 Human tuberculous granuloma
Mtb-infected macrophages are surrounded by various leukocytes including monocytes, lymphocytes, and macrophages. Multinucleated giant cells, lipid-filled foamy macrophages, and epithelioid cells are frequently seen in TB granulomas. The granuloma containing caseum is demarcated by a ring of fibrous capsule.

epithelioid cells, multinucleated giant cells, and foamy macrophages (foam cells). Adipocytes and steroidogenic cells are classical lipid droplets-containing cells, but all cell types including neutrophils and macrophages have the potential to develop lipid droplets under the condition of elevated fatty acid levels [114]. Unlike classical lipids-storing cells, leukocytes contain few lipid droplets under normal conditions; human neutrophils and eosinophils are known to contain 1 to 5 lipid droplets per cell, and the number increases dramatically in inflammatory response [115-116]. The number of lipid droplets in leukocytes increases in conditions such as atherosclerosis, obesity, sepsis, infectious diseases, and type II diabetes. Studies have shown that lipid droplet formation in leukocytes is highly regulated and this process is cell- and stimuli-dependent; unsaturated fatty acids induce lipid droplet formation in neutrophils, monocytes, eosinophils, and macrophages [117-118]; modified low density lipoprotein (e.g. acetylated-, oxidized-LDL), leptin, and CCL2 affect macrophages [119-122]; lipopolysaccharide and mycobacterial LAM stimulate neutrophils and macrophages [123-124]. Lipid droplets in leukocytes are also known to be major sites for eicosanoid (e.g. leukotriene C_4 and prostaglandin E_2) generation [120, 124-129], cytokine (e.g. TNF-α) storage [130], and compartmentalization of cell signaling molecules (e.g. mitogen-activated protein (MAP) kinases) [127].

Mycobacterial Cell Wall

Mtb has a unique cell wall structure [9, 131-132]. Studies have shown that Mtb is protected by a highly lipophilic barrier, consisting of lipids up to 60% of the dry weight of the bacillus [8, 133]. Mycolic acids are intercalated to arabinogalactan, which is linked to peptidoglycan connected with cell membrane (Figure 1.2) [131]. Phthiocerol dimycoserosates, phenolic glycolipids, trehalose-containing glycolipids, and sulfolipids are known to be arrayed freely in the outer membrane, and PIMs,

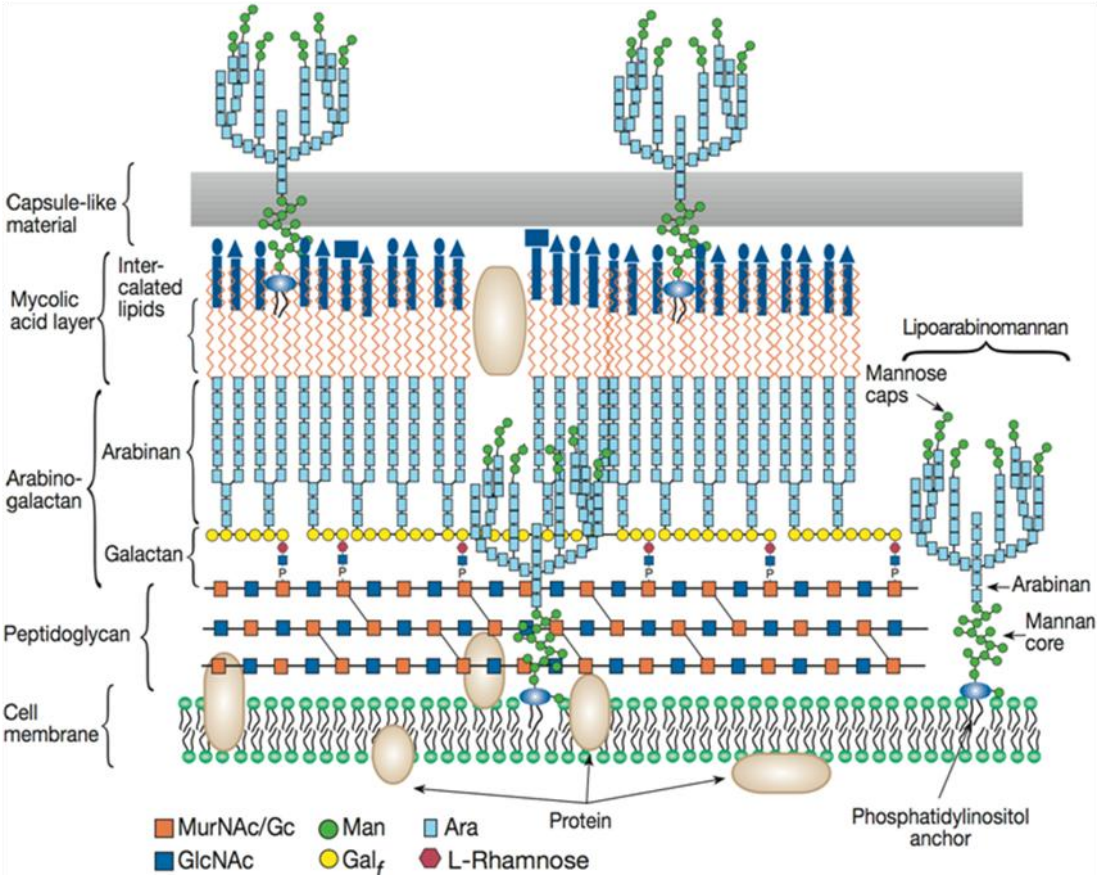

Figure 1.2 Structure of mycobacterial cell wall
Brennan PJ and Crick DC (2007) *Curr. Top. Med. Chem.* 7: 475–488

LAM, and lipomannan are anchored to the plasma membrane through phosphatidyl-*myo*-inositol anchor. Many of these lipids show potent biological activities and are considered virulence factors.

Mycolic acids (mycolates) from Mtb are long-chain high molecular weight α-alkyl β-hydroxy fatty acids consisting of a meromycolate moiety, with carbon chain lengths of up to C_{56} and a long saturated α-branch, C_{20} to C_{24}. Mycolates give rise to important characteristics of Mtb such as resistance to chemical injury, resistance to dehydration, low permeability to hydrophobic antibiotics, and the ability to persist within the host cells [134]. Mycolates are divided into α-mycolates and oxygenated mycolates; α-mycolates do not contain oxygen functionality and oxygenated mycolates include keto- and methoxymycolates containing *cis*- and *trans*-cyclopropane rings. Cyclopropanation of mycolates has been demonstrated to suppress Mtb-induced inflammation and virulence and to be essential for viability, drug resistance, and cell wall integrity of Mtb [135-136].

Trehalose-6,6'-dimycolates (TDM), also known as cord factor, is the most extensively studied mycolate. Even though TDM represents a small percentage of the total mycolates, this petroleum ether-extractable glycolipid is an extremely potent modulator of the proinflammatory response. Lung cells from mice treated with TDM were shown to secrete IL-4, IL-6, IL-10, and TNF-α, and bronchoalveolar lavage cells produced NO, and peritoneal macrophages treated with TDM *in vitro* also produced IL-6, IL-10, IL-12, IFN-γ, and TNF-α [137]. TDM also elicits the production of chemokines, monocytes chemoattractant protein 1 (MCP-1), macrophage inflammatory protein 1α (MIP-1α) [138-139]. The granulomatous response of TDM is also associated with the increased pro-coagulant activity and the decreased level of serum cortisol [140-146], and with the secretion of vascular endothelial growth factor (VEGF) from neutrophils and macrophages [147].

TDM exhibits toxicity in cells, disrupting mitochondrial respiratory chain and oxidative phosphorylation [148-149] and has been shown to have anti-tumor activity most likely via TNF-α, NO, and NK cells, hence clinicians have used TDM for treating cancers such as colon cancer, melanoma, small lung cancer, prostate cancer, and astrocytoma [150-151]. TDM also induces apoptosis, cytotoxicity, cachexia, and death in mice [152-154].

Models for Tuberculosis Research

The limited availability of human TB tissue samples poses an obstacle for detailed study of the disease. Mice, guinea pigs, rabbits, and nonhuman primates are commonly used as models of TB [111, 155-158]. Since TB transmission mainly occurs in secondary TB, guinea pigs which develop both primary and secondary TB lesions provide a unique system for the evaluation of vaccine and chemotherapeutic candidates [159]. Granulomas in rabbits liquefy and cavitate, resembling human TB granulomas [155, 160]. The major drawbacks of guinea pig and rabbit models are the high expense and the limitation of reagents. Monkey TB shows very similar lung pathology to human TB; caseation, liquefaction, cavitation, fibrosis, and calcification of granulomas [156]. However, the cost of monkeys in research is very high and bio-containment is another hurdle. Mice have been used for TB research most extensively, but they do not show similar pathologies and bacterial growth to human infection; absence of true latent infection, differences in granuloma structure, and lack of certain molecules including leukocyte defensins, TLR10 (pseudogene), CD1a, CD1b, CD1c, FcαRI, FcγRIIA, caspase 10, and intercellular adhesion molecule 3 (ICAM3) [157-158, 161-169]. Another attractive model is zebrafish, *Danio rerio*, which is a natural host for *M. marinum* infection [170-171]. There are several remarkable similarities between *M. marinum* and Mtb such as genetic makeup, cell

wall synthesis, granuloma formation, and secretion. Furthermore, the absence of acquired immunity in zebrafish embryos allows examining innate and acquired immunities separately in mycobacterial pathogenesis.

Murine Granuloma Model

Work done in Dr. David Russell's laboratory showed that mycobacterial cell wall lipids were trafficked out of mycobacteria-containing phagosomes and could be transferred to bystander cells [69, 172]. Further studies identified the released lipid species and determined the bioactivities of individual lipid by using a granuloma model developed by the Russell laboratory [173-175]. In this model, each lipid species is coated onto the surface of 90 μm-diameter polystyrene microspheres, mixed with syngeneic macrophages, suspended in growth factor-reduced Matrigel, and then injected into the peritoneal cavity of mice [175]. The injected macrophages phagocytose lipids off the microspheres and secrete cytokines and chemokines to initiate the immune response. Matrigel (BD) is a mixture of extracellular matrix proteins from Engelbreth-Holm-Swarm (EHS) mouse sarcoma cells, mimicking the complex extracellular environment of tissues. As Matrigel is solidified at body temperature, the mixture of Matrigel with mycobacterial lipids forms a mass that can be easily removed for analyzing cell recruitment, cytokine production, and histopathology. Our study has shown that TDM is the most inflammatory and granulomatous species among mycobacterial cell wall lipids [174]. In the current study (Chapter 6), the granuloma model is used with slight modifications; Matrigel mixture is prepared without syngeneic macrophages and injected subcutaneously.

Aims of this study

The purpose of the following work is to understand the biology of tuberculous granuloma. Chapter 2 presents data that delineate the transcriptional profiles of caseous human pulmonary TB granulomas. Three genes involved in lipid metabolism (*ADFP*, *ACSL1*, and *PSAP* (SapC)) were selected for further analysis. Chapter 3 examines the localization of ADFP, ACSL1, and SapC in human TB granulomas. Chapter 4 analyzes the lipid composition of the caseum from human TB granulomas. Chapter 5 investigates the macrophage response to *Mycobacterium tuberculosis* infection *in vitro*. By using the murine granuloma model, Chapter 6 explores the *in vivo* response to mycobacterial cell wall lipid, trehalose dimycolate, which is reminiscent of human TB.

REFERENCES

1. Koch, R., *Die Aetiologie der Tuberkulose.* Journal of Molecular Medicine, 1932. **11**(12): p. 490-492.
2. Smith, N.H., et al., *Ecotypes of the Mycobacterium tuberculosis complex.* J Theor Biol, 2006. **239**(2): p. 220-5.
3. Smith, N.H., et al., *Bottlenecks and broomsticks: the molecular evolution of Mycobacterium bovis.* Nat Rev Microbiol, 2006. **4**(9): p. 670-81.
4. Cole, S.T., et al., *Deciphering the biology of Mycobacterium tuberculosis from the complete genome sequence.* Nature, 1998. **393**(6685): p. 537-44.
5. Camus, J.C., et al., *Re-annotation of the genome sequence of Mycobacterium tuberculosis H37Rv.* Microbiology, 2002. **148**(Pt 10): p. 2967-73.
6. Rohde, K.H., R.B. Abramovitch, and D.G. Russell, *Mycobacterium tuberculosis invasion of macrophages: linking bacterial gene expression to environmental cues.* Cell Host Microbe, 2007. **2**(5): p. 352-64.
7. Cole, S.T., *Learning from the genome sequence of Mycobacterium tuberculosis H37Rv.* FEBS Lett, 1999. **452**(1-2): p. 7-10.
8. Daffe, M. and P. Draper, *The envelope layers of mycobacteria with reference to their pathogenicity.* Adv Microb Physiol, 1998. **39**: p. 131-203.
9. Brennan, P.J. and H. Nikaido, *The envelope of mycobacteria.* Annu Rev Biochem, 1995. **64**: p. 29-63.
10. Munoz-Elias, E.J., et al., *Replication dynamics of Mycobacterium tuberculosis in chronically infected mice.* Infect Immun, 2005. **73**(1): p. 546-51.
11. Gill, W.P., et al., *A replication clock for Mycobacterium tuberculosis.* Nat Med, 2009. **15**(2): p. 211-4.

12. Vashishtha, V.M., *WHO Global Tuberculosis Control Report 2009: Tuberculosis elimination is a distant dream.* Indian Pediatr, 2009. **46**(5): p. 401-2.
13. Corbett, E.L., et al., *The growing burden of tuberculosis: global trends and interactions with the HIV epidemic.* Arch Intern Med, 2003. **163**(9): p. 1009-21.
14. Lawn, S.D. and G. Churchyard, *Epidemiology of HIV-associated tuberculosis.* Curr Opin HIV AIDS, 2009. **4**(4): p. 325-33.
15. Vitoria, M., et al., *The global fight against HIV/AIDS, tuberculosis, and malaria: current status and future perspectives.* Am J Clin Pathol, 2009. **131**(6): p. 844-8.
16. WHO, *Global Tuberculosis Control: Surveillance, Planning, Financing.* . WHO/TB, 2003.
17. Dye, C., C.J. Watt, and D. Bleed, *Low access to a highly effective therapy: a challenge for international tuberculosis control.* Bull World Health Organ, 2002. **80**(6): p. 437-44.
18. Andersen, P. and T.M. Doherty, *The success and failure of BCG - implications for a novel tuberculosis vaccine.* Nat Rev Microbiol, 2005. **3**(8): p. 656-62.
19. Rodrigues, L.C., et al., *Effect of BCG revaccination on incidence of tuberculosis in school-aged children in Brazil: the BCG-REVAC cluster-randomised trial.* Lancet, 2005. **366**(9493): p. 1290-5.
20. Clark-Curtiss, J.E. and S.E. Haydel, *Molecular genetics of Mycobacterium tuberculosis pathogenesis.* Annu Rev Microbiol, 2003. **57**: p. 517-49.
21. Svenson, S., et al., *Towards new tuberculosis vaccines.* Hum Vaccin. **6**(4).
22. Daley, C.L., *Update in tuberculosis 2009.* Am J Respir Crit Care Med. **181**(6): p. 550-5.

23. Ibrahim, M., et al., *Sterilizing activity of R207910 (TMC207)-containing regimens in the murine model of tuberculosis.* Am J Respir Crit Care Med, 2009. **180**(6): p. 553-7.

24. Alcala, L., et al., *In vitro activities of linezolid against clinical isolates of Mycobacterium tuberculosis that are susceptible or resistant to first-line antituberculous drugs.* Antimicrob Agents Chemother, 2003. **47**(1): p. 416-7.

25. Williams, K.N., et al., *Promising antituberculosis activity of the oxazolidinone PNU-100480 relative to that of linezolid in a murine model.* Antimicrob Agents Chemother, 2009. **53**(4): p. 1314-9.

26. Williams, K.N., et al., *Addition of PNU-100480 to first-line drugs shortens the time needed to cure murine tuberculosis.* Am J Respir Crit Care Med, 2009. **180**(4): p. 371-6.

27. Nuermberger, E.L., et al., *Moxifloxacin-containing regimens of reduced duration produce a stable cure in murine tuberculosis.* Am J Respir Crit Care Med, 2004. **170**(10): p. 1131-4.

28. Nikonenko, B.V., et al., *Drug therapy of experimental tuberculosis (TB): improved outcome by combining SQ109, a new diamine antibiotic, with existing TB drugs.* Antimicrob Agents Chemother, 2007. **51**(4): p. 1563-5.

29. Barry, C.E., 3rd, H.I. Boshoff, and C.S. Dowd, *Prospects for clinical introduction of nitroimidazole antibiotics for the treatment of tuberculosis.* Curr Pharm Des, 2004. **10**(26): p. 3239-62.

30. Singh, R., et al., *PA-824 kills nonreplicating Mycobacterium tuberculosis by intracellular NO release.* Science, 2008. **322**(5906): p. 1392-5.

31. Pomerantz, B.J., et al., *Pulmonary resection for multi-drug resistant tuberculosis.* J Thorac Cardiovasc Surg, 2001. **121**(3): p. 448-53.

32. van Leuven, M., et al., *Pulmonary resection as an adjunct in the treatment of multiple drug-resistant tuberculosis.* Ann Thorac Surg, 1997. **63**(5): p. 1368-72; discussion 1372-3.

33. Cicenas, S. and V. Vencevicius, *Lung cancer in patients with tuberculosis.* World J Surg Oncol, 2007. **5**: p. 22.

34. Freixinet, J., *Surgical indications for treatment of pulmonary tuberculosis.* World J Surg, 1997. **21**(5): p. 475-9.

35. Perelman, M.I. and V.P. Strelzov, *Surgery for pulmonary tuberculosis.* World J Surg, 1997. **21**(5): p. 457-67.

36. Naidoo, R., *Surgery for pulmonary tuberculosis.* Curr Opin Pulm Med, 2008. **14**(3): p. 254-9.

37. Algood, H.M., et al., *TNF influences chemokine expression of macrophages in vitro and that of CD11b+ cells in vivo during Mycobacterium tuberculosis infection.* J Immunol, 2004. **172**(11): p. 6846-57.

38. Peters, W. and J.D. Ernst, *Mechanisms of cell recruitment in the immune response to Mycobacterium tuberculosis.* Microbes Infect, 2003. **5**(2): p. 151-8.

39. Flynn, J.L. and J. Chan, *What's good for the host is good for the bug.* Trends Microbiol, 2005. **13**(3): p. 98-102.

40. Algood, H.M., J. Chan, and J.L. Flynn, *Chemokines and tuberculosis.* Cytokine Growth Factor Rev, 2003. **14**(6): p. 467-77.

41. Gan, H., et al., *Enhancement of antimycobacterial activity of macrophages by stabilization of inner mitochondrial membrane potential.* J Infect Dis, 2005. **191**(8): p. 1292-300.

42. Semenzato, G., et al., *Immune mechanisms in interstitial lung diseases.* Allergy, 2000. **55**(12): p. 1103-20.

43. Flynn, J.L., et al., *Tumor necrosis factor-alpha is required in the protective immune response against Mycobacterium tuberculosis in mice.* Immunity, 1995. **2**(6): p. 561-72.

44. Ehlers, S., *Why does tumor necrosis factor targeted therapy reactivate tuberculosis?* J Rheumatol Suppl, 2005. **74**: p. 35-9.

45. Dheda, K., et al., *Lung remodeling in pulmonary tuberculosis.* J Infect Dis, 2005. **192**(7): p. 1201-9.

46. Price, N.M., et al., *Unopposed matrix metalloproteinase-9 expression in human tuberculous granuloma and the role of TNF-alpha-dependent monocyte networks.* J Immunol, 2003. **171**(10): p. 5579-86.

47. Quiding-Jarbrink, M., D.A. Smith, and G.J. Bancroft, *Production of matrix metalloproteinases in response to mycobacterial infection.* Infect Immun, 2001. **69**(9): p. 5661-70.

48. Flynn, J.L., et al., *An essential role for interferon gamma in resistance to Mycobacterium tuberculosis infection.* J Exp Med, 1993. **178**(6): p. 2249-54.

49. Cooper, A.M., et al., *Disseminated tuberculosis in interferon gamma gene-disrupted mice.* J Exp Med, 1993. **178**(6): p. 2243-7.

50. Mogues, T., et al., *The relative importance of T cell subsets in immunity and immunopathology of airborne Mycobacterium tuberculosis infection in mice.* J Exp Med, 2001. **193**(3): p. 271-80.

51. Kleinnijenhuis, J., et al., *Transcriptional and inflammasome-mediated pathways for the induction of IL-1beta production by Mycobacterium tuberculosis.* Eur J Immunol, 2009. **39**(7): p. 1914-22.

52. Fantuzzi, G. and C.A. Dinarello, *The inflammatory response in interleukin-1 beta-deficient mice: comparison with other cytokine-related knock-out mice.* J Leukoc Biol, 1996. **59**(4): p. 489-93.

53. Tsao, T.C., et al., *Increased TNF-alpha, IL-1 beta and IL-6 levels in the bronchoalveolar lavage fluid with the upregulation of their mRNA in macrophages lavaged from patients with active pulmonary tuberculosis.* Tuber Lung Dis, 1999. **79**(5): p. 279-85.

54. Kishimoto, T., et al., *Interleukin-6 family of cytokines and gp130.* Blood, 1995. **86**(4): p. 1243-54.

55. Yokoyama, A., et al., *Interleukin 6 activity in pleural effusion. Its diagnostic value and thrombopoietic activity.* Chest, 1992. **102**(4): p. 1055-9.

56. Law, K., et al., *Increased release of interleukin-1 beta, interleukin-6, and tumor necrosis factor-alpha by bronchoalveolar cells lavaged from involved sites in pulmonary tuberculosis.* Am J Respir Crit Care Med, 1996. **153**(2): p. 799-804.

57. Xirouchaki, N., et al., *Diagnostic value of interleukin-1alpha, interleukin-6, and tumor necrosis factor in pleural effusions.* Chest, 2002. **121**(3): p. 815-20.

58. Mazzarella, G., et al., *T lymphocyte phenotypic profile in lung segments affected by cavitary and non-cavitary tuberculosis.* Clin Exp Immunol, 2003. **132**(2): p. 283-8.

59. Geijtenbeek, T.B., et al., *Mycobacteria target DC-SIGN to suppress dendritic cell function.* J Exp Med, 2003. **197**(1): p. 7-17.

60. Tailleux, L., et al., *DC-SIGN is the major Mycobacterium tuberculosis receptor on human dendritic cells.* J Exp Med, 2003. **197**(1): p. 121-7.

61. Ehlers, S., *DC-SIGN and mannosylated surface structures of Mycobacterium tuberculosis: a deceptive liaison.* Eur J Cell Biol, 2010. **89**(1): p. 95-101.

62. Vannberg, F.O., et al., *CD209 genetic polymorphism and tuberculosis disease.* PLoS One, 2008. **3**(1): p. e1388.

63. Schaefer, M., et al., *Decreased pathology and prolonged survival of human DC-SIGN transgenic mice during mycobacterial infection.* J Immunol, 2008. **180**(10): p. 6836-45.

64. Gordon, S., *The macrophage: past, present and future.* Eur J Immunol, 2007. **37 Suppl 1**: p. S9-17.

65. Ehlers, M.R. and M. Daffe, *Interactions between Mycobacterium tuberculosis and host cells: are mycobacterial sugars the key?* Trends Microbiol, 1998. **6**(8): p. 328-35.

66. Armstrong, J.A. and P.D. Hart, *Response of cultured macrophages to Mycobacterium tuberculosis, with observations on fusion of lysosomes with phagosomes.* J Exp Med, 1971. **134**(3 Pt 1): p. 713-40.

67. Fratti, R.A., et al., *Role of phosphatidylinositol 3-kinase and Rab5 effectors in phagosomal biogenesis and mycobacterial phagosome maturation arrest.* J Cell Biol, 2001. **154**(3): p. 631-44.

68. Fratti, R.A., et al., *Mycobacterium tuberculosis glycosylated phosphatidylinositol causes phagosome maturation arrest.* Proc Natl Acad Sci U S A, 2003. **100**(9): p. 5437-42.

69. Beatty, W.L., et al., *Trafficking and release of mycobacterial lipids from infected macrophages.* Traffic, 2000. **1**(3): p. 235-47.

70. Vergne, I., et al., *Mechanism of phagolysosome biogenesis block by viable Mycobacterium tuberculosis.* Proc Natl Acad Sci U S A, 2005. **102**(11): p. 4033-8.

71. Sturgill-Koszycki, S., et al., *Lack of acidification in Mycobacterium phagosomes produced by exclusion of the vesicular proton-ATPase.* Science, 1994. **263**(5147): p. 678-81.

72. De Voss, J.J., et al., *Iron acquisition and metabolism by mycobacteria.* J Bacteriol, 1999. **181**(15): p. 4443-51.

73. Bellamy, R., et al., *Variations in the NRAMP1 gene and susceptibility to tuberculosis in West Africans.* N Engl J Med, 1998. **338**(10): p. 640-4.

74. Cooper, A.M., et al., *Transient loss of resistance to pulmonary tuberculosis in p47(phox-/-) mice.* Infect Immun, 2000. **68**(3): p. 1231-4.

75. Darwin, K.H., et al., *The proteasome of Mycobacterium tuberculosis is required for resistance to nitric oxide.* Science, 2003. **302**(5652): p. 1963-6.

76. Stenger, S., K.R. Niazi, and R.L. Modlin, *Down-regulation of CD1 on antigen-presenting cells by infection with Mycobacterium tuberculosis.* J Immunol, 1998. **161**(7): p. 3582-8.

77. Johnson, C.M., et al., *Mycobacterium tuberculosis aerogenic rechallenge infections in B cell-deficient mice.* Tuber Lung Dis, 1997. **78**(5-6): p. 257-61.

78. Turner, J., et al., *The progression of chronic tuberculosis in the mouse does not require the participation of B lymphocytes or interleukin-4.* Exp Gerontol, 2001. **36**(3): p. 537-45.

79. Maglione, P.J., J. Xu, and J. Chan, *B cells moderate inflammatory progression and enhance bacterial containment upon pulmonary challenge with Mycobacterium tuberculosis.* J Immunol, 2007. **178**(11): p. 7222-34.

80. Maglione, P.J. and J. Chan, *How B cells shape the immune response against Mycobacterium tuberculosis.* Eur J Immunol, 2009. **39**(3): p. 676-86.

81. Ulrichs, T., et al., *Human tuberculous granulomas induce peripheral lymphoid follicle-like structures to orchestrate local host defence in the lung.* J Pathol, 2004. **204**(2): p. 217-28.

82. Tsai, M.C., et al., *Characterization of the tuberculous granuloma in murine and human lungs: cellular composition and relative tissue oxygen tension.* Cell Microbiol, 2006. **8**(2): p. 218-32.

83. Bosio, C.M., D. Gardner, and K.L. Elkins, *Infection of B cell-deficient mice with CDC 1551, a clinical isolate of Mycobacterium tuberculosis: delay in dissemination and development of lung pathology.* J Immunol, 2000. **164**(12): p. 6417-25.

84. Hansch, H.C., et al., *Mechanisms of granuloma formation in murine Mycobacterium avium infection: the contribution of CD4+ T cells.* Int Immunol, 1996. **8**(8): p. 1299-310.

85. Tsao, T.C., et al., *Shifts of T4/T8 T lymphocytes from BAL fluid and peripheral blood by clinical grade in patients with pulmonary tuberculosis.* Chest, 2002. **122**(4): p. 1285-91.

86. Caruso, A.M., et al., *Mice deficient in CD4 T cells have only transiently diminished levels of IFN-gamma, yet succumb to tuberculosis.* J Immunol, 1999. **162**(9): p. 5407-16.

87. Behar, S.M., et al., *Susceptibility of mice deficient in CD1D or TAP1 to infection with Mycobacterium tuberculosis.* J Exp Med, 1999. **189**(12): p. 1973-80.

88. Rolph, M.S., et al., *MHC class Ia-restricted T cells partially account for beta2-microglobulin-dependent resistance to Mycobacterium tuberculosis.* Eur J Immunol, 2001. **31**(6): p. 1944-9.

89. Sousa, A.O., et al., *Relative contributions of distinct MHC class I-dependent cell populations in protection to tuberculosis infection in mice.* Proc Natl Acad Sci U S A, 2000. **97**(8): p. 4204-8.

90. Serbina, N.V. and J.L. Flynn, *Early emergence of CD8(+) T cells primed for production of type 1 cytokines in the lungs of Mycobacterium tuberculosis-infected mice.* Infect Immun, 1999. **67**(8): p. 3980-8.

91. Cho, S., et al., *Antimicrobial activity of MHC class I-restricted CD8+ T cells in human tuberculosis.* Proc Natl Acad Sci U S A, 2000. **97**(22): p. 12210-5.

92. De Libero, G., I. Flesch, and S.H. Kaufmann, *Mycobacteria-reactive Lyt-2+ T cell lines.* Eur J Immunol, 1988. **18**(1): p. 59-66.

93. Serbina, N.V., et al., *CD8+ CTL from lungs of Mycobacterium tuberculosis-infected mice express perforin in vivo and lyse infected macrophages.* J Immunol, 2000. **165**(1): p. 353-63.

94. Woodworth, J.S., Y. Wu, and S.M. Behar, *Mycobacterium tuberculosis-specific CD8+ T cells require perforin to kill target cells and provide protection in vivo.* J Immunol, 2008. **181**(12): p. 8595-603.

95. Smith, S.M., et al., *Decreased IFN- gamma and increased IL-4 production by human CD8(+) T cells in response to Mycobacterium tuberculosis in tuberculosis patients.* Tuberculosis (Edinb), 2002. **82**(1): p. 7-13.

96. Serbina, N.V. and J.L. Flynn, *CD8(+) T cells participate in the memory immune response to Mycobacterium tuberculosis.* Infect Immun, 2001. **69**(7): p. 4320-8.

97. Joyce, S. and L. Van Kaer, *CD1-restricted antigen presentation: an oily matter.* Curr Opin Immunol, 2003. **15**(1): p. 95-104.

98. Schaible, U.E., et al., *Apoptosis facilitates antigen presentation to T lymphocytes through MHC-I and CD1 in tuberculosis.* Nat Med, 2003. **9**(8): p. 1039-46.

99. Szalay, G., et al., *Participation of group 2 CD1 molecules in the control of murine tuberculosis.* Microbes Infect, 1999. **1**(14): p. 1153-7.

100. Bricard, G. and S.A. Porcelli, *Antigen presentation by CD1 molecules and the generation of lipid-specific T cell immunity.* Cell Mol Life Sci, 2007. **64**(14): p. 1824-40.

101. Layre, E., et al., *Mycolic acids constitute a scaffold for mycobacterial lipid antigens stimulating CD1-restricted T cells.* Chem Biol, 2009. **16**(1): p. 82-92.

102. Fischer, K., et al., *Mycobacterial phosphatidylinositol mannoside is a natural antigen for CD1d-restricted T cells.* Proc Natl Acad Sci U S A, 2004. **101**(29): p. 10685-90.

103. Winau, F., et al., *Saposin C is required for lipid presentation by human CD1b.* Nat Immunol, 2004. **5**(2): p. 169-74.

104. Bermudez, L.E. and J. Goodman, *Mycobacterium tuberculosis invades and replicates within type II alveolar cells.* Infect Immun, 1996. **64**(4): p. 1400-6.

105. Mehta, P.K., et al., *Comparison of in vitro models for the study of Mycobacterium tuberculosis invasion and intracellular replication.* Infect Immun, 1996. **64**(7): p. 2673-9.

106. Balasubramanian, V., et al., *Pathogenesis of tuberculosis: pathway to apical localization.* Tuber Lung Dis, 1994. **75**(3): p. 168-78.

107. Means, T.K., et al., *Human toll-like receptors mediate cellular activation by Mycobacterium tuberculosis.* J Immunol, 1999. **163**(7): p. 3920-7.

108. Brightbill, H.D., et al., *Host defense mechanisms triggered by microbial lipoproteins through toll-like receptors.* Science, 1999. **285**(5428): p. 732-6.

109. Korbel, D.S., B.E. Schneider, and U.E. Schaible, *Innate immunity in tuberculosis: myths and truth.* Microbes Infect, 2008. **10**(9): p. 995-1004.

110. Berrington, W.R. and T.R. Hawn, *Mycobacterium tuberculosis, macrophages, and the innate immune response: does common variation matter?* Immunol Rev, 2007. **219**: p. 167-86.

111. Rhoades, E.R., A.A. Frank, and I.M. Orme, *Progression of chronic pulmonary tuberculosis in mice aerogenically infected with virulent Mycobacterium tuberculosis.* Tuber Lung Dis, 1997. **78**(1): p. 57-66.

112. Farer, L.S., A.M. Lowell, and M.P. Meador, *Extrapulmonary tuberculosis in the United States.* Am J Epidemiol, 1979. **109**(2): p. 205-17.

113. Kim, J.H., A.A. Langston, and H.A. Gallis, *Miliary tuberculosis: epidemiology, clinical manifestations, diagnosis, and outcome.* Rev Infect Dis, 1990. **12**(4): p. 583-90.

114. Martin, S. and R.G. Parton, *Caveolin, cholesterol, and lipid bodies.* Semin Cell Dev Biol, 2005. **16**(2): p. 163-74.

115. Weller, P.F. and A.M. Dvorak, *Arachidonic acid incorporation by cytoplasmic lipid bodies of human eosinophils.* Blood, 1985. **65**(5): p. 1269-74.

116. Weller, P.F., et al., *Cytoplasmic lipid bodies of human neutrophilic leukocytes.* Am J Pathol, 1989. **135**(5): p. 947-59.

117. Bozza, P.T., et al., *Leukocyte lipid body formation and eicosanoid generation: cyclooxygenase-independent inhibition by aspirin.* Proc Natl Acad Sci U S A, 1996. **93**(20): p. 11091-6.

118. Weller, P.F., et al., *Cytoplasmic lipid bodies of neutrophils: formation induced by cis-unsaturated fatty acids and mediated by protein kinase C.* J Cell Biol, 1991. **113**(1): p. 137-46.

119. McGookey, D.J. and R.G. Anderson, *Morphological characterization of the cholesteryl ester cycle in cultured mouse macrophage foam cells.* J Cell Biol, 1983. **97**(4): p. 1156-68.

120. Pacheco, P., et al., *Monocyte chemoattractant protein-1/CC chemokine ligand 2 controls microtubule-driven biogenesis and leukotriene B4-synthesizing*

function of macrophage lipid bodies elicited by innate immune response. J Immunol, 2007. **179**(12): p. 8500-8.

121. de Assis, E.F., et al., *Synergism between platelet-activating factor-like phospholipids and peroxisome proliferator-activated receptor gamma agonists generated during low density lipoprotein oxidation that induces lipid body formation in leukocytes.* J Immunol, 2003. **171**(4): p. 2090-8.
122. Maya-Monteiro, C.M., et al., *Leptin induces macrophage lipid body formation by a phosphatidylinositol 3-kinase- and mammalian target of rapamycin-dependent mechanism.* J Biol Chem, 2008. **283**(4): p. 2203-10.
123. Pacheco, P., et al., *Lipopolysaccharide-induced leukocyte lipid body formation in vivo: innate immunity elicited intracellular Loci involved in eicosanoid metabolism.* J Immunol, 2002. **169**(11): p. 6498-506.
124. D'Avila, H., et al., *Mycobacterium bovis bacillus Calmette-Guerin induces TLR2-mediated formation of lipid bodies: intracellular domains for eicosanoid synthesis in vivo.* J Immunol, 2006. **176**(5): p. 3087-97.
125. Triggiani, M., et al., *Migration of human inflammatory cells into the lung results in the remodeling of arachidonic acid into a triglyceride pool.* J Exp Med, 1995. **182**(5): p. 1181-90.
126. Vieira-de-Abreu, A., et al., *Allergic challenge-elicited lipid bodies compartmentalize in vivo leukotriene C4 synthesis within eosinophils.* Am J Respir Cell Mol Biol, 2005. **33**(3): p. 254-61.
127. Yu, W., et al., *Co-compartmentalization of MAP kinases and cytosolic phospholipase A2 at cytoplasmic arachidonate-rich lipid bodies.* Am J Pathol, 1998. **152**(3): p. 759-69.
128. Bandeira-Melo, C., M. Phoofolo, and P.F. Weller, *Extranuclear lipid bodies, elicited by CCR3-mediated signaling pathways, are the sites of chemokine-*

enhanced leukotriene C4 production in eosinophils and basophils. J Biol Chem, 2001. **276**(25): p. 22779-87.

129. Weller, P.F., et al., *Cytoplasmic lipid bodies of human eosinophils. Subcellular isolation and analysis of arachidonate incorporation.* Am J Pathol, 1991. **138**(1): p. 141-8.

130. Beil, W.J., et al., *Ultrastructural immunogold localization of subcellular sites of TNF-alpha in colonic Crohn's disease.* J Leukoc Biol, 1995. **58**(3): p. 284-98.

131. Brennan, P.J. and D.C. Crick, *The cell-wall core of Mycobacterium tuberculosis in the context of drug discovery.* Curr Top Med Chem, 2007. **7**(5): p. 475-88.

132. Camacho, L.R., et al., *Analysis of the phthiocerol dimycocerosate locus of Mycobacterium tuberculosis. Evidence that this lipid is involved in the cell wall permeability barrier.* J Biol Chem, 2001. **276**(23): p. 19845-54.

133. Minnikin, D.E., *Lipids: complex lipids, their chemistry, biosynthesis and roles*. In C. Ratledge and J. Stanford ed. The Biology of Mycobacteria. 1982, London, United Kingdom: Academic Press, Ltd.

134. Yuan, Y., et al., *MMAS-1, the branch point between cis- and trans-cyclopropane-containing oxygenated mycolates in Mycobacterium tuberculosis.* J Biol Chem, 1997. **272**(15): p. 10041-9.

135. Barkan, D., et al., *Mycolic acid cyclopropanation is essential for viability, drug resistance, and cell wall integrity of Mycobacterium tuberculosis.* Chem Biol, 2009. **16**(5): p. 499-509.

136. Rao, V., et al., *Trans-cyclopropanation of mycolic acids on trehalose dimycolate suppresses Mycobacterium tuberculosis -induced inflammation and virulence.* J Clin Invest, 2006. **116**(6): p. 1660-7.

137. Lima, V.M., et al., *Role of trehalose dimycolate in recruitment of cells and modulation of production of cytokines and NO in tuberculosis.* Infect Immun, 2001. **69**(9): p. 5305-12.

138. Yamagami, H., et al., *Trehalose 6,6'-dimycolate (cord factor) of Mycobacterium tuberculosis induces foreign-body- and hypersensitivity-type granulomas in mice.* Infect Immun, 2001. **69**(2): p. 810-5.

139. Indrigo, J., R.L. Hunter, Jr., and J.K. Actor, *Influence of trehalose 6,6'-dimycolate (TDM) during mycobacterial infection of bone marrow macrophages.* Microbiology, 2002. **148**(Pt 7): p. 1991-8.

140. Hamasaki, N., et al., *In vivo administration of mycobacterial cord factor (Trehalose 6, 6'-dimycolate) can induce lung and liver granulomas and thymic atrophy in rabbits.* Infect Immun, 2000. **68**(6): p. 3704-9.

141. Bekierkunst, A., *Acute granulomatous response produced in mice by trehalose-6,6-dimycolate.* J Bacteriol, 1968. **96**(4): p. 958-61.

142. Bekierkunst, A., et al., *Granuloma formation induced in mice by chemically defined mycobacterial fractions.* J Bacteriol, 1969. **100**(1): p. 95-102.

143. Behling, C.A., et al., *Induction of pulmonary granulomas, macrophage procoagulant activity, and tumor necrosis factor-alpha by trehalose glycolipids.* Ann Clin Lab Sci, 1993. **23**(4): p. 256-66.

144. Perez, R.L., et al., *Cytokine message and protein expression during lung granuloma formation and resolution induced by the mycobacterial cord factor trehalose-6,6'-dimycolate.* J Interferon Cytokine Res, 2000. **20**(9): p. 795-804.

145. Perez, R.L., et al., *Extravascular coagulation and fibrinolysis in murine lung inflammation induced by the mycobacterial cord factor trehalose-6,6'-dimycolate.* Am J Respir Crit Care Med, 1994. **149**(2 Pt 1): p. 510-8.

146. Actor, J.K., et al., *Mycobacterial glycolipid cord factor trehalose 6,6'-dimycolate causes a decrease in serum cortisol during the granulomatous response.* Neuroimmunomodulation, 2002. **10**(5): p. 270-82.

147. Sakaguchi, I., et al., *Trehalose 6,6'-dimycolate (Cord factor) enhances neovascularization through vascular endothelial growth factor production by neutrophils and macrophages.* Infect Immun, 2000. **68**(4): p. 2043-52.

148. Kato, M., *Site II-specific inhibition of mitochondria oxidative phosphorylation by trehalose-6,6'-dimycolate (cord factor) of Mycobacterium tuberculosis.* Arch Biochem Biophys, 1970. **140**(2): p. 379-90.

149. Woodbury, J.L. and W.W. Barrow, *Radiolabelling of Mycobacterium avium oligosaccharide determinant and use in macrophage studies.* J Gen Microbiol, 1989. **135**(7): p. 1875-84.

150. Bekierkunst, A., I.S. Levij, and E. Yarkoni, *Suppression of urethan-induced lung adenomas in mice treated with trehalose-6,6-dimycolate (cord factor) and living bacillus Calmette Guerin.* Science, 1971. **174**(15): p. 1240-2.

151. Ryll, R., Y. Kumazawa, and I. Yano, *Immunological properties of trehalose dimycolate (cord factor) and other mycolic acid-containing glycolipids--a review.* Microbiol Immunol, 2001. **45**(12): p. 801-11.

152. Bekierkunst, A. and L.J. Berry, *Cytotoxic Effect of Mycobacteria on Ehrlich Ascites Cells.* J Bacteriol, 1965. **89**: p. 205-11.

153. Ozeki, Y., et al., *In vivo induction of apoptosis in the thymus by administration of mycobacterial cord factor (trehalose 6,6'-dimycolate).* Infect Immun, 1997. **65**(5): p. 1793-9.

154. Bloch, H., *Studies on the virulence of tubercle bacilli; isolation and biological properties of a constituent of virulent organisms.* J Exp Med, 1950. **91**(2): p. 197-218, pl.

155. Dannenberg, A.M., Jr. and F.M. Collins, *Progressive pulmonary tuberculosis is not due to increasing numbers of viable bacilli in rabbits, mice and guinea pigs, but is due to a continuous host response to mycobacterial products.* Tuberculosis (Edinb), 2001. **81**(3): p. 229-42.

156. Capuano, S.V., 3rd, et al., *Experimental Mycobacterium tuberculosis infection of cynomolgus macaques closely resembles the various manifestations of human M. tuberculosis infection.* Infect Immun, 2003. **71**(10): p. 5831-44.

157. Nuermberger, E., *Using animal models to develop new treatments for tuberculosis.* Semin Respir Crit Care Med, 2008. **29**(5): p. 542-51.

158. Basaraba, R.J., *Experimental tuberculosis: the role of comparative pathology in the discovery of improved tuberculosis treatment strategies.* Tuberculosis (Edinb), 2008. **88 Suppl 1**: p. S35-47.

159. McMurray, D.N., *Hematogenous reseeding of the lung in low-dose, aerosol-infected guinea pigs: unique features of the host-pathogen interface in secondary tubercles.* Tuberculosis (Edinb), 2003. **83**(1-3): p. 131-4.

160. Dannenberg, A.M., Jr. and M. Sugimoto, *Liquefaction of caseous foci in tuberculosis.* Am Rev Respir Dis, 1976. **113**(3): p. 257-9.

161. Geijtenbeek, T.B., et al., *Identification of DC-SIGN, a novel dendritic cell-specific ICAM-3 receptor that supports primary immune responses.* Cell, 2000. **100**(5): p. 575-85.

162. Mestas, J. and C.C. Hughes, *Of mice and not men: differences between mouse and human immunology.* J Immunol, 2004. **172**(5): p. 2731-8.

163. Risso, A., *Leukocyte antimicrobial peptides: multifunctional effector molecules of innate immunity.* J Leukoc Biol, 2000. **68**(6): p. 785-92.

164. Monteiro, R.C. and J.G. Van De Winkel, *IgA Fc receptors.* Annu Rev Immunol, 2003. **21**: p. 177-204.

165. Daeron, M., *Fc receptor biology.* Annu Rev Immunol, 1997. **15**: p. 203-34.

166. Dutronc, Y. and S.A. Porcelli, *The CD1 family and T cell recognition of lipid antigens.* Tissue Antigens, 2002. **60**(5): p. 337-53.

167. Farrar, J.D., et al., *Selective loss of type I interferon-induced STAT4 activation caused by a minisatellite insertion in mouse Stat2.* Nat Immunol, 2000. **1**(1): p. 65-9.

168. Crocker, P.R., et al., *Species heterogeneity in macrophage expression of the CD4 antigen.* J Exp Med, 1987. **166**(2): p. 613-8.

169. van Kooyk, Y. and T.B. Geijtenbeek, *A novel adhesion pathway that regulates dendritic cell trafficking and T cell interactions.* Immunol Rev, 2002. **186**: p. 47-56.

170. Tobin, D.M. and L. Ramakrishnan, *Comparative pathogenesis of Mycobacterium marinum and Mycobacterium tuberculosis.* Cell Microbiol, 2008. **10**(5): p. 1027-39.

171. Stamm, L.M. and E.J. Brown, *Mycobacterium marinum: the generalization and specialization of a pathogenic mycobacterium.* Microbes Infect, 2004. **6**(15): p. 1418-28.

172. Beatty, W.L. and D.G. Russell, *Identification of mycobacterial surface proteins released into subcellular compartments of infected macrophages.* Infect Immun, 2000. **68**(12): p. 6997-7002.

173. Rhoades, E., et al., *Identification and macrophage-activating activity of glycolipids released from intracellular Mycobacterium bovis BCG.* Mol Microbiol, 2003. **48**(4): p. 875-88.

174. Geisel, R.E., et al., *In vivo activity of released cell wall lipids of Mycobacterium bovis bacillus Calmette-Guerin is due principally to trehalose mycolates.* J Immunol, 2005. **174**(8): p. 5007-15.

175. Rhoades, E.R., et al., *Cell wall lipids from Mycobacterium bovis BCG are inflammatory when inoculated within a gel matrix: characterization of a new model of the granulomatous response to mycobacterial components.* Tuberculosis (Edinb), 2005. **85**(3): p. 159-76.

CHAPTER TWO

TRANSCRIPTIONAL PROFILING OF HUMAN PULMONARY TUBERCULOUS GRANULOMAS

ABSTRACT

The macrophages infected with *Mycobacterium tuberculosis* (Mtb) secrete various cytokines and chemokines that recruit other leukocytes to the site of infection. This leads to the formation of tuberculous (TB) granulomas, a hallmark of TB, at the local foci. Surrounded by immunological cells and their effectors, Mtb cannot easily escape the well-stratified granuloma. Immunocompetent people infected with Mtb can maintain this granuloma structure, thereby controlling the infection. However, in immunecompromised people, the center of TB granuloma caseates extensively, liquefies, and erodes into the airway space, transmitting numerous Mtb bacilli to new hosts. The mechanism for the development of dormant TB granulomas into active lesions is not well-understood yet. In this study, we demonstrate genome-wide transcriptional profiles of caseous human pulmonary TB granulomas compared to human normal lung tissues, by using laser capture microdissection (LCM) to select TB granulomas only, excluding uninvolved areas. This technique is also applied to select for normal lung parenchyma. The amplified messenger RNAs from dissected segments are used for genome-wide microarray. This is the first description of transcriptional profiles for human pulmonary TB granulomas and provides invaluable tools for further investigation of TB pathogenesis.

INTRODUCION

Granulomatous diseases occurring in the lung can be divided into caseating, non-caseating, and the diseases are categorized into infectious or non-infectious. Infectious ones include tuberculosis (TB), histoplasmosis, cryptococcosis, and blastomycosis, whereas sarcoidosis, berylliosis, Wegener's granulomatosis, Churg-Strauss disease, and aspiration pneumonia belong to non-infectious granulomatous diseases [1]. The term caseation derives from the gross cheesy appearance of TB granuloma. *Mycobacterium tuberculosis* (Mtb) infection results in the formation of TB granuloma, a collection of immune cells. Most immunocompetent people confine the infectious bacilli inside the TB granulomas or completely resolve the infection foci. However, some TB granulomas develop a caseating center, caseation, or caseum. The caseum of TB granuloma may liquefy and cavitate. At this stage, it is believed that Mtb bacilli multiply exponentially and are released into the open airways via the cavitated granulomas. The formation of caseum in TB granuloma is histologically manifest in TB patients with an active disease; however, it is still unclear how TB granulomas acquire a caseous center and ultimately liquefy and cavitate at the late stage of the disease. Despite the importance of TB granulomas in TB pathogenesis, gene regulation of human TB granulomas is not well-characterized.

In the past years, microarray analysis has been employed in many research areas to understand gene regulation [2]. There are a few reports of gene expression profiles from bronchial alveolar lavage fluid (BALF) samples, peripheral blood mononuclear cells (PBMCs) or human cell lines in response to Mtb infection, using real-time quantitative RT-PCR and/or microarray for a subset of genes [3-6]. Although these previous studies provide us valuable information, we feel that the characterization of global gene expression will provide an indispensable understanding of TB pathogenesis.

In this study, we examined the transcriptional profiles of caseous human pulmonary TB granulomas. Since the granuloma is an isolated structure, it is prudent to analyze the granulomas only, thereby excluding uninvolved lung tissues. Chan and colleagues [7] performed laser capture microdissection (LCM) on murine pulmonary TB granulomas and compared gene expression from LCM samples with that from whole lung tissues by real-time quantitative RT-PCR. Their data demonstrated that the true gene expression profile of affected lung lesions was diluted by introducing unaffected lung parts to the analysis; therefore LCM technique is useful to procure more homogeneous populations of cells from defined regions of tissues for examining the transcriptional profiles [7-8]. The successful microarray analyses on human pulmonary TB granulomas are presented here.

MATERIALS and METHODS

Human Subjects

Human subjects were included in this study according to protocols approved by Institutional Review Boards at University of Cape Town, South Africa, the Public Health Research Institute, Newark, NJ, and Cornell University, Ithaca, NY. Informed consent was obtained from all of patients.

Tissue specimens

We have obtained human TB lung tissue specimens which were surgically excised when TB patients had extensive lung cavitation and tissue degeneration, with no response to the antibiotics. The TB patients in our study did not have human immunodeficiency virus (HIV) infection or acquired immune deficiency syndrome (AIDS) at the time of surgery. Snap-frozen tissues were transported from Groote Schuur Hospital of Cape Town to PHRI, and then transferred to our biosafety level-3

(BL3) laboratory. Frozen samples were embedded in O.C.T. compound (Tissue-Tek®), cut into 10 µm-thick sections at −25°C on a Cryocut 1800 cryostat (Leica Microsystems) and attached onto PET-membrane frame slides (Leica Microsystems) for laser capture microdissection or Superfrost Plus Micro slides (Erie Scientific) for histological examination.

Histological examination

Cryosections are fixed in 1% paraformaldehyde in PBS for 40 min, which has been proven to kill Mtb. After washing in water, sections are stained with hematoxylin and eosin, dehydrated, cleared, and mounted with Permount® (Fisher Scientific). Areas of interest were microscopically matched to the unstained sections on the PET-membrane frame slides for LCM.

Laser Capture Microdissection

Tissue sections mounted onto PET-membrane slides were fixed in graded ethanol (70%, 75%, 96%, and 100%) containing 0.5% sodium azide for 30 sec per each step. Slides were air dried briefly and stored at −80°C until further processing. Areas of interest were dissected by using Leica AS LMD system (Leica Microsystems), and the dissected samples were collected in RNase free 0.5 ml tubes (Eppendorf) by gravity and placed on dry ice until processing.

RNA Isolation from LCM samples

Successful RNA isolation from LCM samples has been documented in multiple publications [7-12]. Using the PicoPure™ RNA Isolation Kit (Arcturus), total RNA is extracted from LCM-derived materials by incubating in extraction buffer at 42°C for 30 min. Subsequently, RNA is isolated following the manufacturer protocol, coupled

with DNase treatment using TURBO DNA-free™ (Ambion). Purity, quality, and quantity of RNA are assessed by the Agilent NanoChip Bioanalyzer assay, spectrophotometer, and reverse-transcription PCR (RT-PCR) for β-actin (234 bp), glyceraldehyde-3-phosphate dehydrogenase (GAPDH, 189 bp), 18S rRNA (236 bp), and ubiquitin (198 bp).

Two-round linear amplification and biotin-Labeling of RNA

The reproducibility and validity of RNA amplification methods allow microarray analysis from a limited amount of RNA [9, 11-12]. To obtain sufficient quantities of biotin-labeled RNA for hybridization onto microarray, two-rounds of linear amplification of RNA were conducted, using RiboAmp HS™ RNA Amplification Kit (Arcturus). Briefly, using a T7-Oligo (dT) primer, a T7 promoter was incorporated during the conversion of 10-20 ng of total cellular RNA into double-stranded cDNA. Double-stranded cDNA was then transcribed *in vitro* by T7 RNA polymerase to generate multiple antisense RNA (aRNA) copies in the sample. Next, a second round of linear amplification was performed using aRNA from the first round as the template for cDNA synthesis. Finally, using the BioArray High Yield™ RNA Transcript Labeling Kit (T7) (Enzo Life Sciences, Inc.), biotin-labeled ribonucleotides were incorporated into aRNA during the second *in vitro* transcription (IVT) reaction. Two-rounds of linear amplification from 10-20 ng of total RNA yielded up to 10-20 μg of biotinylated target. The quality and quantity of the amplified aRNA were checked by using spectrophotometer and Agilent NanoChip Bioanalyzer.

Hybridization and scanning

Fifteen microgram of biotin-labeled aRNA was fragmented and the quality and quantity of the fragmented aRNA were checked by using spectrophotometer and

Agilent NanoChip Bioanalyzer. Fragmented aRNA was hybridized onto GeneChip® Human X3P Array (Affymetrix) for 16 hours at 45°C at Cornell Microarray Core Facility. Genechips were washed and stained in Affymetrix Fluidics Station FS450 and scanned using Affymetrix GeneChip Scanner 3000 7G at Cornell Microarray Core Facility.

Microarray Data analysis

We performed three independent arrays on the LCM-derived granuloma sample from one patient, which confirmed the reliability of the technique. Thereafter, two other granuloma samples from two patients were further analyzed by microarray for biological replicates.

For the generation of a hierarchical list of absolute gene expression profile in caseous human pulmonary TB granulomas, raw CEL files were analyzed at the probe level using R and Bioconductor. Only PM probes were included in the estimation for expression level of probe sets. Raw PM intensities from each array were subjected to local background correction using MAS5 method, $\log_2$-transformed and median-centered. Informative PM probes from each probe set were selected as having the highest mean across all arrays. In this study, the mean signal of top 5 informative PM probes of each probe set was used to represent its expression level.

The data for caseous granulomas and normal lung parenchyma were analyzed using GeneSpring GX 10.0.2 program (Agilent). MAS5 method was used to summarize raw CHP files. Normalization was done by scaling to median of all samples and the baseline was transformed to the median of all samples. List of genes differentially expressed between caseous human pulmonary TB granulomas and normal lung parenchyma was generated.

The networks between gene products were generated by using Ingenuity Pathway Analysis (Ingenuity® Systems, www.ingenuity.com).

Statistical analysis

The statistical significance of differences in gene expressions between normal human lung tissues and caseous human pulmonary TB granulomas was calculated using an unpaired t test with Benjamini-Hochberg correction. Results with a P value less than 0.05 were considered significant.

RESULTS and DISCUSSION

In an effort to understand how the host responds to Mtb infection, we examined the regulation of genes in human pulmonary TB granulomas. Depending on the stage of the granuloma development, TB granulomas differ histologically. For this study, we specifically selected caseous granulomas because caseous granulomas represent a histologically-defined structure that is used as a diagnostic marker of progression to active disease, bacillary growth and transmission. The cryosection of human TB lung tissues shows a chromogenic area, which corresponds to the caseous granuloma (Figure 2.1). Each cryosection from TB lung tissues was fixed and immediately processed for LCM. Since tissues from TB patients were degenerate due to the extreme disease state, therefore, RNA isolation from LCM-derived samples was technically challenging. PicoPure™ RNA Isolation Kit and RiboAmp HS™ RNA Amplification Kit allowed the successful isolation and amplification of RNA from such tissue samples and generated sufficient RNA for microarray analysis. In the current study, tissue samples from three TB patients were used for biological replicates, and one of the three samples was used as a technical replicate. Even though the uninvolved lung tissues in our archive looked histologically normal, RNA of

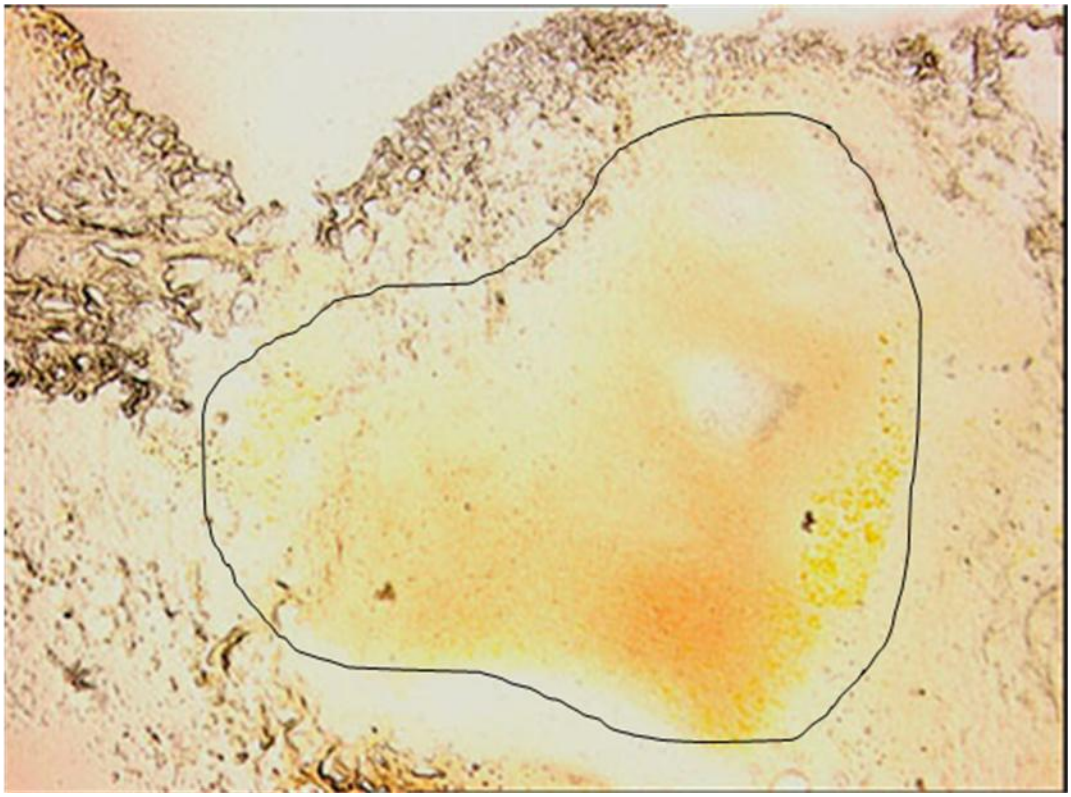

Figure 2.1 Cryosection of caseous human pulmonary TB granuloma (circled) appears chromogenic indicating the abundance of lipid. ×4

quality good enough for microarray was generated from only one sample. The paucity of intact RNA may be due to the low number of cells present in normal lung tissues. The parenchyma of control lung tissue was processed as TB granulomas, and the sample was technically replicated.

The normal tissues are typically used as a control for diseased tissues. However, the cell lineage of TB granulomas is strikingly different when compared to normal lung parenchyma; thus the validity of using normal lung tissues as a control was questionable. Therefore, we generated gene lists by two different ways; one list shows the absolute gene expression levels from TB granulomas only, whereas the other list shows the differential gene expression levels of TB granulomas compared to normal lung tissue. Interestingly, transcriptional profiles of TB granulomas derived both methods were comparable. For the ease of data interpretation, we present the microarray data analyzed by differential gene expressions between TB granuloma and normal lung tissues.

The microarray data analysis on caseous human pulmonary TB granulomas in this study revealed top biological functions; e.g. cell death, cell-mediated immune response, tissue morphology, and infection mechanism (Table 2.1). Human PBMC-derived macrophages from TB patients were shown to upregulate expressions of *CCL3*, *CCL4*, *CXCL1*, *CXCL2*, *CXCL10*, *IL1B*, and *IL10* in response to Mtb infection [13], and BALF-cells from TB patients had upregulated genes such as *IL7R*, *IL8*, *CXCR4*, and *CCL18* [14]. These reported genes for cytokines, chemokines, and their receptors were also highly upregulated in our microarray data (Table 2.2). We previously showed that the cytokine production of macrophages in response to Mtb infection and mycobacterial trehalose dimycolate (TDM) requires CD14, MARCO, and TLR2 [15]; it is noteworthy that transcripts for these molecules are highly upregulated in human TB granulomas (Table 2.2).

Table 2.1 Top Biological Functions in Caseous Human Pulmonary TB Granulomas. The microarray data were analyzed by using Ingenuity Pathway Analysis®.

Diseases and Disorders		
Name	***p*-value**	**No. of molecules**
Infectious Disease	9.48^{-15}–2.79^{-4}	633
Infection Mechanism	3.53^{-14}–2.79^{-4}	498
Immunological Disease	6.34^{-11}–3.39^{-4}	995
Cancer	1.05^{-10}–3.20^{-4}	1406
Reproductive System Disease	8.00^{-10}–2.80^{-5}	352
Molecular and Cellular Functions		
Name	***p*-value**	**No. of molecules**
Cell death	4.46^{-26}–3.00^{-4}	1224
Post-Translational Modification	2.08^{-18}–3.21^{-4}	517
Cellular Development	1.05^{-16}–3.28^{-4}	821
Cellular Function and Maintenance	1.70^{-15}–3.14^{-4}	512
RNA Post-Transcriptional Modification	1.05^{-13}–2.79^{-4}	136
Physiological System Development and Function		
Name	***p*-value**	**No. of molecules**
Organismal Survival	9.11^{-13}–4.57^{-5}	488
Hematological System Development and Function	1.05^{-16}–3.39^{-4}	663
Hematopoiesis	1.05^{-16}–1.12^{-4}	388
Tissue Morphology	4.68^{-10}–4.74^{-6}	258
Cell-Mediated Immune Response	1.70^{-15}–1.03^{-4}	272
Top Canonical Pathways		
Name	***p*-value**	**Ratio**
Protein Ubiquitination Pathway	1.27^{-9}	98/201 (0.488)
Molecular Mechanisms of Cancer	1.61^{-9}	155/372 (0.417)
Death Receptor Signaling	3.15^{-9}	40/64 (0.625)
Lymphotoxin β Receptor Signaling	1.62^{-8}	37/61 (0.607)
Induction of Apoptosis by Human Immunodeficiency Virus 1	2.63^{-10}	42/65 (0.646)
Top Toxicity Lists		
Name	***p*-value**	**Ratio**
Pro-Apoptosis	2.16^{-6}	28/42 (0.667)
Mitochondrial Dysfunction	2.43^{-5}	61/125 (0.488)
Nuclear Factor-Kappa B signaling Pathway	2.19^{-4}	53/112 (0.473)
Retinoic Acid Receptor Activation	4.39^{-4}	60/133 (0.451)
Oxidative Stress Response Mediated by Nuclear Factor 2-Related Factor 2	5.99^{-4}	86/205 (0.42)

Table 2.2 Caseous human pulmonary TB granulomas show upregulated gene expressions for immune response ($P < 0.05$).

Cluster of Differentiation molecules					
Gene	**Description**	**Fold change**	**Gene**	**Description**	**Fold change**
CD3D	CD3D molecule	48.6	*CD59*	CD59 molecule	107.3
CD8A	CD8A molecule	96.3	*CD74*	CD74 molecule	110.8
CD14	CD14 molecule	399.6	*CD80*	CD80 molecule	13.1
CD33	CD33 molecule	177.0	*CD83*	CD83 molecule	162.5
CD44	CD44 molecule	106.3	*CD86*	CD86 molecule	48.7
CD46	CD46 molecule	21.0	*CD96*	CD96 molecule	8.1
CD53	CD53 molecule	162.2	*CD163*	CD163 molecule	890.1
CD55	CD55 molecule	38.3	*CD276*	CD276 molecule	44.2
Major Histocompatibility Complex molecules					
Gene	**Description**	**Fold change**	**Gene**	**Description**	**Fold change**
HLA-A	MHC class I, A	52.2	*HLA-DMA*	MHC class II, DM alpha	55.2
HLA-B	MHC class I, B	328.6	*HLA-DRA*	MHC class II, DR alpha	95.7
HLA-C	MHC class I, C	645.2	*HLA-DRB1*	MHC class II, DR beta 1	411.5
HLA-DOA	MHC class II, DO alpha	28.4	*HLA-E*	MHC class I, E	256.2
HLA-DQB1	MHC class II, DQ, beta 1	86.2	*HLA-F*	MHC class I, F	848.7
Receptors/Antigen recognition					
Gene	**Description**	**Fold change**	**Gene**	**Description**	**Fold change**
C3AR1	Complement component 3a receptor 1	56.1	*MRC1*	Mannose receptor, C type 1	64.3
C5AR1	Complement component 5a receptor 1	12.1	*MRC2*	Mannose receptor, C type 2	93.4
FCER1G	Fc fragment of IgE, high affinity I, receptor for; gamma polypeptide	141.7	*MSR1*	Macrophage scavenger receptor 1	81.5
FCGR2A (CD32)	Fc fragment of IgG, low affinity, IIa, receptor	126.8	*SCARA5*	Scavenger receptor class A, member 5	25.5
FCGR2B (CD32)	Fc fragment of IgG, low affinity, IIb, receptor	15.6	*SCARB2*	Scavenger receptor class B, member 2	33.1
FCGR3A (CD16a)	Fc fragment of IgG, low affinity, IIIa, receptor	12.2	*SCARF1*	Scavenger receptor class F, member 1	22.5
FCGR3B (CD16b)	Fc fragment of IgG, low affinity, IIIb, receptor	44.5	*TLR1*	Toll-like receptor 1	57.4
MARCO	Macrophage receptor with collagenous structure	106.2	*TLR2*	Toll-like receptor 2	78.5
			TLR4	Toll-like receptor 4	20.1

Table 2.2 (Continued)

Cytokines and cytokine receptors					
Gene	**Description**	**Fold change**	**Gene**	**Description**	**Fold change**
CSF1	Colony stimulating factor 1	46.5	*IL27RA*	Interleukin 27 receptor, alpha	14.0
FAS	Fas	44.8	*IL32*	Interleukin 32	39.4
FASLG	Fas ligand	9.1	*LTA*	Lymphotoxin alpha	10.0
IFNGR1	Interferon gamma receptor 1	91.1	*LTB*	Lymphotoxin beta	70.2
IFNGR2	Interferon gamma receptor 2	131.0	*MIF*	Macrophage migration inhibitory factor	14.5
IL1B	Interleukin 1, beta	26.9	*MST1*	Macrophage stimulating 1	16.3
IL2RB	Interleukin 2 receptor, beta	43.0	*SCYE1*	Small inducible cytokine subfamily E, member 1	43.0
IL4R	Interleukin 4 receptor	12.7	*TNFAIP1*	TNF, alpha-induced protein 1	3.8
IL6R	Interleukin 6 receptor	9.2	*TNFAIP2*	TNF, alpha-induced protein 2	195.8
IL7R	Interleukin 7 receptor	27.8	*TNFAIP3*	TNF, alpha-induced protein 3	165.5
IL8	Interleukin 8	43.6	*TNFAIP8*	TNF, alpha-induced protein 8	115.7
IL10	Interleukin 10	28.1	*TNFRSF1A*	TNF receptor superfamily, member 1A	32.5
IL12RB1	Interleukin 12 receptor, beta 1	36.0	*TNFRSF1B*	TNF superfamily, member 1B	21.0
IR13RA1	Interleukin 13 receptor, alpha 1	49.8	*TNFRSF10B*	TNF receptor superfamily, member 10b	148.8
IL15	Interleukin 15	28.8	*TNFRSF14*	TNF receptor superfamily, member 14	42.0
IL15RA	Interleukin 15 receptor, alpha	8.6	*TNFRSF21*	TNF receptor superfamily, member 21	50.8
IL17RA	Interleukin 17, receptor A	26.7	*TNFSF4*	TNF (ligand) superfamily, member 4	12.8
IL17RC	Interleukin 17, receptor C	15.7	*TNFSF10*	TNF (ligand) superfamily, member 10	50.7
IL21R	Interleukin 21 receptor	17.0	*TNFSF13B*	TNF (ligand) superfamily, member 13b	497.7

Table 2.2 (Continued)

Chemokines and chemokine receptors					
Gene	**Description**	**Fold change**	**Gene**	**Description**	**Fold change**
CCL1	Chemokine (C-C motif) ligand 1	14.0	*CCRL2*	Chemokine (C-C motif) receptor-like 2	17.7
CCL2	Chemokine (C-C motif) ligand 2	242.2	*CKLF*	Chemokine-like factor	146.8
CCL3	Chemokine (C-C motif) ligand 3	1028.9	*CMKLR1*	Chemokine-like receptor 1	11.3
CCL4	Chemokine (C-C motif) ligand 4	19.3	*CXCL1*	Chemokine (C-X-C motif) ligand 1	17.8
CCL5	Chemokine (C-C motif) ligand 5	17.3	*CXCL2*	Chemokine (C-X-C motif) ligand 2	7.1
CCL8	Chemokine (C-C motif) ligand 8	41.4	*CXCL9*	Chemokine (C-X-C motif) ligand 9	141.6
CCL18	Chemokine (C-C motif) ligand 18	85.7	*CXCL10*	Chemokine (C-X-C motif) ligand 10	474.1
CCR1	Chemokine (C-C motif) receptor 1	277.4	*CXCL12*	Chemokine (C-X-C motif) ligand 12	39.6
CCR2	Chemokine (C-C motif) receptor 2	5.9	*CXCL16*	Chemokine (C-X-C motif) ligand 16	12.8
CCR5	Chemokine (C-C motif) receptor 5	138.4	*CXCR4*	Chemokine (C-X-C motif) receptor 4	602.2
CCR7	Chemokine (C-C motif) receptor 7	39.2	*CXCR7*	Chemokine (C-X-C motif) receptor 7	40.2

Table 2.2 (Continued)

Signaling					
Gene	**Description**	**Fold change**	**Gene**	**Description**	**Fold change**
IFIT1	Interferon-induced protein with tetratricopeptide repeats 1	15.1	*MSN*	Moesin	61.0
IFIT3	Interferon-induced protein with tetratricopeptide repeats 3	67.1	*MYD88*	Myeloid differentiation primary response gene (88)	18.6
IL6ST	Interleukin 6 signal transducer (gp130)	22.4	*PAG1*	Phosphoprotein associated with glycosphingolipid microdomains 1	1115.8
INHBA	Inhibin, beta A	54.5	*SMAD3*	SMAD family member 3	10.1
INSIG1	Insulin induced gene 1	121.3	*STAT6*	Signal transducer and activator of transcription 6, interleukin 4-induced	10.0
IRAK2	Interleukin-1 receptor-associated kinase 2	30.1	*SYK*	Spleen tyrosine kinase	121.7
IRAK3	Interleukin-1 receptor-associated kinase 3	66.0	*TGFBR1*	Transforming growth factor, beta receptor 1	91.2
MAP3K5	Mitogen-activated protein kinase kinase kinase 5	340.8	*TNIP3*	TNFAIP3 interacting protein 3	25.4
MAPK1	Mitogen-activated protein kinase 1	89.0	*TRAF1*	TNF receptor-associated factor 1	8.1
MAPK14	Mitogen-activated protein kinase 14	125.5	*TRAF3*	TNF receptor-associated factor 3	385.6

As well as immune response, other interesting themes have emerged from the microarray data: angiogenesis and tissue remodeling. The formation of TB granuloma as an isolated independent structure in the lung parenchyma results from the recruitment of immunological cells from the blood stream and angiogenesis, followed by tissue remodeling [16-17]. While the tightly formed granuloma protects the host from Mtb dissemination to other parts of the body, the extensive tissue remodeling at the terminal stage of active TB leads to the granuloma liquefaction and erosion. Our microarray study clearly demonstrates that tissue remodeling is very active in TB granuloma at the transcriptional level (Table 2.3). Particularly, the increased secretion of MMP1 and MMP9 has been implicated in active TB disease in human [18-22]; these genes are highly upregulated (Table 2.3), and we observed MMP activity in human pulmonary TB granulomas by using *in situ* zymography (By Dr. Kaori Sakamoto, unpublished data).

The most interesting theme from the microarray study is lipid metabolism. An increasing body of literature has indicated that the host lipid metabolism changes upon mycobacterial infection. Histological examination has demonstrated abundant lipids at the periphery of human TB granulomas and the presence of Mtb bacilli in lipid-rich areas including foamy macrophages and adipose tissues, and *in vitro* and *in vivo* mycobacterial infection studies indicate the accumulation of lipids in macrophages [23-28]. While the caseous center of human TB granuloma has been proposed to be filled with lipids, our microarray data present the first molecular evidence that lipid metabolism is highly active in caseous human TB granulomas. Table 2.4 shows a subset of upregulated genes involved in lipid metabolism, and Ingenuity Pathway Analysis® generated pathway indicates most of upregulated genes are interconnected (Figure 2.2). Moreover, many of them are unified around the pro-inflammatory

Table 2.3 Caseous human pulmonary TB granulomas show upregulated gene expressions for angiogenesis and tissue remodeling ($P < 0.05$).

Proteolysis					
Gene	**Description**	**Fold change**	**Gene**	**Description**	**Fold change**
ADAMTS1	ADAM metallopeptidase with thrombospondin type 1 motif, 1	4.3	*MMP1*	Matrix metallopeptidase 1	606.2
ADAMTS5	ADAM metallopeptidase with thrombospondin type 1 motif, 5	16.0	*MMP2*	Matrix metallopeptidase 2	16.2
ADAMTS6	ADAM metallopeptidase with thrombospondin type 1 motif, 6	9.9	*MMP9*	Matrix metallopeptidase 9	199.9
ADAMTS12	ADAM metallopeptidase with thrombospondin type 1 motif, 12	7.3	*MMP10*	Matrix metallopeptidase 10	14.9
CASP2	Caspase 2	7.7	*MMP19*	Matrix metallopeptidase 19	123.6
CASP4	Caspase 4	24.4			
CASP6	Caspase 6	11.3	*SERPINA1*	Serpin peptidase inhibitor, clade A, member 1	18.1
CASP7	Caspase 7	5.9			
CASP8	Caspase 8	114.7	*SERPINB1*	Serpin peptidase inhibitor, clade B, member 1	189.2
CASP9	Caspase 9	16.0			
CASP10	Caspase 10	11.9	*SERPINB9*	Serpin peptidase inhibitor, clade B, member 9	41.7
CHI3L1	Chitinase-3-like 1	1042.5			
CTSA	Cathepsin A	109.6	*SERPINE1*	Serpin peptidase inhibitor, clade E, member 1	141.4
CTSB	Cathepsin B	127.6			
CTSC	Cathepsin C	8.9	*SERPINF1*	Serpin peptidase inhibitor, clade F, member 1	34.2
CTSH	Cathepsin H	9.3			
CTSK	Cathepsin K	36.9	*TIMP1*	TIMP metallopeptidase inhibitor 1	112.4
CTSL1	Cathepsin L1	63.5			
CTSS	Cathepsin S	340.3	*TIMP2*	TIMP metallopeptidase inhibitor 2	44.3
CTSZ	Cathepsin Z	61.5			

Table 2.3 (Continued)

Fibrosis					
Gene	**Description**	**Fold change**	**Gene**	**Description**	**Fold change**
COL1A1	Collagen, type I, alpha 1	9.7	*COL12A1*	Collagen, type XII, alpha 1	11.8
COL3A1	Collagen, type III, alpha 1	254.4	*COL14A1*	Collagen, type XIV, alpha 1	8.5
COL4A1	Collagen, type IV, alpha 1	1.7	*COL16A1*	Collagen, type XVI, alpha 1	2.2
COL4A3BP	Collagen, type I, alpha 1, alpha 3 binding protein	81.9	*COL18A1*	Collagen, type XVIII, alpha 1	4.6
COL5A1	Collagen, type V, alpha 1	24.8	*COL21A1*	Collagen, type XXI, alpha 1	6.2
COL5A2	Collagen, type V, alpha 2	92.7	*COL24A1*	Collagen, type XXIV, alpha 1	4.7
COL5A3	Collagen, type V, alpha 3	23.9	*COL25A1*	Collagen, type XXV, alpha 1	8.4
COL6A2	Collagen, type VI, alpha 2	36.5	*FBLN2*	Fibulin 2	10.7
COL6A3	Collagen, type VI, alpha 3	90.0	*ITGA5*	Integrin, alpha 5	29.2
COL8A2	Collagen, type VIII, alpha 2	25.9	*ITGB1*	Integrin, beta 1	103.8
COL11A1	Collagen, type XI, alpha 1	142.0	*LUM*	Lumican	14.8
Angiogenesis					
Gene	**Description**	**Fold change**	**Gene**	**Description**	**Fold change**
CTGF	Connective tissue growth factor	235.3	*PLAU*	Plasminogen activator, urokinase	272.4
HIF1A	Hypoxia inducible factor 1, alpha subunit	61.0	*PLAT*	Plasminogen activator, tissue	161.0
NRP1	Neuropilin 1	52.4	*THBS2*	Thrombospondin 2	95.7
PDGFC	Platelet derived growth factor C	21.7	*THBS3*	Thrombospondin 3	18.5
PDGFRA	Platelet derived growth factor receptor, alpha polypeptide	11.3	*VCAN*	Versican	89.5
PDGFRB	Platelet derived growth factor receptor, beta polypeptide	13.8	*VEGFA*	Vascular endothelial growth factor A	17.6

Table 2.4 Caseous human pulmonary TB granulomas show upregulated gene expressions for lipid metabolism ($P < 0.05$).

Lipid synthesis and sequestration					
Gene	**Description**	**Fold change**	**Gene**	**Description**	**Fold change**
ABHD5	Abhydrolase domain containing 5	34.3	*GBA*	Glucosidase, beta, acid	32.0
ACLY	ATP citrate lyase	22.7	*GLA*	Galactosidase, alpha	152.5
ACSL1	Acyl CoA synthetase long chain family member 1	39.4	*GLB1*	Galactosidase, beta 1	19.9
ACSL3	Acyl CoA synthetase long chain family member 3	71.2	*GPD2*	Glycerol-3-phosphate dehydrogenase 2	60.9
ACSL4	Acyl CoA synthetase long chain family member 4	261.5	*HADHA*	Hydroxyacyl-Coenzyme A dehydrogenase/3-ketoacyl-Coenzyme A thiolase/enoyl-Coenzyme A hydratase, alpha subunit	11.0
ACSL5	Acyl CoA synthetase long chain family member 5	75.5	*HMGCR*	3-hydroxy-3methylglutaryl-Coenzyme A reductase	8.9
ADFP	Adipose differentiation-related protein	19.1	*IDI1*	Isopentenyl-diphosphate delta isomerase 1	10.9
CRAT	Carnitine O-acetyltransferase	14.8	*LIPA*	Lipase A, lysosomal acid, cholesterol esterase	12.6
CYP1B1	Cytochrome P450, family 1, subfamily B, polypeptide 1	36.5	*LSS*	Lanosterol synthase	11.0
CYP27A1	Cytochrome P450, family 27, subfamily A, polypeptide 1	48.0	*PLSCR1*	Phospholipid scramblase 1	11.8
DEGS1	Degenerative spermatocyte homolog 1, lipid desaturase	180.2	*PSAP*	Prosaposin (precursor of sapC)	14.6
DHCR7	7-dehydrocholesterol reductase	8.8	*SCD*	Stearoyl-CoA desaturase	13.1
EBP	Emopamil binding protein	18.3	*SC5DL*	Sterol-C5-desaturase	10.1
ELOVL5	Elovl family member 5, elongation of long chain fatty acids	36.8	*SOAT1*	Sterol O-acyltransferase 1	10.3
FADS1	Fatty acid desaturase 1	45.0	*SPHK2*	Sphingosine kinase 2	11.6
FDPS	Farnesyl diphosphate synthase	8.6	*TPI1*	Triosephosphate isomerase 1	12.4

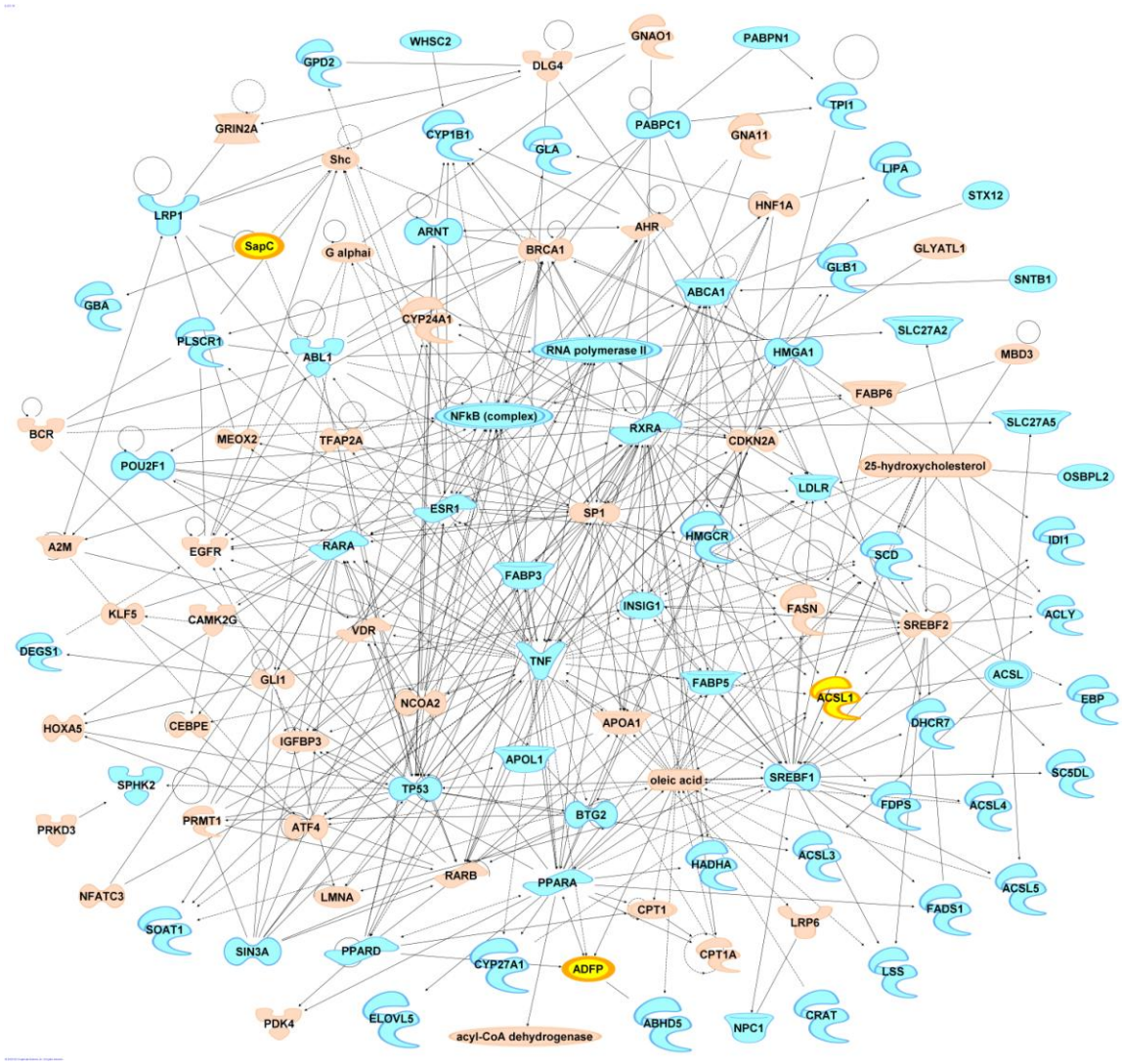

Figure 2.2 The network of genes involved in lipid metabolism. This was generated by using Ingenuity Pathway Analysis® program. Genes in blue and yellow are upregulated in the array and shown in Table 2.4.

Figure 2.2 (Continued)

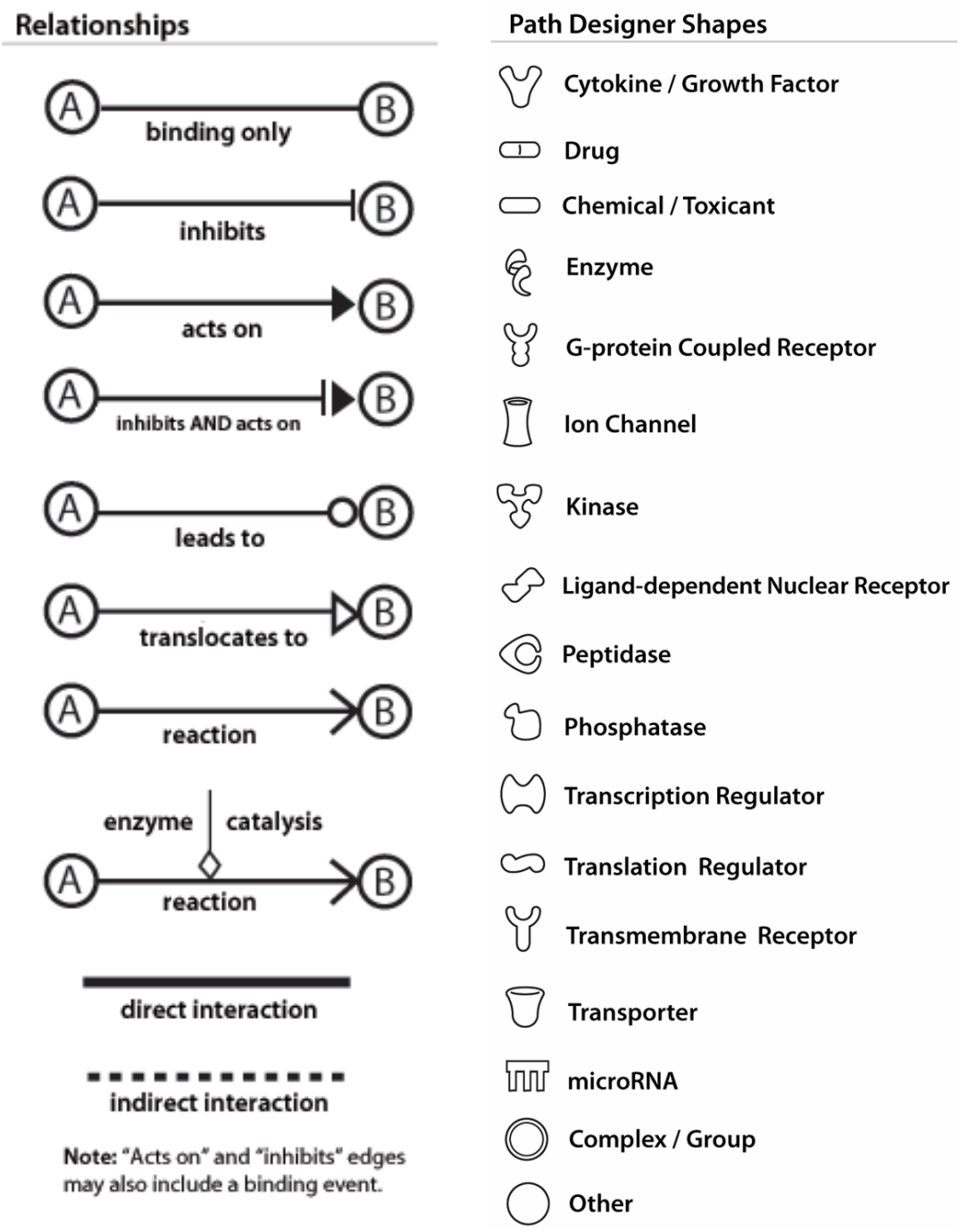

cytokine tumor necrosis factor-α (TNF-α), indicating that this response is consistent with a sustained pro-inflammatory stimulation.

Despite the importance of understanding the granuloma biology in human TB pathogenesis, little has been known. The current study has generated a genome-wide transcriptional profile of caseous human pulmonary TB granulomas and opened new avenues to investigate TB pathogenesis. Future work includes further investigation of genes selected from the microarray data: especially in lipid metabolism, cellular transmigration, and ER stress.

ACKNOWLEDGEMENTS

I would like to thank Drs. Helen Wainwright, Gabriele Walther, and Linda-Gail Bekker for providing the valuable human lung tissues, Dr. Wei Wang for the advice on microarray data analysis, and Cornell University Microarray Core Facility for hybridizing and scanning GeneChip slides.

REFERENCE

1. El-Zammar, O.A. and A.L. Katzenstein, *Pathological diagnosis of granulomatous lung disease: a review.* Histopathology, 2007. **50**(3): p. 289-310.
2. Heller, M.J., *DNA microarray technology: devices, systems, and applications.* Annu Rev Biomed Eng, 2002. **4**: p. 129-53.
3. Grassi, M., et al., *Transcriptional profile of the immune response in the lungs of patients with active tuberculosis.* Clin Immunol, 2006. **121**(1): p. 100-7.
4. Volpe, E., et al., *Gene expression profiling of human macrophages at late time of infection with Mycobacterium tuberculosis.* Immunology, 2006. **118**(4): p. 449-60.
5. Ragno, S., et al., *Changes in gene expression in macrophages infected with Mycobacterium tuberculosis: a combined transcriptomic and proteomic approach.* Immunology, 2001. **104**(1): p. 99-108.
6. Kim, D.K., et al., *Microarray analysis of gene expression associated with extrapulmonary dissemination of tuberculosis.* Respirology, 2006. **11**(5): p. 557-65.
7. Zhu, G., et al., *Gene expression in the tuberculous granuloma: analysis by laser capture microdissection and real-time PCR.* Cell Microbiol, 2003. **5**(7): p. 445-53.
8. Emmert-Buck, M.R., et al., *Laser capture microdissection.* Science, 1996. **274**(5289): p. 998-1001.
9. Caretti, E., et al., *Comparison of RNA amplification methods and chip platforms for microarray analysis of samples processed by laser capture microdissection.* J Cell Biochem, 2008. **103**(2): p. 556-63.

10. Mikulowska-Mennis, A., et al., *High-quality RNA from cells isolated by laser capture microdissection.* Biotechniques, 2002. **33**(1): p. 176-9.
11. Luzzi, V., et al., *Accurate and reproducible gene expression profiles from laser capture microdissection, transcript amplification, and high density oligonucleotide microarray analysis.* J Mol Diagn, 2003. **5**(1): p. 9-14.
12. King, C., et al., *Reliability and reproducibility of gene expression measurements using amplified RNA from laser-microdissected primary breast tissue with oligonucleotide arrays.* J Mol Diagn, 2005. **7**(1): p. 57-64.
13. Thuong, N.T., et al., *Identification of tuberculosis susceptibility genes with human macrophage gene expression profiles.* PLoS Pathog, 2008. **4**(12): p. e1000229.
14. Raju, B., et al., *Gene expression profiles of bronchoalveolar cells in pulmonary TB.* Tuberculosis (Edinb), 2008. **88**(1): p. 39-51.
15. Bowdish, D.M., et al., *MARCO, TLR2, and CD14 are required for macrophage cytokine responses to mycobacterial trehalose dimycolate and Mycobacterium tuberculosis.* PLoS Pathog, 2009. **5**(6): p. e1000474.
16. Marquis, J.F., et al., *Fibrotic response as a distinguishing feature of resistance and susceptibility to pulmonary infection with Mycobacterium tuberculosis in mice.* Infect Immun, 2008. **76**(1): p. 78-88.
17. Dheda, K., et al., *Lung remodeling in pulmonary tuberculosis.* J Infect Dis, 2005. **192**(7): p. 1201-9.
18. Elkington, P.T., et al., *Synergistic up-regulation of epithelial cell matrix metalloproteinase-9 secretion in tuberculosis.* Am J Respir Cell Mol Biol, 2007. **37**(4): p. 431-7.

19. Taylor, J.L., et al., *Role for matrix metalloproteinase 9 in granuloma formation during pulmonary Mycobacterium tuberculosis infection.* Infect Immun, 2006. **74**(11): p. 6135-44.

20. Hrabec, E., et al., *Circulation level of matrix metalloproteinase-9 is correlated with disease severity in tuberculosis patients.* Int J Tuberc Lung Dis, 2002. **6**(8): p. 713-9.

21. O'Kane, C.M., et al., *STAT3, p38 MAP Kinase and NF-{kappa}B Drive Unopposed Monocyte-dependent Fibroblast MMP-1 Secretion in Tuberculosis.* Am J Respir Cell Mol Biol, 2009.

22. Elkington, P.T., et al., *Mycobacterium tuberculosis, but not vaccine BCG, specifically upregulates matrix metalloproteinase-1.* Am J Respir Crit Care Med, 2005. **172**(12): p. 1596-604.

23. Hunter, R.L., et al., *Multiple roles of cord factor in the pathogenesis of primary, secondary, and cavitary tuberculosis, including a revised description of the pathology of secondary disease.* Ann Clin Lab Sci, 2006. **36**(4): p. 371-86.

24. Hunter, R.L., et al., *Trehalose 6,6'-dimycolate and lipid in the pathogenesis of caseating granulomas of tuberculosis in mice.* Am J Pathol, 2006. **168**(4): p. 1249-61.

25. Hunter, R.L., C. Jagannath, and J.K. Actor, *Pathology of postprimary tuberculosis in humans and mice: contradiction of long-held beliefs.* Tuberculosis (Edinb), 2007. **87**(4): p. 267-78.

26. Peyron, P., et al., *Foamy macrophages from tuberculous patients' granulomas constitute a nutrient-rich reservoir for M. tuberculosis persistence.* PLoS Pathog, 2008. **4**(11): p. e1000204.

27. Neyrolles, O., et al., *Is adipose tissue a place for Mycobacterium tuberculosis persistence?* PLoS One, 2006. **1**: p. e43.

28. D'Avila, H., et al., *Mycobacterium bovis bacillus Calmette-Guerin induces TLR2-mediated formation of lipid bodies: intracellular domains for eicosanoid synthesis in vivo.* J Immunol, 2006. **176**(5): p. 3087-97.

CHAPTER THREE

LOCALIZATION OF ADFP, ACSL1, AND SAPC ON HUMAN PULMONARY TUBERCULOUS GRANULOMAS

ABSTRACT

Mycobacterium tuberculosis (Mtb) infection leads to the formation of granuloma at the infection site, and the well-stratified tuberculous (TB) granuloma prevents the escape of Mtb bacilli to other parts of the body but also provides a niche for Mtb, thereby protecting them from the host immune system. Immunocompetent individuals may resolve TB granulomas by calcification or maintain the granuloma structure under control by constant immune system. However, with unknown mechanism, TB granulomas start to extensively caseate or necrotize, and ultimately liquefy and cavitate into the open airway, transmitting the deadly Mtb bacilli to other individuals. Based on our microarray analysis showing upregulation of lipid metabolism, we examined localization of proteins involved in three different lipid metabolism processes on human pulmonary TB granulomas by immunohistology: adipose differentiation-related protein (ADFP), acyl-CoA synthetase long-chain family member 1 (ACSL1), and saposin C (SapC). Our data show that caseous and fibrocaseous TB granulomas have strong expressions of ADFP, ACSL1, and SapC, whereas old, resolved TB granulomas do not. SapC expression is detected in early TB granulomas. In summary, our data indicate that Mtb infection causes dysregulated lipid metabolism in the human host, and this transition correlates with the accumulation of lipids as caseum in human TB granuloma.

INTRODUCTION

Shortly after infection, the tissue site becomes organized into a granuloma, which comprises of the core of infected macrophages surrounded by foamy and epithelioid macrophages, monocytes, and multinucleated giant cells (MGCs). The periphery of the granuloma is marked by fibroblasts that lay down a fibrous capsule around the macrophage-rich granuloma. Once the capsule is formed, lymphocytes are scarce within the granuloma center and are most abundant outside this fibrous capsule. In this state, the granuloma represents a stable structure that maintains a constant bacterial load but does not cause any overt signs of disease in the infected individual. Immunocompetent or antibiotic-treated individuals can resolve tuberculous (TB) granulomas, disaggregating recruited leukocytes, dissolving extracellular matrix, thereby restoring the normal pulmonary structure. However, 5~10 % of infected individuals develop active TB disease after the initial infection. Pulmonary TB disease is seen about 85% of individuals with active disease [1], although this proportion dramatically changes in human immunodeficiency virus (HIV)-infected individuals who develop pulmonary TB (38%), extrapulmonary TB (30%), and both pulmonary and extrapulmonary (32%) [2-3]. As TB transmission occurs via Mtb-containing aerosols released from the cavitated, ruptured pulmonary granuloma, it is critical to understand the mechanism of TB granuloma development.

Accumulation of lipids has been linked to metabolic syndromes and diseases including diabetes, sepsis, Chagas' disease, hepatitis C virus infection, and acquired immune deficiency syndrome (AIDS) [4-8]. Foamy or lipid-droplet filled macrophages are the fundamental component of atherosclerosis and are becoming recognized as a consequence of chronic inflammatory stimuli [9]. Previous reports documented the abundance of foam cells in human TB lung tissues [10-11]. In addition, virulent Mtb or *M. bovis* Bacillus Calmette-Guérin (BCG) infection triggers

accumulation of lipid droplets in macrophages *in vitro* [11-12], suggesting Mtb stimulates the accumulation of host lipids. The progression of latent TB toward active disease correlates with the increased accumulation of caseum, which is thought to result from the death of macrophages and other leukocytes in the granuloma center. The granuloma becomes increasingly necrotic until the center liquefies, and it cavitates and ruptures into the lung airway [13-14]. Our microarray data have indicated that tissue remodeling is active in caseous human pulmonary TB granulomas (Table 2.2) and genes for lipid metabolism are also highly upregulated (Table 2.3 and Figure 2.2).

To test our hypothesis that the extensive lipid accumulation as caseum contributes to the expansion of the granuloma with the ultimate tissue breakdown, we decided to examine whether proteins responsible for lipid synthesis and sequestration could be detected on human pulmonary TB granulomas. By immunohistological analysis, it was very clear that three proteins, ADFP, ACSL1, and SapC, were highly expressed in cells of caseous and fibrocaseous granulomas, but resolved granulomas did not show any appreciable expression. These data argue that the host undergoes metabolic shift during Mtb infection and that lipids accumulate inside progressive TB granulomas.

MATERIALS and METHODS

Human Subjects

Human subjects were included in this study according to protocols approved by Institutional Review Boards at University of Cape Town, South Africa, the Public Health Research Institute, Newark, NJ, and Cornell University, Ithaca, NY. Informed consent was obtained from all of the patients.

Histology

Human TB lung tissues embedded in paraffin were cut at 3 µm thickness and stained with hematoxylin and eosin for histological examination, after which images were taken by Leica CM300 camera (v1.0, Leica Microsystems) attached to Axiophot (Carl Zeiss MicroImaging) with Leica IM50 software (v1.20, Leica Microsystems). All the slides were reviewed by a pathologist, M. Locketz (Department of Pathology, University of Cape Town, South Africa).

For the detection of neutral lipids, cryosections of human TB lung tissues were fixed in 4% paraformaldehyde in PBS for 30 min and either stained with 0.3% Oil Red O (Alfa Aesar) and counterstained with hematoxylin or stained with 10µg/ml BODIPY 493/503 (Invitrogen) and 1µg/ml DAPI (Invitrogen). Images were photographed by AxioCam HRc attached to Zeiss Axio Imager with AxioVision LE software (Carl Zeiss MicroImaging).

Immunohistology

For immunohistological study of human pulmonary TB tissues, paraffin-embedded sections were cut at 3 µm thickness, heat-fixed, deparaffinized and rehydrated. Epitopes were heat-retrieved in a pressure cooker with 1 mM EDTA buffer pH 8.0, and tissue sections were blocked with 0.2% gelatin in PBS with 0.05% Tween-20 (PBS-T) at room temperature for 1 h. Mouse monoclonal antibody against human ADFP (1:100, RDI division of Fitzgerald Industrial Intl.), rabbit polyclonal antibody against human ACSL1 (1:150, GenWay Biotech), or rabbit polyclonal antibody against human SapC (1:50, Santa Cruz Biotechnology) were applied to the samples at 37°C for 1 h. After washing with PBS-T three times, samples were incubated with 1% Sudan Black B (Sigma) in 70% ethanol at room temperature for 10 min. Sections were washed with PBS-T three times and incubated with Cy3™-goat antibody against

mouse (H+L) (1:250, Jackson ImmunoResearch) or Cy3™-goat antibody against rabbit (H+L) (1:250, Jackson ImmunoResearch) at room temperature for 45 min. After PBS-T wash, nuclei were stained with 1μg/ml of DAPI at room temperature for 10 min, followed by thorough wash with PBS-T. Slides without primary antibodies and normal lung tissues were included as controls. Tissue sections were mounted in ProLong Gold Antifade Reagent and images were captured by AxioCam MRm attached to Zeiss Axioskop 40 epifluorescence microscope with AxioVision 4.3 software (Carl Zeiss MicroImaging). Further image analysis was done by AxioVision LE software (Carl Zeiss MicroImaging) and Adobe Photoshop CS2 (Adobe).

RESULTS and DISCUSSION

Despite the critical importance of understanding TB granuloma biology, few studies have looked beyond immune mechanisms to probe the underlying pathology required to generate active disease. As recent studies and our microarray study on human TB granulomas (Chapter 2) point to the involvement of lipid metabolism in TB pathogenesis [10-12], we decided to investigate whether proteins involved in lipid metabolism could be detected in human TB granulomas by immunohistology.

From the upregulated genes in human TB granulomas (Table 2.3 and Figure 2.2), we focused on three proteins relevant to three different aspects of lipid sequestration and metabolism: ADFP, ACSL1, and SapC. Excess lipids are stored in an organelle, the lipid droplet, which is formed through either the sequestration of cholesteryl esters (CE) from LDL-derived cholesterol or from lipids synthesized *de novo* by cells. ADFP is known to be required for lipid droplet formation and it remains strongly associated with the periphery of lipid droplets [15]. Upregulated ADFP expression increases sequestration of CE, increases synthesis of long-chain fatty acid (LCFA) and triacylglycerols (TAG), and inhibits catalysis of lipids through

the β-oxidation pathway [15-18]. ADFP mRNA is increased by excess LCFA, fasting, modified low density lipoprotein (LDL), Peroxisome proliferator-activated receptor (PPAR) agonists, or transcription factors that play a role in lipid homeostasis [19-23]. ACSL1, the acyl-CoA synthetase, can also lead to lipid droplet formation through the *de novo* synthesis of long chain fatty acids that are incorporated into TAG [24-25]. ACSL1 mediates the formation of fatty acyl-CoA esters from fatty acids of carbon length 14 to 24, a key step for lipid biosynthesis, and it is proposed to be present on the plasma membrane, mitochondria, and lipid droplets. Finally, the prosaposin product, saposin C (SapC, sphingolipid activator protein), is required for the turnover of glycosphingolipids into ceramide and sphingosine in the inner endosomal and lysosomal membranes, an essential activity to maintain the balance of lipid species in biological membranes [26-27]. In addition to glycolipid degradation, SapC is known to function as a transfer protein by loading Mtb glycolipid, lipoarabinomannan (LAM), onto the antigen-presenting molecule, CD1b [28-29]. For our study, we focused on the role of SapC in glycosphingolipid metabolism.

Using immunohistological analysis, we investigated the localization and relative expression levels of ADFP, ACSL1, and SapC on human pulmonary TB granulomas representing different stages of disease progression. Granulomas from 32 cases were categorized into four stages: nascent (n=28), caseous (n=16), fibrocaseous (n=66), and resolved granulomas (n=9) (Figure 3.1).

The expression profile of the lipid droplet-associated protein, ADFP, varied markedly at each stage of granuloma development. Nascent granulomas showed weak or minimal staining, whereas caseous and fibrocaseous granulomas showed the abundant expression of ADFP (Figure 3.2 A–F). Macrophages and MGCs around the fibrotic capsule showed the most intense staining pattern. It is noteworthy that the actual caseum of several granulomas revealed strong expression of ADFP mingled

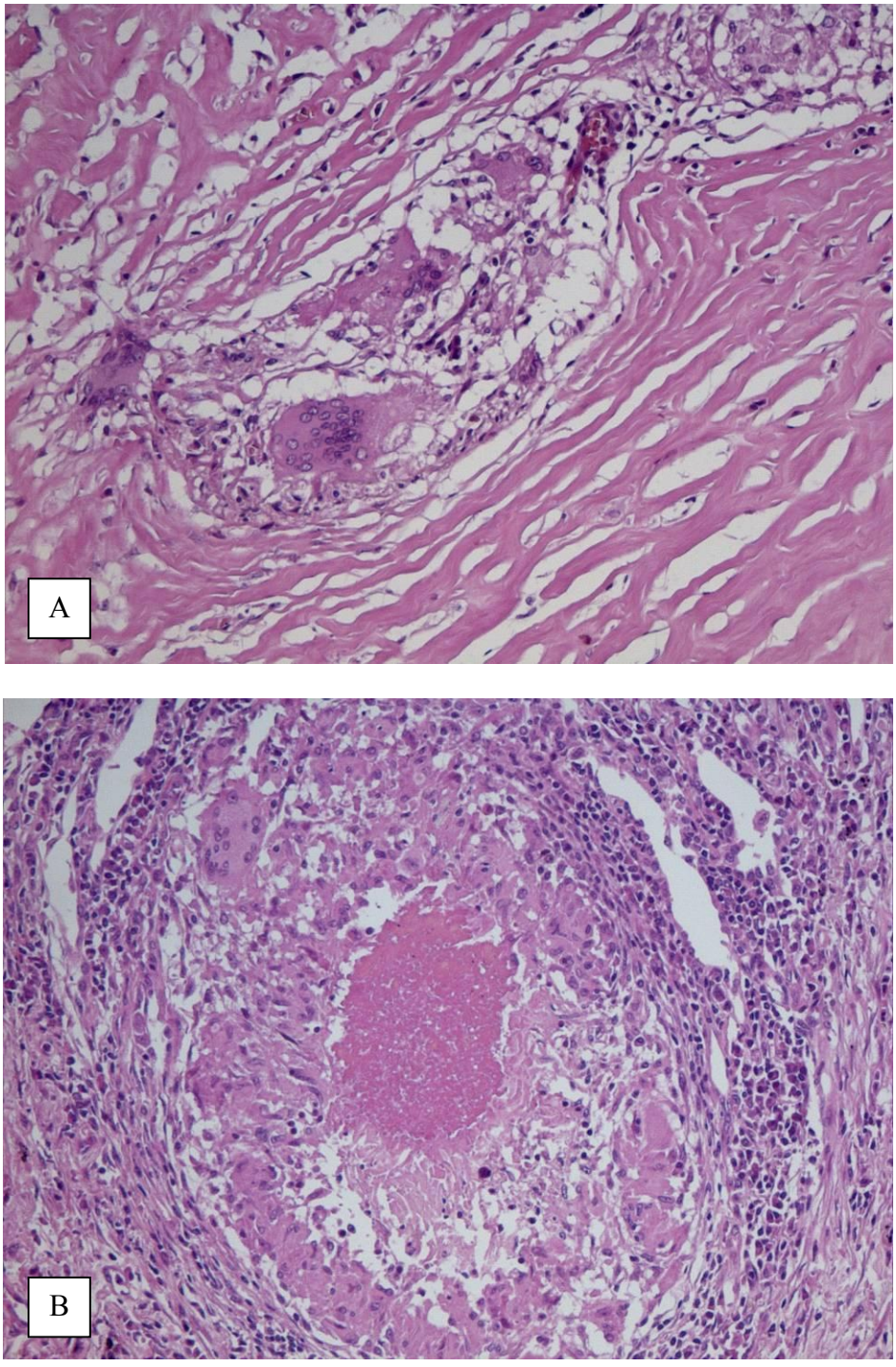

Figure 3.1 Human pulmonary TB granulomas are categorized into four stages Nascent (A: ×10) Caseous (B: ×10) Fibrocaseous (C: ×4) Resolved (D: ×4)

Figure 3.1 (Continued)

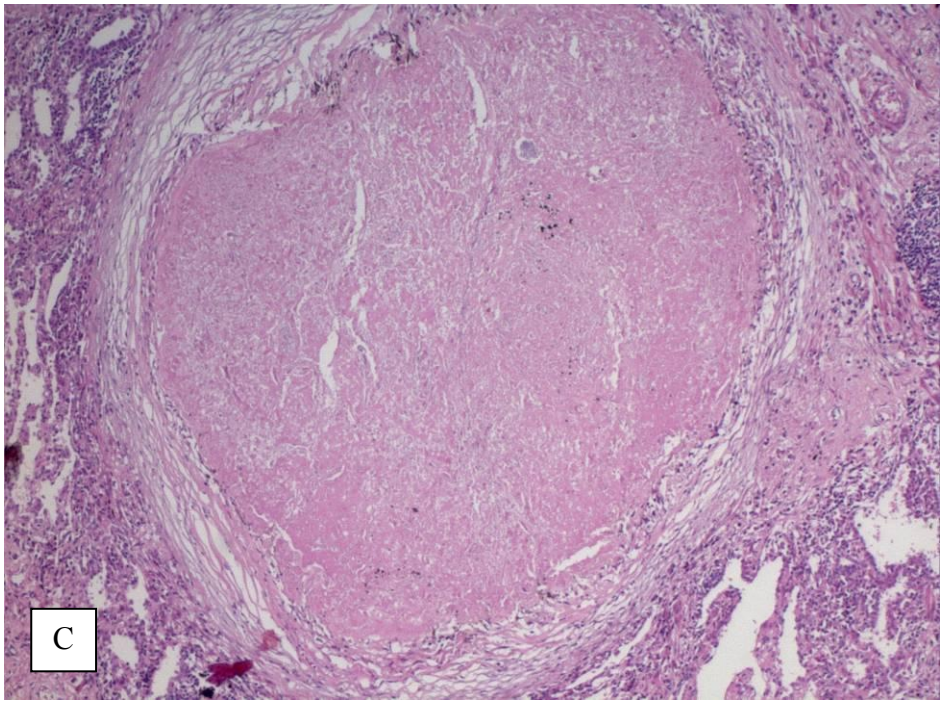

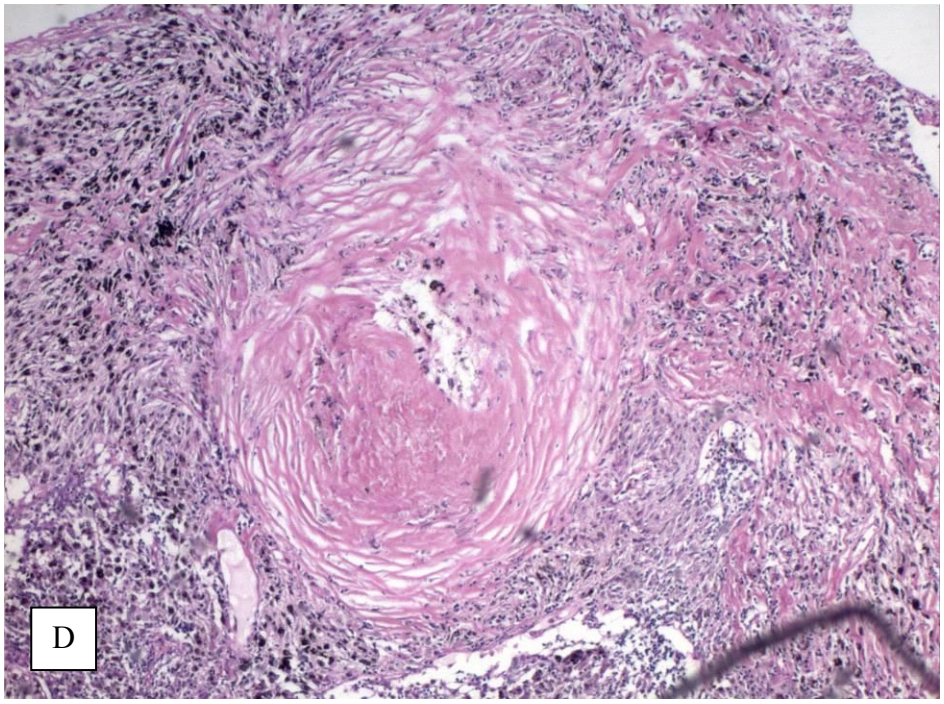

Figure 3.2 ADFP expression pattern at different stages of human pulmonary TB granulomas.
Representative images are shown here. The same exposure time was used for all of the images.
A: ADFP (red) expression in early granulomas (nuclei in blue) is shown here. Its corresponding area is shown in a box in B. ×20
B: H&E-stained early granuloma. ×10
C: ADFP (red) expression in caseous granulomas (nuclei in blue) is shown here. Its corresponding area is shown in a box in D. ×200
D: H&E-stained caseous granuloma. ×1.25
E: ADFP (red) expression in fibrocaseous granulomas (nuclei in blue) is shown here. Its corresponding area is shown in a box in F. ×20
F: H&E-stained fibrocaseous granuloma. ×1.25
G: ADFP (red) expression at the caseous center (nuclei in blue). Its corresponding area is shown in a box in H. ×20
H: H&E-stained caseous granuloma. ×4
I: ADFP (red) expression in resolved granulomas (nuclei in blue) is shown here. Its corresponding area is shown in a box in I. ×20
J: H&E-stained caseous granuloma. ×4
K: ADFP (red) expression in normal lung parenchyma (nuclei in blue). ×20

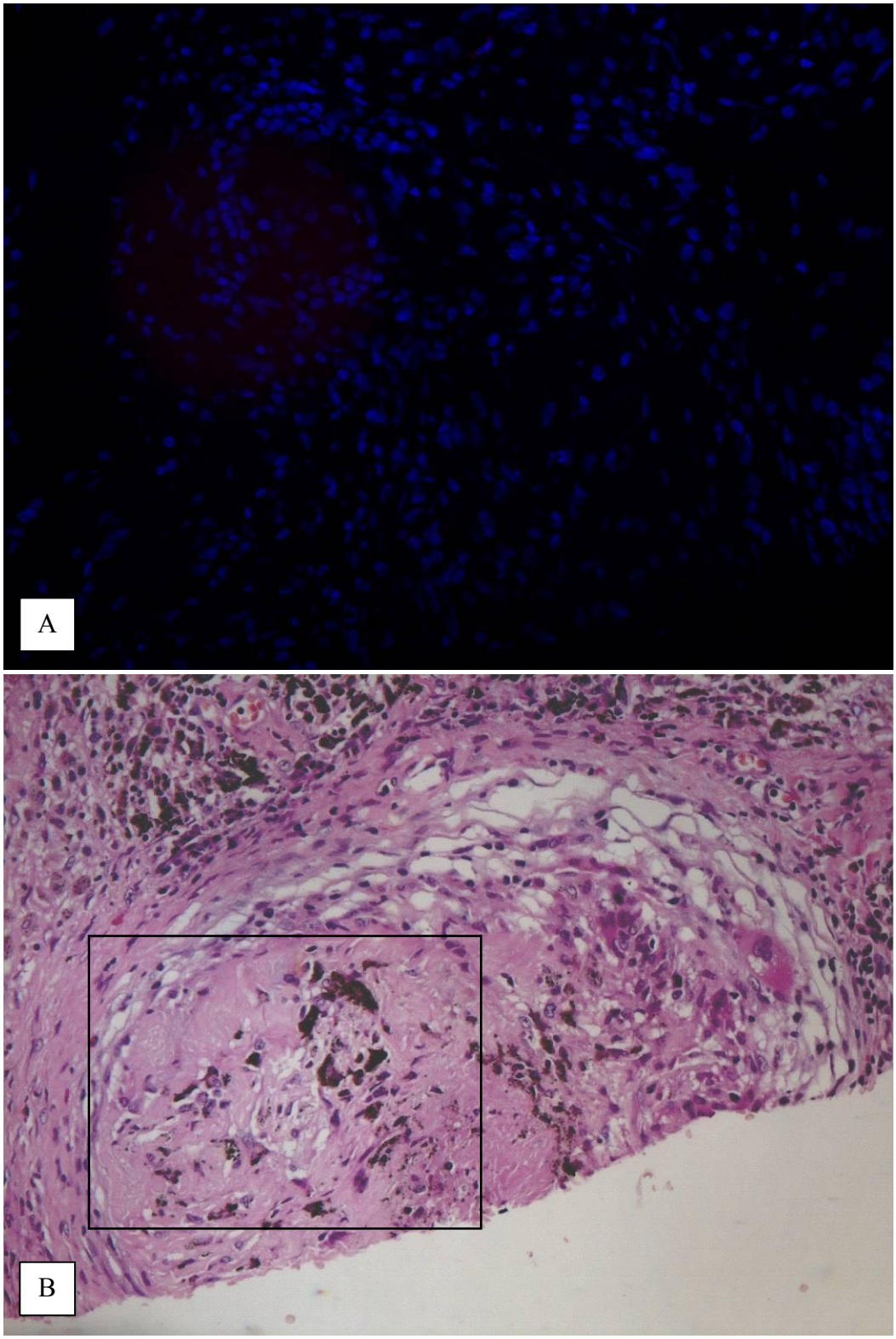
A
B

Figure 3.2 (Continued)

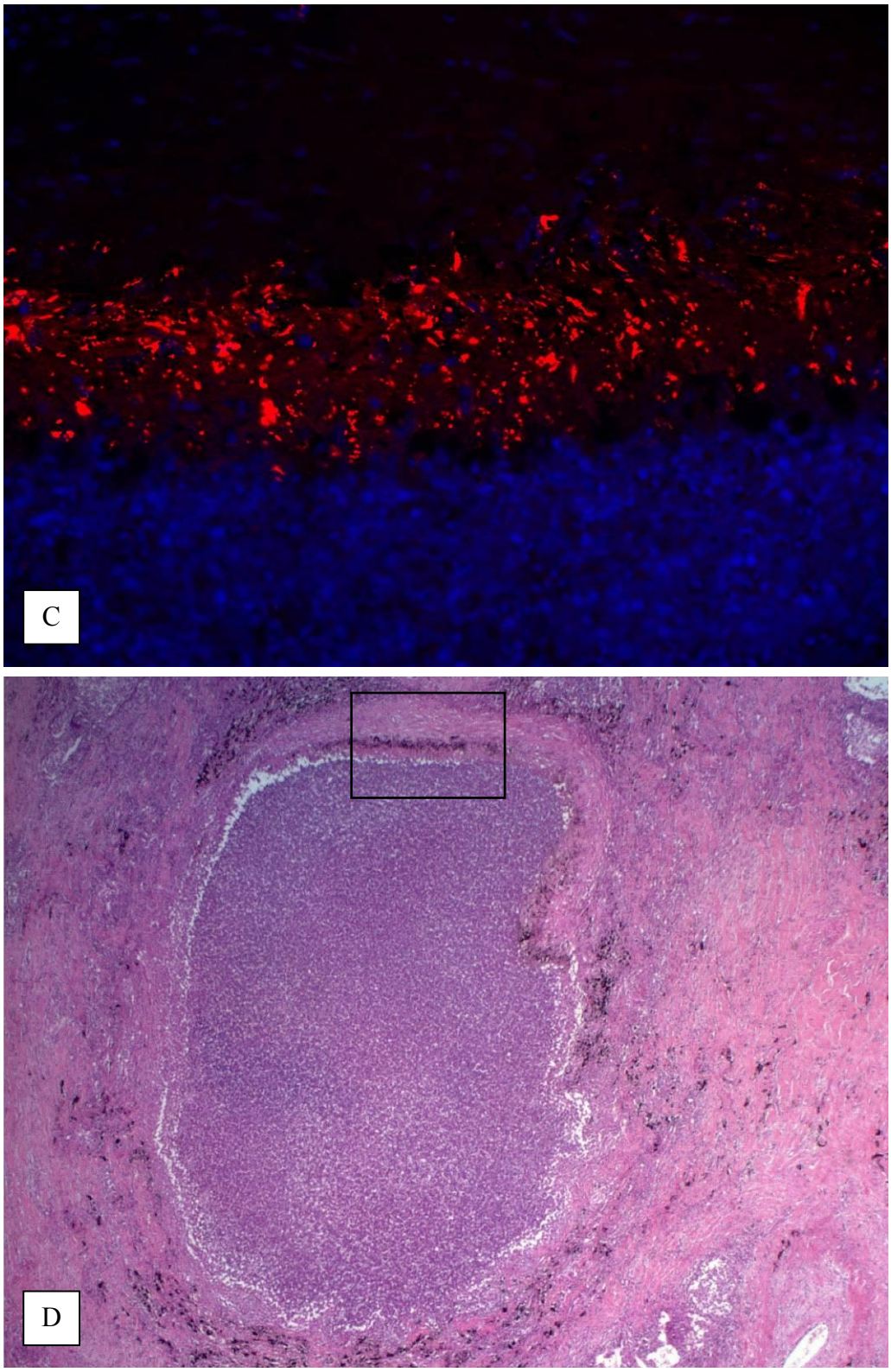

Figure 3.2 (Continued)

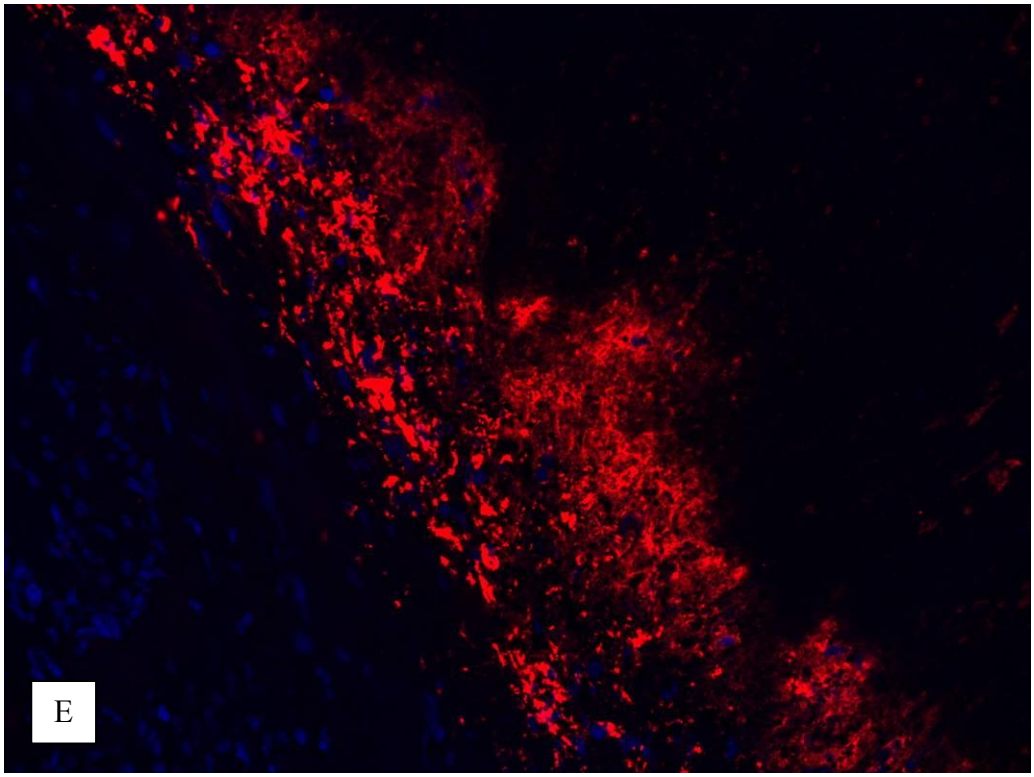

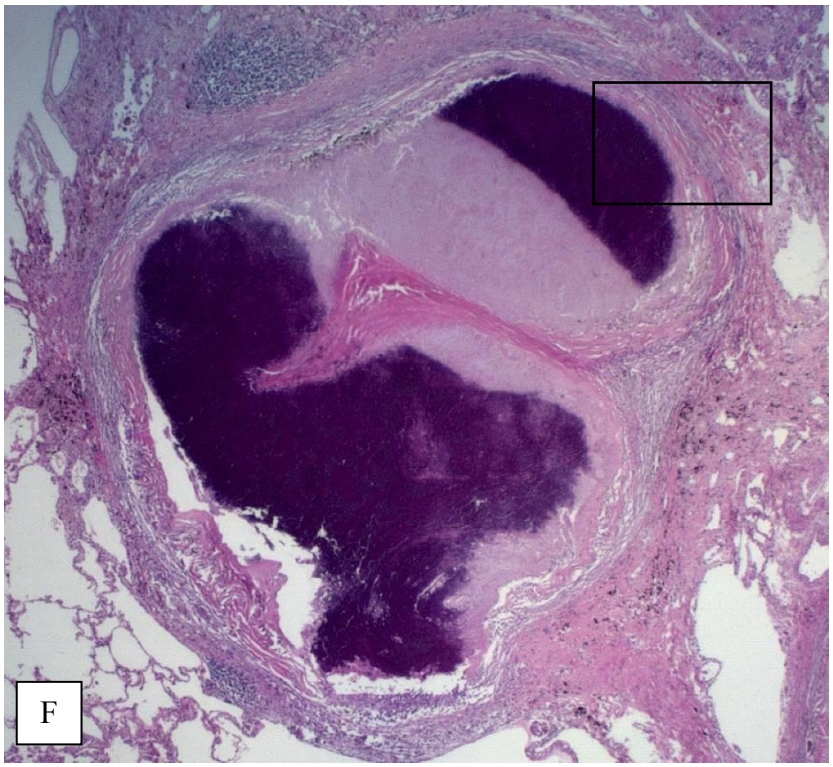

Figure 3.2 (Continued)

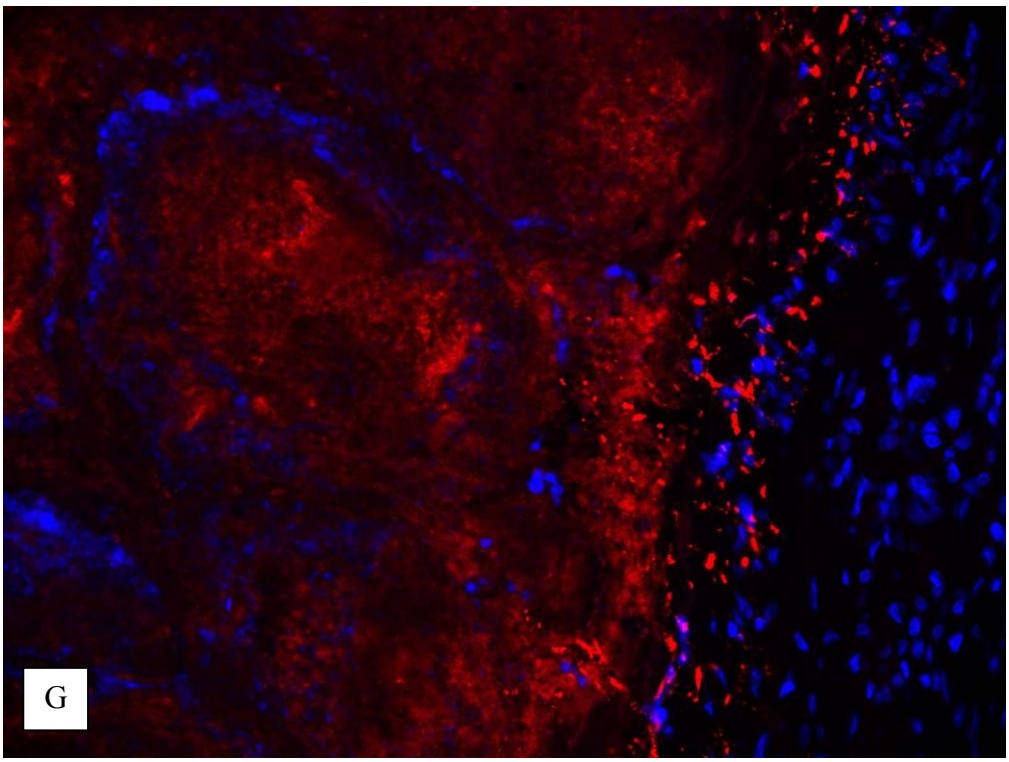

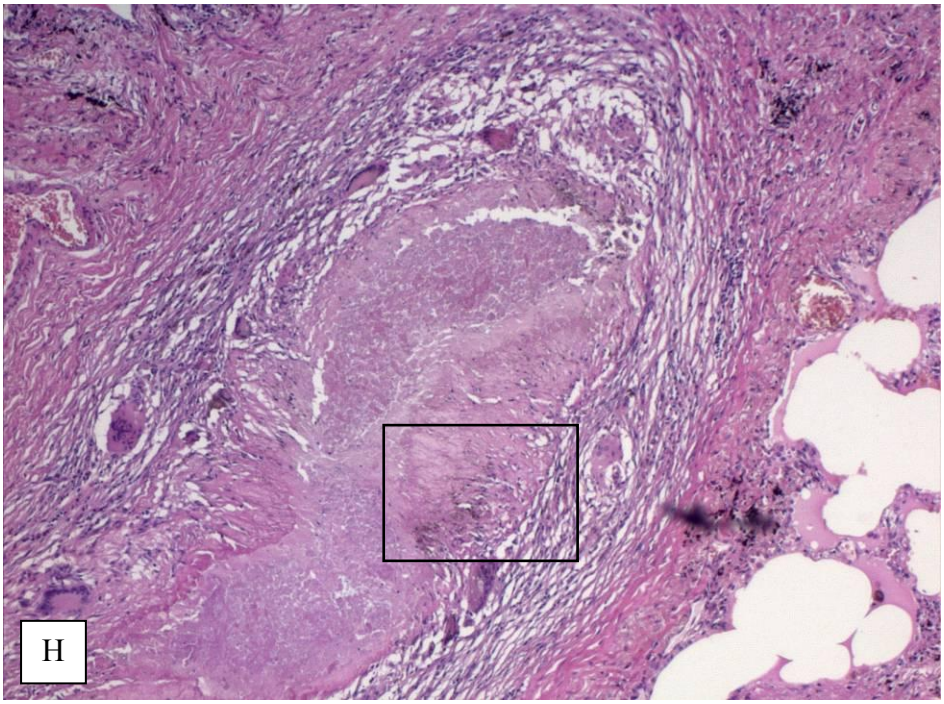

Figure 3.2 (Continued)

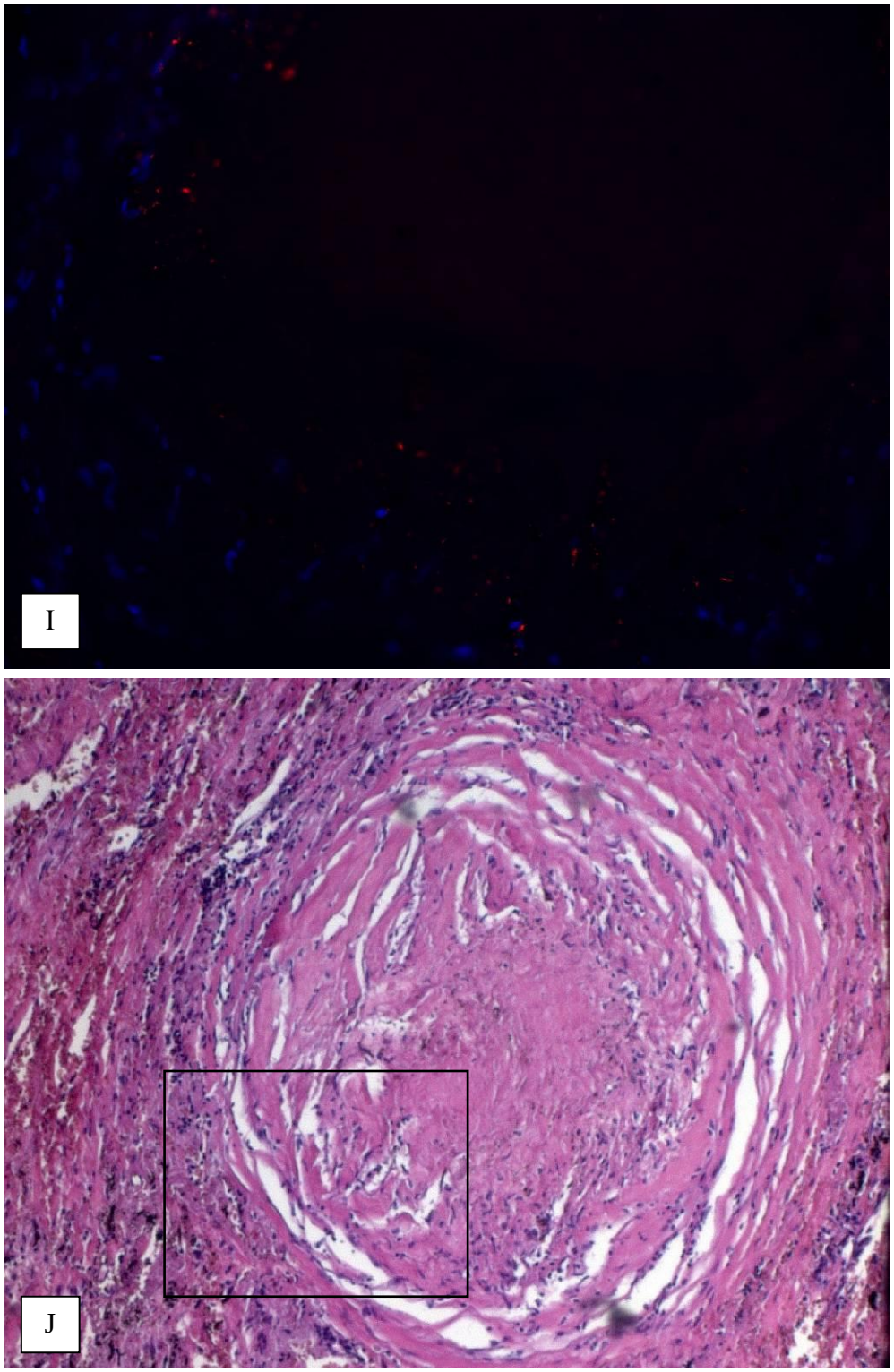

Figure 3.2 (Continued)

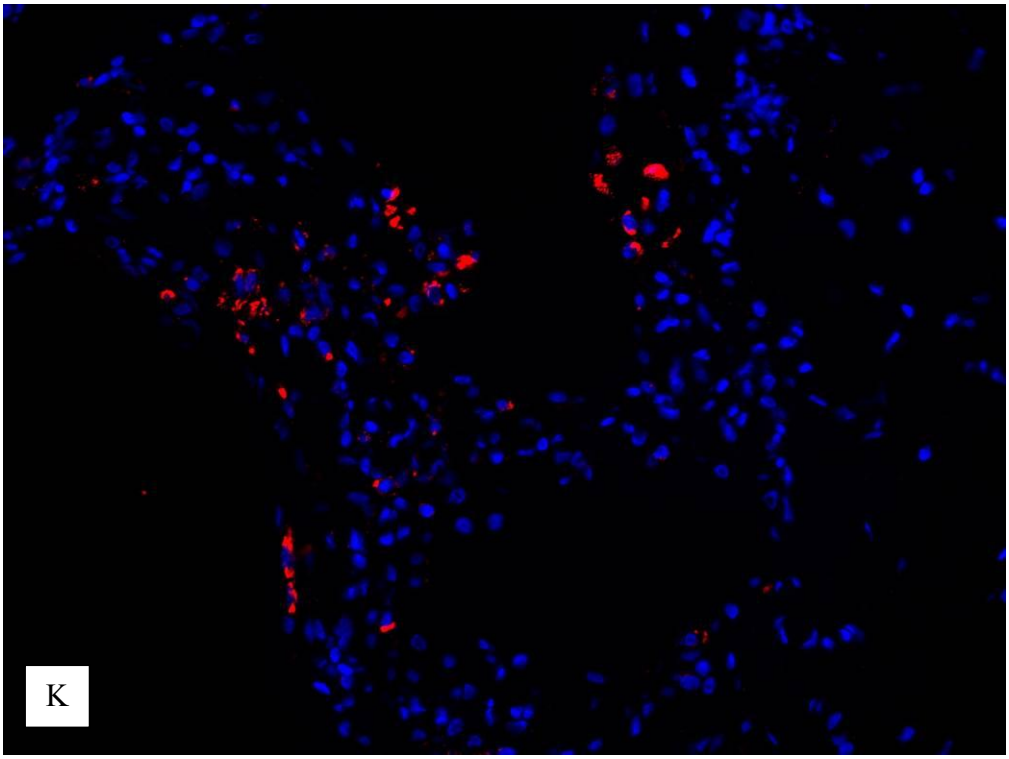

with nuclear debris, indicating that the lipids of the caseum were likely derived from lipid droplets sequestered within foam cells upon apoptotic or necrotic cell death (Figure 3.2 G&H). Finally, resolved or calcified granulomas lacked detectable ADFP label (Figure 3.2 I&J). Type II pneumocytes produce surfactant proteins to reduce surface tension, and the surfactant proteins are recycled by type II pneumocytes and alveolar macrophages. As a result, those cells possess lipid droplets, and ADFP was detected in healthy lung parenchyma (Figure 3.2 K).

The expression pattern of ACSL1 was very similar to that of ADFP. Nascent granulomas had almost no staining, while MGCs occasionally showed very weak staining (Figure 3.3 A&B). In contrast, the cellular regions subtending the capsules of caseous and fibrocaseous granulomas were robustly stained with ACSL1 antibody (Figure 3.3 C-F). Similar to ADFP, resolved granulomas showed no ACSL1 expression, with the exception of a few cells (Figure 3.3 G&H). Since ACSL1 is important for normal cellular functions, it was detectable in the normal lung parenchyma (Figure 3.3 I).

SapC expression was different from both ADFP and ACSL1 in that it was strongly expressed in macrophages and MGCs even in nascent granulomas (Figure 3.4 A&B). In caseous and fibrocaseous granulomas, SapC was expressed along the capsule that contained many macrophages and MGCs (Figure 3.4 C–F). Similarly to ADFP and ACSL1, SapC expression was not detected in resolved granulomas (Figure 3.4 G&H). By immunohistology, there was no detectable level of SapC expression in normal lung tissues (data not shown).

In addition to the detection of proteins involved in lipid synthesis and accumulation, lipid-laden foam cells were frequently seen in caseous granulomas and in the alveoli and respiratory bronchioles (Figure 3.5 A&B). Lipids were readily detected by neutral lipid staining (Figure 3.5 C&D).

Figure 3.3 ACSL1 expression pattern at different stages of human pulmonary TB granulomas. Representative images are shown here. The same exposure time was used for all of the images.
A: ACSL1 (red) expression in early granulomas (nuclei in blue) is shown here. Its corresponding area is shown in a box in B. ×20
B: H&E-stained early granuloma. ×10
C: ACSL1 (red) expression in caseous granulomas (nuclei in blue) is shown here. Its corresponding area is shown in a box in D. ×20
D: H&E-stained caseous granuloma. ×4
E: ACSL1 (red) expression in fibrocaseous granulomas (nuclei in blue) is shown here. Its corresponding area is shown in a box in F. ×20
F: H&E-stained fibrocaseous granuloma. ×4
G: ACSL1 (red) expression in resolved granulomas (nuclei in blue) is shown here. Its corresponding area is shown in a box in I. ×20
H: H&E-stained caseous granuloma. ×4
I: ACSL1 (red) expression in normal lung parenchyma (nuclei in blue). ×20

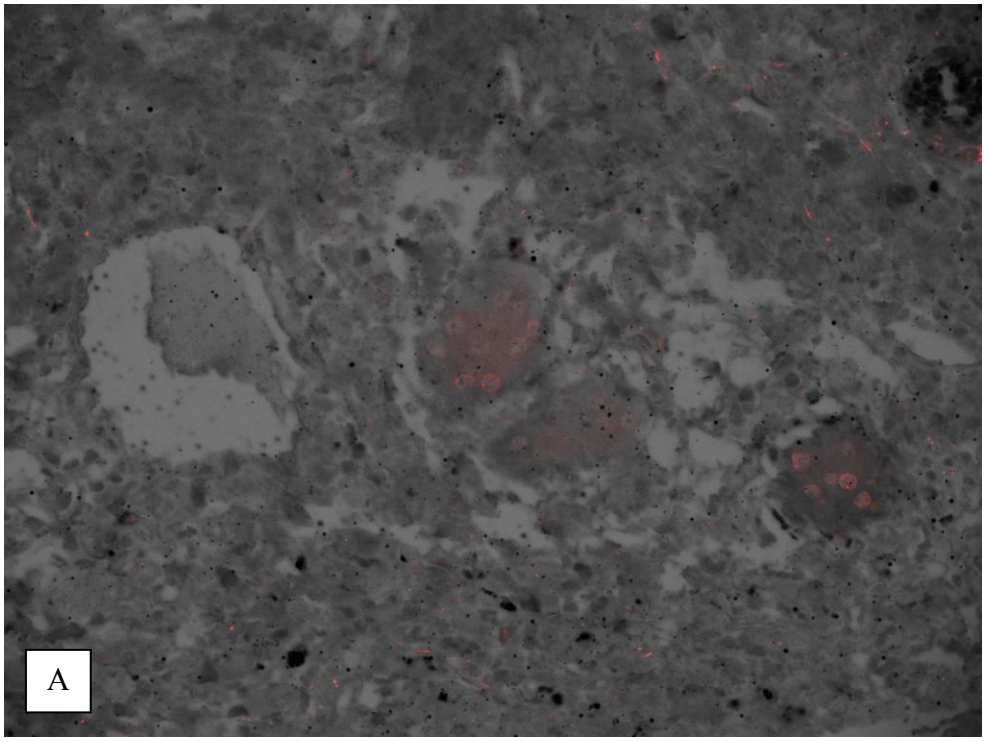
A

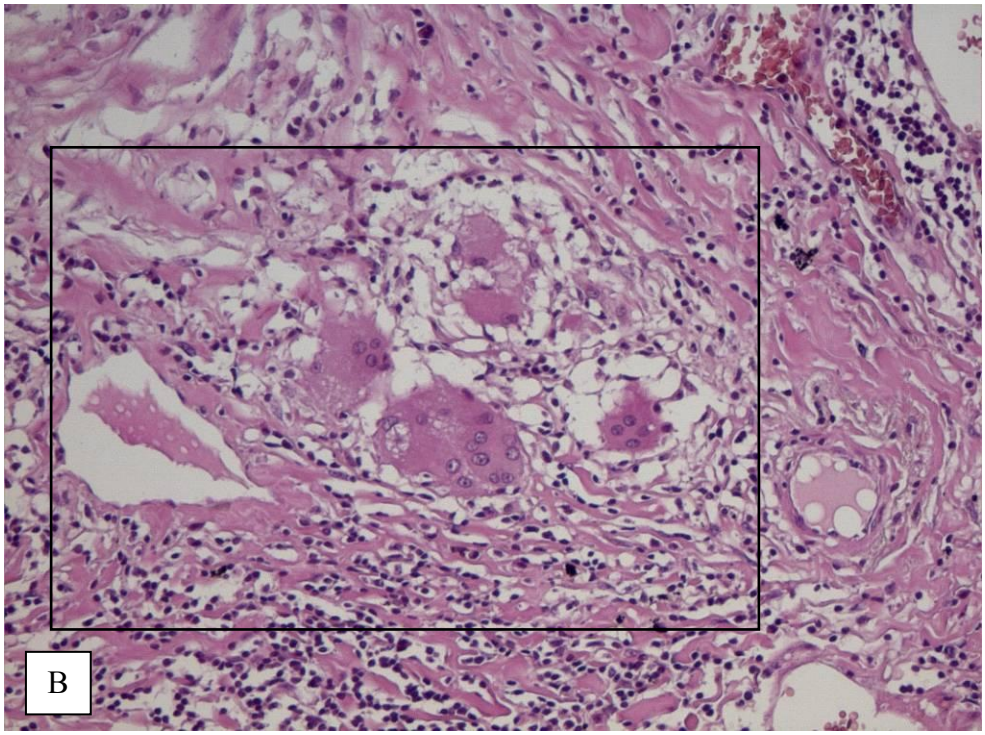
B

Figure 3.3 (Continued)

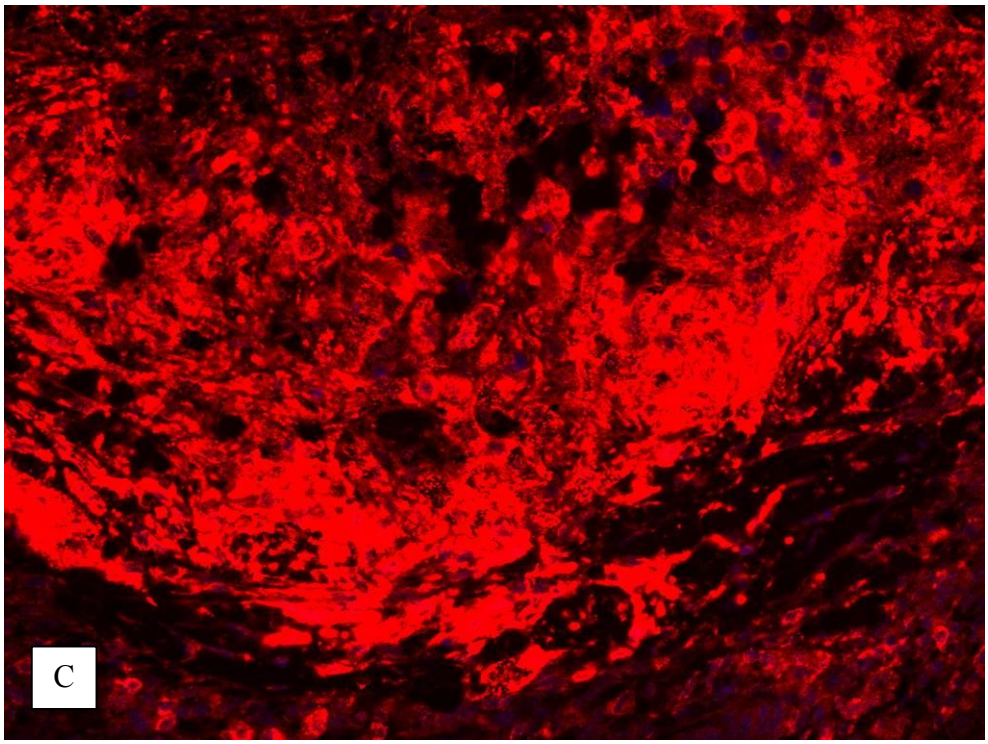

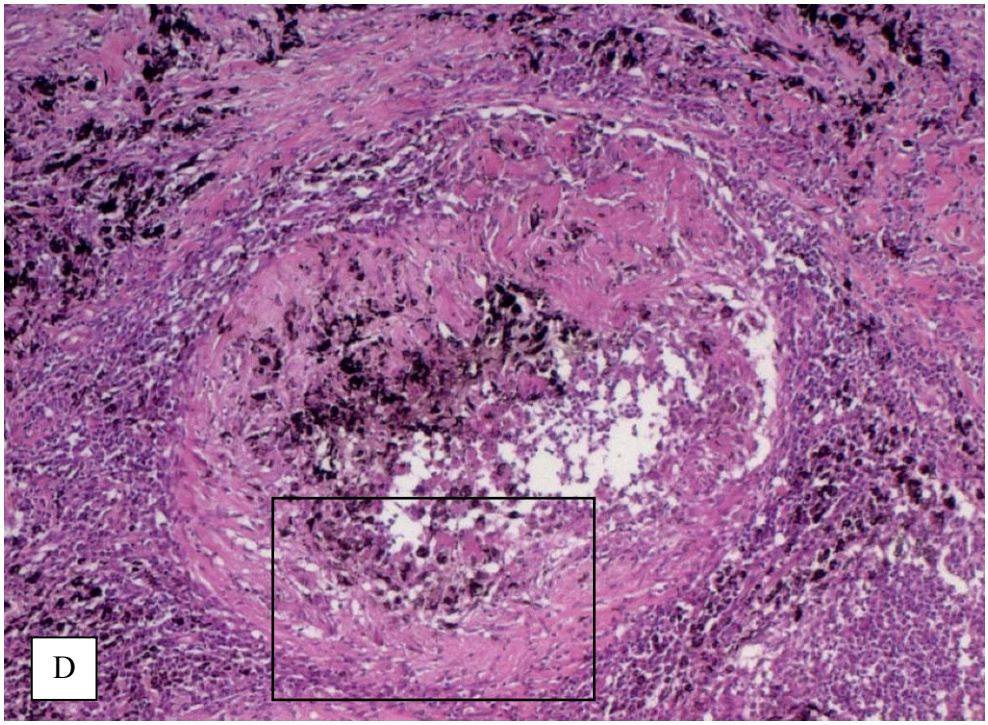

Figure 3.3 (Continued)

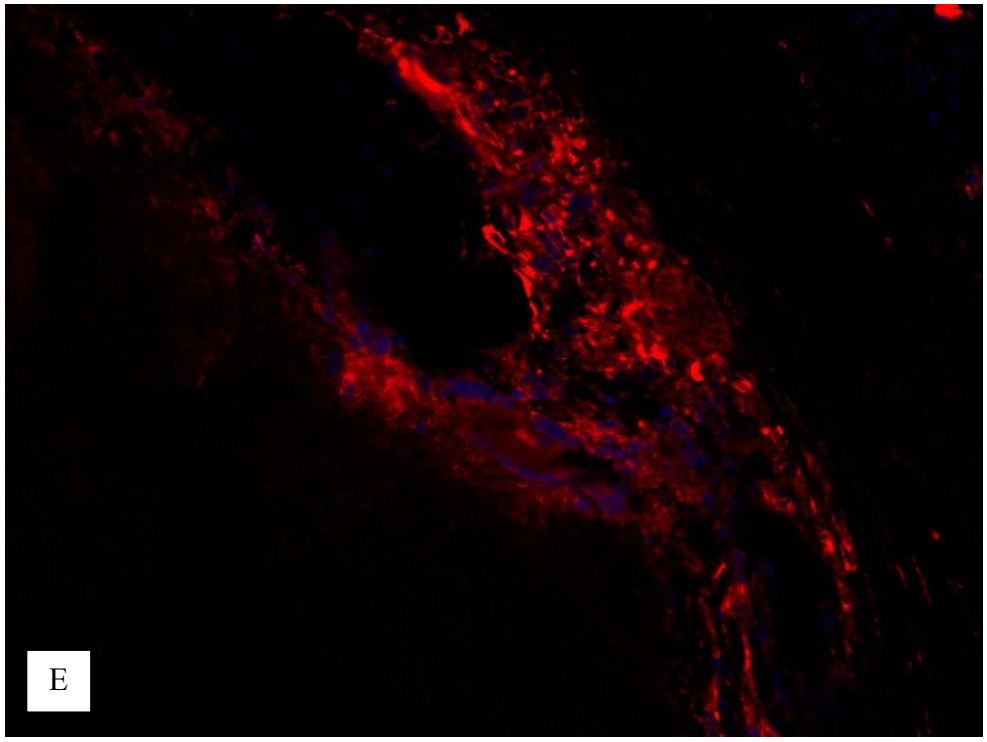

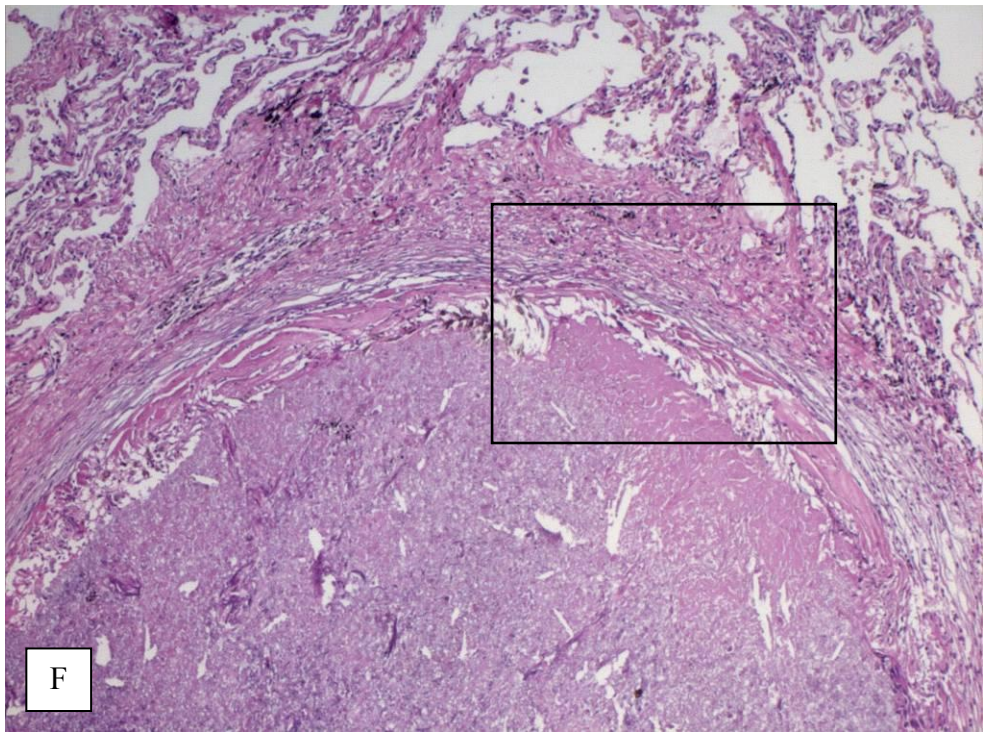

Figure 3.3 (Continued)

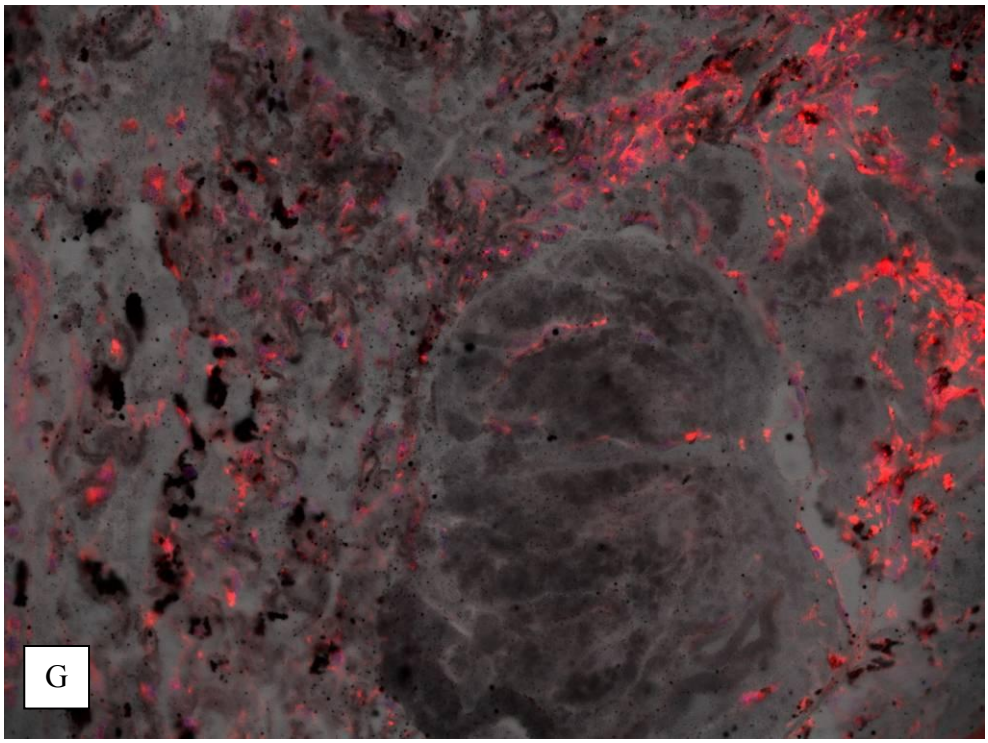

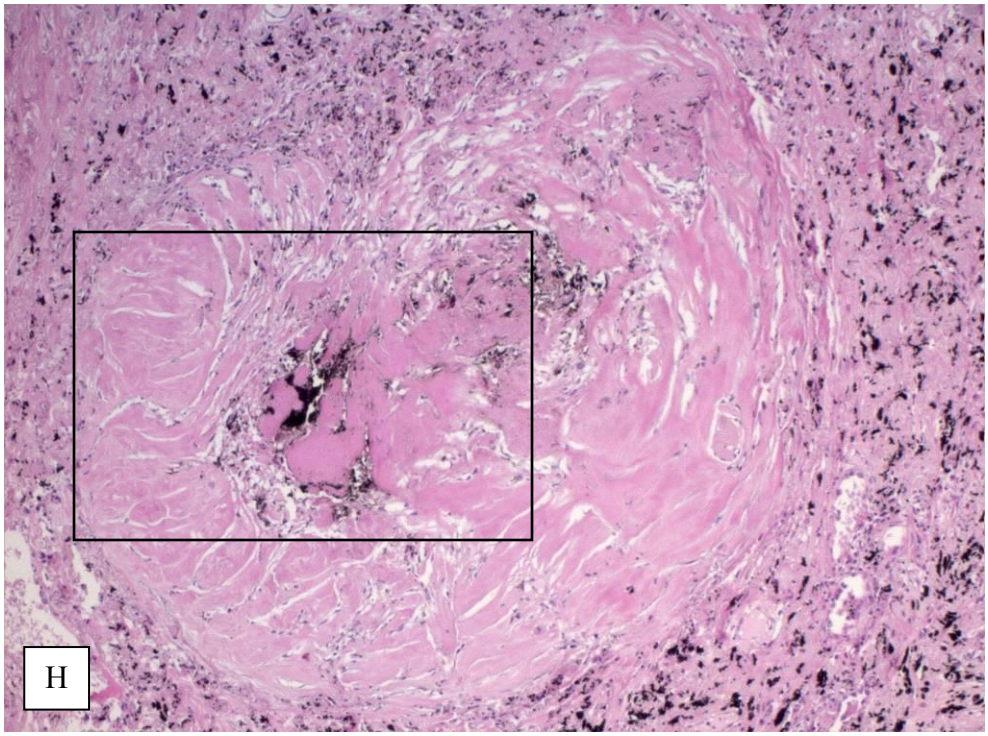

Figure 3.3 (Continued)

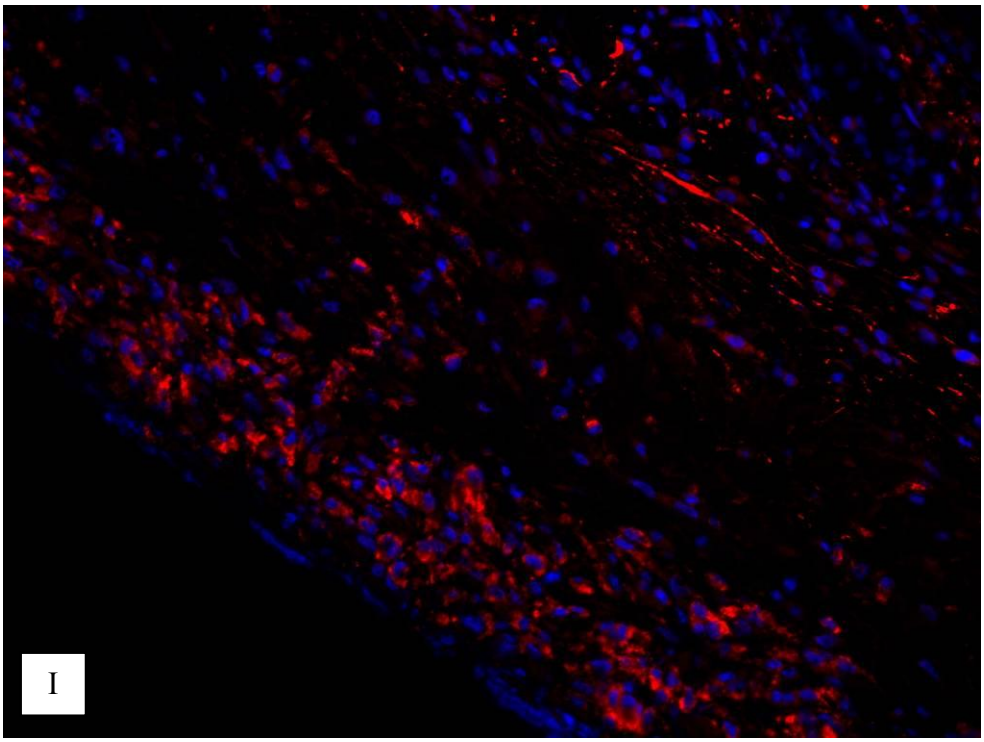

Figure 3.4 SapC expression pattern at different stages of human pulmonary TB granulomas.
Representative images are shown here.
A: SapC (red) expression in early granulomas (nuclei in blue) is shown here. Its corresponding area is shown in a box in B. ×20
B: H&E-stained early granuloma. ×10
C: SapC (red) expression in caseous granulomas (nuclei in blue) is shown here. Its corresponding area is shown in a box in D. ×20
D: H&E-stained caseous granuloma. ×4
E: SapC (red) expression in fibrocaseous granulomas (nuclei in blue) is shown here. Its corresponding area is shown in a box in F. ×20
F: H&E-stained fibrocaseous granuloma. ×1.25
G: SapC (red) expression in resolved granulomas (nuclei in blue) is shown here. Its corresponding area is shown in a box in I. ×20
H: H&E-stained caseous granuloma. ×4

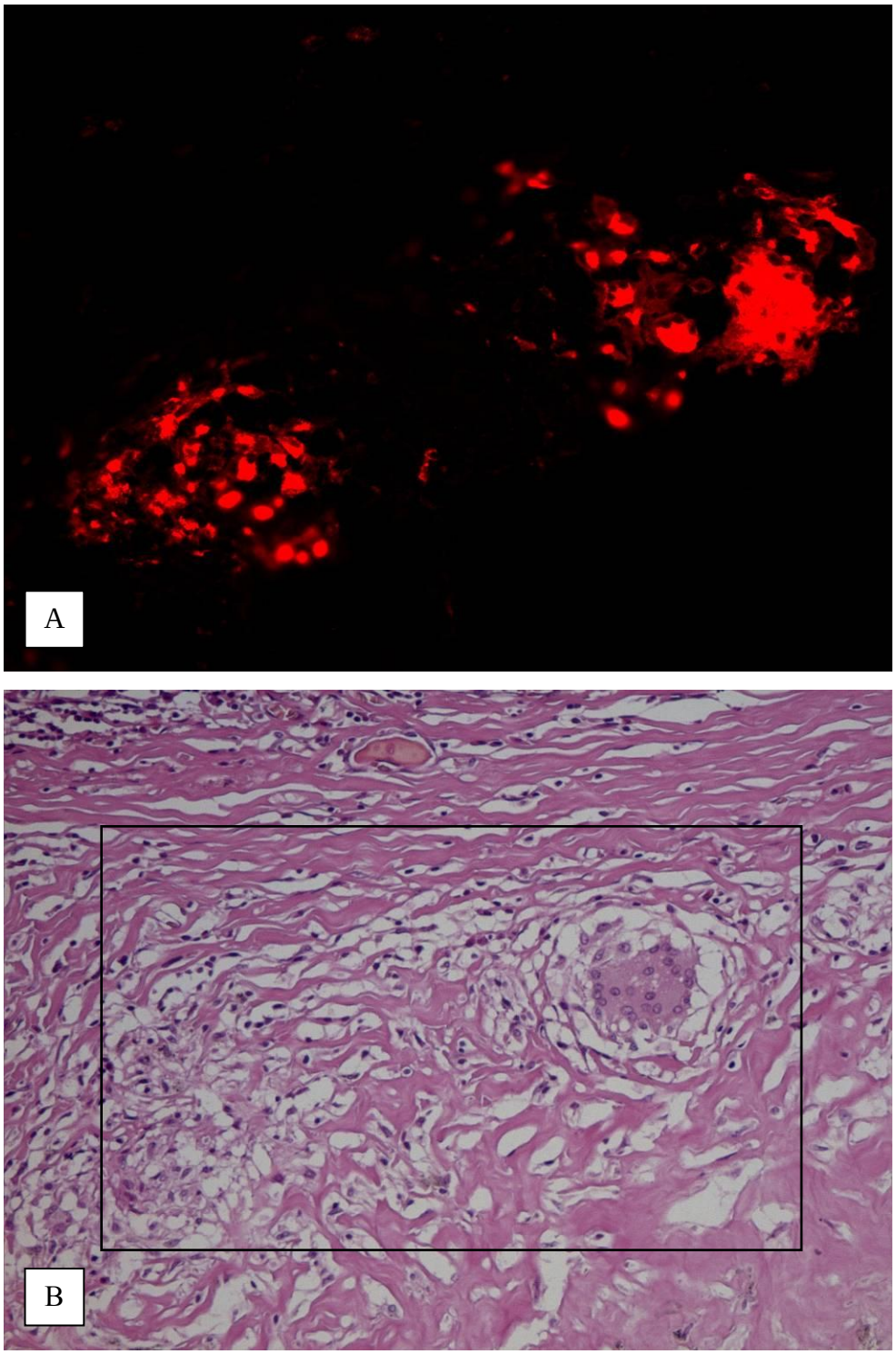
A
B

Figure 3.4 (Continued)

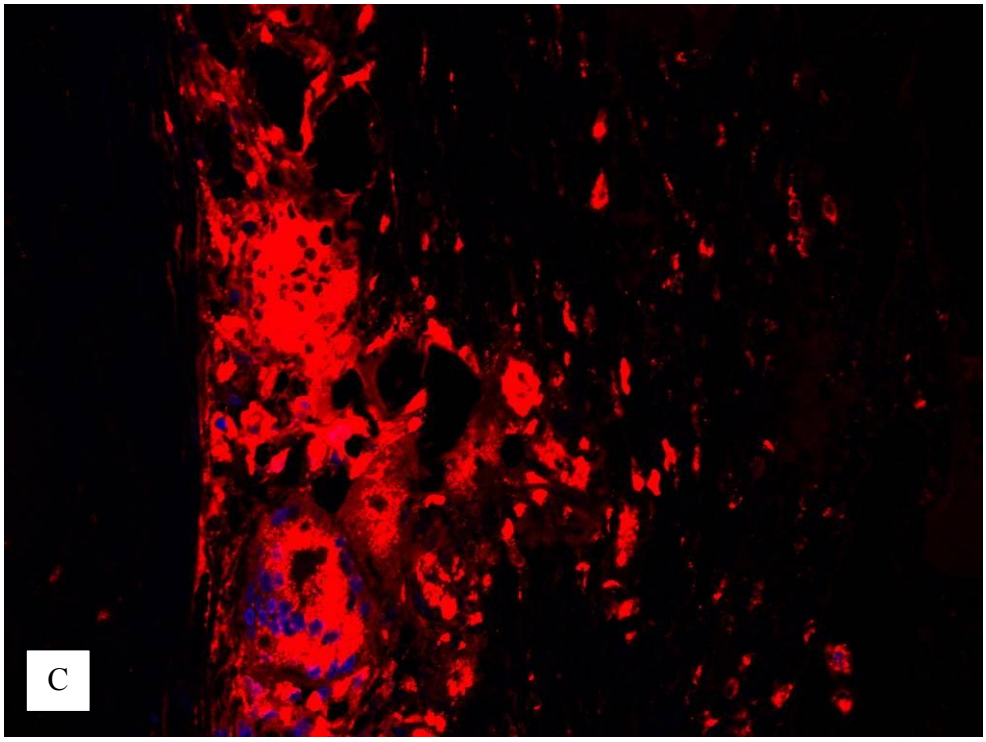

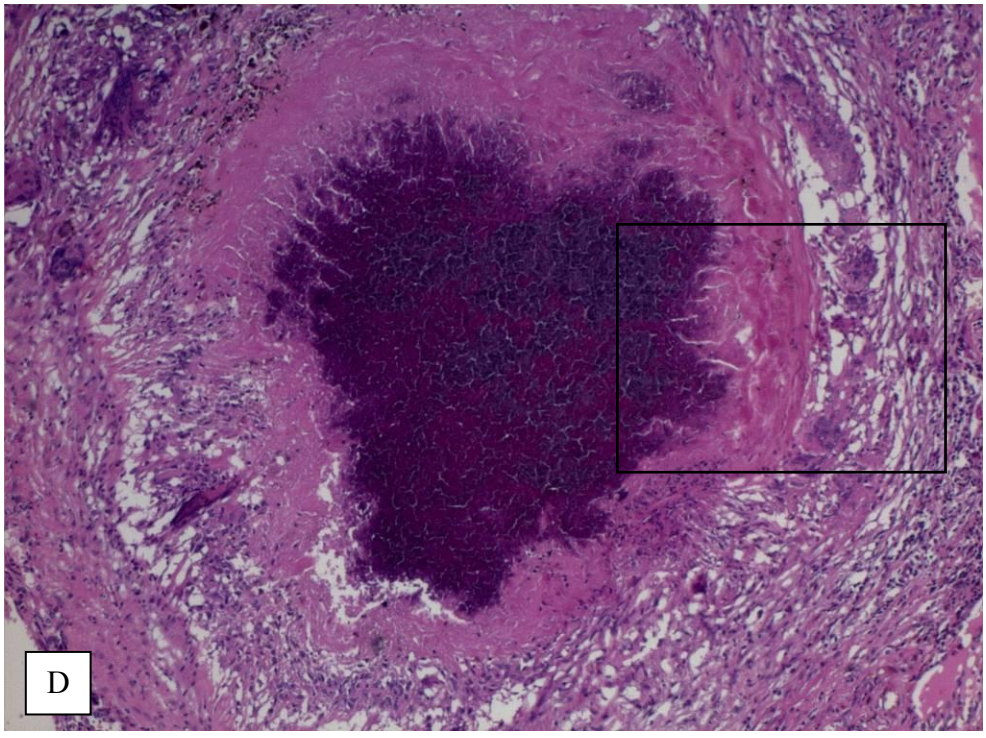

Figure 3.4 (Continued)

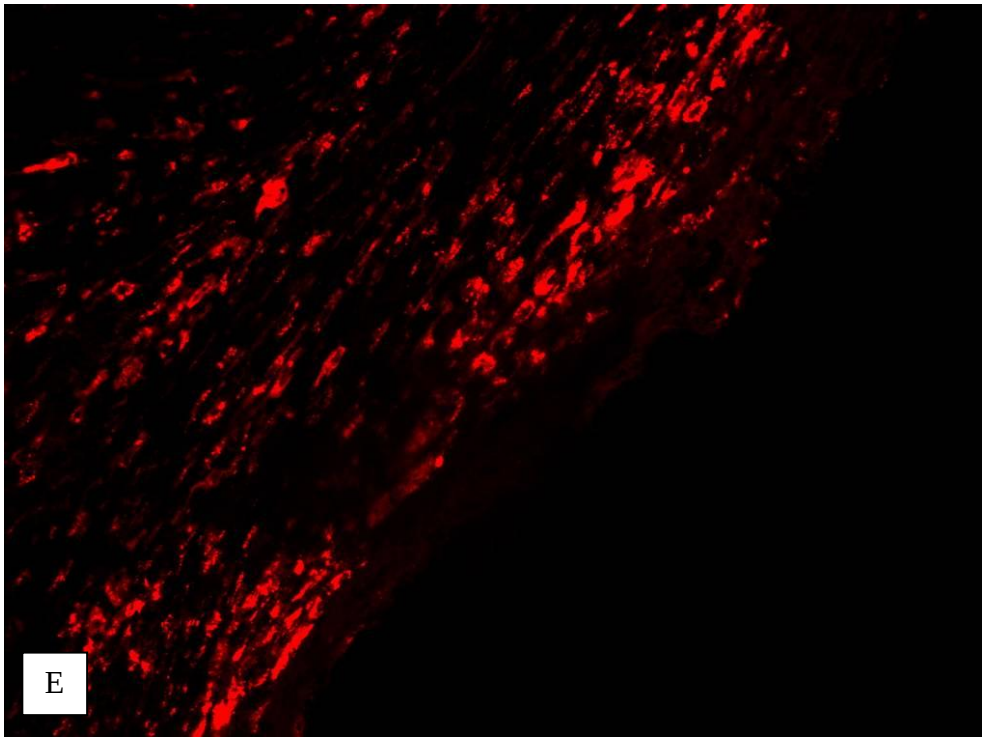

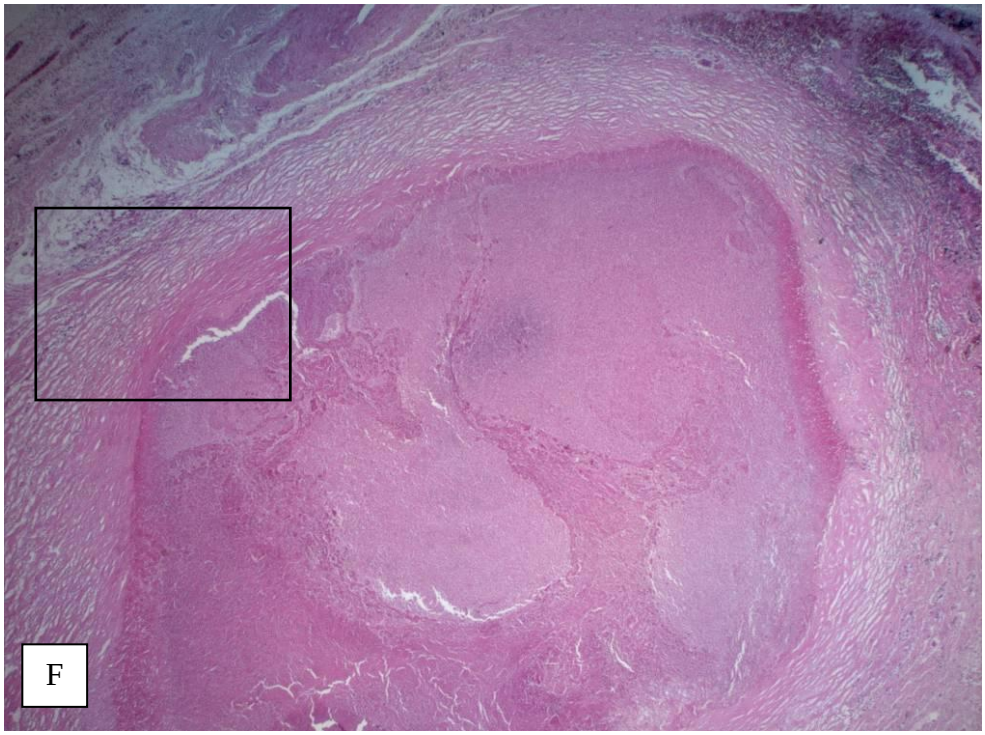

Figure 3.4 (Continued)

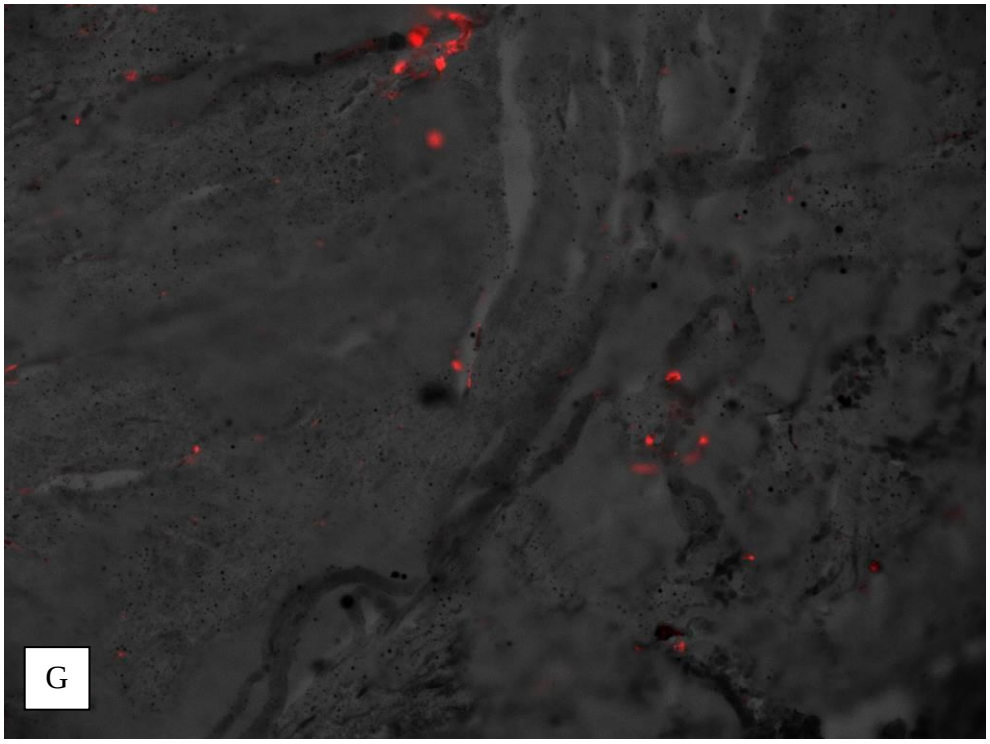

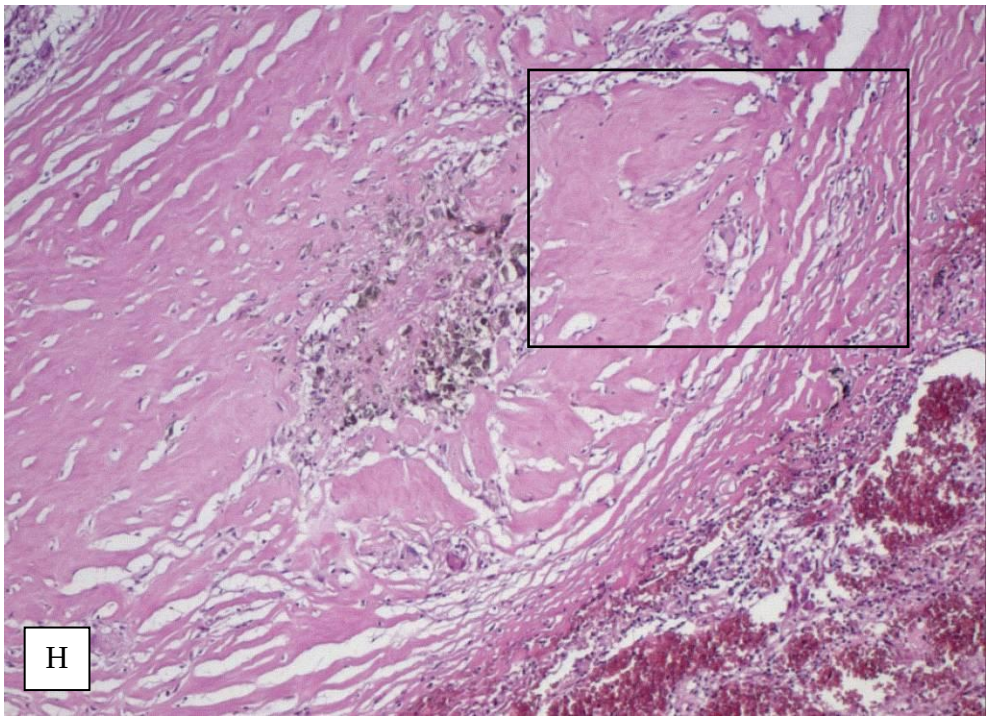

Figure 3.5 Lipid-laden foam cells in caseous granulomas and alveolar spaces. Alveoli and respiratory bronchioles are full of foamy macrophages (A: ×20, H&E on paraffin section, C: Oil red O staining for neutral lipids on cryosection). Foam cells are present at the periphery of caseous granulomas (B: ×20, H&E on paraffin section, D: Oil red O staining for neutral lipids on cryosection).
Arrows indicate foam cells.

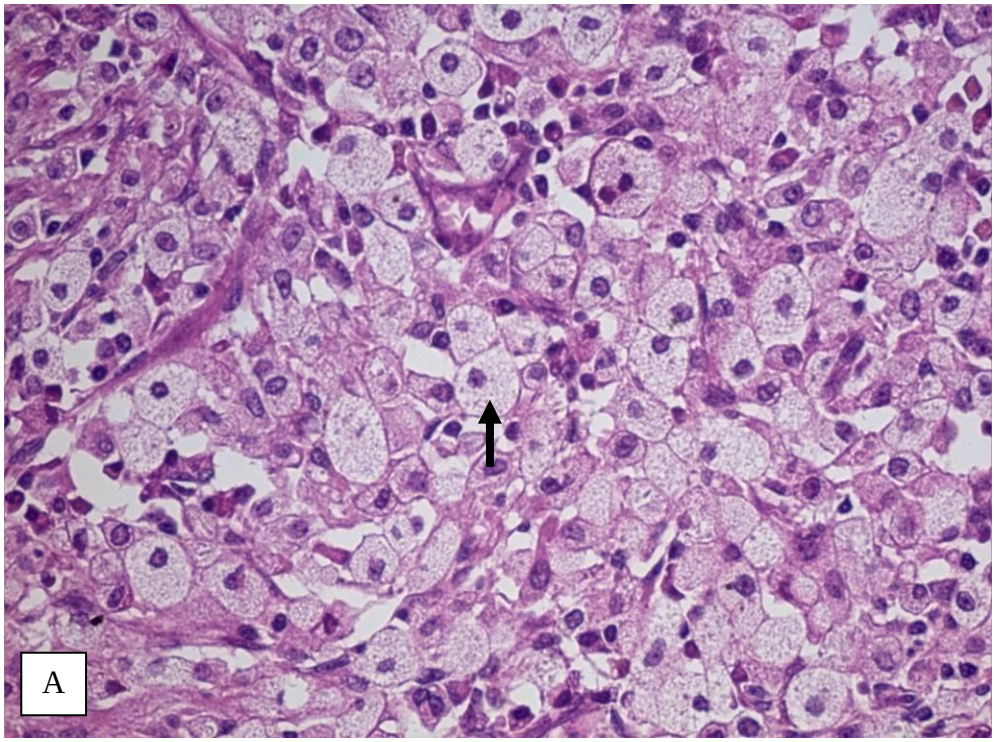
A

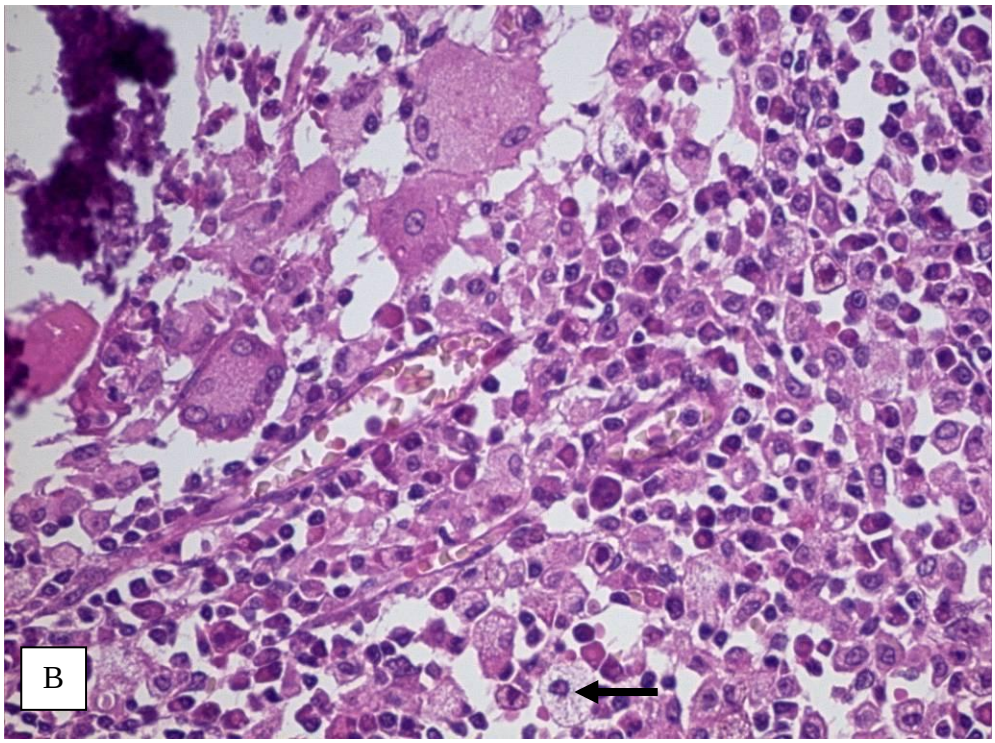
B

Figure 3.5 (Continued)

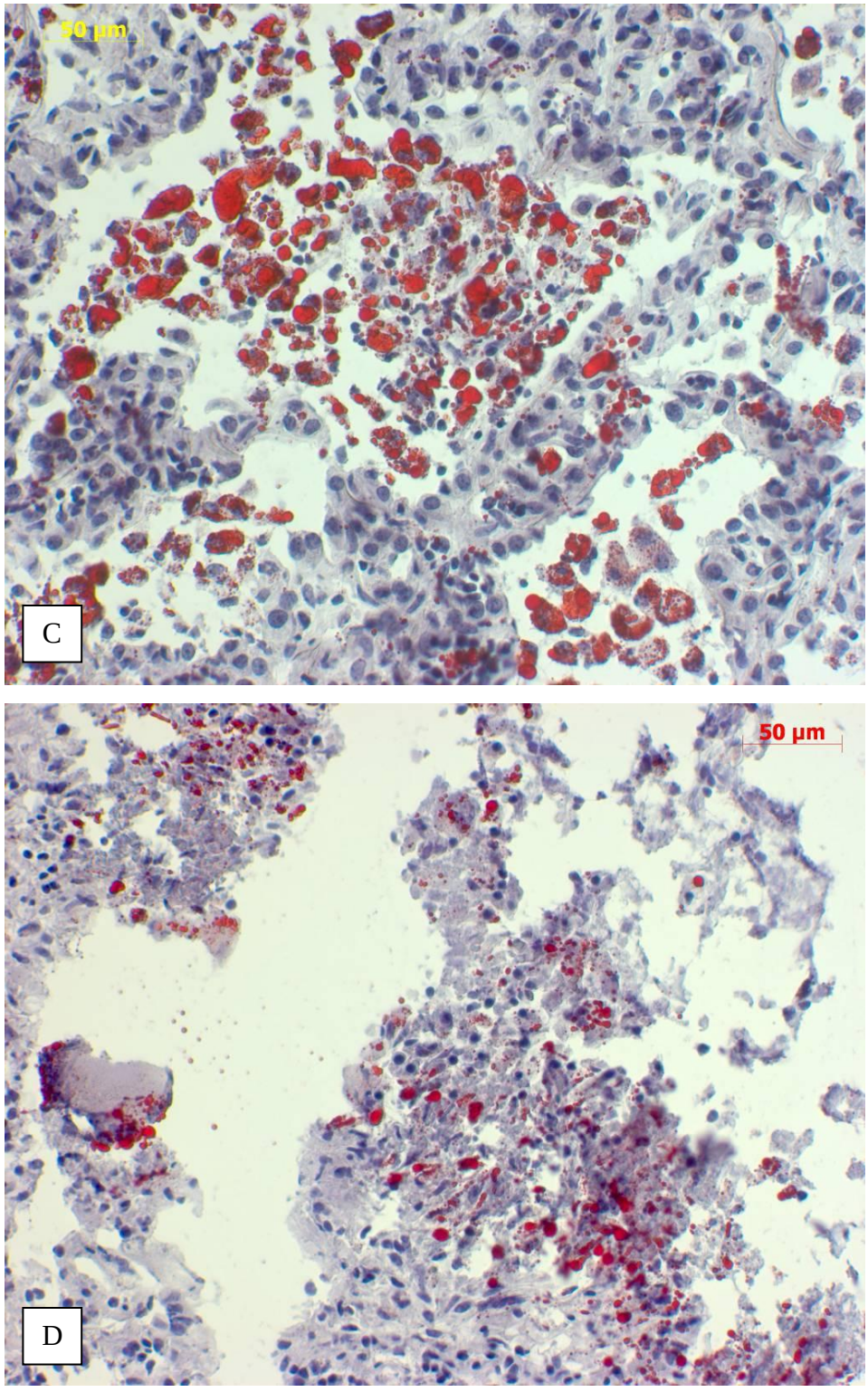

The immunohistological analysis of human TB granulomas has generated a picture that enables us to form a more dynamic interpretation of granuloma progression. Both ADFP and ACSL1 play a role in lipid accumulation through either sequestration or *de novo* synthesis, and the increased expression of ADFP and ACSL1 in caseous and fibrocaseous granulomas indicates that the advanced form of TB granulomas accumulate lipids. In contrast to ADFP and ACSL1, SapC was expressed very strongly in nascent granulomas, and this may indicate that cells undergo a metabolic shift early on before starting to accumulate the massive amount of lipids in the form of caseum. SapC in TB granulomas may play a role in transferring Mtb lipid antigens for T cell activation.

The data presented here provide compelling evidence that the development of the lipid-rich caseum in the human TB granuloma results from a re-alignment in lipid metabolism within the granuloma. Ongoing and future studies include the investigation of specific host and Mtb factors that drive the accumulation of lipids inside TB granulomas. Investigations to understand the temporal and spatial regulation of lipid metabolism in human TB granulomas of different stages are warranted.

ACKNOWLEDGEMENTS

I would like to thank Drs. Helen Wainwright, Christopher Maske, and Michael Locketz and Ms. Annalie Visser for providing human tissues and inputs while I was performing immunohistology in Cape Town, South Africa.

REFERENCES

1. Farer, L.S., A.M. Lowell, and M.P. Meador, *Extrapulmonary tuberculosis in the United States.* Am J Epidemiol, 1979. **109**(2): p. 205-17.
2. Small, P.M., et al., *Treatment of tuberculosis in patients with advanced human immunodeficiency virus infection.* N Engl J Med, 1991. **324**(5): p. 289-94.
3. Havlir, D.V. and P.F. Barnes, *Tuberculosis in patients with human immunodeficiency virus infection.* N Engl J Med, 1999. **340**(5): p. 367-73.
4. Desruisseaux, M.S., et al., *Adipocyte, adipose tissue, and infectious disease.* Infect Immun, 2007. **75**(3): p. 1066-78.
5. Ducharme, N.A. and P.E. Bickel, *Lipid droplets in lipogenesis and lipolysis.* Endocrinology, 2008. **149**(3): p. 942-9.
6. Guilherme, A., et al., *Adipocyte dysfunctions linking obesity to insulin resistance and type 2 diabetes.* Nat Rev Mol Cell Biol, 2008. **9**(5): p. 367-77.
7. McLauchlan, J., *Lipid droplets and hepatitis C virus infection.* Biochim Biophys Acta, 2009. **1791**(6): p. 552-9.
8. Murphy, D.J., *The biogenesis and functions of lipid bodies in animals, plants and microorganisms.* Prog Lipid Res, 2001. **40**(5): p. 325-438.
9. Schmitz, G. and M. Grandl, *Lipid homeostasis in macrophages - implications for atherosclerosis.* Rev Physiol Biochem Pharmacol, 2008. **160**: p. 93-125.
10. Hunter, R.L., C. Jagannath, and J.K. Actor, *Pathology of postprimary tuberculosis in humans and mice: contradiction of long-held beliefs.* Tuberculosis (Edinb), 2007. **87**(4): p. 267-78.
11. Peyron, P., et al., *Foamy macrophages from tuberculous patients' granulomas constitute a nutrient-rich reservoir for M. tuberculosis persistence.* PLoS Pathog, 2008. **4**(11): p. e1000204.

12. D'Avila, H., et al., *Mycobacterium bovis bacillus Calmette-Guerin induces TLR2-mediated formation of lipid bodies: intracellular domains for eicosanoid synthesis in vivo.* J Immunol, 2006. **176**(5): p. 3087-97.

13. Dannenberg, A.M., Jr. and M. Sugimoto, *Liquefaction of caseous foci in tuberculosis.* Am Rev Respir Dis, 1976. **113**(3): p. 257-9.

14. Dannenberg, A.M., Jr., *Roles of cytotoxic delayed-type hypersensitivity and macrophage-activating cell-mediated immunity in the pathogenesis of tuberculosis.* Immunobiology, 1994. **191**(4-5): p. 461-73.

15. Robenek, H., et al., *Lipid droplets gain PAT family proteins by interaction with specialized plasma membrane domains.* J Biol Chem, 2005. **280**(28): p. 26330-8.

16. Chang, B.H. and L. Chan, *Regulation of Triglyceride Metabolism. III. Emerging role of lipid droplet protein ADFP in health and disease.* Am J Physiol Gastrointest Liver Physiol, 2007. **292**(6): p. G1465-8.

17. Bickel, P.E., J.T. Tansey, and M.A. Welte, *PAT proteins, an ancient family of lipid droplet proteins that regulate cellular lipid stores.* Biochim Biophys Acta, 2009. **1791**(6): p. 419-40.

18. Larigauderie, G., et al., *Adipophilin enhances lipid accumulation and prevents lipid efflux from THP-1 macrophages: potential role in atherogenesis.* Arterioscler Thromb Vasc Biol, 2004. **24**(3): p. 504-10.

19. Dalen, K.T., et al., *PPARalpha activators and fasting induce the expression of adipose differentiation-related protein in liver.* J Lipid Res, 2006. **47**(5): p. 931-43.

20. Edvardsson, U., et al., *PPARalpha activation increases triglyceride mass and adipose differentiation-related protein in hepatocytes.* J Lipid Res, 2006. **47**(2): p. 329-40.

21. Gao, J. and G. Serrero, *Adipose differentiation related protein (ADRP) expressed in transfected COS-7 cells selectively stimulates long chain fatty acid uptake.* J Biol Chem, 1999. **274**(24): p. 16825-30.

22. Wang, X., et al., *Induced expression of adipophilin mRNA in human macrophages stimulated with oxidized low-density lipoprotein and in atherosclerotic lesions.* FEBS Lett, 1999. **462**(1-2): p. 145-50.

23. Wei, P., et al., *Expression of adipose differentiation-related protein (ADRP) is conjointly regulated by PU.1 and AP-1 in macrophages.* J Biochem, 2005. **138**(4): p. 399-412.

24. Soupene, E., H. Fyrst, and F.A. Kuypers, *Mammalian acyl-CoA:lysophosphatidylcholine acyltransferase enzymes.* Proc Natl Acad Sci U S A, 2008. **105**(1): p. 88-93.

25. Parkes, H.A., et al., *Overexpression of acyl-CoA synthetase-1 increases lipid deposition in hepatic (HepG2) cells and rodent liver in vivo.* Am J Physiol Endocrinol Metab, 2006. **291**(4): p. E737-44.

26. Harzer, K., M. Hiraiwa, and B.C. Paton, *Saposins (sap) A and C activate the degradation of galactosylsphingosine.* FEBS Lett, 2001. **508**(1): p. 107-10.

27. Kolter, T. and K. Sandhoff, *Principles of lysosomal membrane digestion: stimulation of sphingolipid degradation by sphingolipid activator proteins and anionic lysosomal lipids.* Annu Rev Cell Dev Biol, 2005. **21**: p. 81-103.

28. Winau, F., et al., *Saposin C is required for lipid presentation by human CD1b.* Nat Immunol, 2004. **5**(2): p. 169-74.

29. Kolter, T., et al., *Lipid-binding proteins in membrane digestion, antigen presentation, and antimicrobial defense.* J Biol Chem, 2005. **280**(50): p. 41125-8.

CHAPTER FOUR

LIPID ANALYSIS OF CASEUM FROM HUMAN PULMONARY TUBERCULOUS GRANULOMAS

ABSTRACT

In response to *Mycobacterium tuberculosis* (Mtb) infection, host cells secrete various cytokines and chemokines, recruiting leukocytes to the site of infection. This process results in the formation of tuberculous (TB) granuloma at the infection focus. Immunocompetent individuals infected with Mtb control the infection by confining the bacilli inside TB granuloma or by eliminating the bacilli completely. However, people with immunosuppressive conditions develop an active disease, at which TB granulomas extensively caseate, liquefy and cavitate. Since TB transmission occurs via Mtb-containing aerosol droplets released from the cavitated granulomas, it is important to understand how TB granuloma caseates and cavitates. It has been hypothesized that the caseum is filled with lipids. Therefore, we performed lipid analysis of caseum of human pulmonary TB granulomas and demonstrated that the caseum contained more neutral lipids, cholesterol (CHO), cholesteryl esters (CE), and triacylglycerols (TAG), and glycosphingolipid, lactosylceramide, than normal lung parenchyma. We propose that, during active TB state, the host undergoes a dramatic shift in lipid metabolism, accompanied by the accumulation of lipids in form of caseum, and that the expansion of lipid contents in the caseum may result in the liquefaction and cavitation. Furthermore, these lipids may also serve as a carbon source for Mtb bacilli.

INTRODUCTION

Mycobacterium tuberculosis (Mtb)-containing aerosol droplets are inhaled by the host, followed by phagocytosis by alveolar macrophages. The infected cells secrete various cytokines and chemokines and recruit leukocytes to the site of the infection. The leukocytes form a solid structure, tuberculous (TB) granuloma. TB granuloma is two-sided in that it protects the host by confining Mtb bacilli into the localized nodule, and on the other hand, it protects Mtb bacilli from host immunity within the stratified nodule. When the host fails to keep the infection under control or the bacteria succeed in multiplying and destroying the host cells, TB is reactivated. At this stage, the caseous TB granuloma liquefies and cavitates, and the TB granuloma ruptures into the airway space, and Mtb bacilli grow on the open surface of cavitary granuloma [1-3]. It is still unclear what drives the latency into active TB, although immunosuppressive conditions including aging, acquired immune deficiency syndrome (AIDS), cancer, and malnutrition are known to raise the risk of developing active TB.

Based on the cheesy appearance, the center of the granuloma is called caseum or caseous center. The caseum of human pulmonary TB granulomas has been thought to be filled with lipids, although there is no direct biochemical evidence. Pagel's group reported abundant lipids in Mtb-infected human tissues histologically [4], followed by Caldwell who analyzed the lipid composition of caseous materials that included human and bovine lymph nodes and livers. Their studies demonstrated that a higher percentage of cholesterol (CHO) was found in caseous materials as compared to control tissue samples [5]. Further, Kondo *et al.* [6-7] demonstrated that virulent Mtb infection induced the accumulation of cholesteryl esters (CE) in murine lung *in vivo* and murine peritoneal macrophages *in vitro*. Recent findings that virulent Mtb or *Mycobacterium bovis* Bacillus Calmette Guérin (BCG) infection triggers the formation

of lipid droplets in macrophages *in vitro* indicate the active involvement of the bacilli in modulating the host lipid metabolism [8-9].

We have shown that genes involved in lipid metabolism were highly upregulated in caseous human pulmonary TB granulomas and also that adipose differentiation-related protein (ADFP), acyl CoA-synthetase long chain family member 1 (ACSL1), and saposin C (SapC), responsible for lipid metabolism and storage, were expressed very strongly in caseous granulomas (Chapter 2&3). These data argue that recruited cells to the site of infection undergo a dramatic change in lipid metabolism in response to Mtb infection and that lipids accumulate progressively inside human TB granulomas in the form of caseum. To test our hypothesis, we analyzed the lipid composition of caseum from human pulmonary TB granulomas. By using thin layer chromatography (TLC) and mass spectrometry (MS) analyses, our data showed that caseum had more CHO, CE, and triacylglycerols (TAG) than normal lung parenchyma. Moreover, we found a unique lipid species that was significantly abundant in caseum but low in normal tissues. This lipid was identified as lactosylceramide (LacCer). In addition, Mtb bacilli were detected histologically throughout the granuloma including caseum. These data support our hypothesis that, in the localized nodule, leukocytes experience a metabolic shift in response to Mtb infection, culminating in the extensive accumulation of neutral lipids and glycolipids, in the form of caseum.

MATERIALS AND METHODS

Lipid analysis

Frozen human TB lung tissues or normal lung tissues were thawed, and caseum or normal tissue segments were isolated and transferred into glass vials (Wheaton Science) and then mixed with chloroform:methanol (2:1, v/v). The corresponding

materials were microscopically confirmed by histological staining. After sonication at 50°C for 1 h, the extracts were filtered through a 0.2 µm-pore size PTFE membrane (GD/X® syringe filter, Whatman) and dried down using nitrogen. TLC plates (aluminum-backed Silica gel 60 plates, EMD) were pre-run in chloroform:methanol (90:10, v/v) to remove any contaminants from silica gel followed by heat-activation at 110°C for 30 min. Total lipids were developed either in a dual solvent system of chloroform:methanol:water (65:25:4, v/v/v) and petroleum ether:ethyl ether:acetic acid (70:30:2, v/v/v) or in a single solvent system of chloroform:methanol:water (65:25:4, v/v/v). Plates were sprayed with 50% sulfuric acid in ethanol and charred for detecting lipid species. The lipid standards used were cholesteryl oleate, TAG, cardiolipin, and phosphatidylcholine (Sigma), CHO (MP Biomedicals), sphingomyelin (SM) (Avanti Polar Lipids), and neutral glycosphingolipid qualmix (Matreya).

Electrospray (ESI) tandem quadrupole mass spectrometric analysis of lipids

Structural analysis of lipids including SM, LacCer, CE, and TAG were carried out by a Finnigan TSQ-7000 triple stage quadrupole mass spectrometer (Thermo Electron Corporation, CA) equipped with a Finnigan ESI source and controlled by Finnigan ICIS software operated on a DEC alpha workstation. Lipid extract dissolved in methanol/chloroform (2:1, v/v) were continuously infused into the ESI source with a Harvard syringe pump at a flow rate of 1µL/min. The skimmer was at ground potential, and the electrospray needle was at 4.5 kV. The heated capillary temperature was 250°C. The collisionally activated dissociation (CAD) tandem mass spectra were obtained under collision energy from 30 to 45 eV, and argon (2.3 mTorr) was used as target gas. The product ion spectra were acquired in the profile mode at the scan rate of one scan per 3 sec. Structural characterization of CH was conducted by Agilent 5973 MSD GC/MS system operated by ChemStation software. Lipid extract in

methanol/chloroform (2:1, v/v) was injected into a Hewett-Packard 6890 GC in a splitless mode and analyzed with a 15 m DB-1701 column (0.25 mm i.d, 0.25 μm film thickness; J & W Scientific). The initial temperature of GC was set at 100°C for 1 min, increased to 220°C at a rate of 50°C/min, then to 290°C at a rate of 10°C/min and maintained at 290°C for another 10 min. The temperatures of the injector, transfer line of the GC column and of the ion-source were set at 280°C, 280°C and 230°C, respectively. The full scan mass spectra (50–500 Da) were acquired at a rate of 1 scan/0.25 Sec. Mass spectrometry was performed by Dr. Fong-Fu Hsu (Washington University School of Medicine).

Mycobacterium staining on human lung tissues

Paraffin-embedded sections of human TB lung tissues were heat-fixed, deparaffinized, and rehydrated. The sections were incubated with auramine-rhodamine (EM Science) for 30 min at 60°C, washed with dd-H_2O, differentiated in 1% HCl in 70% ethanol for 30 sec, and washed. The section was blocked with 1% Sudan Black in 70% ethanol, washed with dd-H_2O, counterstained with Harris hematoxylin, and then mounted with Fluoromount G (Southern Biotech). Images were captured by AxioCam HRc attached to Zeiss Axio Imager with AxioVision LE software (Carl Zeiss MicroImaging).

RESULTS and DISCUSSION

Since TB transmission occurs via Mtb-containing aerosols released from cavitated pulmonary TB granulomas, it is critical to understand the biology of TB granulomas. TB granuloma is a collection of leukocytes formed upon Mtb infection. It can be resolved or remain dormant. However, it is with still unclear how TB granuloma caseates and cavitates. To understand this process, we examined gene and protein expression of human pulmonary TB granulomas (Chapter 2&3) and showed

that lipid metabolism plays an important role in cells of caseous granulomas. In order to determine if upregulated expression of genes and proteins for lipid metabolism lead to any change in lipid profiles, we analyzed lipids of actual caseum from human pulmonary TB granulomas.

Total lipids were extracted from the caseum of caseous and fibrocaseous granulomas and they were compared to lipids obtained from normal lung tissues. TLC analysis revealed significant differences in lipid profiles; caseum materials showed increased amounts of neutral lipids, CHO, CE, and TAG (Figure 4.1). In addition, a unique lipid double band was detected in the caseum which was not detectable in normal lung tissues (Figure 4.2). It showed the same color and migration pattern to standard lactosylceramide (LacCer).

We also performed mass spectrometry (MS) to confirm lipid identities. The MS profile of SM was obtained by precursor-ion scan of *m/z* 184. The spectrum contained the whole array of the protonated SM species consisting of 18:1-sphingosine long chain base with 16:0 (*m/z* 703), 22:0 (*m/z* 787), 24:2 (*m/z* 811), 24:1 (*m/z* 813), and 24:0 (*m/z* 815) fatty acyl groups, respectively (Figure 4.3 A). This profile was similar to that obtained by neutral loss scan of *m/z* 183 (Figure 4.3 B), which contained the ion series at *m/z* 725, *m/z* 809, *m/z* 833, *m/z* 835, and *m/z* 837 that were 22 Da heavier than the corresponding $[M + H]^+$ ions, further supporting the presence of sphingomyelins. The MS profile of LacCer was obtained by neutral loss scan of *m/z* 162, an unique loss of a sugar moiety that specifically detects the $[M + Na]^+$ ions of LacCer (Figure 4.3 C). The spectrum was dominated by the ion at *m/z* 884, corresponding to a d18/16:0-LacCer, along with ions at *m/z* 968, *m/z* 994, and *m/z* 996, representing the $[M + Na]^+$ ions of d18:1/22:0, d18:1/24:1, and d18:1/24:0 LacCer, respectively. The tandem mass spectrum was obtained by precursor-ion scan of *m/z* 369, a signature fragment ion that is commonly seen for CE, following collision

Figure 4.1 Lipid analysis of caseum and normal lung tissue by thin-layer chromatography.
Total lipids were extracted from normal lung tissues (lane 4-6, 120 µg) and caseum (lane 7-9, 120 µg), and then run in parallel with total lipids from Mtb CDC1551 (lane 1, 400 µg), and standard lipids, cardiolipin (lane 2, 50 µg), phosphatidylcholine (lane 3, 50 µg), cholesterol (CHO, lane 10, 20 µg), cholesteryl ester (CE, lane 11, 25 µg), and triacylglycerol (TAG, lane 12, 20 µg). The caseum reveals higher amounts of CHO, CE, and TAG (dual solvent system). Caseum samples were derived from granulomas of seven TB patients, and normal lung tissue samples were from unaffected lung areas of another seven TB patients. Three representative lipids of caseum and normal lung tissue are shown in this analysis.

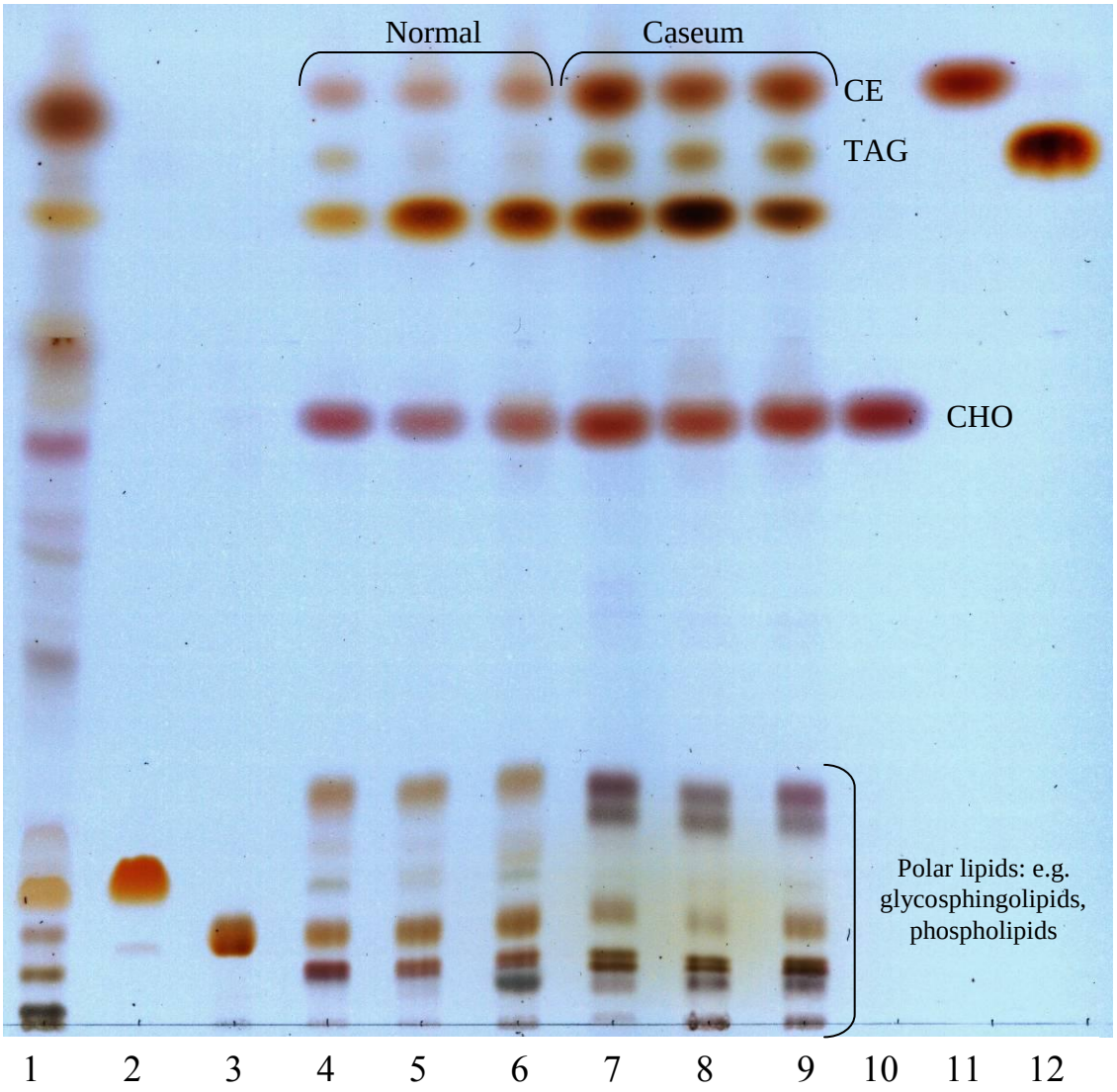
Normal
Caseum
CE
TAG
CHO
Polar lipids: e.g. glycosphingolipids, phospholipids
1
2
3
4
5
6
7
8
9
10
11
12

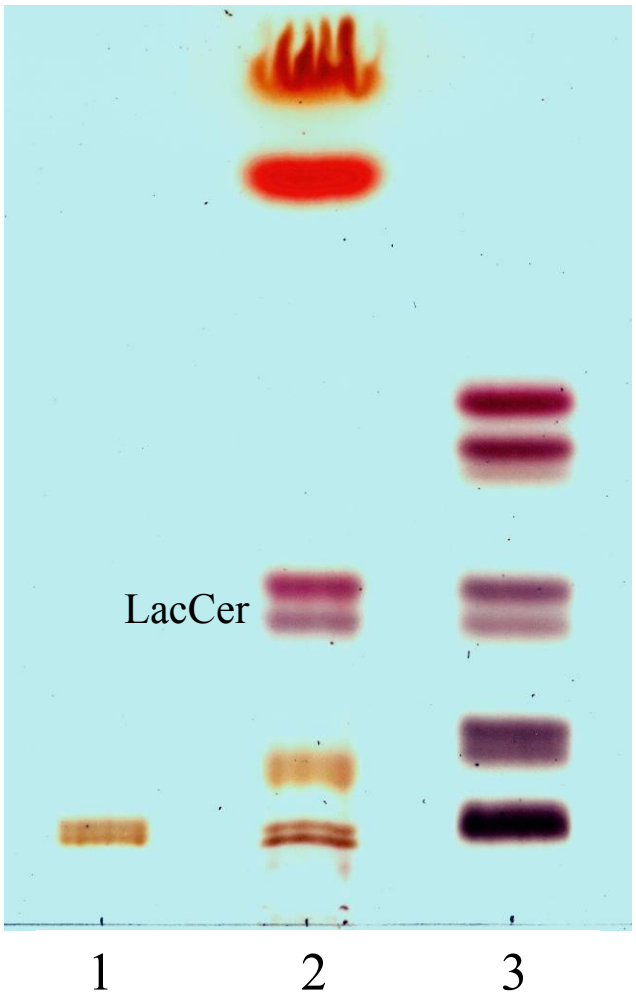

Figure 4.2 Lipid analysis of caseum by thin-layer chromatography.
Total lipids from the caseum (lane 2, 120 µg) were separated by TLC. As standards, sphingomyelin (SM, lane 1, 5 µg) and neutral glycosphingolipids (lane 3, 30 µg) were used. Caseum samples derived from granulomas of seven TB patients showed the same pattern, and one representative sample is shown in this analysis. LacCer is indicated.

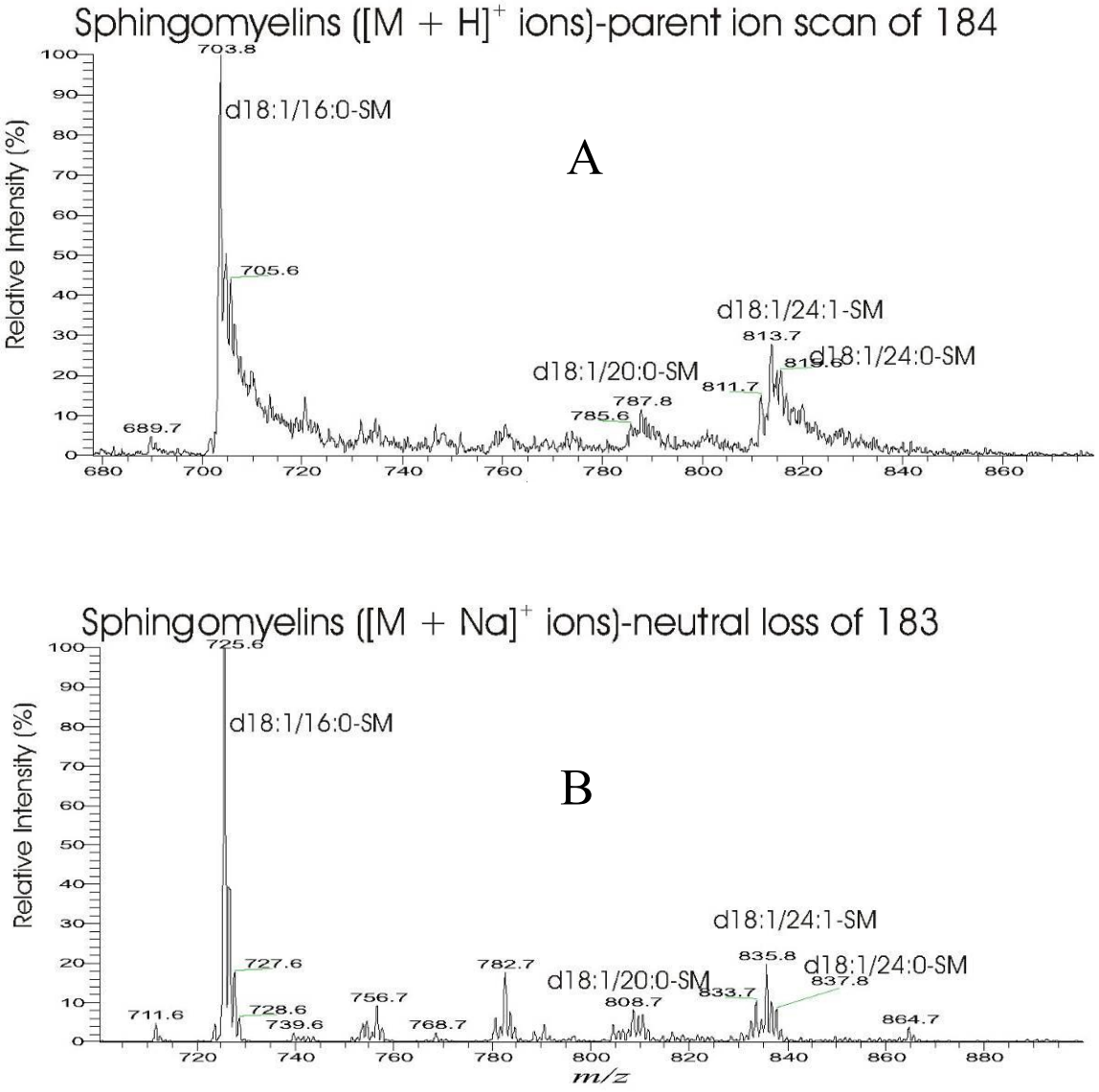

Figure 4.3 Mass spectrometric analyses of sphingomyelin (A&B), lactosylceramide (C), cholesteryl esters (D), triacylglycerols (E), and cholesterol (F&G) derived from caseum of human pulmonary TB granulomas. Data from one representative sample are shown.

Figure 4.3 (Continued)

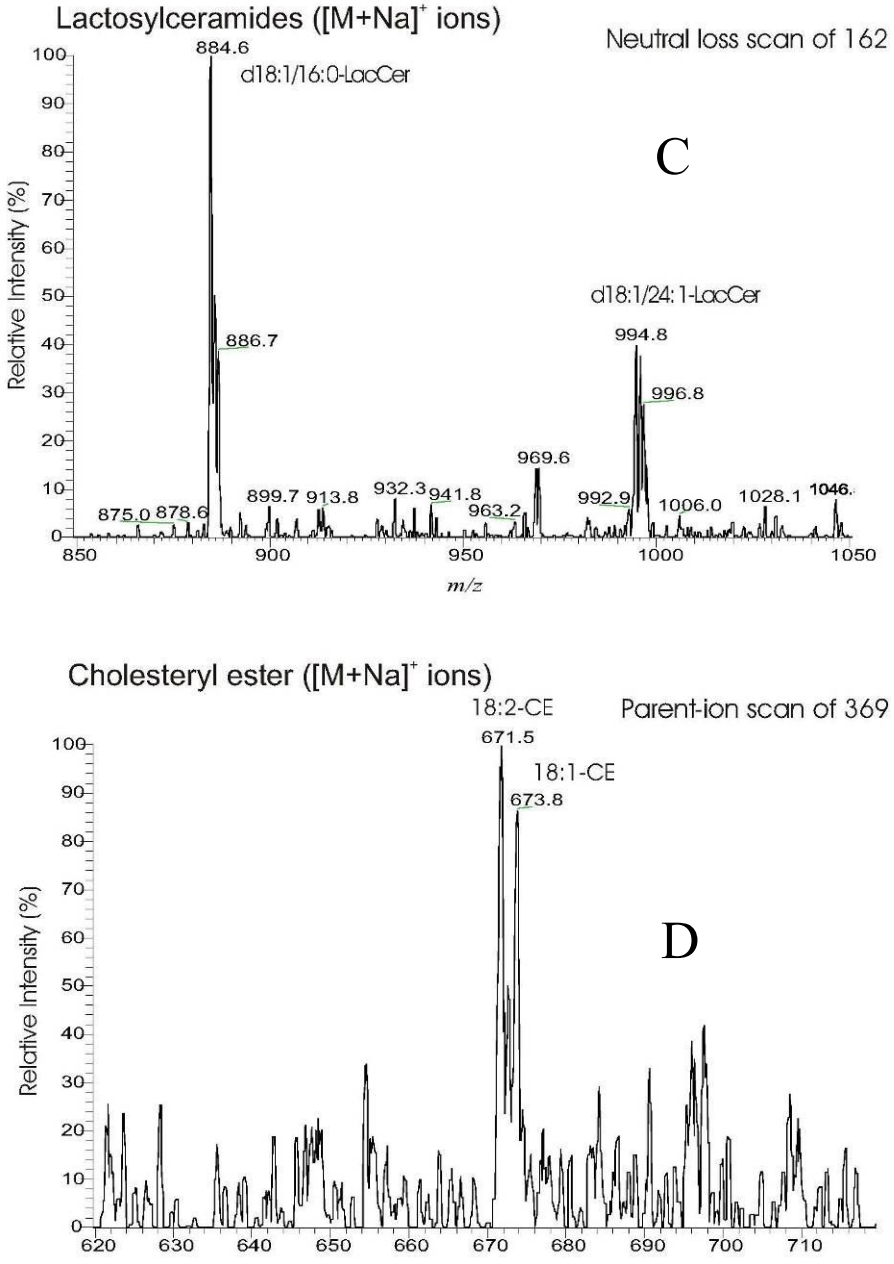

Figure 4.3 (Continued)

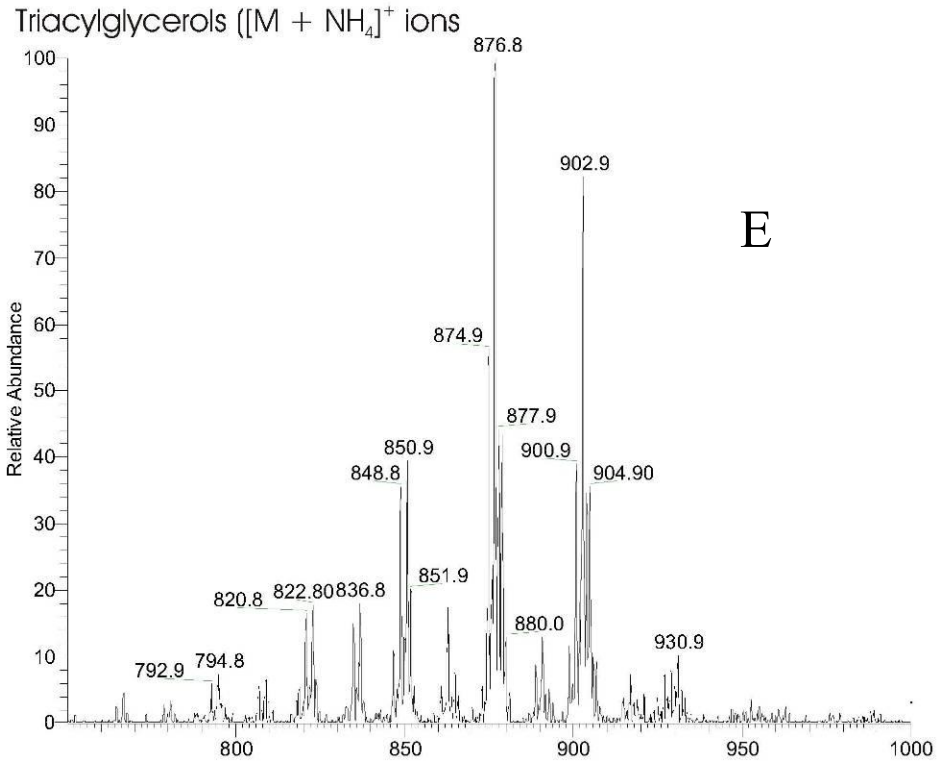

Figure 4.3 (Continued)

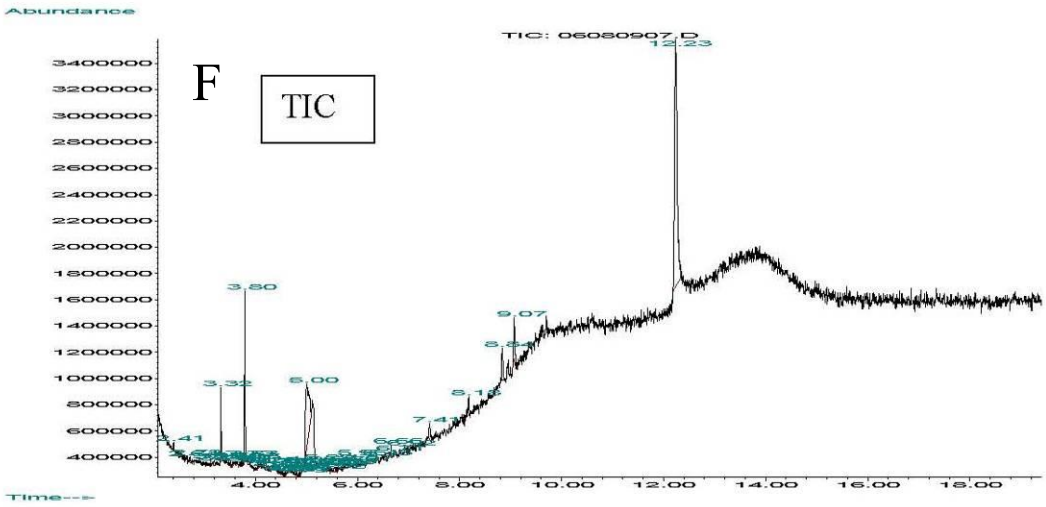

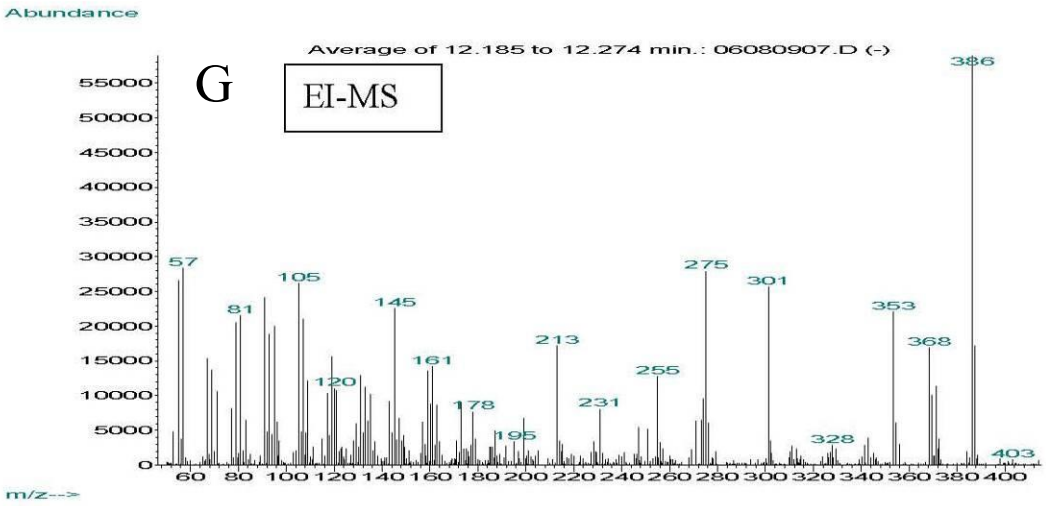

activation dissociation on the $[M + Na]^+$ ions. The spectrum contained the major ions at *m/z* 671 and *m/z* 673, corresponding to the sodiated species of cholesteryl linoleate and cholesteryl oleate, respectively (Figure 4.3 D). The MS profile revealed the major $[M + NH_4]^+$ ions of TAG that consisted of 16:0-, 16:1-, 18:0-, 18:1-, and 18:2-fatty acid substituents on the glycerol backbone (Figure 4.3 E). The spectrum was dominated by the ions at *m/z* 876 corresponding to the ammoniated TAG species possessing a total of C_{52} with the presence of 2 total unsaturated bonds situated on the fatty acyl chains (52:2), and at *m/z* 902 (54:3), *m/z* 820 (48:2), *m/z* 822 (48:1), *m/z* 834 (49:2), *m/z* 836 (49:1), *m/z* 848 (50:2), *m/z* 850 (50:1), *m/z* 874 (52:3), *m/z* 900 (54:4), and *m/z* 904 (54:2). The electron impact (EI) gas chromatography/mass spectrometry (GC/MS) and total ion current (TIC) chromatogram gave a peak at 12.23 min (Figure 4.3 F) and an EI mass spectrum (Figure 4.3 G) identical to that arising from CHO standard, and the retention time is also identical to that of authentic standard, confirming the presence of cholesterol.

CHO has long been linked to TB, although its role in TB pathogenesis is contradictory. The administration of CHO-rich diets to TB patients reduced the number of bacilli in the sputum [10-13]. In contrast to the beneficial effects of cholesterol on TB patients, when hypercholesterolemia was induced in mice through deletion of *ApoE* prior to Mtb infection, the high cholesterol accelerated bacterial growth and exacerbated the lung pathology [14]. Recent studies demonstrated the ability of Mtb to utilize host-derived CHO *in vitro* and *in vivo* [15-18]. It is also known that CHO-enriched microdomains of phagocytes facilitate mycobacterial uptake and ensure bacterial intracellular survival [19-20]. As TB patients are weakened by the disease, administration of CHO-rich diet is likely to benefit patients. On the other hand, the confined environment of TB granuloma with CHO-rich caseum may promote the survival of Mtb bacillus by its capability to degrade CHO as a carbon

source [15, 17-18]. However, further investigations are needed to characterize the role(s) of CHO in TB pathogenesis.

Mycobacteria are also known to accumulate TAG under stress, e.g. starvation and hypoxia, and utilize it during the chronic infection period. Mtb bacilli containing TAG-rich intracellular lipophilic inclusions (ILIs) were detected in sputum samples from TB patients [21-24]. However, further studies need to be done to determine whether dysregulated lipid metabolism of the host contributes to TAG accumulation in the caseum.

In addition to CHO and TAG, Mtb infection was shown to induce the accumulation of CE *in vitro* and *in vivo* [6-7]. Interestingly, the presence of CE in caseous intracranial TB granulomas has been proposed to be a disease marker [25]. It is not clear if CE serves as a carbon source for Mtb or is a product of pathological changes in the host. However, it is clear from our data and previous literature that Mtb infection leads to dysregulated lipid metabolism of the host and this culminates in the accumulation of CE in the form of caseum.

LacCer is an extremely interesting glycosphingolipid to be found in TB granuloma caseum with respect to its biological properties. LacCer is normally present in trace amounts in mammalian cells because it is an intermediate in the glycosphingolipids biosynthesis. Its accumulation in cells could result from either increased ceramide synthase activity, increased catabolism of complex ceramides or proinflammatory factors [26]. LacCer in phagocytes is also implicated in innate immunity by forming membrane microdomains; LacCer may serve as a pattern recognition receptor for pathogens including mycobacteria, thereby leading to signal transduction and phagocytosis [27-30]. Particularly, LacCer that contains very long fatty acid C24:0 and C24:1 chains is known to be critical for LacCer-mediated functions [31], and LacCer identified in our analysis on caseum of human TB

granuloma also contained long chain fatty acids (Figure 4.3 C, and page 6). Even though we cannot rule out the role of LacCer in bacterial recognition, our biochemical data seem to point to the role(s) of LacCer in glycosphingolipid metabolism rather than phagocytic function. The excess accumulation of LacCer in the caseum is tightly associated with the high expression of SapC in nascent and caseous granulomas; SapC mediates the degradation of LacCer into glucosylceramide (GlcCer) by β-galactosidase [32]. Since we did not see any detectable level of GlcCer in caseum by TLC analysis, LacCer synthase may exceed the activity of SapC and β-galactosidase as TB granuloma progresses. However, the relationship and roles of LacCer and SapC in TB pathogenesis need to be further elucidated.

We also examined human TB granulomas to localize Mtb bacilli. Even though it is not clear how the metabolism of Mtb is regulated within human TB granulomas, it is obvious that Mtb can survive within granulomas [33-34]. Furthermore, lipids identified in our study were shown to be a carbon source for Mtb during chronic infection [15-18, 23]. Despite the poor sensitivity of traditional methods [35-37], auramine-rhodamine staining detected acid fast bacilli (AFB) in nascent granulomas, caseous granulomas, and fibrocaseous granulomas, and the bacilli were also seen within caseum (Figure 4.4). Even though the bacterial number is low, the amplification of the response to Mtb and its released virulence factors could explain the extreme tissue reaction observed in human TB granulomas.

It is very intriguing that two different diseases, TB and atherosclerosis, share the same lipid species implicated in pathogenesis: CHO, CE, TAG, and LacCer [38-39]. The accumulation of apolipoprotein-B containing lipoproteins in arterial intima triggers the endothelium to secrete cytokines and chemokines, thereby recruiting blood monocytes which differentiate into macrophages and engulf lipoproteins [40-41]. These macrophages, namely foam cells, being full of lipid droplets, attract more

Figure 4.4 Localization of Mtb bacilli on human TB granulomas.
Macrophage in nascent granuloma harbors Mtb bacillus as indicated by auramine-rhodamine staining (A, merged with bright field). The corresponding area is also shown by hematoxylin & eosin (H&E) staining (B). Caseating granuloma harbors several Mtb bacilli within the caseum (C, merged with bright field), and its corresponding area is shown in D. Note that B and D are mirrored images of A and C, respectively. For clarity, B and D are flipped. The arrow in red indicates Mtb bacillus. Some macrophages (mostly alveolar macrophages) are deposited with carbon, therefore presenting black dots. Representative images are shown.

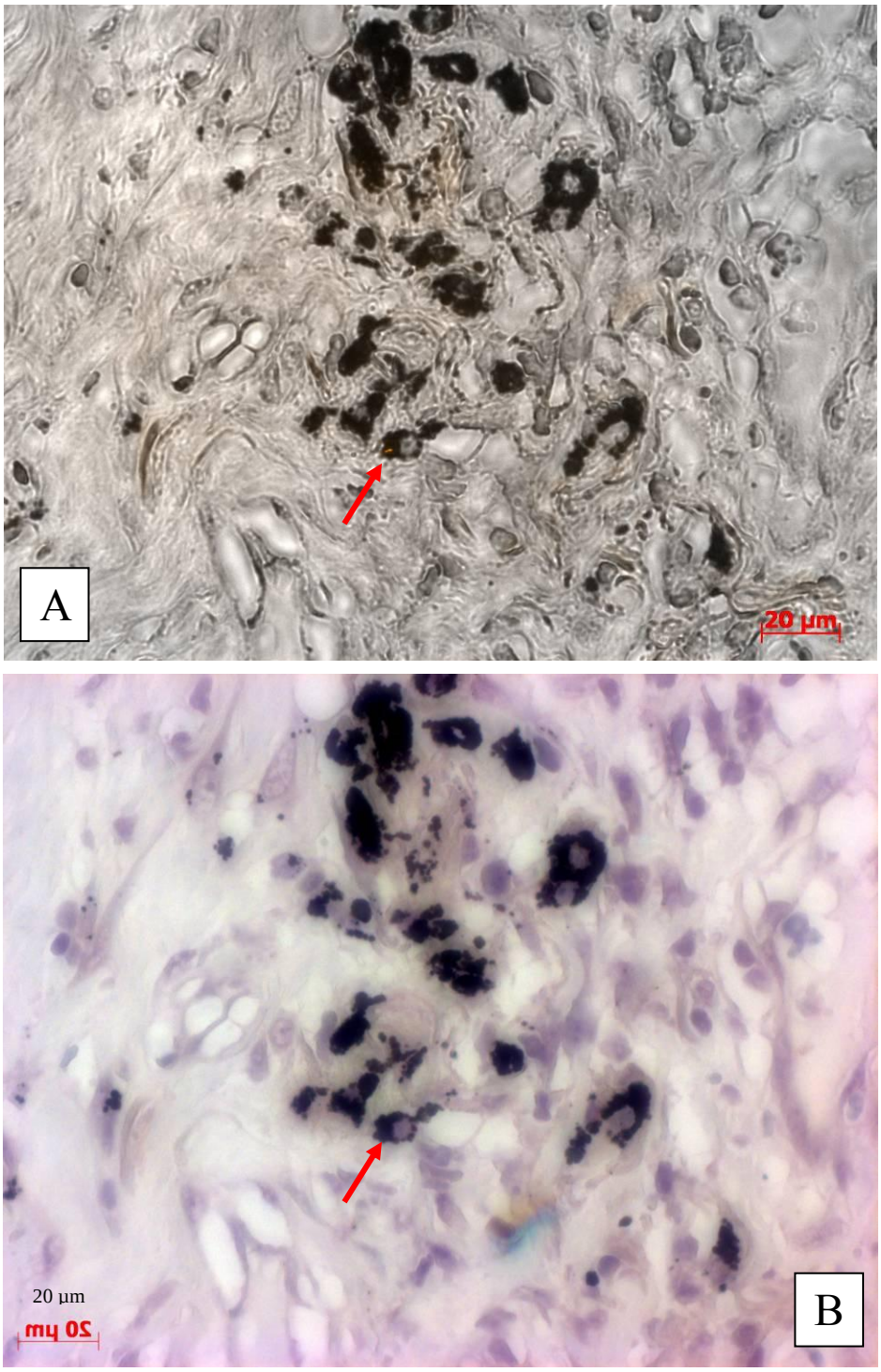
A
20 µm
20 µm
B

Figure 4.4 (Continued)

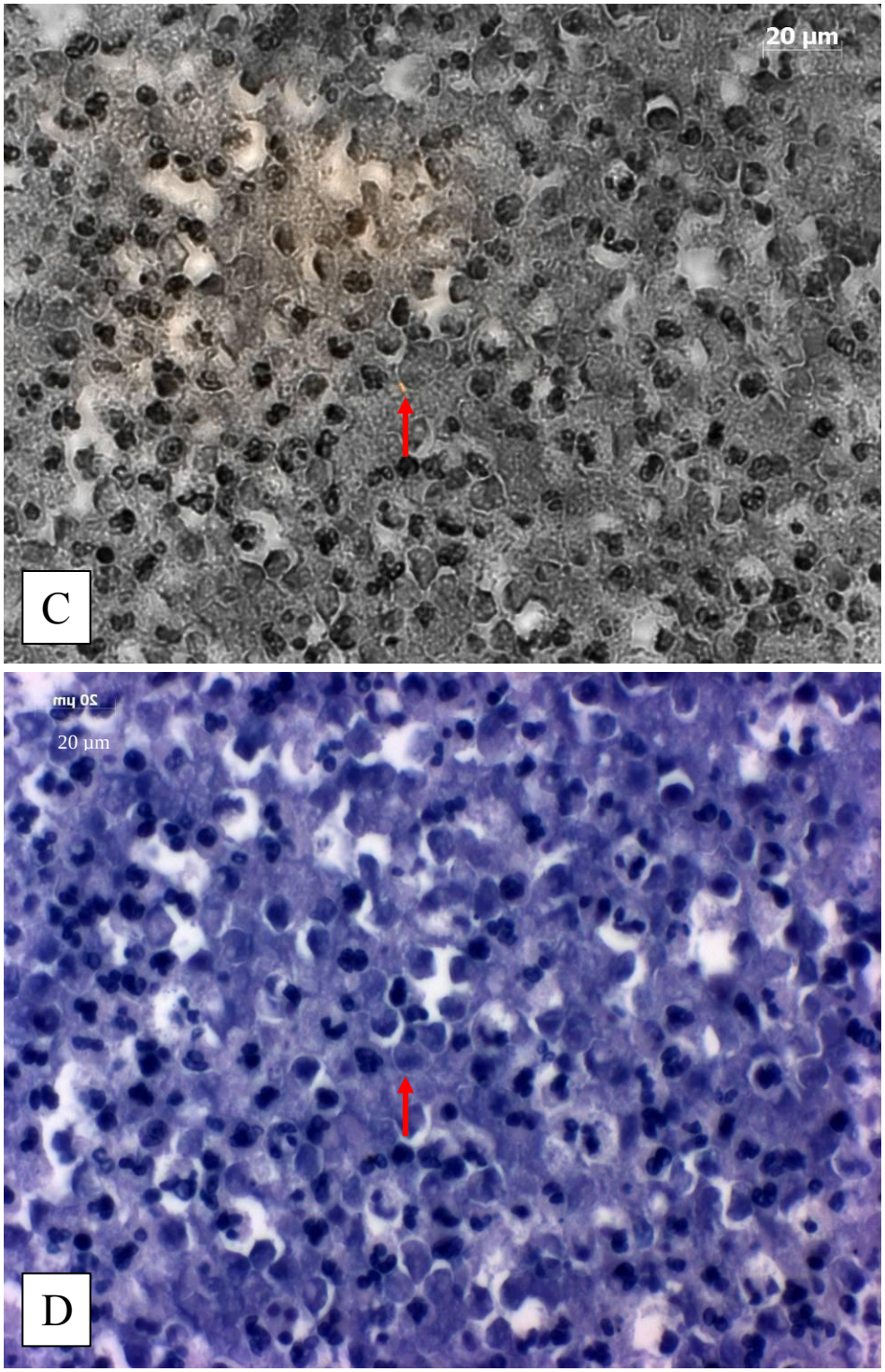

monocytes, T cells, mast cells, and neutrophils to the lesion. Smooth muscle cells (SMC) are also recruited and form a fibrous cap around the necrotic, lipid-rich core. The rupture of the fragile lesion results in thrombosis and heart failure. CHO and TAG of atherosclerotic plaques are mostly derived from low-density lipoprotein (LDL), and LacCer is also known to markedly accumulate in plaque intima [42] and to be highly excreted in urine of hypercholesterolemic patients [43]. Interestingly, our microarray data (Chapter 2) using caseous human pulmonary TB granulomas showed upregulation of genes for lipoprotein receptors including low-density lipoprotein receptor (LDLR), macrophage receptor with collagenous structure (MARCO), and macrophage scavenger receptor 1 (MSR1). In addition to the deposition of neutral lipids and glycosphingolipids, the development and rupture of atherosclerotic plaque is strikingly similar to that of caseous human TB granuloma.

A recent study on *Mycobacterium leprae*-infected lepromatous leprosy patients demonstrated that genes involved in lipid metabolism were highly upregulated and host-derived oxidized phospholipids induced by *M. leprae* infection modified the host immunity by inhibiting TLR2/1 activation [44]. Intriguingly, several of the genes reported as upregulated in our study (Chapter 2) overlap with those observed in lepromatous leprosy lesions, including *ADFP* and *PSAP* [44]. Another study showed increased amounts of CHO and CE in lesions of lepromatous leprosy patients [45]. These data indicate that there are many parallels to the metabolic reprogramming induced by both Mtb and *M. leprae*. The point at which the two infection sites diverge could hinge on the formation of the fibrous capsule in TB granuloma, which may focus and constrain the inflammatory response leading to the accumulation of the sequestered lipids forming the caseum. The pathology is unique to Mtb and precedes the liquefaction and cavitation of the granuloma.

In summary, the current study showed that caseum from human TB

granulomas is significantly enriched with CHO, CE, TAG, and LacCer, and this biochemical analysis is in line with our microarray and immunohistology analyses (Chapter 2&3). Due to the limited sensitivity of TLC, we cannot exclude other lipid species that could be important for TB granulomas. Drug development for TB treatment has been focused on inhibition and/or elimination of Mtb; however, our data suggest that preventing lipid-laden TB granuloma from liquefying and rupturing into the airway space may modulate the progression of TB disease. In analogy with atherosclerosis treatment, manipulation of excess inflammation, lipid accumulation, and lipid-mediated cell death at the localized TB granuloma may accelerate the treatment of TB patients receiving antibiotics.

Future work would include identifying the origin of lipids from the caseum, how Mtb interfere host lipid trafficking, and finally whether lipids from foam cells are responsible for making up caseum.

ACKNOWLEDGEMENTS

I would like to thank Dr. Fong-Fu Hsu at Washington University School of Medicine for performing mass-spectrometry.

REFERENCES

1. Dannenberg, A.M., Jr. and M. Sugimoto, *Liquefaction of caseous foci in tuberculosis.* Am Rev Respir Dis, 1976. **113**(3): p. 257-9.
2. Dannenberg, A.M., Jr., *Roles of cytotoxic delayed-type hypersensitivity and macrophage-activating cell-mediated immunity in the pathogenesis of tuberculosis.* Immunobiology, 1994. **191**(4-5): p. 461-73.
3. Hunter, R.L., et al., *Multiple roles of cord factor in the pathogenesis of primary, secondary, and cavitary tuberculosis, including a revised description of the pathology of secondary disease.* Ann Clin Lab Sci, 2006. **36**(4): p. 371-86.
4. Pagel, W. and M. Pagel, *Zur Histochemie der Lungentuberkulose, mit besonderer Berücksichtigung der Fettsubstanzen und Lipoide.* Virchows Archiv, 1925. **256**(3): p. 629-640.
5. Caldwell, G.T., *Chemical Changes in Tuberculous Tissues.* The Journal of Infectious Diseases, 1919. **24**(2): p. 81-113.
6. Kondo, E. and K. Kanai, *Accumulation of cholesterol esters in macrophages incubated with mycobacteria in vitro.* Jpn J Med Sci Biol, 1976. **29**(3): p. 123-37.
7. Kondo, E., et al., *Analysis of host-originated lipids associated with "in vivo grown tubercle bacilli".* Jpn J Med Sci Biol, 1970. **23**(5): p. 315-26.
8. Peyron, P., et al., *Foamy macrophages from tuberculous patients' granulomas constitute a nutrient-rich reservoir for M. tuberculosis persistence.* PLoS Pathog, 2008. **4**(11): p. e1000204.

9. D'Avila, H., et al., *Mycobacterium bovis bacillus Calmette-Guerin induces TLR2-mediated formation of lipid bodies: intracellular domains for eicosanoid synthesis in vivo.* J Immunol, 2006. **176**(5): p. 3087-97.
10. Deniz, O., et al., *Serum total cholesterol, HDL-C and LDL-C concentrations significantly correlate with the radiological extent of disease and the degree of smear positivity in patients with pulmonary tuberculosis.* Clin Biochem, 2007. **40**(3-4): p. 162-6.
11. Kozarevic, D., et al., *Serum cholesterol and mortality: the Yugoslavia Cardiovascular Disease Study.* Am J Epidemiol, 1981. **114**(1): p. 21-8.
12. Perez-Guzman, C., et al., *A cholesterol-rich diet accelerates bacteriologic sterilization in pulmonary tuberculosis.* Chest, 2005. **127**(2): p. 643-51.
13. Taylor, G.O. and A.E. Bamgboye, *Serum cholesterol and diseases in Nigerians.* Am J Clin Nutr, 1979. **32**(12): p. 2540-5.
14. Martens, G.W., et al., *Hypercholesterolemia impairs immunity to tuberculosis.* Infect Immun, 2008. **76**(8): p. 3464-72.
15. Pandey, A.K. and C.M. Sassetti, *Mycobacterial persistence requires the utilization of host cholesterol.* Proc Natl Acad Sci U S A, 2008. **105**(11): p. 4376-80.
16. Brzostek, A., et al., *Mycobacterium tuberculosis is able to accumulate and utilize cholesterol.* J Bacteriol, 2009. **191**(21): p. 6584-91.
17. Chang, J.C., et al., *Identification of Mycobacterial genes that alter growth and pathology in macrophages and in mice.* J Infect Dis, 2007. **196**(5): p. 788-95.
18. Chang, J.C., et al., *igr Genes and Mycobacterium tuberculosis cholesterol metabolism.* J Bacteriol, 2009. **191**(16): p. 5232-9.
19. Gatfield, J. and J. Pieters, *Essential role for cholesterol in entry of mycobacteria into macrophages.* Science, 2000. **288**(5471): p. 1647-50.

20. Peyron, P., et al., *Nonopsonic phagocytosis of Mycobacterium kansasii by human neutrophils depends on cholesterol and is mediated by CR3 associated with glycosylphosphatidylinositol-anchored proteins.* J Immunol, 2000. **165**(9): p. 5186-91.

21. Deb, C., et al., *A novel lipase belonging to the hormone-sensitive lipase family induced under starvation to utilize stored triacylglycerol in Mycobacterium tuberculosis.* J Biol Chem, 2006. **281**(7): p. 3866-75.

22. Mishra, K.C., et al., *Functional role of the PE domain and immunogenicity of the Mycobacterium tuberculosis triacylglycerol hydrolase LipY.* Infect Immun, 2008. **76**(1): p. 127-40.

23. Low, K.L., et al., *Triacylglycerol utilization is required for regrowth of in vitro hypoxic nonreplicating Mycobacterium bovis bacillus Calmette-Guerin.* J Bacteriol, 2009. **191**(16): p. 5037-43.

24. Garton, N.J., et al., *Intracellular lipophilic inclusions of mycobacteria in vitro and in sputum.* Microbiology, 2002. **148**(Pt 10): p. 2951-8.

25. Subramanian, A., et al., *NMR spectroscopic identification of cholesterol esters, plasmalogen and phenolic glycolipids as fingerprint markers of human intracranial tuberculomas.* NMR Biomed, 2008. **21**(3): p. 272-88.

26. Chatterjee, S. and A. Pandey, *The Yin and Yang of lactosylceramide metabolism: implications in cell function.* Biochim Biophys Acta, 2008. **1780**(3): p. 370-82.

27. Sonnino, S., et al., *Role of very long fatty acid-containing glycosphingolipids in membrane organization and cell signaling: the model of lactosylceramide in neutrophils.* Glycoconj J, 2009. **26**(6): p. 615-21.

28. Yoshizaki, F., et al., *Role of glycosphingolipid-enriched microdomains in innate immunity: microdomain-dependent phagocytic cell functions.* Biochim Biophys Acta, 2008. **1780**(3): p. 383-92.

29. Iwabuchi, K., et al., *Involvement of very long fatty acid-containing lactosylceramide in lactosylceramide-mediated superoxide generation and migration in neutrophils.* Glycoconj J, 2008. **25**(4): p. 357-74.

30. Nakayama, H., et al., *Lyn-coupled LacCer-enriched lipid rafts are required for CD11b/CD18-mediated neutrophil phagocytosis of nonopsonized microorganisms.* J Leukoc Biol, 2008. **83**(3): p. 728-41.

31. Iwabuchi, K., et al., *Significance of glycosphingolipid fatty acid chain length on membrane microdomain-mediated signal transduction.* FEBS Lett, 2010. **584**(9): p. 1642-52.

32. Kolter, T. and K. Sandhoff, *Principles of lysosomal membrane digestion: stimulation of sphingolipid degradation by sphingolipid activator proteins and anionic lysosomal lipids.* Annu Rev Cell Dev Biol, 2005. **21**: p. 81-103.

33. Opie, J.D.A.E.L., *TUBERCLE BACILLI IN LATENT TUBERCULOUS LESIONS AND IN LUNG TISSUE WITHOUT TUBERCULOUS LESIONS.* Archives of Pathology and Laboratory Medicine, July 1927. **4**: p. 1-21.

34. Ulrichs, T., et al., *Modified immunohistological staining allows detection of Ziehl-Neelsen-negative Mycobacterium tuberculosis organisms and their precise localization in human tissue.* J Pathol, 2005. **205**(5): p. 633-40.

35. Garg, S.K., et al., *Diagnosis of tuberculosis: available technologies, limitations, and possibilities.* J Clin Lab Anal, 2003. **17**(5): p. 155-63.

36. Shapiro, H.M. and T. Hanscheid, *Fuchsin fluorescence in Mycobacterium tuberculosis: the Ziehl-Neelsen stain in a new light.* J Microbiol Methods, 2008. **74**(2-3): p. 119-20.

37. Mert, A., et al., *Ziehl-Neelsen staining and polymerase chain reaction study of tissue from tuberculous granulomas.* Respirology, 2003. **8**(4): p. 548.

38. Martin, S. and R.G. Parton, *Lipid droplets: a unified view of a dynamic organelle.* Nat Rev Mol Cell Biol, 2006. **7**(5): p. 373-8.

39. Tabas, I., *Macrophage death and defective inflammation resolution in atherosclerosis.* Nat Rev Immunol. **10**(1): p. 36-46.

40. Tabas, I., K.J. Williams, and J. Boren, *Subendothelial lipoprotein retention as the initiating process in atherosclerosis: update and therapeutic implications.* Circulation, 2007. **116**(16): p. 1832-44.

41. Lusis, A.J., *Atherosclerosis.* Nature, 2000. **407**(6801): p. 233-41.

42. Chatterjee, S.B., et al., *Accumulation of glycosphingolipids in human atherosclerotic plaque and unaffected aorta tissues.* Glycobiology, 1997. **7**(1): p. 57-65.

43. Chatterjee, S., C.S. Sekerke, and P.O. Kwiterovich, Jr., *Increased urinary excretion of glycosphingolipids in familial hypercholesterolemia.* J Lipid Res, 1982. **23**(4): p. 513-22.

44. Cruz, D., et al., *Host-derived oxidized phospholipids and HDL regulate innate immunity in human leprosy.* J Clin Invest, 2008. **118**(8): p. 2917-28.

45. Mattos, K.A., et al., *Lipid droplet formation in leprosy: Toll-like receptor-regulated organelles involved in eicosanoid formation and Mycobacterium leprae pathogenesis.* J Leukoc Biol. **87**(3): p. 371-84.

CHAPTER FIVE

MYCOBACTERIUM TUBERCULOSIS INDUCES THE FORMATION OF LIPID DROPLETS IN MACROPHAGES IN VITRO

ABSTRACT

Mycobacterium tuberculosis (Mtb) is transmitted via Mtb-containing aerosol droplets. Once inhaled, Mtb is engulfed by alveolar macrophages, which is followed by the recruitment of leukocytes such as monocytes, neutrophils, B-cells, and T-cells to the site of infection. Mtb bacillus mainly resides in macrophages and utilizes the host machinery for its survival. Our data have shown that Mtb infection leads to the dysregulation of host lipid metabolism as indicated by the accumulation of lipids within tuberculous (TB) granuloma. Next, we examined gene regulation and protein expression in Mtb-infected macrophages. Herein, we demonstrate that Mtb *in vitro* infection leads to the formation of lipid droplets in macrophages and this phenomenon is accompanied by upregulation of transcripts and proteins for adipose differentiation-related protein (ADFP), acyl-CoA synthetase long-chain family member 1 (ACSL1), and saposin C (SapC). Moreover, mRNA expression of *ADFP*, *ACSL1*, and *SapC* can be reduced by mevastatin, an inhibitor of 3-hydroxy-3-methyl-glutaryl-CoA reductase (HMGCR) that blocks mevalonate and ultimately cholesterol synthesis.

INTRODUCTION

Mycobacterium tuberculosis (Mtb) is phagocytosed by macrophages via several receptors including complement receptors (CRs), mannose receptor (MR), CD14, surfactant protein (SP) and type A&B scavenger receptors [1-10] and establishes a niche within macrophages, by circumventing phagosomal maturation, lysosomal fusion and acidification [11-16]. It also has been shown that Mtb enters via cholesterol (CHO)-enriched microdomains and CH mediates phagosomal association of tryptophan-alanine-rich coat protein (TACO), which prevents mycobacterial degradation in lysosomes [17]. Mtb-containing phagosomes retain early endosomal markers such as small GTPase Rab5 and exclude vesicular H^+ ATPase from the vacuole, thereby maintaining the inner environment just slightly acidic at pH 6.2 [11, 18]. These phagosomes that do not fuse with lysosomes can still interact with host cell recycling pathway, possibly supplying essential nutrients to intraphagosomal Mtb [19-20].

Recent studies have shed light on the mechanism of Mtb survival during chronic infection. As murine tuberculous (TB) granuloma progresses, lipid droplets accumulate as well and these organelles are in close proximity to Mtb-containing phagosomes, suggesting that Mtb may acquire a carbon source from lipid droplets [21]. Moreover, Mtb is shown to be able to degrade host-derived lipids *in vitro* and *in vivo* [22-25]. Our studies on human TB granulomas have revealed that the human host undergoes dramatic changes in lipid metabolism, and this is correlated with the accumulation of neutral lipids and glycosphingolipids within the granuloma in the form of caseum (Chapter 2&3&4). These data combined with our earlier observation indicate that Mtb infection leads to lipid accumulation in the granuloma.

In this study, we report that murine or human macrophages infected with Mtb accumulate lipid droplets and this phenomenon is associated with upregulation of

transcripts of adipose differentiation-related protein (*ADFP*), acyl-CoA synthetase long-chain family member 1 (*ACSL1*), and saposin C (*SapC*), all involved in lipid metabolism and lipid accumulation. The gene expression level of *ADFP*, *ACSL1*, and *SapC* could be lowered by mevastatin that inhibits 3-hydroxy-3-methyl-glutaryl-CoA reductase (HMGR) of HMG-CoA pathway that produces cholesterol. This implies that the host response to Mtb infection, manifested by lipid accumulation, can be lowered by chemicals.

MATERIALS and METHODS

Animals

C57BL/6J mice were obtained from the Jackson Laboratory and housed under specific-pathogen-free conditions. All experiments were approved by Cornell University Institutional Animal Care and Use Committee.

Mycobacterial culture

Mtb strain H37Rv was grown in 7H9 broth (Difco) medium supplemented with 10% oleic acid/albumin/dextrose/catalase (OADC) and 0.05% Tween-80. Bacteria of exponential phase ($O.D._{600}$ = 0.6) were homogenized through 27G needle (BD) and used for macrophage infection.

Culture and in vitro infection of murine macrophages

Bone marrow cells were isolated from femurs and tibias of 6-8 week-old female C57BL/6J mice and cultured in Dulbecco's Modified Eagle Medium (DMEM, Gibco) supplemented with 20% L-929 cell-conditioned medium, 10% heat-inactivated fetal calf serum (HI-FCS; Hyclone), 2 mM L-glutamine (Gibco), 1 mM sodium pyruvate (Gibco), and 100 U/ml penicillin-100 µg/ml streptomycin (Gibco) at 37°C, 5% CO_2,

and 90% humidity for five days. For confocal microscopy, mature bone marrow-derived macrophages (BMMΦ) were seeded onto coverslips (Fisher Scientific) at a density of 1×10^5 cells per well in 24-well plates (TPP) for immunostaining or at a density of 1×10^7 cells into 75 cm^2 flask (TPP) for quantitative real-time RT-PCR analysis. BMMΦ were incubated with Mtb H37Rv at a multiplicity of infection 20:1 (bacteria per macrophage) for 2h, washed with PBS three times and cultured in DMEM medium without antibiotics.

Culture and in vitro infection of human macrophages

Monocytes were isolated from human blood (Zen-Bio Inc.) by gradient separation. Briefly, blood was mixed with an equal volume of PBS, and 25 ml of this mixture was laid over 12ml of Histopaque®-10771 (Sigma, density=1.0771 g/ml). The mixture was centrifuged at 900×*g* for 30 min at room temperature. The leukocytes-containing layer was harvested and PBS was added up to 50 ml. Leukocytes were centrifuged at 250 ×*g* for 10 min at room temperature. This PBS wash was repeated until all the platelets were washed away. Leukocytes were counted and seeded in Dulbecco's Modified Eagle Medium (DMEM; Gibco) supplemented with 10% heat-inactivated fetal calf serum (HI-FCS; Hyclone), 2 mM L-glutamine (Gibco), 1 mM sodium pyruvate (Gibco), and 100 U/ml penicillin-100 µg/ml streptomycin (Gibco) at 37°C, 5% CO_2, and 90% humidity. Medium was changed every two days, and fully differentiated macrophages were obtained after seven to eight days. Macrophages were seeded at a density of 1×10^5 cells per well in 24-well plates (TPP) for immunostaining (with coverslips, Fisher Scientific) or quantitative real-time RT-PCR analysis. Cells were incubated with Mtb H37Rv at a multiplicity of infection 10:1 (bacteria per macrophage) for 2h, washed with PBS three times and cultured in

DMEM medium without antibiotics. For the inhibition of cholesterol synthesis, 10 μM of Mevastatin (Sigma) was added to macrophages that were infected with Mtb.

Confocal microscopy

Cells were fixed in 4% paraformaldehyde in PBS for 30 min, washed with PBS three times and blocked with 5% bovine serum albumin (Sigma), 1.5% glycine (VWR International), and 0.1% saponin in PBS at room temperature for 1h. Cells were incubated with guinea pig polyclonal antibody against murine Adfp or mouse monoclonal antibody against human ADFP (1:100, RDI division of Fitzgerald Industries Intl.), rabbit polyclonal antibody against human ACSL1 (1:200, GenWay Biotech), or rabbit polyclonal antibody against human SapC (1:50, Santa Cruz Biotechnology) at 37°C for 1 h. After washing with PBS three times, cells were incubated with Texas Red®-donkey antibody against guinea pig or mouse IgG (H+L) (1:250, Jackson ImmunoResearch) or Texas Red®-goat antibody against rabbit IgG (H+L) (1:250, Jackson ImmunoResearch) and BODIPY® 493/503 (1 μg/ml, Invitrogen) for lipid droplets, at room temperature for 1 h. Cells were washed with PBS three times, and nuclei were stained with 5 μg/ml of bisbenzimide (Sigma) in PBS at room temperature for 5 min. After washing in PBS, cells were mounted in ProLong Gold Antifade Reagent (Molecular Probes®). Cells without primary antibody staining were included as negative controls. Images were captured using Leica TCS SP5 confocal laser scanning microscope (Leica Microsystems) using a 63× oil immersion lens.

Quantitative real-time RT-PCR

Infected and uninfected macrophages were lysed with TRIZOL® Reagent (Invitrogen) and homogenized by passing cell lysate through a pipette. The homogenized samples

were mixed with 0.2 volume of chloroform per 1 volume of TRIZOL® Reagent. The RNA-containing aqueous phase was column-purified using RNeasy mini kit (Qiagen). RNA samples were treated with DNase using TURBO DNA-*free*™ (Ambion). cDNA was synthesized using iScript™ cDNA Synthesis Kit (BIO-RAD) and used for real-time PCR using iTaq™ SYBR® Green Supermix with ROX (BIO-RAD) in 7500 Fast Real-Time PCR System (Applied Biosystems).

Forward and reverse primers designed by using Primer3 [26].

The primers used in PCR for murine genes are as follows:

Acsl1 forward, 5'-GTCCTGGGCACAGAAGAGAG-3'

Acsl1 reverse, 5'-GTCAGAAGGCCGTTGTCAAT-3'

Adfp forward, 5'-GGAGTGGAAGAGAAGCATCG-3'

Adfp reverse, 5'-TGGCATGTAGTCTGGAGCTG-3'

SapC forward, 5'-GATCCTGCCAGAACCAAGTG-3'

SapC reverse, 5'-CTCAAGTGCCTCCACCAACT-3'

18S rRNA forward, 5'-GCAATTATTCCCCATGAACG-3'

18S rRNA reverse, 5'-GGCCTCACTAAACCATCCAA-3'

The primers used in PCR for human genes are as follows:

ACSL1 forward, 5'-CCAGAAGGGCTTCAAGACTG-3'

ACSL1 reverse, 5'-GCCTTCTCTGGCTTGTCAAC-3'

ADFP forward, 5'-ACTGGCTGGTAGGTCCCTTT-3'

ADFP reverse, 5'-TGCTTCCCAATTTAGGGTTG-3'

SapC forward, 5'-GGTGACCAAGCTGATTGACA-3'

SapC reverse, 5'-GTACGTGTCCACCACCTCCT-3'

18S rRNA, 5'-GATATGCTCATGTGGTGTTG-3'

18S rRNA, 5'-AATCTTCTTCAGTCGCTCCA-3'

Each PCR was performed in triplicates, and PCR conditions for selected genes are as follows: initial activation at 95°C for 2 min and 40 cycles of denaturation at 95°C for 30 sec and annealing and extension at 53°C for 45 sec. The calculated threshold cycle (C_t) value for each gene was normalized to C_t of house-keeping gene 18S rRNA, and then the fold induction of gene of interest between control macrophages and Mtb-infected macrophages was calculated and expressed by using the formula, $2^{-\Delta\Delta Ct}$.

RESULTS and DISCUSSION

Macrophages not only phagocytose and digest the pathogen but also provide a niche for the intracellular pathogen. Mtb has many strategies to subvert the killing mechanisms of the host cell, and moreover, it utilizes host-derived lipids as its own carbon source. Previous studies have indicated that host cells accumulate lipids in response to Mtb infection [27-28]. Moreover, our microarray and immunohistology data (Chapter 2&3&4) indicated that caseum of human TB granulomas were abundant with lipids, and particularly, ADFP, ACSL1, and SapC important for lipid synthesis and sequestration were highly expressed in granulomas.

In the current study, we investigated if Mtb *in vitro* infection in macrophages upregulates the same transcripts as seen in human TB granulomas; *Adfp*, *Acsl1*, and *SapC*. We used murine bone-marrow derived macrophages (BMMΦ) and human peripheral blood monocyte-derived macrophages (PBMM) for Mtb infection.

At day 1 post-infection, murine BMMΦ showed high expression levels of *Adfp*, *Acsl1*, and *SapC* (Table 5.1), which were lower at other time points. We also observed Adfp, Acsl1, and SapC expressions in Mtb-infected cells by immunostaining on BMMΦ of day 1 post-infection (Figure 5.1A–F). However, the antibodies against Adfp and SapC cross-reacted with Mtb bacilli (green Mtb bacilli can be seen in Figure 5.1 F, arrow).

Table 5.1 BMMΦ genes in response to Mtb H37Rv infection
Murine BMMΦ were infected with Mtb H37Rv, and the mRNA levels of *Adfp*, *Acsl1*, and *Psap* (SapC) were determined by quantitative real-time RT-PCR. The experiments were repeated at least three times, and the representative result is shown. Three technical replicates were included for all conditions and genes. The fold change was calculated as described in the method section, and the average of replicates is shown.

Fold induction-normalized to 18S rRNA						
Gene	**Day1**	**Day2**	**Day3**	**Day5**	**Day6**	**Day12**
Adfp	4.2	1.27	0.8	1.05	0.81	0.87
Acsl1	26.25	3.27	2.3	1.68	1.58	0.72
***Psap* (SapC)**	2.46	1.07	0.71	0.82	0.82	1.26

Figure 5.1 Expressions of Adfp, Acsl1, and SapC in murine BMMΦ are induced by Mtb infection.
Murine BMMΦ were infected with Mtb H37Rv for one day and immunostained antigens were observed by confocal microscope.
Representative images are shown here. Antigens are in green and nuclei in blue.
A. Adfp expression in control cells
B. Adfp expression in Mtb infected cells
C. Acsl1 expression in control cells
D. Acsl1 expression in Mtb infected cells
E. SapC expression in control cells
F. SapC expression in Mtb infected cells, an arrow indicates Mtb bacillus.

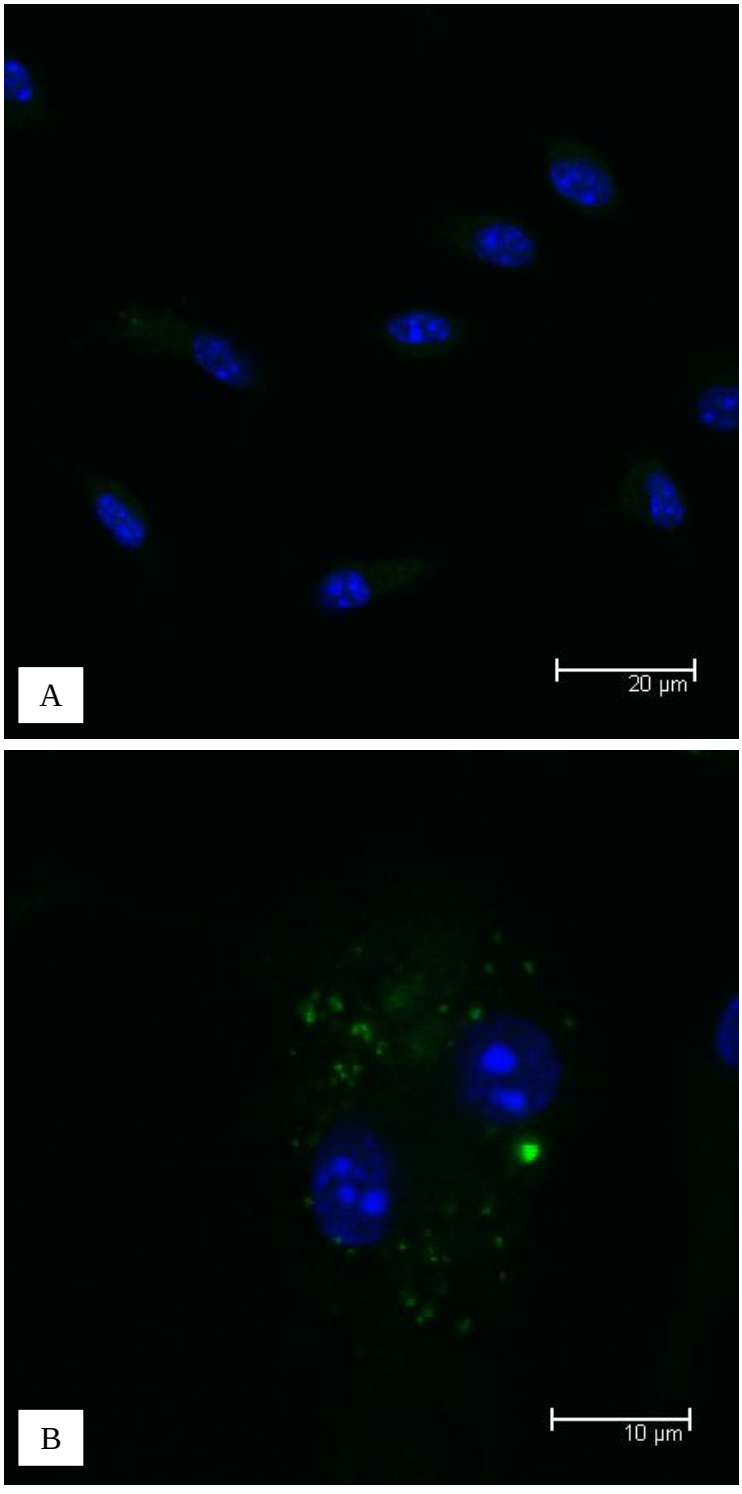
A
20 µm
B
10 µm

Figure 5.1 (Continued)

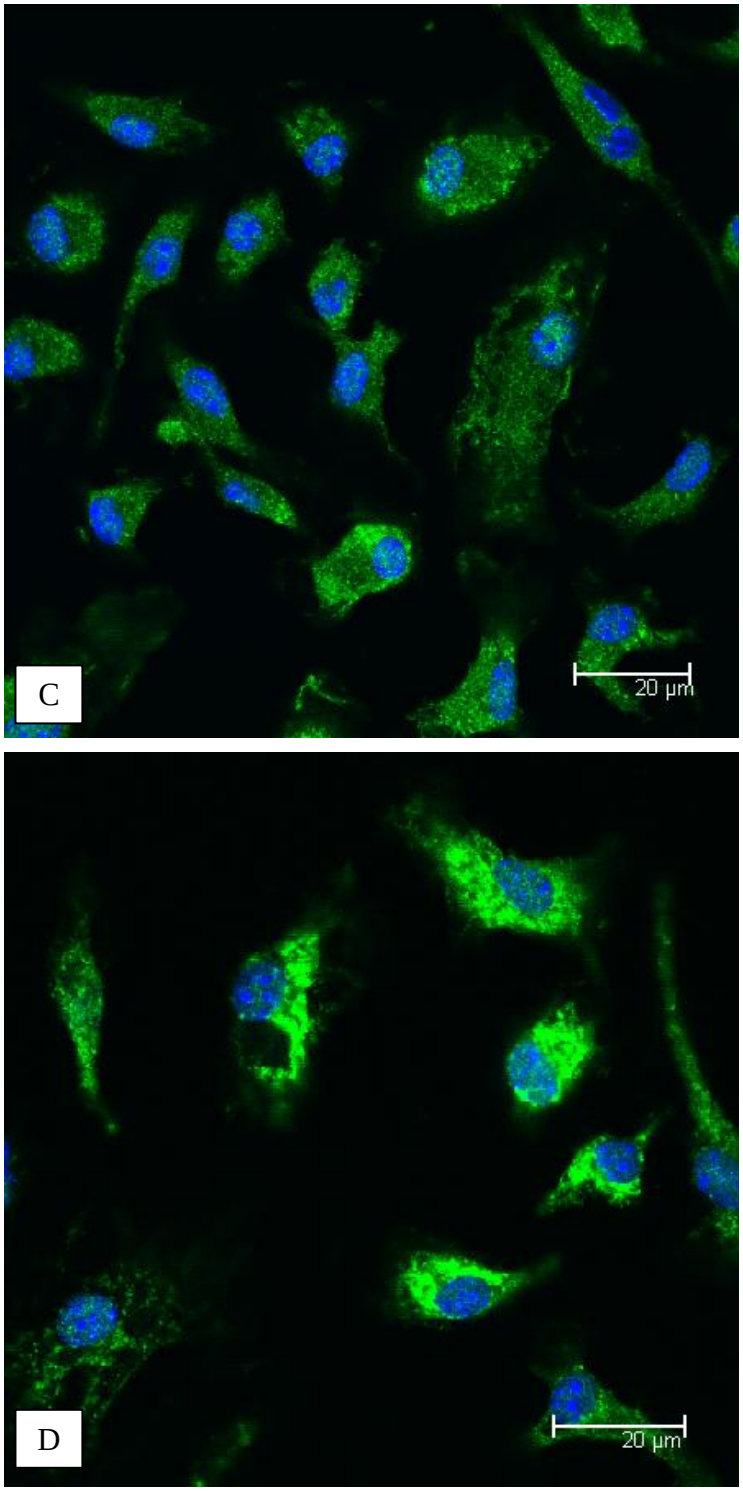

Figure 5.1 (Continued)

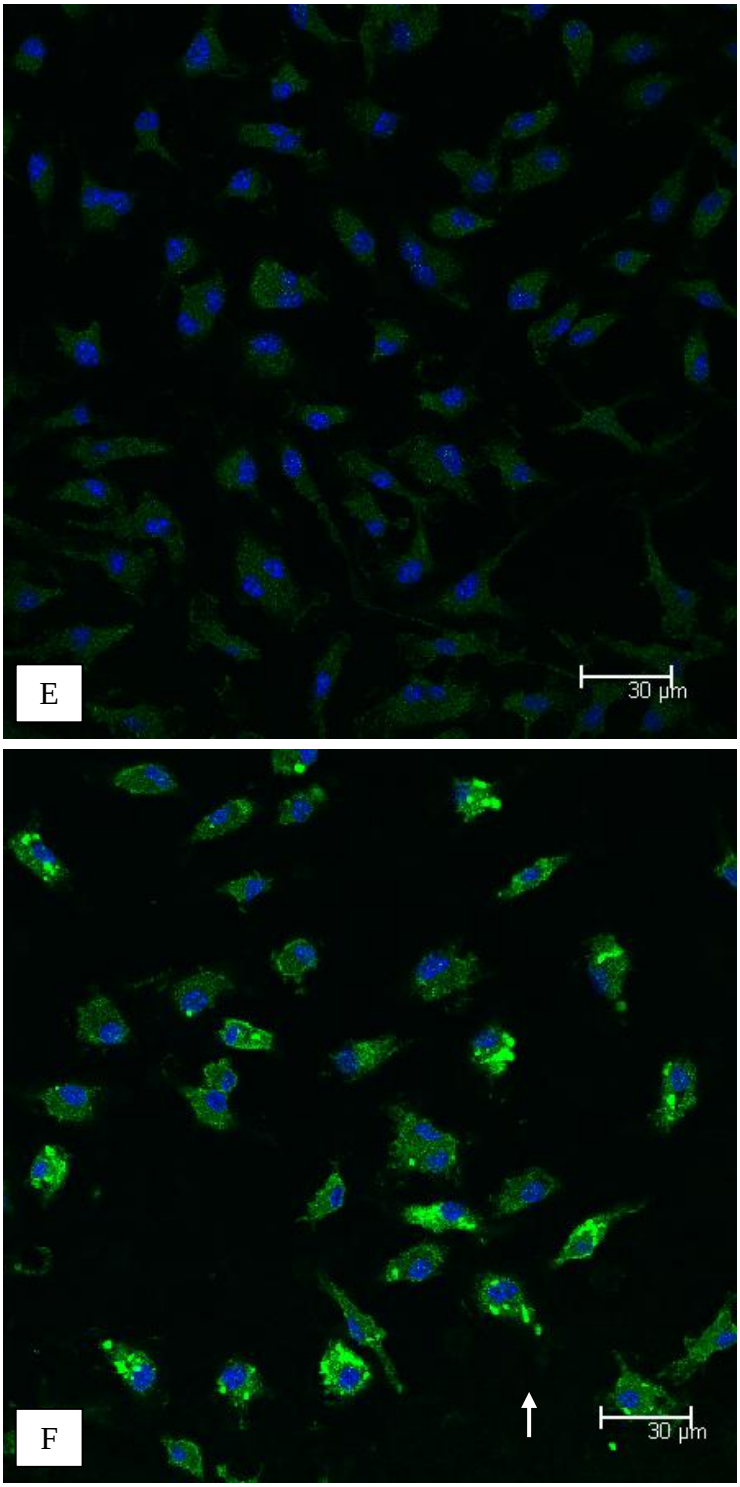

Table 5.2 PBMM genes in response to Mtb H37Rv infection
Human PBMM were infected with Mtb H37Rv for 4 days in the absence or presence of Mevastatin, and then total RNAs were prepared from three replicates. The mRNA levels of *ADFP*, *ACSLL*, and *PSAP* (SapC) were determined by quantitative real-time RT-PCR. Three technical replicates were included for all conditions and genes for the assay. The fold change for each replicate was calculated as described in the method section, and the average of replicates is shown here.

Fold induction-normalized to 18S rRNA		
Gene	**Mtb**	**Mtb + Mevastatin**
ADFP	1.22	1
ACSL1	1.86	1.63
***PSAP* (SapC)**	1.37	1.09

Figure 5.2 Expressions of ADFP, ACSL1, and SapC in PBMM are induced by Mtb infection

Human PBMM were infected with Mtb H37Rv for 4 days, and immunostained antigens were observed by confocal microscope.

Representative images are shown here. Antigens are in red, neutral lipids in green, and nuclei in blue.

A. ADFP expression in control cells

B. ADFP expression in Mtb infected cells. It is expressed at the surface of lipid droplets.

C. ACSL1 expression in control cells

D. ACSL1 expression in Mtb infected cells. Its expression is also detected at the surface of lipid droplets.

E. SapC expression in control cells

F. SapC expression in Mtb infected cells

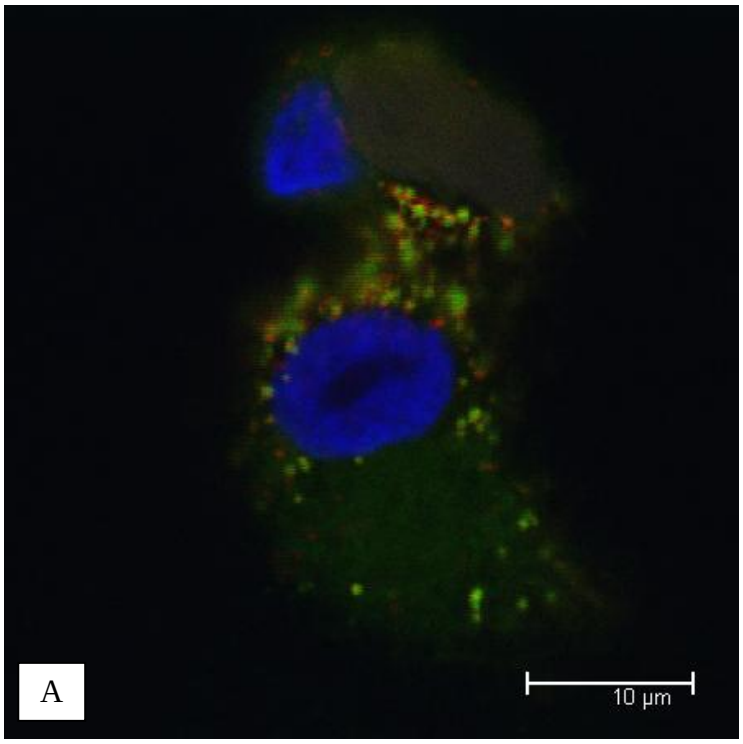
A
10 µm

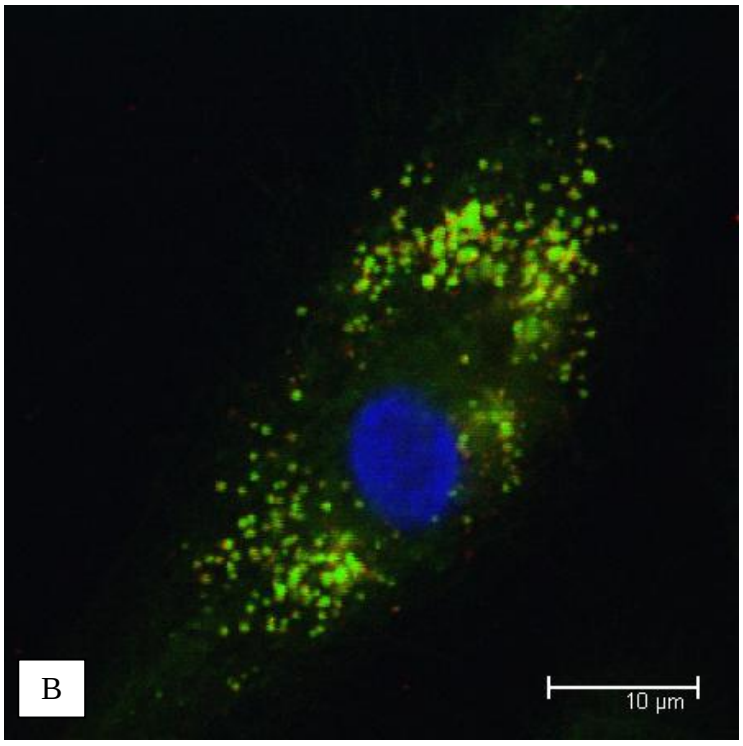
B
10 µm

Figure 5.2 (Continued)

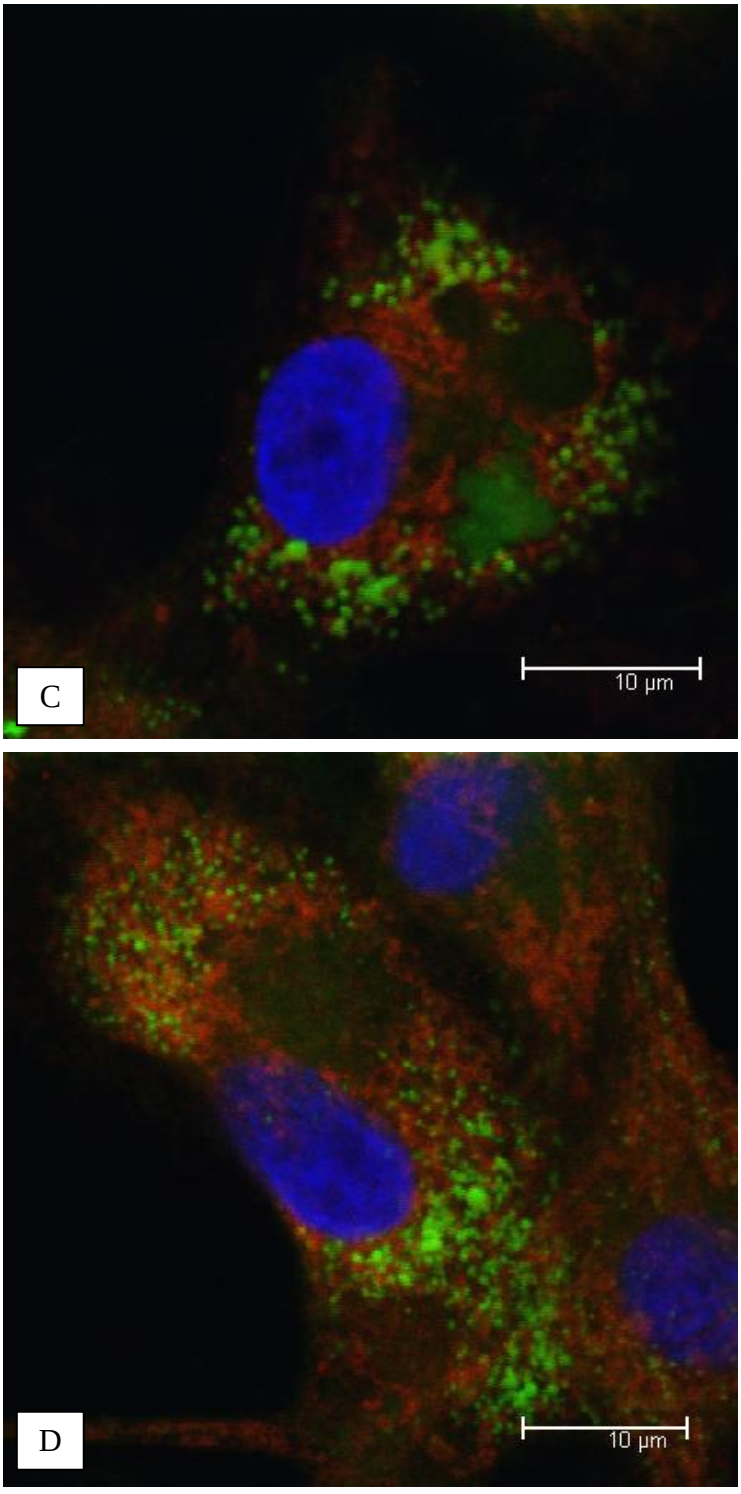

Figure 5.2 (Continued)

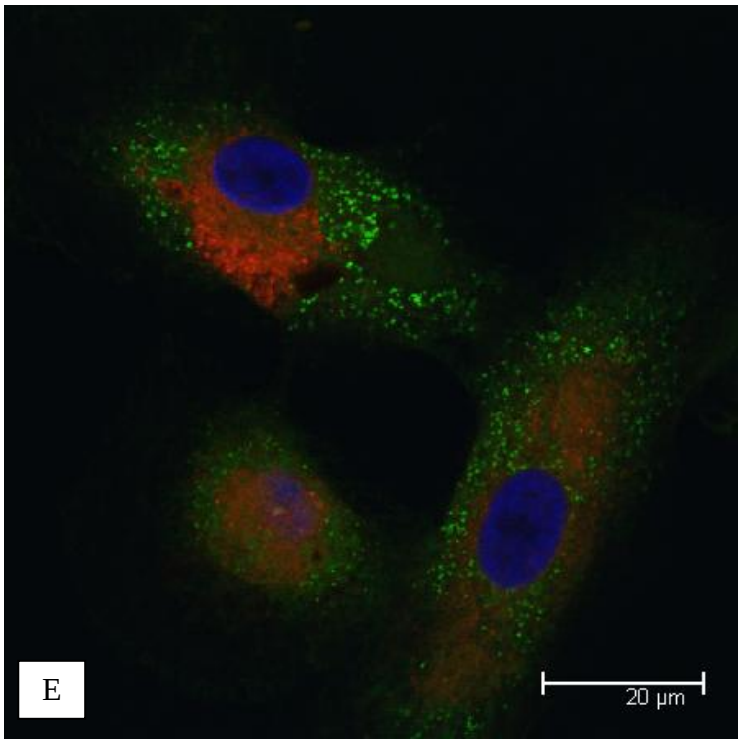

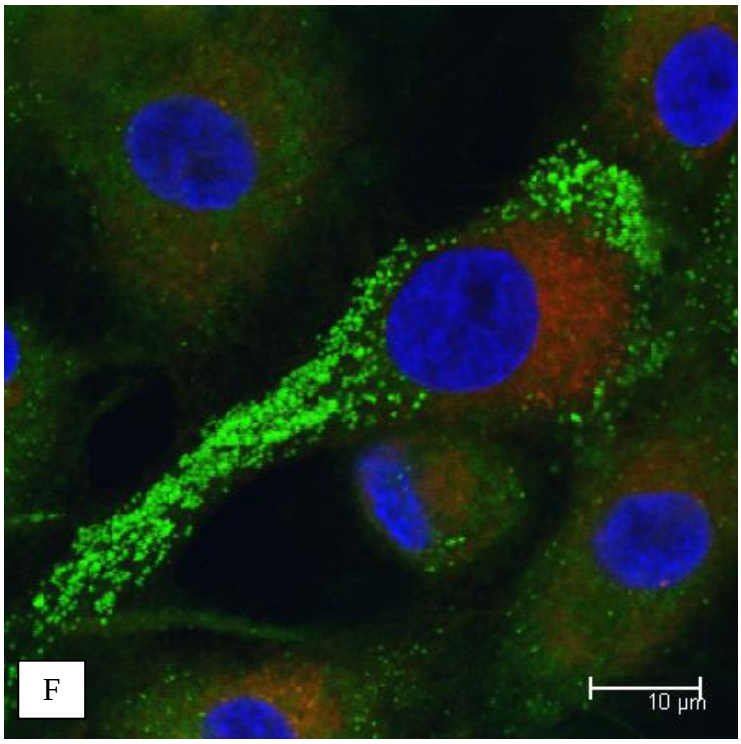

Human PBMM were infected with Mtb H37Rv for 4 days and examined for mRNA and protein expressions. We observed a slight increase of transcripts in Mtb-infected cells (Table 5.2) and also proteins as shown by confocal microscopy (Figure 5.2A–F). However, the control cells also showed lipid droplets. The addition of Mevastatin lowered the gene expression [29], but we could not detect any changes in protein expression by confocal microscopy; lipid droplets were still present (data not shown).

In summary, the current study has shown that Mtb infection leads to the accumulation of lipid droplets in murine or human macrophages, which is accompanied by the upregulated transcripts and proteins of ADFP, ACSL1, and SapC. This data is in line with previous reports that macrophages or murine lung infected with virulent Mtb accumulates neutral lipids [21, 27-28, 30]. Moreover, this corroborates our analyses on human TB pulmonary granulomas that the host undergoes metabolic shift during Mtb infection which results in the accumulation of lipids as caseum.

Many questions are remained unanswered. Future work should include whether lipid droplets-derived lipids contribute to the formation of caseum, Mtb-derived lipids intersect with host-derived lipids, and lipid droplets-derived lipids are used for Mtb survival directly or they are merely byproducts of host inflammation. The information about the essential carbon source for Mtb within host cells will help to design novel drugs.

REFERENCES

1. Hirsch, C.S., et al., *Complement receptor-mediated uptake and tumor necrosis factor-alpha-mediated growth inhibition of Mycobacterium tuberculosis by human alveolar macrophages.* J Immunol, 1994. **152**(2): p. 743-53.
2. Schlesinger, L.S., *Macrophage phagocytosis of virulent but not attenuated strains of Mycobacterium tuberculosis is mediated by mannose receptors in addition to complement receptors.* J Immunol, 1993. **150**(7): p. 2920-30.
3. Schlesinger, L.S., et al., *Phagocytosis of Mycobacterium tuberculosis is mediated by human monocyte complement receptors and complement component C3.* J Immunol, 1990. **144**(7): p. 2771-80.
4. Stokes, R.W., et al., *Mycobacteria-macrophage interactions. Macrophage phenotype determines the nonopsonic binding of Mycobacterium tuberculosis to murine macrophages.* J Immunol, 1993. **151**(12): p. 7067-76.
5. Ernst, J.D., *Macrophage receptors for Mycobacterium tuberculosis.* Infect Immun, 1998. **66**(4): p. 1277-81.
6. Gaynor, C.D., et al., *Pulmonary surfactant protein A mediates enhanced phagocytosis of Mycobacterium tuberculosis by a direct interaction with human macrophages.* J Immunol, 1995. **155**(11): p. 5343-51.
7. Peterson, P.K., et al., *CD14 receptor-mediated uptake of nonopsonized Mycobacterium tuberculosis by human microglia.* Infect Immun, 1995. **63**(4): p. 1598-602.
8. Haworth, R., et al., *The macrophage scavenger receptor type A is expressed by activated macrophages and protects the host against lethal endotoxic shock.* J Exp Med, 1997. **186**(9): p. 1431-9.

9. Philips, J.A., E.J. Rubin, and N. Perrimon, *Drosophila RNAi screen reveals CD36 family member required for mycobacterial infection.* Science, 2005. **309**(5738): p. 1251-3.

10. Bowdish, D.M., et al., *MARCO, TLR2, and CD14 are required for macrophage cytokine responses to mycobacterial trehalose dimycolate and Mycobacterium tuberculosis.* PLoS Pathog, 2009. **5**(6): p. e1000474.

11. Via, L.E., et al., *Arrest of mycobacterial phagosome maturation is caused by a block in vesicle fusion between stages controlled by rab5 and rab7.* J Biol Chem, 1997. **272**(20): p. 13326-31.

12. Armstrong, J.A. and P.D. Hart, *Response of cultured macrophages to Mycobacterium tuberculosis, with observations on fusion of lysosomes with phagosomes.* J Exp Med, 1971. **134**(3 Pt 1): p. 713-40.

13. Armstrong, J.A. and P.D. Hart, *Phagosome-lysosome interactions in cultured macrophages infected with virulent tubercle bacilli. Reversal of the usual nonfusion pattern and observations on bacterial survival.* J Exp Med, 1975. **142**(1): p. 1-16.

14. Kyei, G.B., et al., *Rab14 is critical for maintenance of Mycobacterium tuberculosis phagosome maturation arrest.* Embo J, 2006. **25**(22): p. 5250-9.

15. Crowle, A.J., et al., *Evidence that vesicles containing living, virulent Mycobacterium tuberculosis or Mycobacterium avium in cultured human macrophages are not acidic.* Infect Immun, 1991. **59**(5): p. 1823-31.

16. Sturgill-Koszycki, S., et al., *Lack of acidification in Mycobacterium phagosomes produced by exclusion of the vesicular proton-ATPase.* Science, 1994. **263**(5147): p. 678-81.

17. Gatfield, J. and J. Pieters, *Essential role for cholesterol in entry of mycobacteria into macrophages.* Science, 2000. **288**(5471): p. 1647-50.

18. Deretic, V. and R.A. Fratti, *Mycobacterium tuberculosis phagosome.* Mol Microbiol, 1999. **31**(6): p. 1603-9.

19. Clemens, D.L. and M.A. Horwitz, *The Mycobacterium tuberculosis phagosome interacts with early endosomes and is accessible to exogenously administered transferrin.* J Exp Med, 1996. **184**(4): p. 1349-55.

20. Sturgill-Koszycki, S., U.E. Schaible, and D.G. Russell, *Mycobacterium-containing phagosomes are accessible to early endosomes and reflect a transitional state in normal phagosome biogenesis*. Embo J, 1996. **15**(24): p. 6960-8.

21. Caceres, N., et al., *Evolution of foamy macrophages in the pulmonary granulomas of experimental tuberculosis models.* Tuberculosis (Edinb), 2009. **89**(2): p. 175-82.

22. Pandey, A.K. and C.M. Sassetti, *Mycobacterial persistence requires the utilization of host cholesterol.* Proc Natl Acad Sci U S A, 2008. **105**(11): p. 4376-80.

23. Brzostek, A., et al., *Mycobacterium tuberculosis is able to accumulate and utilize cholesterol.* J Bacteriol, 2009. **191**(21): p. 6584-91.

24. Chang, J.C., et al., *Identification of Mycobacterial genes that alter growth and pathology in macrophages and in mice.* J Infect Dis, 2007. **196**(5): p. 788-95.

25. Chang, J.C., et al., *igr Genes and Mycobacterium tuberculosis cholesterol metabolism.* J Bacteriol, 2009. **191**(16): p. 5232-9.

26. Rozen, S. and H. Skaletsky, *Primer3 on the WWW for general users and for biologist programmers.* Methods Mol Biol, 2000. **132**: p. 365-86.

27. Kondo, E. and K. Kanai, *Accumulation of cholesterol esters in macrophages incubated with mycobacteria in vitro.* Jpn J Med Sci Biol, 1976. **29**(3): p. 123-37.

28. Kondo, E., et al., *Analysis of host-originated lipids associated with "in vivo grown tubercle bacilli".* Jpn J Med Sci Biol, 1970. **23**(5): p. 315-26.

29. Campia, I., et al., *Geranylgeraniol prevents the cytotoxic effects of mevastatin in THP-1 cells, without decreasing the beneficial effects on cholesterol synthesis.* Br J Pharmacol, 2009. **158**(7): p. 1777-86.

30. Peyron, P., et al., *Foamy macrophages from tuberculous patients' granulomas constitute a nutrient-rich reservoir for M. tuberculosis persistence.* PLoS Pathog, 2008. **4**(11): p. e1000204.

CHAPTER SIX

HOST RESPONSE TO MYCOBACTERIAL TREHALOSE DIMYCOLATE

ABSTRACT

Mycobacterium tuberculosis (Mtb) infection triggers the formation of tuberculous (TB) granuloma in the host. In human TB, the mechanism of granuloma development and breakdown is not well-characterized. Multiple mycobacterial cell wall components are shown to be responsible for the granulomatous response including trehalose dimycolate (TDM). In this study, we demonstrate that macrophages in TDM-induced murine granulomas (TDM-granulomas) are filled with lipid droplets, which are associated with expression of adipose differentiation-related protein (Adfp) and acyl-CoA synthetase long-chain family member 1 (Acsl1). TDM-granulomas secrete proinflammatory cytokines, interleukin (IL)-6 and tumor necrosis factor (TNF)-α, and show tissue-damaging pathology. These phenomena are not dependent of B- or T-cells in mice. Similar to human TB, microarray analysis on TDM-granuloma reveals a striking resemblance to caseous human TB granuloma with regard to lipid accumulation, tissue remodeling, inflammatory response, and many other biological processes. These results show that a single mycobacterial cell wall component, TDM, induces foam cell formation in mice and is capable of forming granulomas which mimic human TB granulomas. Thus murine TDM-granulomas serve as a good model of human TB pathogenesis, especially regarding characterization of individual host factors involved in cellular recruitment, metabolic dysregulation, and tissue remodeling.

INTRODUCTION

Mycobacterium tuberculosis (Mtb) infection results in the formation of well-organized granuloma where the bacteria are sequestered and remain dormant unless tuberculosis (TB) is reactivated. The mechanism of TB reactivation is still unclear, although conditions such as acquired immune deficiency syndrome (AIDS), aging, malnutrition, and other diseases predispose Mtb- infected individuals to active TB. TB transmission occurs via Mtb-containing aerosols coughed up by patients with active disease, when the granuloma is cavitated. Due to limited availability of human TB tissues, it is prudent to develop alternative models in studying the mechanism of granuloma development and breakdown.

The granulomatous response by Mtb infection has been shown to be triggered by Mtb cell wall components such as lipoarabinomannan (LAM), phosphatidylinositol mannosides (PIM), and trehalose dimycolate (TDM) [1]. Our previous work has shown that mycobacterial lipids are continuously released from infected cells and transferred to bystander cells [2-3]. Of the released lipids, TDM is a major immunostimulatory factor, eliciting proinflammatory cytokine production and induces a strong granulomatous response in mice [4-6]. We also have shown that TDM-induced stimulation of macrophages requires the presence of toll-like receptor (TLR) adaptor protein myeloid differentiation factor 88 (MyD88), TLR2, CD14, and macrophage receptor with collagenous structure (Marco) [4, 7]. Patients with cavitary TB were shown to have bacteria growing on the open cavitary surface, and these bacilli were covered with a membrane, which might consist of TDM released from continuously growing bacteria at the interface between the airway and liquefactive granuloma [8-9]. Recently, Peyron *et al*. showed that TDM, particularly oxygenated species that are present in virulent Mtb (e.g. keto- and methoxy-mycolates) is capable of inducing foam cell formation *in vitro* [10]. This is of particular interest since foam

cells were seen in TB-affected lung tissues of mice and human [9-11]. Our analyses on human pulmonary TB granulomas also have revealed the upregulation of genes and proteins involved in lipid synthesis and accumulation including adipose differentiation-related protein (ADFP), acyl-CoA synthetase long-chain family member 1 (ACSL1), and saposin C (SapC), which were implicated in the formation of lipid-filled caseum (Chapter 2&3). In addition, our analysis on lipid composition showed the abundance of neutral lipids and glycosphingolipids in caseum (Chapter 4). Furthermore, macrophages infected with Mtb *in vitro* upregulated transcripts for ADFP, ACSL1, and SapC (Chapter 5). These data indicate that Mtb or Mtb-derived factors influence the host lipid metabolism, thereby leading to lipid accumulation.

In this study, we examined murine TDM-induced granulomas in comparison to human TB granulomas. TDM, coated onto polystyrene beads, induced a strong granulomatous response subcutaneously. Numerous lipid-filled foam cells were observed in TDM-granuloma and lipid droplets were tightly associated with Adfp and Acsl1. *Ex vivo* TDM-granulomas also secreted proinflammatory cytokines, e.g. IL-6 and TNF-α. These responses were independent on B- or T-cells, demonstrating that innate immunity is primarily involved in forming lipid droplets upon TDM stimulation. Of special interest was to observe that murine TDM-granulomas presented pathologies similar to human TB granulomas. Microarray analysis on TDM-granuloma further revealed similarities in gene expression profiles with regard to immune response, tissue remodeling, and lipid metabolism. These results show that TDM provokes lipid accumulation in host cells *in vivo*, and therefore, TDM-granuloma may serve as a good model to investigate human TB granuloma.

METHODS and MATERIALS

Animals

Four to six week-old C57BL/6J and *Rag1*$^{-/-}$ (C57BL/6 background) female mice were obtained from the Jackson Laboratory and housed under specific-pathogen-free conditions. All experiments were approved by Cornell University Institutional Animal Care and Use Committee.

In vivo granuloma model

Mycobacterial lipid-bearing beads were prepared as described previously, with slight modifications [4, 6]. Briefly, 9.25×10^3 of 80 μm polystyrene microspheres (Duke Scientific) were coated with 15 μg of Mtb-derived TDM or control lipid phosphatidylglycerol (PG, Sigma) by alternative cycles of vortexing and sonication. The TDM- or PG-coated beads were resuspended in 300 μl of ice-cold growth-factor reduced Matrigel (BD). The mixture was injected subcutaneously into the scruff of the murine neck. At day 3, 6, and 9 post-inoculation, WT and KO mice were sacrificed and granulomas were harvested. Three or four mice were used for the injection of TDM- or PG-Matrigel mixture.

Histology

Granulomas were fixed in 4% paraformaldehyde in PBS at 4°C for over 24 hours and transferred to 70% ethanol. Tissues were embedded in paraffin and cut at 4 μm thickness (Cornell Histology Laboratory). Sections were stained with hematoxylin & eosin for histological examination. Images were captured by Zeiss Axio Imager with AxioVision LE software (Carl Zeiss MicroImaging).

Immunohistology

Paraffin-embedded sections were heat-fixed, deparaffinized and rehydrated. Epitopes were heat-retrieved in 1 mM EDTA buffer pH 8.0, and tissue sections were blocked

with 5% BSA in PBS at room temperature for 1 hour. Guinea pig polyclonal antibody against murine Adfp (1:200, RDI division of Fitzgerald Industrial Intl.) or rabbit polyclonal antibody against human ACSL1 (1:150, GenWay Biotech) was applied to sections at 37°C for 1 hour. After washing with PBS three times, sections were incubated with 1% Sudan Black B (Sigma) in 70% ethanol at room temperature for 10 min. Sections were washed with PBS three times and incubated with Texas Red®-donkey antibody against guinea pig IgG (H+L) (1:250, Jackson ImmunoResearch) or Texas Red®-goat antibody against rabbit IgG (H+L) (1:250, Jackson ImmunoResearch) at room temperature for 45 min. After three washes with PBS, nuclei were stained with 5 µg/ml of bisbenzimide (Sigma) in PBS at room temperature for 5 min. After thorough wash with PBS, sections were mounted in ProLong Gold Antifade Reagent (Molecular Probes®). Sections without primary antibody were included as a negative control. Images were captured by Zeiss Axio Imager with AxioVision LE software (Carl Zeiss MicroImaging).

Cryosections were cut at 10 µm thickness and fixed in 4% paraformaldehyde in PBS for 20 min. The sections were stained with BODIPY 493/503 (10 µg/ml, Invitrogen) or Nile Red (1 µg/ml, Sigma) for neutral lipids and with bisbenzimide for nuclei. Mounted sections were visualized by Zeiss Axio Imager with AxioVision LE software (Carl Zeiss MicroImaging).

Enzyme-Linked Immunosorbent Assay

Portions of harvested PG- or TDM-granulomas were cultured in 1ml DMEM medium supplemented with 10% heat-inactivated fetal calf serum (Hyclone), 2 mM L-glutamine (Gibco), 1 mM sodium pyruvate (Gibco), and 100 U/ml penicillin-100 µg/ml streptomycin (Gibco) at 37°C, 5% CO_2, and 90% humidity for 48 hours. Conditioned media were collected, centrifuged to remove cell debris, and supernatants

were stored at −80°C until use. Sandwich ELISAs for IL-1β, IL-6, and TNF-α were performed according to the manufacturer's instructions (BD Pharmingen).

Lipid analysis

Total lipids were extracted from PG- or TDM-granulomas in chloroform:methanol (2:1, v/v). The mixture was sonicated at 50°C for 1 hour and filtered through 0.2 μm-pore size PTFE membrane (GD/X® syringe filter, Whatman). Lipids were dried down under nitrogen gas. TLC plates (Aluminum-backed Silica gel 60 plates, EMD) were cleaned in chloroform:methanol (90:10, v/v) and heat-activated at 110°C for 30 min. Total lipids were developed in chloroform:methanol:water (65:25:4) for the first half of the plate, and then in ether:ethyl ether: acetic acid (70:30:2, v/v/v) for the entire plate. Plates were sprayed with 50% sulfuric acid in ethanol and charred for detecting components. The lipid standards used were cholesteryl esters, triacylglycerols, and cardiolipin (Sigma), cholesterol (MP Biomedicals), and neutral glycosphingolipid qualmix (Matreya).

Microarray

PG- or TDM-granulomas were lysed with TRIZOL® Reagent (Invitrogen) and homogenized by passing the lysate through a pipette. The homogenized samples were mixed with 0.2 volume of chloroform per 1 volume of TRIZOL, and phases were separated by centrifugation at 12,000 × *g* for 15 min at 4°C. The RNA-containing aqueous phase was column-purified using RNeasy mini kit (Qiagen), according to manufacturer's instructions. RNA samples were treated with DNase using TURBO DNA-*free*® (Ambion). Purity, quality, and quantity of RNA were assessed by the Agilent NanoChip Bioanalyzer assay, spectrophotometric analysis, and reverse-transcription PCR of β-actin (157 bp), 18S rRNA (123 bp), and glyceraldehyde-3-

phosphate dehydrogenase (189 bp). Because PG does not recruit many leukocytes to the PG injection site, harvested RNA was not sufficient for performing microarrays. Therefore, total RNA samples from both PG- and TDM-granulomas were subjected to amplification. Two-rounds of linear amplification using RiboAmp HS^{TM} Amplification Kit (Molecular Devices) generated sufficient RNA. The amplified antisense RNA (aRNA) was biotinylated using BioArray High Yield^{TM} RNA Transcript Labeling Kit (T7) (Enzo Life Sciences, Inc.), followed by fragmentation, hybridization onto GeneChip® Mouse Genome 430 2.0 Array (Affymetrix) and scanning by GeneArray 300 Scanner (Affymetrix). More than three biological replicates were performed for PG- or TDM-induced granulomas.

Microarray Data Analysis

The data were analyzed by using GeneSpring GX 10.0.2 program (Agilent Technologies). Briefly, MAS5 method was used to summarize raw CEL files, the normalization was done by scaling to median of all samples and the baseline was transformed to the median of all samples. Further analysis was done using Ingenuity Pathway Analysis (Ingenuity® Systems, www.ingenuity.com).

Statistical analysis

The statistical significance of differences in gene expressions between PG-granuloma and TDM-granuloma was calculated using an unpaired *t* test. Results with *P* value less than 0.05 were considered statistically significant.

RESULTS and DISCUSSION

In TB patients, Mtb bacilli are maintained in a well-established structure, TB granuloma. Most Mtb-infected individuals control this granuloma during life time

without showing any clinical symptoms, whereas immunocompromised individuals develop active disease accompanied by granuloma breakdown. We have shown that human pulmonary TB granulomas undergo a metabolic shift during active TB disease, with upregulated lipid metabolism and lipid accumulation in the form of caseum (Chapter 2&3&4). Moreover, Mtb *in vitro* infection leads to lipid accumulation in macrophages (Chapter 5).

In the current study, we examined the granuloma formation in mice using TDM. When TDM was injected into mice subcutaneously, it recruited numerous leukocytes to the site of injection. TDM induced a strong granulomatous response as opposed to control lipid PG (Figure 6.1 A&B). Interestingly, foam cells were frequently observed around TDM-bearing beads (Figure 6.2 A). In contrast, control lipid PG-bearing beads recruited barely any cells (Figure 6.3 A). The extent of foam cell formation was higher at later time points, indicating lipid accumulation occurs progressively (data not shown). Foam cells in TDM-granulomas expressed lipid droplet-associated protein, Adfp (Figure 6.2 B), and lipid droplets were observed by neutral lipid staining with Nile Red on cryosections (Figure 6.2 C). PG-granuloma does not have any detectable Adfp expression (Figure 6.3 B).

To examine if the foam cell formation in response to TDM is dependent on cells of acquired immune response, we injected TDM-bearing beads into *Rag1*$^{-/-}$ (KO) mice that do not have B- and T-cells. KO mice developed a granulomatous response similar to wild-type (WT) mice (Figure 6.4 A). Cells surrounding TDM-beads in KO mice also foamy and express Adfp alongside (Figure 6.4 B). On the contrary to TDM-granulomas, PG-granulomas from KO mice did not recruit many leukocytes and Adfp was not detectable (Figure 6.5 A&B). These data suggest that innate immunity is sufficient for the lipid droplet formation in response to TDM in our granuloma model.

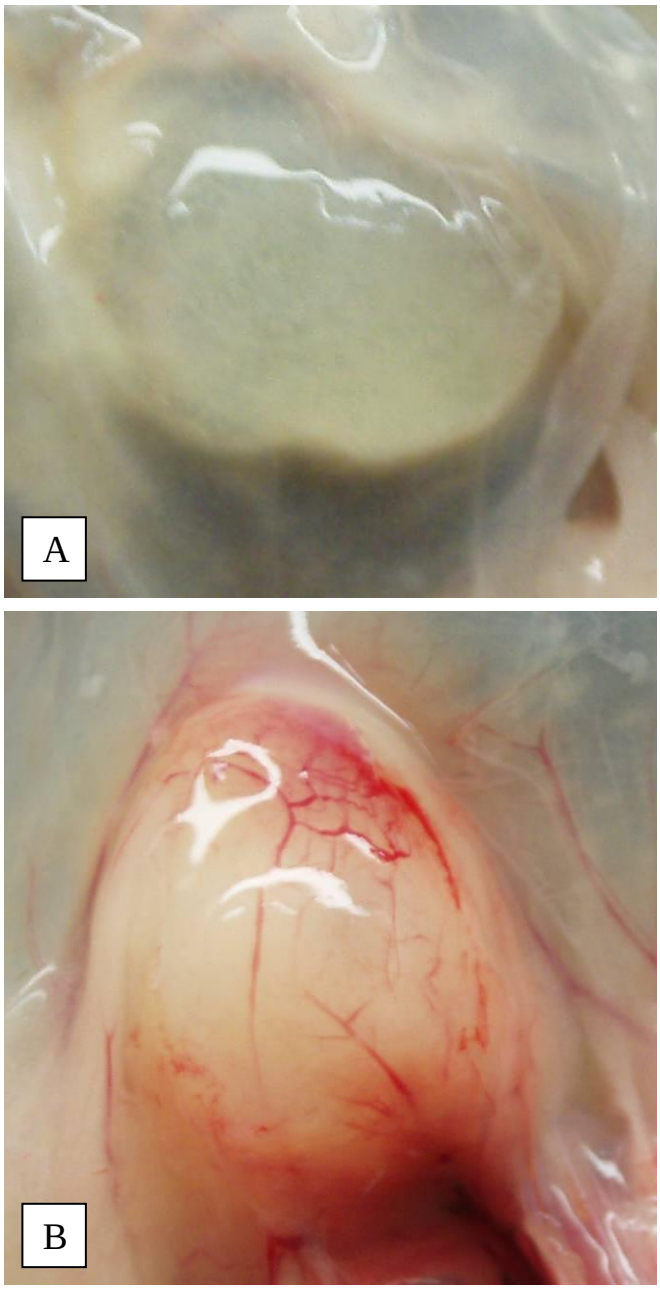

Figure 6.1 The gross feature of PG- and TDM-induced granulomas at day 6. PG-granuloma is pale (A), whereas TDM-granuloma is well vascularized and capsulated (B).

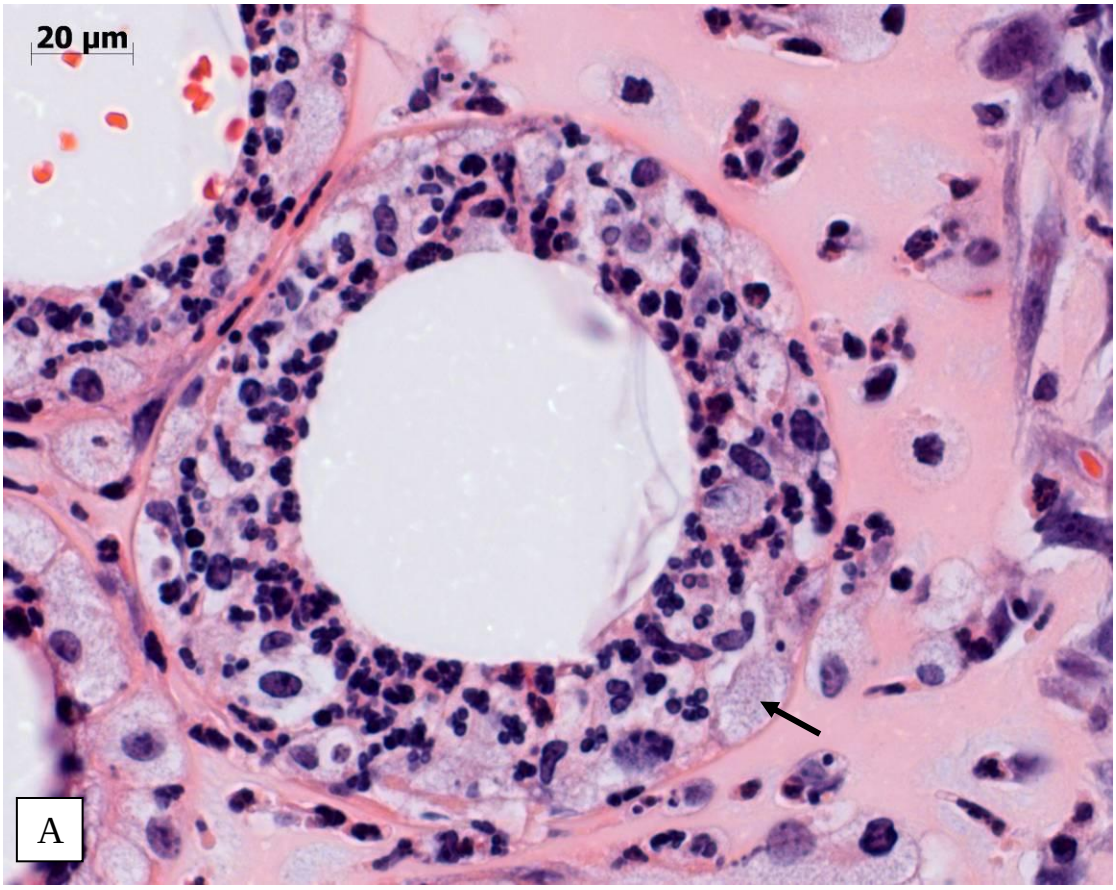

Figure 6.2 TDM induces foam cell formation in mice.
Cells around TDM-beads are foamy, filled with lipid droplets (A). The arrow indicates a foam cell. Foam cells are accompanied by lipid droplet-associated protein, Adfp (B). Adfp is in red and nuclei in blue. The presence of lipid droplets (green) is detected by staining with Nile Red for neutral lipids (C).
Granulomas were harvested at day 6.

Figure 6.2 (Continued)

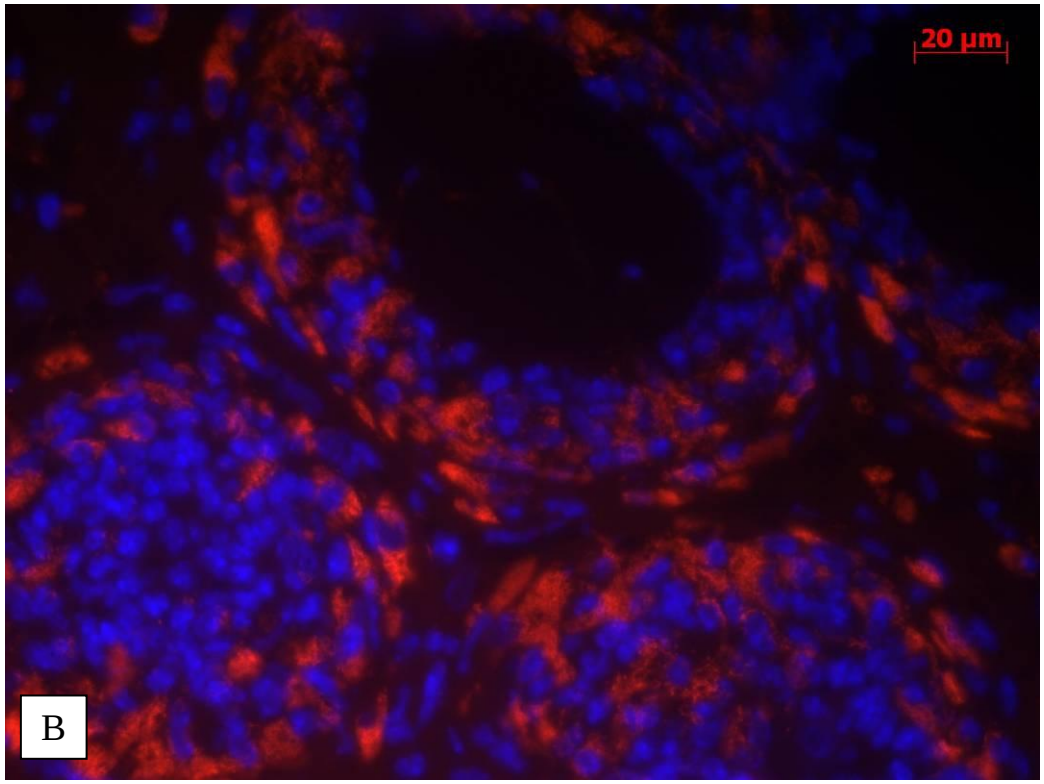

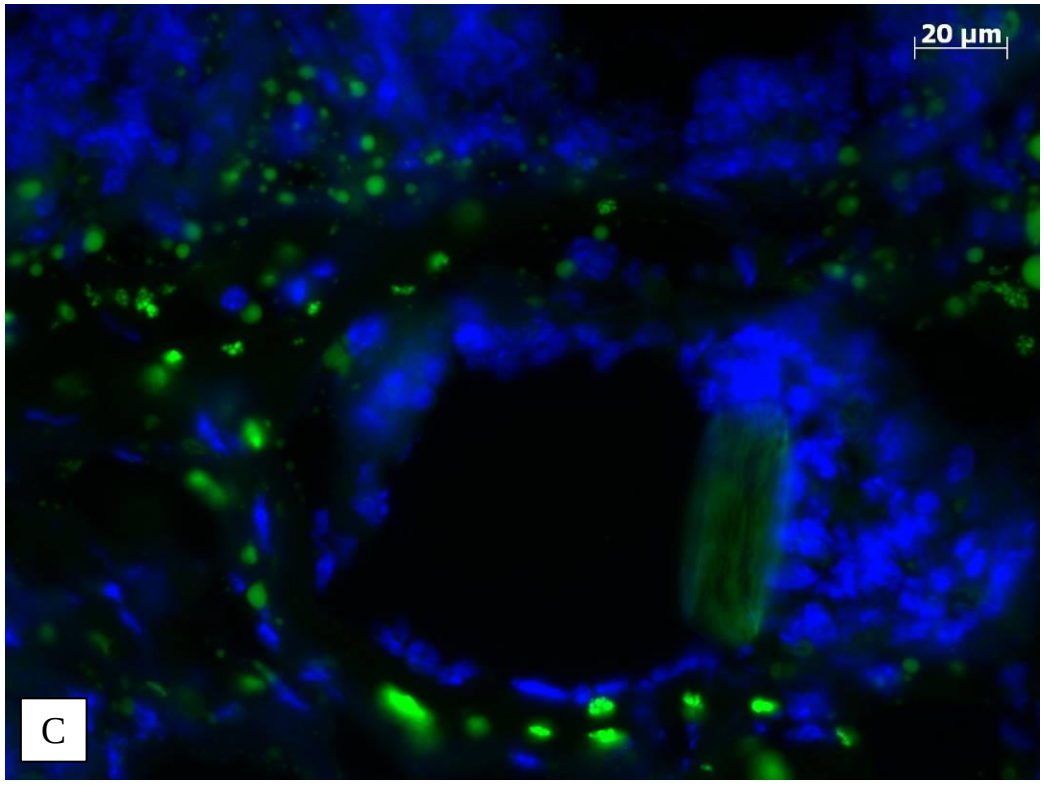

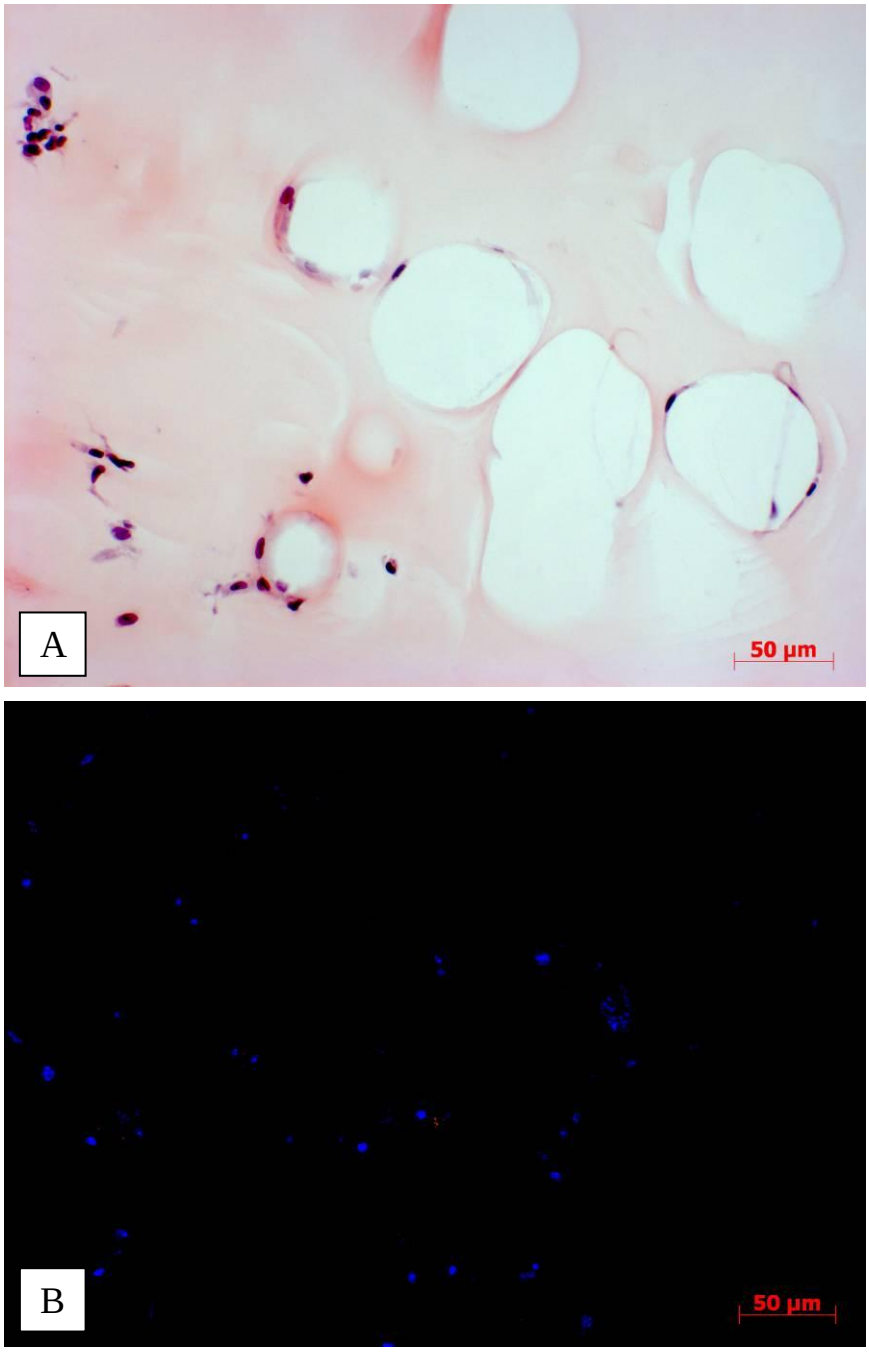

Figure 6.3 PG does not induce a strong granulomatous response.
PG-beads have a few recruited cells (A). Cells around PG-beads show weak Adfp expression (B). Adfp is in red and nuclei in blue.
Granulomas were harvested at day 6.

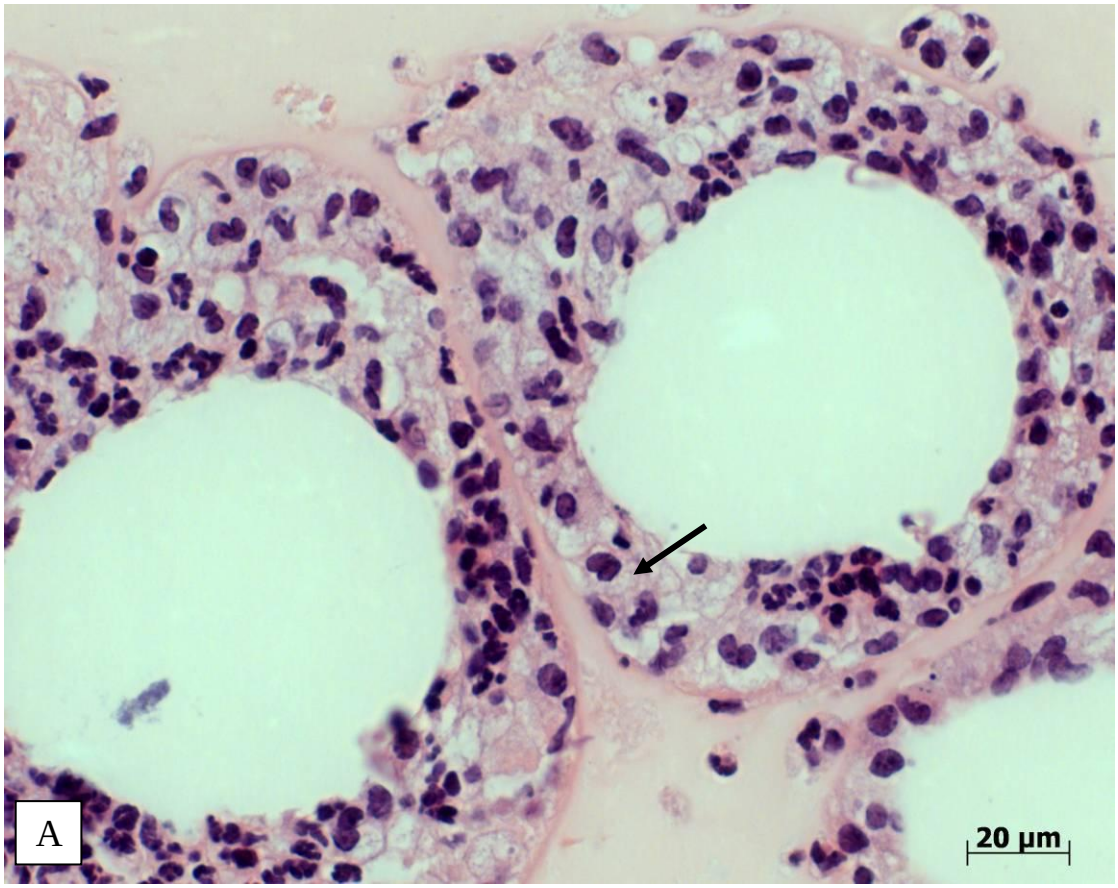

Figure 6.4 TDM induces foam cell formation in *Rag1*$^{-/-}$ mice.
Cells around TDM-beads are foamy, filled with lipid droplets (A). The arrow indicates foam cells. Foam cells are accompanied by lipid droplet-associated protein, Adfp (B). Adfp is in red and nuclei in blue. Granulomas were harvested at day 6.

Figure 6.4 (Continued)

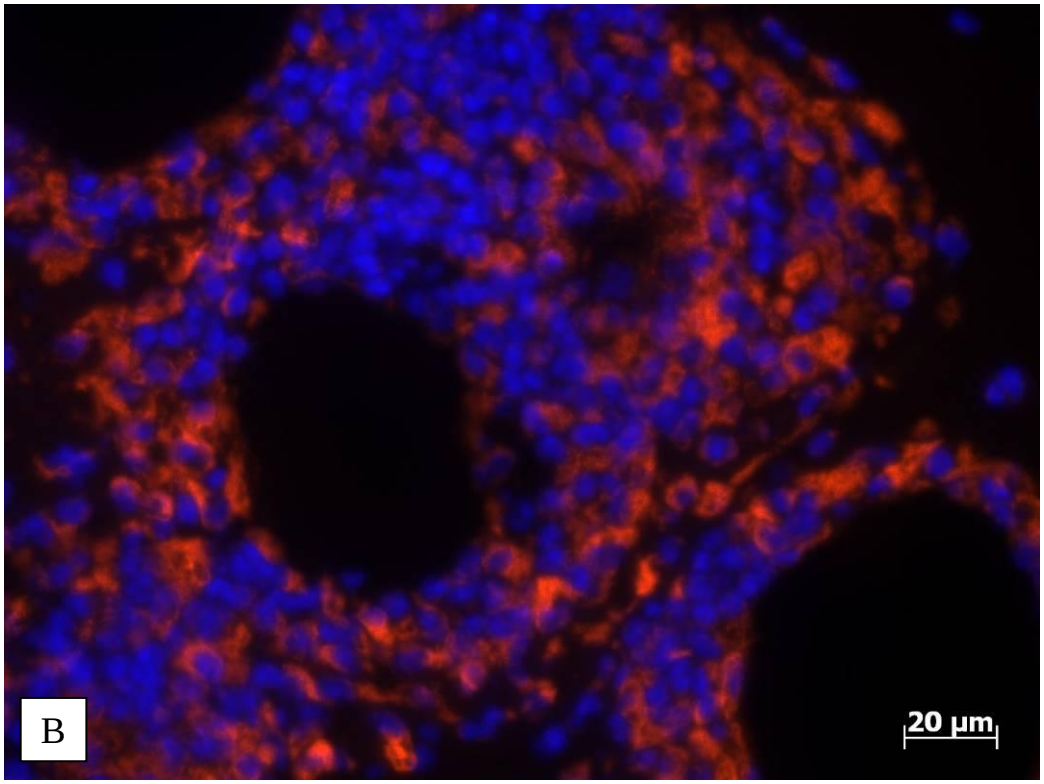

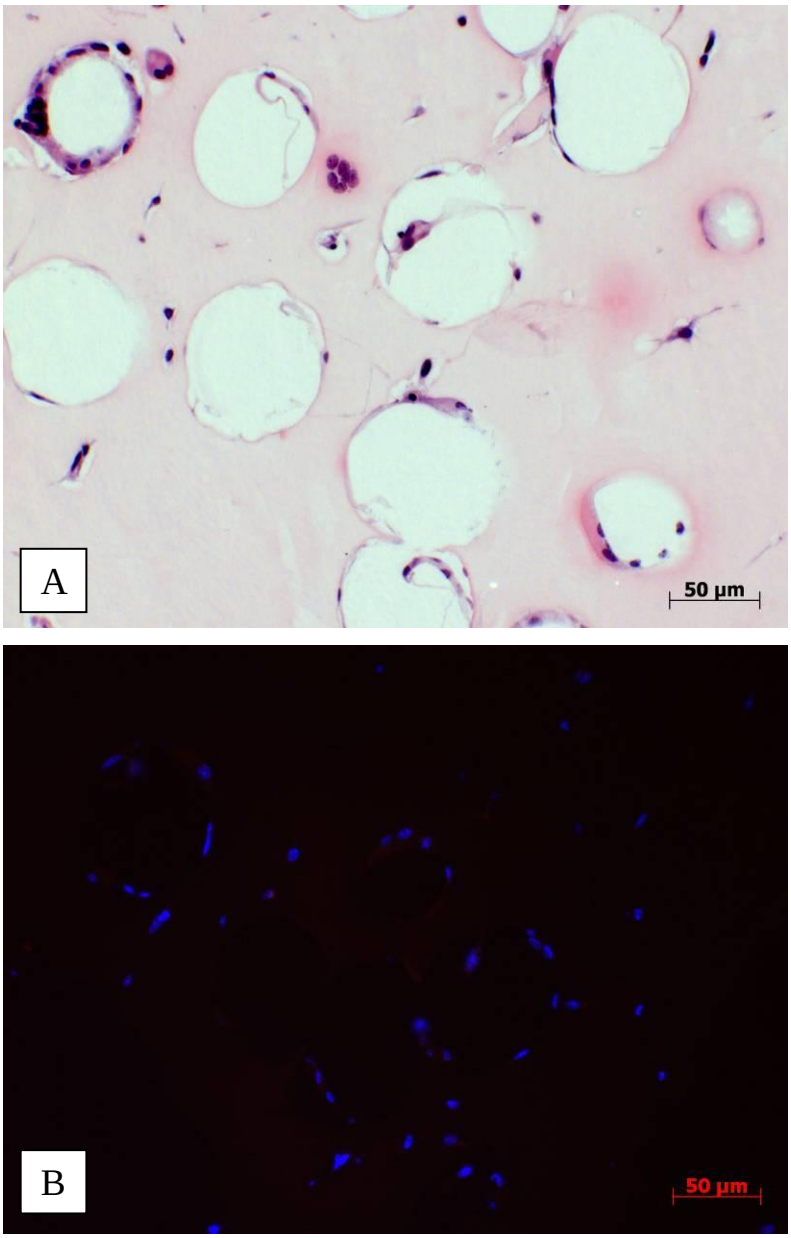

Figure 6.5 PG-induced response in *Rag1*$^{-/-}$ mice.
PG recruited a few cells (A) and Adfp is not detectable (B). Adfp is in red and nuclei in blue. Granulomas were harvested at day 6.

As we observed upregulated transcripts for Adfp, Acsl1, and SapC in Mtb-infected macrophages (Chapter 5), we examined the expression of Acsl1 and SapC in TDM-granulomas. Only Acsl1 was detected by immunohistology (Figure 6.6).

Previous work in our laboratory has shown that *ex vivo* TDM-granuloma secrete proinflammatory cytokines [4, 6]. Since the histology of WT and KO mice was similar, we compared cytokine production in WT and KO TDM granulomas. There were no statistically significant differences in IL-6 and TNF-α production between WT and KO TDM granulomas (Figure 6.7). Although we cannot exclude the role of lymphocytes or lymphocyte-derived factors in regulating the host response to TDM, our data propose that the accumulation of lipids in response to a mycobacterial lipid is driven mainly by innate immunity.

In addition to lipid accumulation in TDM-granulomas, we also observed tissue degeneration and necrotizing center, which are strikingly similar to caseous necrosis in human TB granulomas (Figure 6.8). For further investigation, we performed microarray analysis on TDM-granulomas to examine gene regulation. About 74% of oligonucleotide probe sets that were differentially expressed in murine TDM-granulomas ($P < 0.05$) overlapped with those that were differentially expressed in caseous human pulmonary TB granulomas; totally 4757 genes are common to both murine TDM-granulomas and human TB granulomas ($P < 0.05$) (Figure 6.9). Ingenuity Pathway Analysis® of 4757 common genes showed top bio functions occurring in both murine-TDM granulomas and human TB granulomas including inflammatory response, cell death, cellular movement, and tissue morphology (Table 6.1). Moreover, many biological processes were significantly upregulated in murine TDM-granulomas as observed in human TB granulomas, e.g. immune response, tissue remodeling, and lipid metabolism (Table 6.2–6.4). Consistent with Adfp and Acsl1 protein expressions in TDM-granulomas as shown by immunohistology (Figure 6.2&

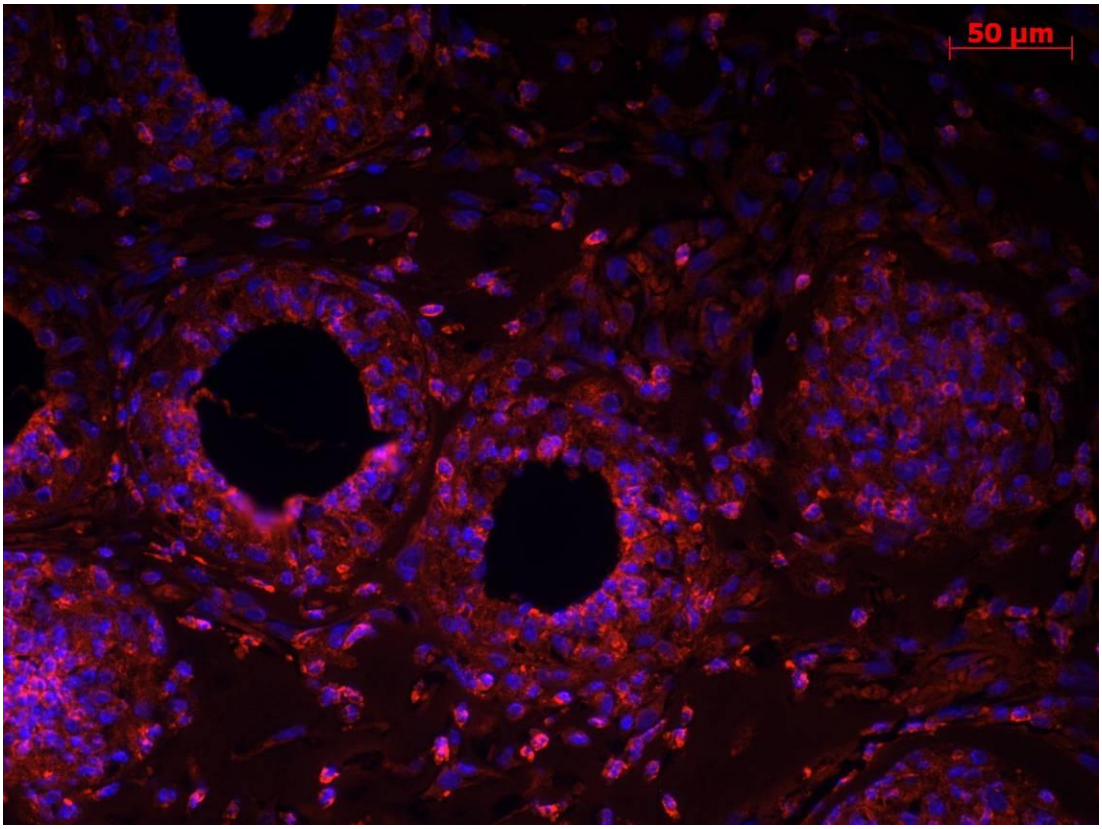

Figure 6.6 TDM-granulomas express Acsl1.
Cells surrounding TDM-bearing beads express lipid synthesis-associated protein, Acsl1. Acsl1 is in red and nuclei in blue. Granulomas from WT mice were harvested at day 6.

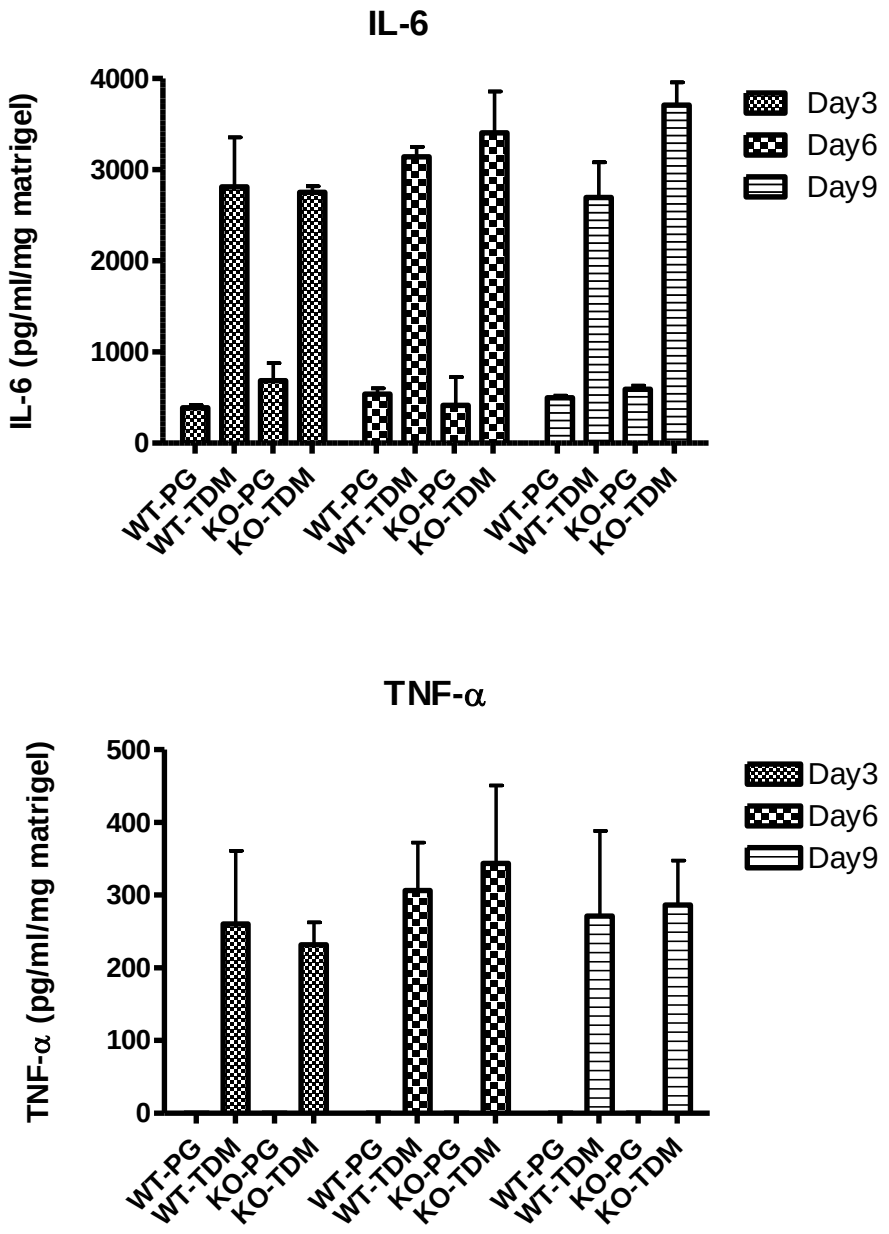

Figure 6.7 *Ex vivo* TDM-granulomas from WT and KO (*Rag1*$^{-/-}$) mice produce comparable amounts of proinflammatory cytokines. Levels of IL-6 and TNF-α were measured by Enzyme-Linked Immunosorbent Assay (ELISA). Data from 3 mice are shown as mean ± S.D.

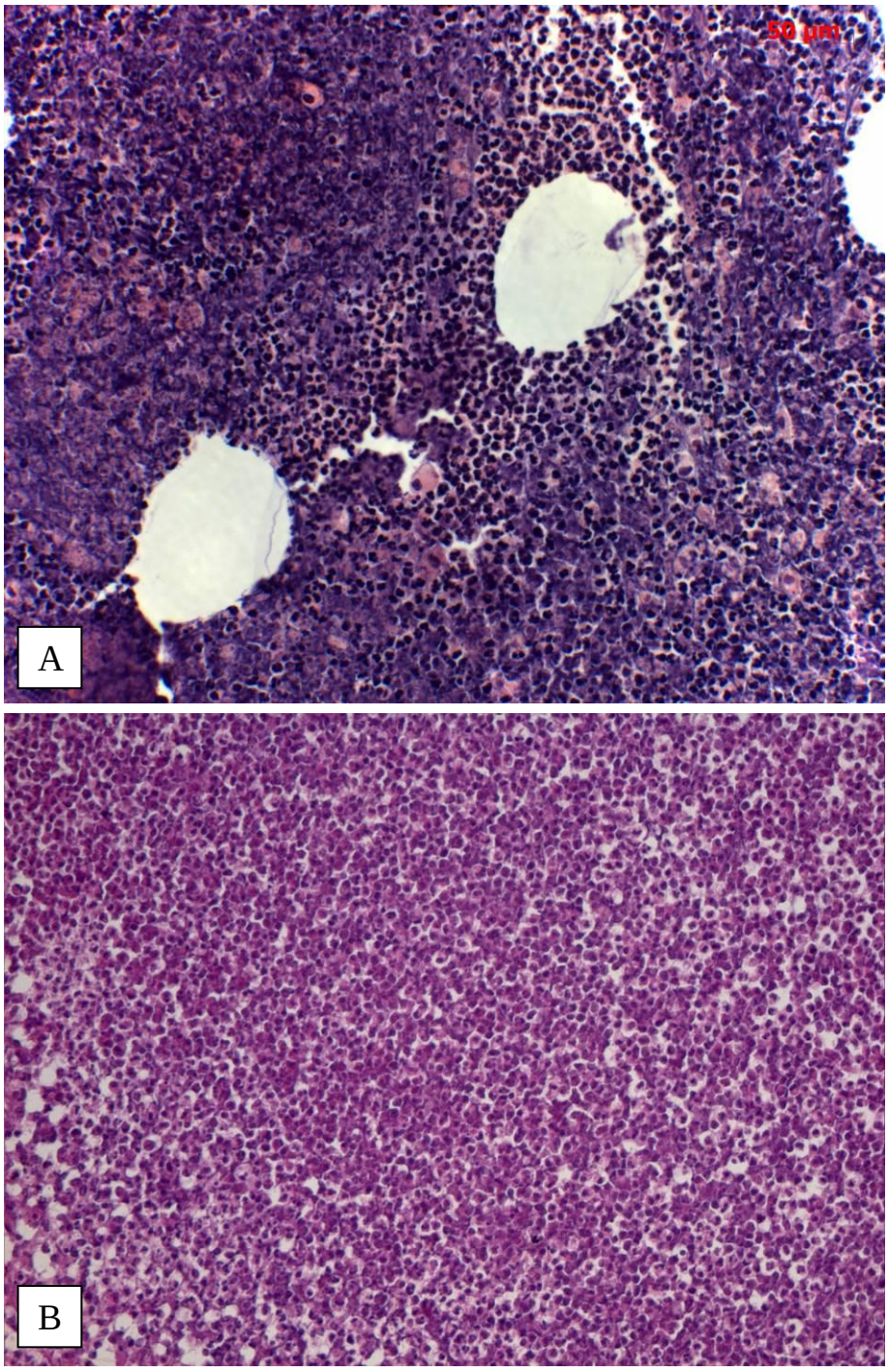

Figure 6.8 The pathology of murine TDM-granuloma is similar to that of caseous human TB granuloma. TDM-granuloma (A) shows tissue degeneration in a similar way to the caseation in human TB granuloma (B, caseous center, caseum).

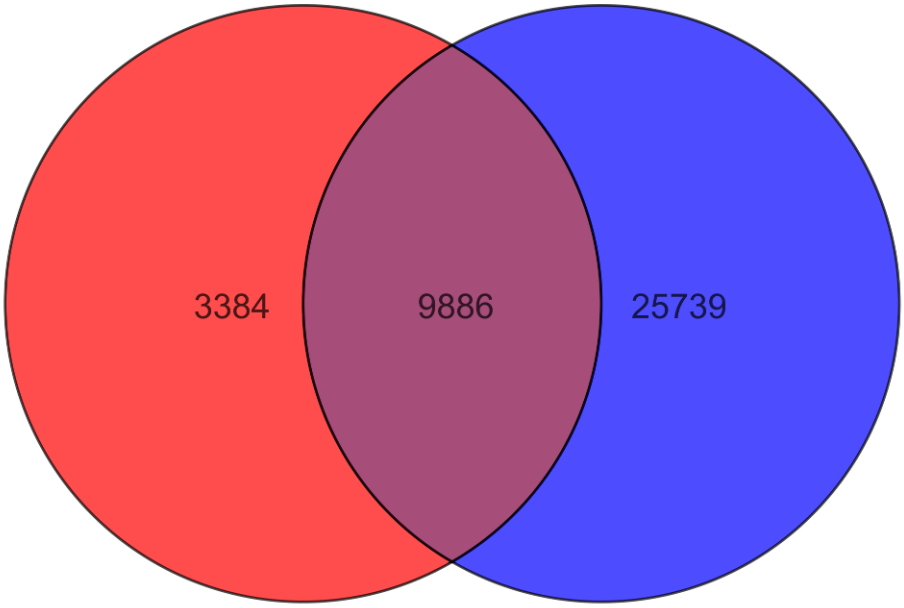

Figure 6.9 Differentially expressed genes in murine TDM-granulomas overlap with those in caseous human pulmonary TB granulomas. Totally, 4757 genes represent 9886 probes that overlap between TDM-granulomas and TB granulomas. Probes from TDM-granulomas are in red and probes from human TB granulomas in blue. $P < 0.05$ Mouse Genome 430 2.0 GeneChip contains 45,000 probes for 39,000 transcripts. Human X3P GeneChip contains 61,000 probes for 47,000 transcripts.

Table 6.1 Top Biological Functions common to both Murine TDM-Granulomas and Caseous Human Pulmonary TB Granulomas. The microarray data were analyzed by using Ingenuity Pathway Analysis®.

Diseases and Disorders		
Name	***p*-value**	**No. of molecules**
Inflammatory Response	2.97^{-16}–5.92^{-7}	541
Inflammatory Disease	3.69^{-19}–6.01^{-7}	1002
Cancer	2.25^{-20}–5.56^{-7}	1267
Neurological Disease	2.97^{-20}–1.28^{-7}	1379
Hematological Disease	6.22^{-22}–6.08^{-7}	435
Molecular and Cellular Functions		
Name	***p*-value**	**No. of molecules**
Cell death	2.74^{-48}–5.08^{-7}	1135
Cellular growth and proliferation	1.61^{-26}–5.68^{-7}	1126
Cellular Development	2.04^{-26}–5.58^{-7}	920
Cellular Movement	4.18^{-26}–4.46^{-7}	661
Cellular Function and Maintenance	2.35^{-20}–4.46^{-7}	426
Physiological System Development and Function		
Name	***p*-value**	**No. of molecules**
Organismal Survival	9.72^{-27}–6.62^{-13}	484
Hematological System Development and Function	3.67^{-24}–5.55^{-7}	661
Hematopoiesis	3.67^{-24}–2.27^{-7}	391
Tissue Morphology	3.06^{-19}–5.96^{-7}	422
Cell-Mediated Immune Response	9.40^{-19}–2.27^{-7}	285
Top Canonical Pathways		
Name	***p*-value**	**Ratio**
Receptor Activator of Nuclear Factor-Kappa B Signaling in Osteoclasts	1.2^{-13}	56/96 (0.583)
Interleukin-10 Signaling	1.69^{-13}	42/70 (0.614)
Role of Protein Kinase R in Interferon Induction and Antiviral Response	1.36^{-12}	32/46 (0.696)
B cell Receptor Signaling	2.41^{-12}	76/154 (0.494)
Induction of Apoptosis by Human Immunodeficiency Virus 1	2.01^{-11}	40/65 (0.615)
Top Toxicity Lists		
Name	***p*-value**	**Ratio**
Nuclear Factor-Kappa B signaling Pathway	1.34^{-10}	61/112 (0.545)
Retinoic Acid Receptor Activation	5.76^{-7}	61/133 (0.459)
Mechanism of Gene Regulation by Peroxisome Proliferators via Peroxisome Proliferator-Activated Receptor Alpha	7.79^{-7}	47/95 (0.495)
Hepatic Cholestasis	2.57^{-6}	60/135 (0.444)
Hepatic Fibrosis	3.09^{-6}	42/85 (0.494)

Table 6.2 Murine TDM-granulomas show upregulated transcripts for immune response. These genes are also upregulated in caseous human pulmonary TB granulomas ($P < 0.05$).

Cluster of Differentiation molecules					
Gene	**Description**	**Fold change**	**Gene**	**Description**	**Fold change**
Cd14	CD14 molecule	9.6	*Cd53*	CD53 molecule	1.9
Cd33	CD33 molecule	3.7	*Cd80*	CD80 molecule	4.7
Cd44	CD44 molecule	3.3	*Cd86*	CD86 molecule	2.3
Major Histocompatibility Complex molecules					
Gene	**Description**	**Fold change**	**Gene**	**Description**	**Fold change**
H2-D1	Histocompatibility 2, D region locus 1	1.7	*H2-Q7*	Histocompatibility 2, Q region locus 7	2.2
H2-L	Histocompatibility 2, D region	1.7	*H2-Q8*	Histocompatibility 2, Q region locus 8	2.7
Receptors/Antigen recognition					
Gene	**Description**	**Fold change**	**Gene**	**Description**	**Fold change**
C5ar1	Complement component 5a receptor 1	2.7	*Msr1*	Macrophage scavenger receptor 1	2.2
Fcer1g	Fc fragment of IgE, high affinity I, receptor for; gamma polypeptide	1.6	*Scarb1*	Scavenger receptor class B, member 1	2.1
Fcgr2b	Fc receptor, IgG, low affinity, IIb	1.9	*Scarb2*	Scavenger receptor class B, member 2	2.1
Marco	Macrophage receptor with collagenous structure	34.2	*Tlr2*	Toll-like receptor 2	5.9
			Tlr4	Toll-like receptor 4	1.9

Table 6.2 (Continued)

Cytokines and cytokine receptors					
Gene	**Description**	**Fold change**	**Gene**	**Description**	**Fold change**
Csf1	Colony stimulating factor 1	2.5	*Ltb*	Lymphotoxin B	8.4
Fas	Fas	11.7	*Tnfaip2*	TNF, alpha-induced protein 2	4.4
Il1b	Interleukin 1, beta	110.1	*TnfaipP3*	TNF, alpha-induced protein 3	5.9
Il13ra1	Interleukin 13 receptor, alpha 1	2.7	*Tnfrsf1a*	TNF receptor superfamily, member 1A	1.5
Il15	Interleukin 15	1.6	*Tnfrsf1b*	TNF superfamily, member 1B	2.5
Il15ra	Interleukin 15 receptor, alpha	1.7	*Tnfrsf21*	TNF receptor superfamily, member 21	1.4
Il17ra	Interleukin 17, receptor A	2.6	*Tnfsf10*	TNF (ligand) superfamily, member 10	2.4
Chemokines and chemokine receptors					
Gene	**Description**	**Fold change**	**Gene**	**Description**	**Fold change**
Ccl3	Chemokine (C-C motif) ligand 3	46.3	*Cmklr1*	Chemokine-like receptor 1	1.2
Ccl4	Chemokine (C-C motif) ligand 4	39.1	*Cxcl11*	Chemokine (C-X-C motif) ligand 1	17.2
Ccr1	Chemokine (C-C motif) receptor 1	6.0	*Cxcl2*	Chemokine (C-X-C motif) ligand 2	38.7
Ccr7	Chemokine (C-C motif) receptor 7	2.1	*Cxcl12*	Chemokine (C-X-C motif) ligand 12	8.4
Ccrl2	Chemokine (C-C motif) receptor-like 2	11.9	*Cxcl16*	Chemokine (C-X-C motif) ligand 16	2.2
Cklf	Chemokine-like factor	1.5	*Cxcr4*	Chemokine (C-X-C motif) receptor 4	7.1
Signaling					
Gene	**Description**	**Fold change**	**Gene**	**Description**	**Fold change**
Inhba	Inhibin, beta A	4.6	*Pag1*	Phosphoprotein associated with glycosphingolipid microdomains 1	3.6
Irak	Interleukin-1 receptor-associated kinase 2	4.3	*Smad3*	MAD homolog 3	2.9
Irak3	Interleukin-1 receptor-associated kinase 3	3.9	*Stat6*	Signal transducer and activator of transcription 6,	1.5
Map3k5	Mitogen-activated protein kinase kinase kinase 5	2.1	*Syk*	Spleen tyrosine kinase	7.3
Mapk1	Mitogen-activated protein kinase 1	1.3	*Traf1*	TNF receptor- associated factor 1	3.9
Msn	Moesin	1.8	*Traf3*	TNF receptor-associated factor 3	3.2
Myd88	Myeloid differentiation primary response gene 88	1.6	*Tnip3*	TNFAIP3 interacting protein 3	25.4

Table 6.3 Murine TDM-granulomas show upregulated transcripts for angiogenesis and tissue remodeling. These genes are also upregulated in caseous human pulmonary TB granulomas ($P < 0.05$).

Proteolysis					
Gene	**Description**	**Fold change**	**Gene**	**Description**	**Fold change**
Casp4	Caspase 4	3.5	*Mmp9*	Matrix metallopeptidase 9	21.6
Casp6	Caspase 6	1.8	*Mmp10*	Matrix metallopeptidase 10	186.5
Casp8	Caspase 8	1.5	*Serpinb9*	Serpin peptidase inhibitor, clade B, member 9	1.3
Chi3l1	Chitinase-3-like 1	48.6	*Timp1*	Tissue inhibitor of metalloproteinase 1	1.3
Fibrosis					
Gene	**Description**	**Fold change**	**Gene**	**Description**	**Fold change**
Col3a1	Collagen, type III, alpha 1	1.7	*Col18a1*	Collagen, type XVIII, alpha 1	4.6
Col4a1	Collagen, type IV, alpha 1	7.2	*Col24a1*	Collagen, type XXIV, alpha 1	1.5
Col4a3bp	Collagen, type I, alpha 1, alpha 3 binding protein	2.4	*Itga5*	Integrin, alpha 5	2.6
Angiogenesis					
Gene	**Description**	**Fold change**	**Gene**	**Description**	**Fold change**
Hif1a	Hypoxia inducible factor 1, alpha subunit	17.8	*Pdgfrb*	Platelet derived growth factor receptor, beta polypeptide	2.3
Pdgfra	Platelet derived growth factor receptor, alpha polypeptide	1.4	*Vcan*	Versican	3.8
			Vegfa	Vascular endothelial growth factor A	1.5

6.6), the transcripts were also upregulated (Table 6.4). Moreover, among genes involved in inflammation, *Cd14*, *Marco*, and *Tlr2* were upregulated, which is line with our previous report on the macrophage response to TDM (Table 6.2) [7].

The lipid analysis indicated that TDM-granulomas have more cholesterol (CHO), cholesteryl esters (CE), and triacylglycerols (TAG), and different compositions of glycosphingolipids and phospholipids, compared to PG-granuloma (Figure 6.10). As lipid droplets are mainly composed of sequestered CHO or CE and TAG, this data is consistent with the histology and microarray analyses on TDM-granulomas.

The formation and development of TB granulomas is a result of the complex relationship between host and Mtb bacilli. Since both host and bacterial factors contribute to this process, it is difficult to pin down one single component that is responsible for TB granuloma development. Our results herein provide a different avenue to examine human TB pathogenesis. TDM, a mycobacterial cell wall lipid, has shown to induce lipid droplets *in vitro* [10, 12] and it is true in our *in vivo* granuloma model. The formation of lipid droplets is not dependent of B- or T-cells, implying that the major host driver for this process is innate immunity. Moreover, gene regulation in TDM-granulomas revealed a considerable overlap with that in caseous human pulmonary TB granulomas. We hypothesize that Mtb (or mainly TDM)-induced lipid droplets contribute to the formation of caseum within the confined granuloma structure, in analogy with the caseum formation in human TB granuloma. In addition to lipid accumulation in TDM-granulomas, tissue remodeling and degeneration was also prominent, similarly to human TB granulomas. Our granuloma model can be used to study essential processes involved human TB granuloma development.

Further investigations into the dynamic biology of the TB granuloma are

Table 6.4 Murine TDM-granulomas show upregulated transcripts for lipid metabolism. These genes are also upregulated in caseous human pulmonary TB granulomas ($P < 0.05$).

Lipid synthesis and sequestration					
Gene	**Description**	**Fold change**	**Gene**	**Description**	**Fold change**
Abhd5	Abhydrolase domain containing 5	1.6	*Degs1*	Degenerative spermatocyte homolog 1, lipid desaturase	1.4
			Gba	Glucosidase, beta, acid	1.4
Acly	ATP citrate lyase	1.2	*Gla*	Galactosidase, alpha	1.7
Acsl1	Acyl CoA synthetase long chain family member 1	8.1	*Gpd2*	Glycerol phosphate dehydrogenase 2, mitochondrial	1.9
Acsl4	Acyl CoA synthetase long chain family member 4	2.3	*Plscr1*	Phospholipid scramblase 1	1.5
Adfp	Adipose differentiation-related protein	2.0	*Soa1*	Sterol O-acyltransferase 1	1.6
Cyp1b1	Cytochrome P450, family 1, subfamily B, polypeptide 1	3.7	*Tpi1*	Triosephosphate isomerase 1	1.7

Figure 6.10 Lipid analysis of PG- and TDM-granulomas
Total lipids from PG-granuloma (4, day 6; 5, day 9; 6, day 9 surrounding adipose tissue and capsule) and TDM-granuloma (7, day 6; 8, day 9; 9, day 9 surrounding adipose tissue and capsule) were extracted from granulomas and separated by thin-layer chromatography, together with standard lipids, oleic acid (1), cardiolipin (2), neutral glycosphingolipids (3), cholesteryl esters (CE) (10), cholesterol (CHO) (11), and triacylglycerol (TAG) (l2). More than three biological replicates per time point (day 6 and 9) were analyzed and representative lipid samples are shown.

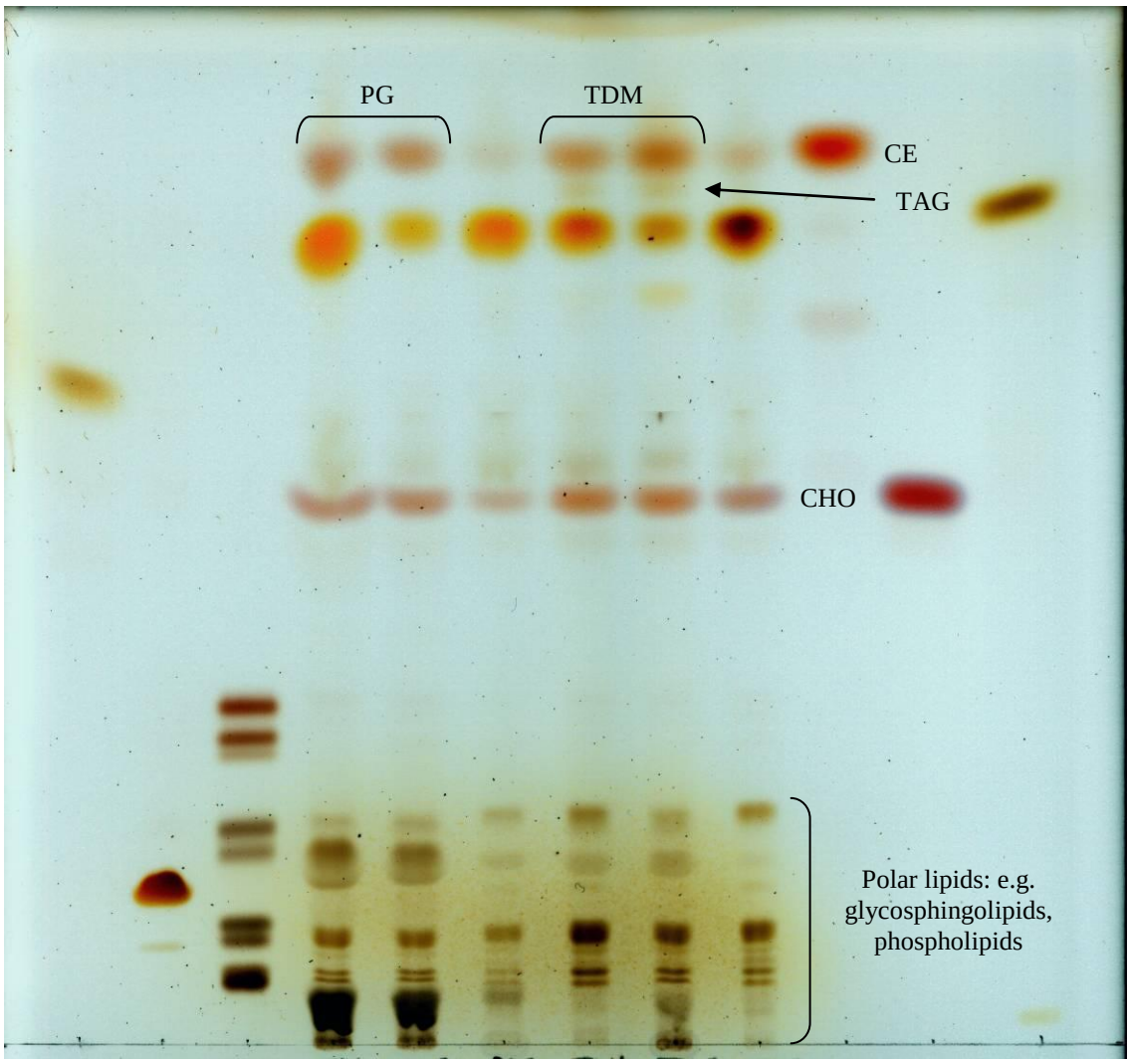
PG
TDM
CE
TAG
CHO
Polar lipids: e.g. glycosphingolipids, phospholipids
1
2
3
4
5
6
7
8
9
10
11
12

imperative. Studies on the characterization of individual host molecules important in lipid accumulation and of minor lipid species involved in inflammatory response will help to advance our knowledge on human TB granuloma development.

ACKNOWLEDEGEMENTS

Special thanks to Drs. Kaori Sakamoto and Elizabeth Rhoades for teaching me the granuloma model.

REFERENCES

1. Takimoto, H., et al., *Interferon-gamma independent formation of pulmonary granuloma in mice by injections with trehalose dimycolate (cord factor), lipoarabinomannan and phosphatidylinositol mannosides isolated from Mycobacterium tuberculosis.* Clin Exp Immunol, 2006. **144**(1): p. 134-41.
2. Beatty, W.L., et al., *Trafficking and release of mycobacterial lipids from infected macrophages.* Traffic, 2000. **1**(3): p. 235-47.
3. Russell, D.G., H.C. Mwandumba, and E.E. Rhoades, *Mycobacterium and the coat of many lipids.* J Cell Biol, 2002. **158**(3): p. 421-6.
4. Geisel, R.E., et al., *In vivo activity of released cell wall lipids of Mycobacterium bovis bacillus Calmette-Guerin is due principally to trehalose mycolates.* J Immunol, 2005. **174**(8): p. 5007-15.
5. Rhoades, E., et al., *Identification and macrophage-activating activity of glycolipids released from intracellular Mycobacterium bovis BCG.* Mol Microbiol, 2003. **48**(4): p. 875-88.
6. Rhoades, E.R., et al., *Cell wall lipids from Mycobacterium bovis BCG are inflammatory when inoculated within a gel matrix: characterization of a new model of the granulomatous response to mycobacterial components.* Tuberculosis (Edinb), 2005. **85**(3): p. 159-76.
7. Bowdish, D.M., et al., *MARCO, TLR2, and CD14 are required for macrophage cytokine responses to mycobacterial trehalose dimycolate and Mycobacterium tuberculosis.* PLoS Pathog, 2009. **5**(6): p. e1000474.
8. Hunter, R.L., N. Venkataprasad, and M.R. Olsen, *The role of trehalose dimycolate (cord factor) on morphology of virulent M. tuberculosis in vitro.* Tuberculosis (Edinb), 2006. **86**(5): p. 349-56.

9. Hunter, R.L., et al., *Multiple roles of cord factor in the pathogenesis of primary, secondary, and cavitary tuberculosis, including a revised description of the pathology of secondary disease.* Ann Clin Lab Sci, 2006. **36**(4): p. 371-86.

10. Peyron, P., et al., *Foamy macrophages from tuberculous patients' granulomas constitute a nutrient-rich reservoir for M. tuberculosis persistence.* PLoS Pathog, 2008. **4**(11): p. e1000204.

11. Pagel, W. and M. Pagel, *Zur Histochemie der Lungentuberkulose, mit besonderer Berücksichtigung der Fettsubstanzen und Lipoide.* Virchows Archiv, 1925. **256**(3): p. 629-640.

12. Korf, J., et al., *The Mycobacterium tuberculosis cell wall component mycolic acid elicits pathogen-associated host innate immune responses.* Eur J Immunol, 2005. **35**(3): p. 890-900.

CHAPTER SEVEN

CONCLUSIONS

Summary

One third of the world population is infected with *Mycobacterium tuberculosis* (Mtb); most of infected individuals do not develop active disease, which is known as chronic or latent infection (or latency). Healthy individuals control Mtb infection by forming a tightly structured granuloma, which is made of leukocytes forming a core around Mtb-infected cells and the fibrous capsule at the periphery. Tuberculous (TB) granuloma protects the host by confining the infection at the local foci but also serves as a niche for Mtb protected from the host immune system. During active TB disease, granulomas liquefy and cavitate, and at this stage Mtb bacilli start to multiply exponentially. The transition of latency to active TB disease and transmission is preceded by the enlargement and liquefaction of caseum (caseous center) and the breakdown of fibrous capsule. Despite the importance of this process, we do not fully understand how gene expression is regulated within TB granulomas, how the caseum develops, and what makes up the caseum.

The work was initiated to advance our knowledge on the biology of TB granulomas by using human TB tissues and *in vitro* and *in vivo* model systems.

Chapter two detailed the microarray analysis on caseous human pulmonary TB granulomas. We used ‘caseous’ ‘pulmonary’ granulomas for our study since the development of caseum precedes the liquefaction and erosion of granulomas and the transmission mainly occurs in pulmonary TB. The microarray data analysis of caseous human pulmonary TB granulomas has generated biological pathways beyond immunological processes (Table 2.1–2.4): e.g. angiogenesis, apoptosis, lipid metabolism, oxidative stress, and tissue remodeling. Previous studies [1-2]

demonstrated the abundance of lipid-filled foam cells in human TB lung tissues and our microarray data also indicated that genes involved in lipid metabolism are highly upregulated in caseous human pulmonary TB granulomas (Table 2.4). These data suggest that Mtb infection leads to the upregulation of genes involved in lipid synthesis and sequestration within TB granulomas, thereby forming foam cells and ultimately caseum.

To further understand the lipid metabolism implicated in human TB granulomas, in Chapter three, we examined the expression of selected proteins involved in lipid synthesis and sequestration by immunohistological analysis of human TB lung tissues; adipose differentiation-related protein (ADFP), acyl-CoA long chain family member 1 (ACSL1), and saposin C (SapC) that represent three different pathways of lipid metabolism were chosen for the analysis (Figure 2.2 and Table 2.4). Strikingly disproportionate expression of ADFP, ACSL1, and SapC was observed (Figure 3.2–3.4), which was accompanied by the formation of lipid droplet-filled foam cells in caseous granulomas and inflamed respiratory bronchioles (Figure 3.5). The high expression of ADFP, ACSL1, and SapC together with the observation of lipid droplets implies that lipid synthesis and accumulation are upregulated within caseous human pulmonary TB granulomas.

Biochemical analysis showed that the caseum of TB granulomas was significantly enriched with neutral lipids, especially, cholesterol (CHO), cholesteryl esters (CE), triacylglycerols (TAG), and glycosphingolipid lactosylceramide (LacCer) (Figure 4.1–4.3). This finding is very interesting since the accumulation of neutral lipids is facilitated by ACSL1 and ADFP activity and that SapC is implicated in LacCer metabolism. Together, these biochemical (Chapter four), transcriptional (Chapter two), and immunohistological (Chapter three) data support our hypothesis that lipids accumulate within human TB granulomas, forming a caseum, and this

process is accompanied by the upregulation of genes and proteins involved in lipid synthesis and sequestration. In analogy to atherosclerosis, the accumulated lipids within TB granulomas may exacerbate inflammation and make the center of TB granulomas more necrotic, which leads to the rupture of granulomas into airways. These lipids within necrotic caseum that is isolated from host immune system may promote Mtb survival by providing carbon source.

In Chapter five, we examined the effect of Mtb on macrophages *in vitro*. Mtb-infected murine or human macrophages showed upregulation of the same transcripts as seen in human TB granulomas: *ADFP*, *ACSL1*, and *PSAP* (SapC) (Table 5.1&5.2). By using confocal microscopy, we could detect foam cells accompanied with ADFP, ACSL1, and SapC expression in Mtb-infected cells (Figure 5.1&5.2). These data indicate that Mtb infection induces lipid accumulation within host cells.

Our data (Chapter two–five) showed that lipids accumulate within human TB granulomas and that Mtb affects the host lipid metabolism *in vitro*. To examine this process *in vivo*, we used our granuloma model [3] in Chapter six. As demonstrated, the Mtb cell wall lipid, trehalose dimycolate (TDM), induced a strong granulomatous response and foam cell formation in mice (Figure 6.1&6.2). This phenomenon was not dependent on the presence of B- or T-cells (Figure 6.4), indicating that innate immune cells are mainly involved in the formation of foam cells. In addition to lipid accumulation, TDM-induced granulomas showed a striking similarity to human TB granulomas as shown by histology and microarray analyses (Figure 6.8&6.9 and Table 6.1–6.4). Therefore, by using our TDM granuloma model, we can explore mechanisms implicated in human TB pathogenesis. For example; (1) host signaling molecules involved in lipid droplet formation can be investigated by using knockout mice or pharmacological agents, (2) lipid trafficking within live cells can be examined by confocal imaging, (3) identification of inflammatory lipid species that are common

to TDM granuloma and human TB granuloma, (4) elucidation of cell death pathway that leads to the formation of necrotic, caseous center, (5) fibrosis in TDM granulomas can be manipulated pharmacologically or genetically (e.g. targeting plasminogen activator inhibitor-1), and (6) tissue degradation can be modulated by agents such as matrix metalloproteinase inhibitors. The use of murine models to answer questions emerging from human data represents the best of both systems.

Whether Mtb multiplies or remains dormant within human TB granulomas during latency is not clear. Yet, Mtb bacilli survive within granulomas during latency, and they multiply and escape from cavitated granulomas during active TB disease. The bacilli require energy to survive during latency; however, the carbon source within human granulomas is not known. The accumulated neutral lipids in the caseum of human TB granulomas identified in the current study (Chapter four) could serve as a carbon source for Mtb. Recently, *in vitro* and *in vivo* studies demonstrated the capability of Mtb to metabolize CHO [4-7]. However, it should be cautioned that murine TB granulomas do not develop the caseum as seen in human TB granulomas. Therefore, the nature of CHO requirement for Mtb survival within murine granulomas may differ from human granulomas. Our *in vitro* and *in vivo* studies (Chapter five and six) suggest that Mtb infection induces foam cell formation. Neutral lipids and glycosphingolipids sequestered in the caseum are most likely to be derived from host cells. Especially, lipid droplets released from foam cells (rather than other leukocytes) within TB granulomas are likely to be the main source of lipids accumulated in the caseum. Further investigation is necessary to determine if lipids released from foam cells make up the same lipid species identified within the caseum. In addition, the caseum may contain minor lipid species (inflammatory lipids such as prostaglandins and leukotrienes) that might play a role in TB pathogenesis.

Even though the caseum increases in size, Mtb bacilli are not likely to be released from the lesion unless the fibrous capsule breaks down; however, the factors that drive capsule breakdown are not known. Dannenberg *et al*. have shown that cathepsin D activity is upregulated in macrophages in *Mycobacterium bovis*-infected rabbits and proposed that the proteinase activity of cathepsin D may be responsible for the liquefaction of caseum and the subsequent cavitation [8]. Our microarray analysis on murine TDM-granulomas (Chapter six) showed that the expression of cathepsin D transcript was 1.4 fold upregulated compared to control PG-granulomas. Moreover, cathepsin D protein was strongly expressed in murine TDM-granulomas as shown by immunohistology (Figure 7.1A), which was not dependent on the presence of B- or T-cells (TDM-granulomas from *Rag1*$^{-/-}$ mice, Figure 7.1B). This phenomenon is interesting in that the death and degradation of macrophages within TB granulomas is thought to mainly contribute to the formation of caseum. Caseous human pulmonary TB granulomas did not show statistical significance in the upregulation of cathepsin D transcript (Chapter two, 4.9 fold upregulation); however, many genes involved in tissue degradation and remodeling were highly upregulated (Table 2.3). *Chitinase 3-like-1* (*CHI3L1*) is of particular interest. CHI3L1, a 40 kDa glycoprotein, is involved in tissue remodeling and angiogenesis and is highly secreted in human cancers such as lung, breast, colon, liver, prostate, ovaries, brain, and thyroid cancer [9]. CHI3L1 is also implicated in inflammatory diseases including rheumatoid arthritis, liver fibrosis, bacterial septicemia, and inflammatory bowel disease [9]. It is worth investigating the level of CHI3L1 in bronchoalveolar lavage fluid or serum of TB patients; it may be used as a severe TB disease marker. The activity of enzymes such as matrix metallopeptidases, caspases, and urokinase can be tested on human TB granulomas and murine TDM-granulomas, by using *in situ* zymography. Mice that lack genes involved in fibrosis, angiogenesis, or tissue degradation (e.g. fibulin, collagen,

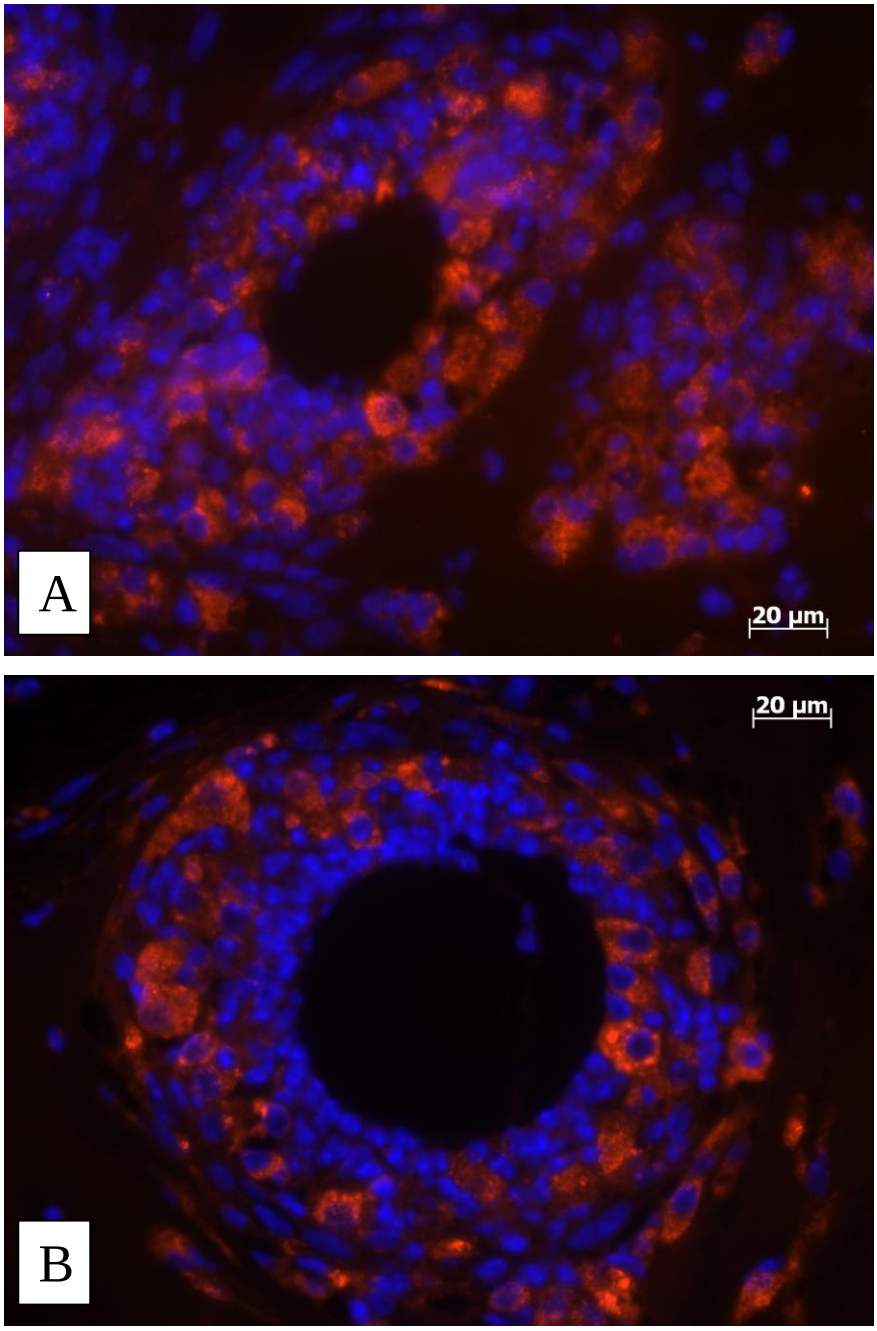

Figure 7.1 Cathepsin D is strongly expressed in murine trehalose dimycolate- induced granulomas. At day 6 of post-inoculation, granulomas were harvested from wild-type (A) and *Rag1*$^{-/-}$ (B) mice and tissue sections were probed with antibody against cathepsin D. Immunofluorescence was performed as described in Chapter six.

integrin, connective tissue growth factor, matrix metallopeptidase, serpin peptidase inhibitor, CHI3L1, and vascular endothelial growth factor A) can be used to study tissue remodeling and granuloma breakdown, in our TDM granuloma model. By using models such as rabbits or non-human primates, pharmacological agents or small interfering RNA that block enzymatic activities can be administered to see if excess caseation and liquefaction, and following breakdown can be modulated.

Ongoing studies

The formation of caseum within TB granulomas is believed to result from the death of cells, mainly macrophages; nonetheless, the mechanism of cell death in TB pathogenesis is not well-characterized. In addition, it is not clear if cell death benefits the host and/or the Mtb bacillus. Whether endoplasmic reticulum (ER) stress-induced apoptosis is involved in TB pathogenesis is not known (Figure 7.2); our microarray analysis on caseous human pulmonary TB granulomas (Chapter two) revealed that genes involved in ER stress were highly upregulated (Table 7.1). Furthermore, Mtb infection leads to the upregulation of transcripts for ER stress in murine macrophages (Table 7.2). We also observed increased expression of CCAAT/enhancer-binding protein homologous protein (CHOP) and cytochrome c somatic (CYCS) in caseous human TB granulomas (Figure 7.3 A&B), and 80–90% of CHOP-positive cells were positive with terminal deoxynucleotidyl transferase dUTP nick end labeling (TUNEL) staining (data not shown). These data indicate that ER stress or ER stress-induced apoptosis is implicated in TB pathogenesis. We are currently preparing a manuscript (Induction of ER stress in macrophages of tuberculosis granulomas; Seimon TA, Kim MJ, Blumenthal A, Koo J, Wainwright H, Kaplan G, Bekker LG, Ehrt S, Nathan C, Tabas I, and Russell DG, submitted to PLoS ONE).

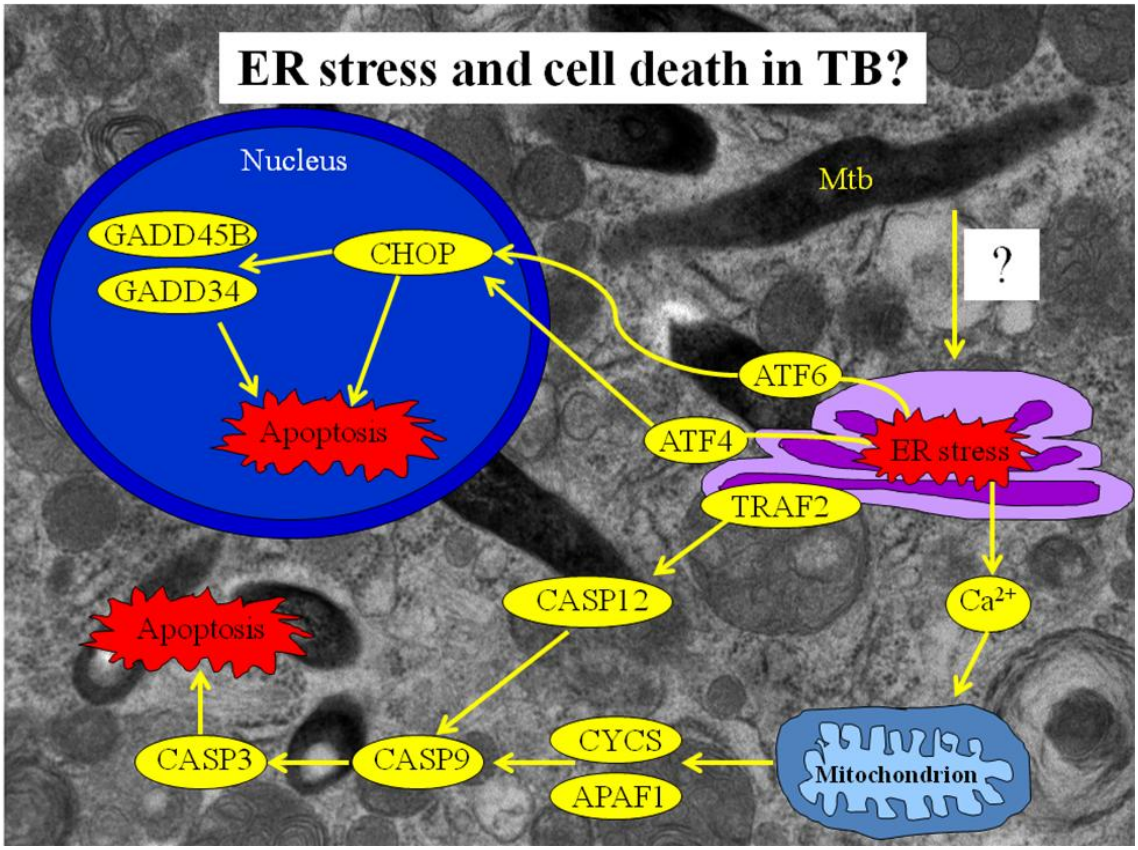

Figure 7.2 Endoplasmic reticulum stress and cell death in tuberculosis pathogenesis The mechanism of cell death in tuberculous granulomas is not well-characterized. This simplified diagram shows some of the key molecules that are involved in endoplasmic reticulum (ER) stress and subsequent cell death.

Table 7.1 Genes relevant for ER stress response are highly upregulated in caseous human pulmonary TB granulomas ($P < 0.05$). The microarray data analysis is described in Chapter two.

Endoplasmic Reticulum (ER) Stress Response		
Gene	**Description**	**Fold upregulation**
APAF1	Apoptotic peptidase activating factor 1	9.0
ATF2	Activating transcription factor 2	20.1
ATF6	Activating transcription factor 6	33.8
CALR	Calreticulin	13.3
CANX	Calnexin	16.9
CASP1	Caspase 1, apoptosis-related cysteine peptidase	35.7
CASP3	Caspase 3, apoptosis-related cysteine peptidase	63.7
CASP4	Caspase 4, apoptosis-related cysteine peptidase	91.7
CASP8	Caspase 8, apoptosis-related cysteine peptidase	114.7
CASP9	Caspase 9, apoptosis-related cysteine peptidase	16.0
CYCS	Cytochrome C, somatic	61.2
DDIT3/*CHOP*	DNA-damage-inducible transcript 3	20.0
EDEM1	ER degradation enhancer, mannosidase alpha-like 1	8.0
ERO1L	Endoplasmic oxidoreductin-1-like protein	54.7
HERPUD1	Homocysteine-inducible, ER stress-inducible, ubiquitin-like domain member 1	43.0
HSP90B1	Heat shock protein 90 kDa beta (Grp94), member 1	72.6
PDIA4	Protein disulfide isomerase family A, member 4	80.3
TRAF2	TNF receptor associated factor 2	14.7
XBP1	X-box binding protein 1	22.5

Table 7.2 Genes relevant for ER stress response are upregulated in Mtb-infected murine macrophages. The quantitative real-time RT-PCR was performed as described in Chapter five. The experiments were repeated at least three times, and the representative result is shown. Three technical replicates were included for all conditions and genes. The fold change was calculated as described in the method section (Chapter five), and the average of replicates is shown.

Endoplasmic Reticulum (ER) Stress Response		
Gene	**Description**	**Fold upregulation**
Atf4	Activating transcription factor 4	1.55
Atf6	Activating transcription factor 6	1.26
Casp3	Caspase 3	1.78
Casp12	Caspase 12	2.53
Ddit3/*Chop*	DNA-damage-inducible transcript 3	26.10
Dapk1	Death associated protein kinase 1	1.48
Edem1	ER degradation enhancer, mannosidase alpha-like 1	1.22
Ero1l	Endoplasmic oxidoreductin-1-like protein	2.19
Gadd34	Growth arrest and DNA-damage-inducible 34	2.53
Gadd45b	Growth arrest and DNA-damage-inducible 45 beta	6.14
Herpud1	Homocysteine-inducible, ER stress-inducible, ubiquitin-like domain member 1	1.1
Jnk1	Mitogen-activated protein kinase 8	1.38

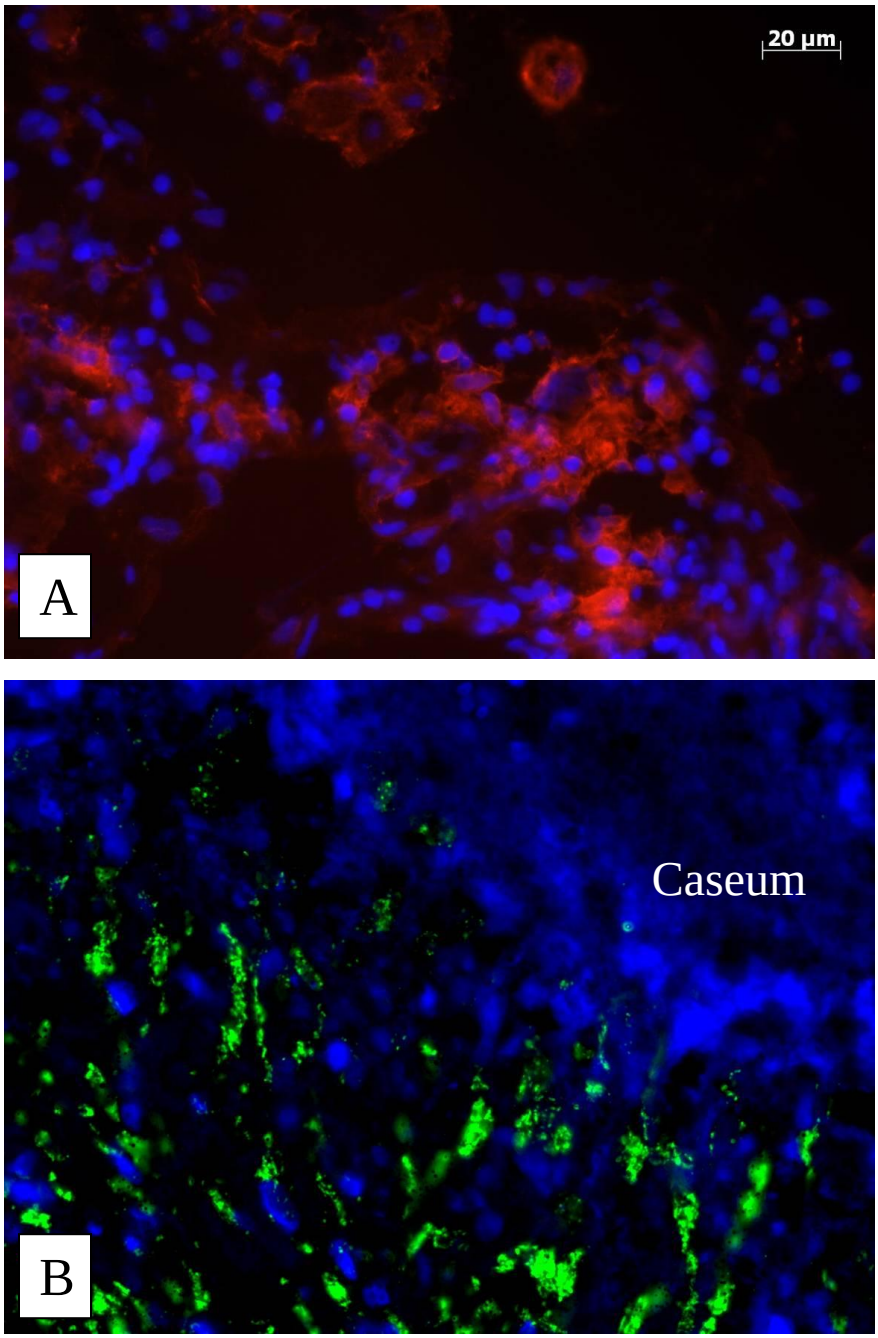

Figure 7.3 ER stress response proteins, DNA-damage-inducible transcript 3 (CHOP, A) and cytochrome c (CYCS), are highly expressed in caseous human pulmonary TB granulomas. The immunohistology on cryosections (A, CHOP in red, nuclei in blue) and paraffin-embedded sections (B, CYCS in green, nuclei in blue, image was taken by using 20× lens) was performed as described in Chapter three.

Another interesting theme emerging from microarray analysis on human TB granulomas is cell transmigration. Though not complete, the recruitment of leukocytes to the site of Mtb infection is known to be driven by various cytokines and chemokines including TNF-α, CCL2, CCL3, and CXCL9 [10-11]. The murine TDM-granulomas showed the massive infiltration of leukocytes to TDM-bearing polystyrene beads (Chapter six and Figure 7.4); we used TDM-granulomas to identify molecules that trigger cell transmigration. At day 6 post-inoculation, murine phosphatidylglycerol (PG)- and TDM-granulomas were excised and incubated in Dulbecco's Modified Eagle Medium (DMEM, without phenol red) for 24 to 48 hours. The conditioned medium was harvested and size-fractionated. We tested fractionated-conditioned medium by using the Transwell system; conditioned medium is placed in the lower compartment and murine bone marrow-derived macrophages are added onto the Matrigel matrix (contains extracellular matrix) (Figure 7.5). Conditioned medium from PG-granulomas did not show any activity, whereas conditioned medium harvested from TDM-granulomas triggered substantial cell transmigration. Interestingly, fractions containing molecules larger than 50 kDa triggered cell transmigration; molecules rather than small chemokines seem to play a role in this process. We have identified 144 molecules in the fraction by mass spectrometric analysis and are currently investigating candidate molecules. It is noteworthy that molecules (larger than 50 kDa) identified in the fraction are also implicated in the transcriptional profiles of human TB granulomas and murine TDM-granulomas (data not shown). These data indicate, to a certain extent, that molecules or pathways of cell transmigration are common to both human TB granulomas and murine TDM granulomas.

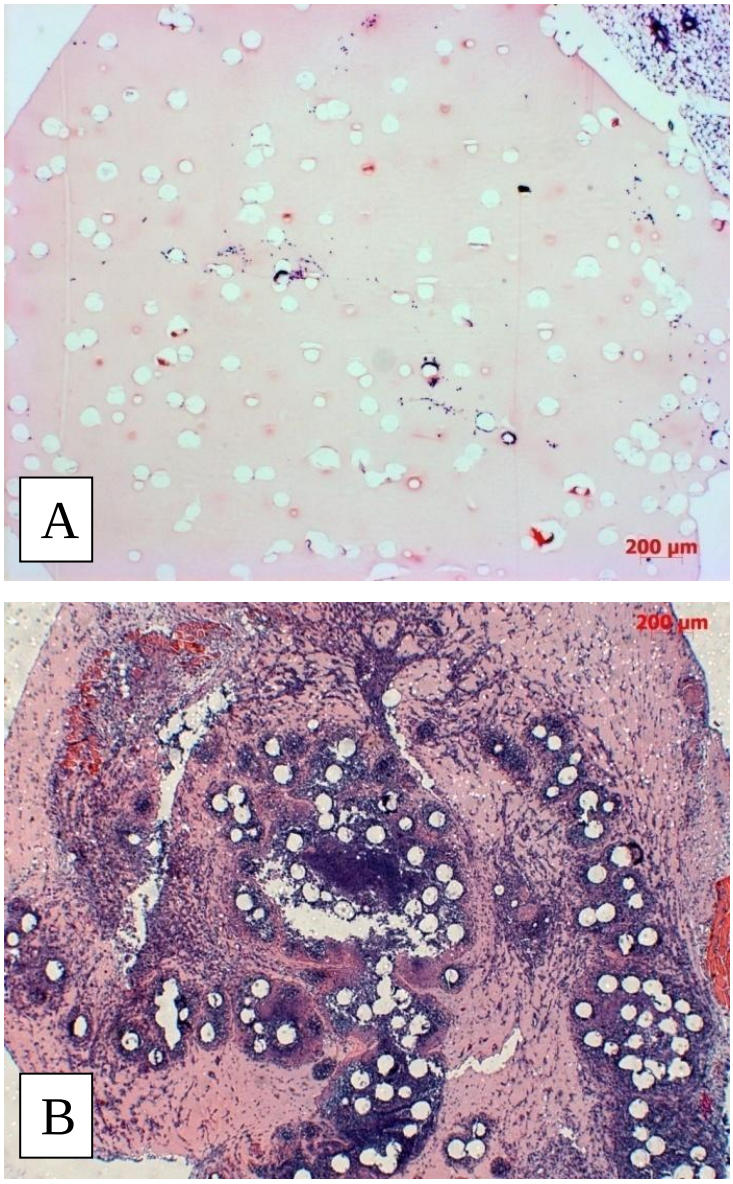

Figure 7.4 Trehalose dimycolate recruits leukocytes to the site of injection in mice. Phosphatidylglycerol (PG) or trehalose dimycolate (TDM) was coated onto polystyrene beads and resuspended in Matrigel matrix. The mixture was injected into mice subcutaneously, and formed granulomas were harvested at day 6. PG (A) does not recruit leukocytes, whereas TDM (B) causes a massive infiltration of leukocytes. Detailed methods are described in Chapter six. Hematoxylin & eosin staining

Figure 7.5 Conditioned medium derived from trehalose dimycolate (TDM)-granulomas triggers cell transmigration. This work is being done in collaboration with Dr. Ute Schwab.
TDM-granulomas harvested from C57BL/6 mice were *ex vivo* incubated in Dulbecco's Modified Eagle Medium (DMEM) for 24 to 48 hours (A). The conditioned medium was placed in the lower compartment of the Transwell system, and the polycarbonate membrane of Transwell was coated with Matrigel matrix (BD) (B). Murine bone-marrow derived macrophages (C57BL/6) which were added onto the top of Matrigel matrix transmigrated through the Matrigel matrix (B&C). The transmigrating macrophages show filopodia in the Matrigel matrix (D, hematoxylin & eosin staining).

A

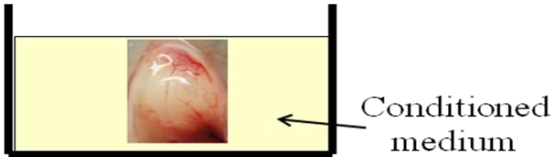
Conditioned
medium

B

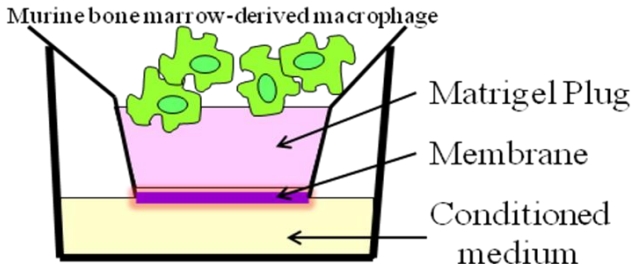
Murine bone marrow-derived macrophage
Matrigel Plug
Membrane
Conditioned
medium

C

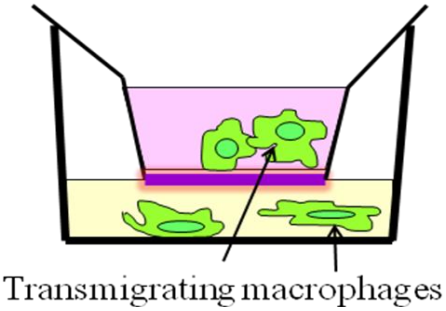
Transmigrating macrophages

D

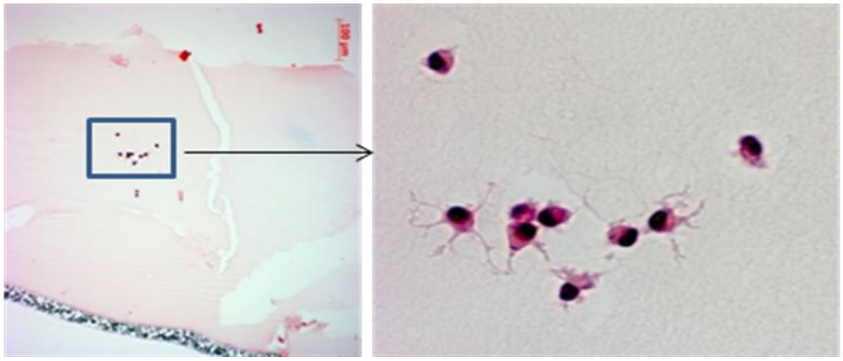

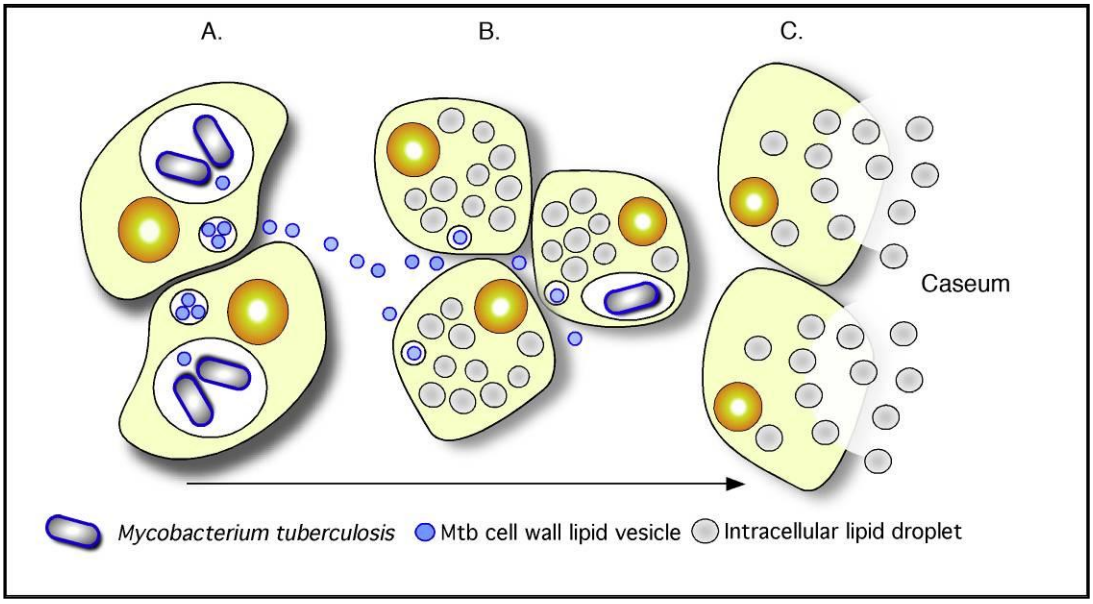

Figure 7.6 A model illustrating the linkages between Mtb-infection, foam cell formation and accumulation of caseum in the human TB granuloma.
A. Intracellular Mtb bacilli synthesize and release cell wall components inside their host cells. We have demonstrated previously that these lipids accumulate in the internal vesicles in multi- vesicular bodies, which are exocytosed from the cell in vesicular form **B**. Because of the release of these vesicles, both infected and uninfected macrophages are exposed to cell wall mycolates and induced to form foamy macrophages, as illustrated in Figure 5. The foamy macrophages have been shown to support the maintenance and growth of persistent bacteria **C**. We now propose that these cells die via an inflammatory, necrotic process and release their lipid droplets into the extracellular milieu within the granuloma. As a result of the fibrotic capsule, the human granuloma is an enclosed, isolated structure with minimal vasculature. The enclosed nature of the human granuloma leads to accumulation of necrotic debris as caseum. In this model, this process is an integral part of the pathology that leads to active disease and transmission.
Kim MJ, Wainwright HC, Locketz M, Bekker LG, Walther GB, Dittrich C, Visser A, Wang W, Hsu FF, Wiehart U, Tsenova L, Kaplan G, and Russell DG.
In press (EMBO molecular medicine)

Conclusion

Overall, this work has presented a better understanding of the biology of TB granulomas, by using molecular, histological, biochemical, and cell biological methods *in vitro* and *in vivo*. Based on our data, we propose a new model for the progression of TB granulomas; Mtb infection drives the dysregulation of host lipid metabolism, thereby leading to the accumulation of lipids within cells (mainly macrophages); furthermore, cell death (including ER stress-induced apoptosis and necrosis) causes the release of sequestered lipids, which ultimately results in the formation of a caseum (Figure 7.6). The data from human TB granulomas will provide opportunities for designing novel therapeutics targeting Mtb and/or modulating host metabolism.

Many questions need to be answered. For example: Are other molecules important roles in lipid metabolism within human TB granulomas? Is there a direct relationship between upregulation of ADFP, ACSL1, and SapC and accumulation of neutral lipids and glycosphingolipids? Which other lipids are present in the caseum? Are the lipids in the caseum made of lipids derived from foam cells? Can Mtb bacilli metabolize the lipids in the caseum of human TB granulomas or are the accumulated lipids a byproduct of the host immune response? How does cell death within TB granulomas occur? Is there a way of preventing the caseum formation and granuloma breakdown?

REFERENCES

1. Pagel, W. and M. Pagel, *Zur Histochemie der Lungentuberkulose, mit besonderer Berücksichtigung der Fettsubstanzen und Lipoide.* Virchows Archiv, 1925. **256**(3): p. 629-640.
2. Hunter, R.L., C. Jagannath, and J.K. Actor, *Pathology of postprimary tuberculosis in humans and mice: contradiction of long-held beliefs.* Tuberculosis (Edinb), 2007. **87**(4): p. 267-78.
3. Geisel, R.E., et al., *In vivo activity of released cell wall lipids of Mycobacterium bovis bacillus Calmette-Guerin is due principally to trehalose mycolates.* J Immunol, 2005. **174**(8): p. 5007-15.
4. Pandey, A.K. and C.M. Sassetti, *Mycobacterial persistence requires the utilization of host cholesterol.* Proc Natl Acad Sci U S A, 2008. **105**(11): p. 4376-80.
5. Brzostek, A., et al., *Mycobacterium tuberculosis is able to accumulate and utilize cholesterol.* J Bacteriol, 2009. **191**(21): p. 6584-91.
6. Chang, J.C., et al., *Identification of Mycobacterial genes that alter growth and pathology in macrophages and in mice.* J Infect Dis, 2007. **196**(5): p. 788-95.
7. Chang, J.C., et al., *igr Genes and Mycobacterium tuberculosis cholesterol metabolism.* J Bacteriol, 2009. **191**(16): p. 5232-9.
8. Converse, P.J., et al., *Cavitary tuberculosis produced in rabbits by aerosolized virulent tubercle bacilli.* Infect Immun, 1996. **64**(11): p. 4776-87.
9. Coffman, F.D., *Chitinase 3-Like-1 (CHI3L1): a putative disease marker at the interface of proteomics and glycomics.* Crit Rev Clin Lab Sci, 2008. **45**(6): p. 531-62.

10. Algood, H.M., J. Chan, and J.L. Flynn, *Chemokines and tuberculosis.* Cytokine Growth Factor Rev, 2003. **14**(6): p. 467-77.

11. Flynn, J.L. and J. Chan, *What's good for the host is good for the bug.* Trends Microbiol, 2005. **13**(3): p. 98-102.